Inhomogeneous Stokes Flow through Porous Media

by

Richard Panko Batycky

S.M., Chemical Engineering (1992)
Massachusetts Institute of Technology

B.Sc., Chemical Engineering (1990)
University of Calgary

Submitted to the Department of Chemical Engineering
in partial fulfillment of the requirements for the degree of

Doctor of Philosophy

at the

MASSACHUSETTS INSTITUTE OF TECHNOLOGY

September 1995

Author .....
Department of Chemical Engineering
August 4, 1995

Certified by .....
Howard Brenner
Willard Henry Dow Professor of Chemical Engineering
Thesis Supervisor

Accepted by .....
Robert E. Cohen
Chairman, Committee for Graduate Students

Inhomogeneous Stokes Flow through Porous Media

by

Richard Panko Batycky

Submitted to the Department of Chemical Engineering
on August 4, 1995, in partial fulfillment of the
requirements for the degree of
Doctor of Philosophy

Abstract

A new technique is proposed for rigorously analyzing, from first principles, the macroscopically inhomogeneous low-Reynolds number flow of an incompressible Newtonian fluid through the interstices of a spatially periodic model of a porous medium. The scheme involves developing a generalized Taylor series expansion of the microscale velocity field $\mathbf{v}$ and pressure field p in terms of a continuous local position vector and a discrete global position vector.

An *exact* microscale solution is developed for an arbitrary incompressible, Newtonian flow field, allowing the velocity and pressure to be 'separated' into a product solution composed of two parts: (i) spatially periodic lattice functions, characterizing the fine-scale, unit cell geometry of the porous medium; (ii) constant arbitrary tensors (related to the Darcy-scale mean velocity gradients), describing the inhomogeneous macroscale flow field. This technique may be used to describe other inhomogeneous transport processes occuring in these types of porous media.

From this exact microscale product representation, a macroscale description of the flow is constructed. The microscale→macroscale 'averaging' scheme is not a volume-average technique, but rather represents a more fundamental approach, drawing on classical macroscale *definitions* to define the mean velocity field $\overline{\mathbf{v}}$ and mean stress field $\overline{\mathbf{P}}$. (The macroscale pressure $\overline{p}$ then follows directly from $\overline{\mathbf{P}}$ without requiring any assumptions about the existence of a pressure field within the interiors of the bed particles, as is characteristic of classical volume-average approaches.) Macroscale linear and angular momentum balances follow naturally from these definitions. As well, constitutive relationships are derived, relating the Darcy-scale external body force density, deviatoric stress, and external body couple density to such Darcy-scale kinematical fields as the velocity, vorticity, and rate-of-strain. All phenomenological coefficients appearing in these macroscale constitutive relations are implicitly expressed as unique functions of the microscale lattice geometry and the interstitial viscosity. Their calculation requires only the solution of Stokes flow problems within a *single* unit cell of the periodic array, despite the non-local, inhomogeneity of the basic flow. The final form of the macroscale linear momentum equation contains not only the usual Darcy permeability dyadic, but also a coupling triadic (relating $\overline{\nabla}\,\overline{p}$ to

$\overline{\nabla}\,\overline{\mathbf{v}}$) and a Brinkman-type viscosity tetradic (relating $\overline{\nabla}\,\overline{p}$ to $\overline{\nabla}\,\overline{\nabla}\,\overline{\mathbf{v}}$). The scheme also allows calculation of higher-order mean velocity gradient terms in the expression for $\overline{\nabla}\,\overline{p}$.

Numerical solutions of the first three unit-cell fields, arising from $\overline{\mathbf{v}}$, $\overline{\nabla}\,\overline{\mathbf{v}}$ and $\overline{\nabla}\,\overline{\nabla}\,\overline{\mathbf{v}}$, respectively, are calculated for various two-dimensional square arrays composed of circular and elliptical cylinders. The macroscale phenomenological coefficients appearing in the several Darcy-scale constitutive relationships are calculated from these unit cell microscale, Stokes-flow fields. Among other things, the effects of particle volume fraction and ellipse eccentricity upon these coefficients are quantified.

Thesis Supervisor: Howard Brenner
Title: Willard Henry Dow Professor of Chemical Engineering

... for Andrena and Anya

I have yet to see any problem, however complicated, which, when you looked at it in the right way, did not become still more complicated.

Poul Anderson, 1969

Whoever, in the pursuit of science, seeks after immediate practical utility may rest assured that he seeks in vain.

Hermann Ludwig Ferdinand von Helmholtz, 1862

Acknowledgments

I would like to thank Howard Brenner and David Edwards for their guidance, encouragement and friendship while writing this thesis. The innumerous meetings with Howard were extremely valuable and insightful. I would also like to thank my wife, family and friends for their support.

This research was supported in part by the Office of Basic Energy Sciences of the Department of Energy.

Contents

List of Figures

List of Tables

Chapter 1

Introduction

1.1 Origin of the Darcy-Brinkman Equation

The slow, quasisteady flow of an incompressible Newtonian fluid through the interstices of a porous medium may be described by Stokes equation,

$$\nabla p = \mu \nabla^2 \mathbf{v}, \tag{1.1-1}$$

together with the continuity equation,

$$\nabla \cdot \mathbf{v} = 0, \tag{1.1-2}$$

valid at every point of the interstitial fluid continuum. Here, p is the pressure, μ is the (isotropic and uniform) fluid viscosity, and $\mathbf{v}$ is the vector velocity. As the particles comprising the porous medium are fixed in space, and the fluid adheres to the surfaces of these particles, the above equations are necessarily subject to the no-slip boundary condition

$$\mathbf{v} = \mathbf{0} \quad \text{on} \quad s_p, \tag{1.1-3}$$

where s_p denotes the particle surfaces. Whereas equations (1.1-1)–(1.1-3) constitute a purely microscale description of flow in a porous material, a macroscale description of the flow is more often used, one which views the combined skeletal porous medium

and fluid as a heterogeneous continuum (see applications in § 2.3).

The first macroscale description of flow through porous materials was proposed by Darcy [44], namely

$$\overline{\nabla}\overline{p} = -\frac{\mu}{k}\overline{\mathbf{v}}, \tag{1.1-4}$$

where overbars represent quantities defined on a coarse scale that views the fluid-particle system as a continuum, k being the permeability of the medium. Coupled with this is the continuity condition,

$$\overline{\nabla} \cdot \overline{\mathbf{v}} = 0 \tag{1.1-5}$$

for incompressible fluids.

As first noted by Brinkman [29, 30, 31], fundamental problems associated with Darcy's equation (1.1-4) exist. First, as (1.1-4) is a first-order equation, it is impossible to formulate rational macroscale boundary conditions, in contrast with Eq. (1.1-1), which is of the second-order. Second, in the limit as the volumetric particle density ϕ shrinks to zero (corresponding to $k \to \infty$) one should presumably recover Stokes equation (1.1-1). For these reasons, Brinkman [30] proposed the following modification of Darcy's equation:

$$\overline{\nabla}\overline{p} = -\frac{\mu}{k}\overline{\mathbf{v}} + \overline{\mu}^*\overline{\nabla}^2\overline{\mathbf{v}}, \tag{1.1-6}$$

where $\overline{\mu}^*$ is an effective viscosity[1] (Brinkman viscosity) of the macroscale continuum. Brinkman used (1.1-6) to compute the force on a sphere embedded in a porous mass [30], but noted that the results were sensitive to the choice of $\overline{\mu}^*$. He suggested that perhaps one could use of Einstein's viscosity result for suspensions [48, 49], namely

$$\frac{\overline{\mu}^*}{\mu} = 1 + \frac{5}{2}\phi. \tag{1.1-7}$$

[1]To avoid confusion, the effective viscosity of a medium composed of particles fixed in space will hereafter be refered to as the Brinkman viscosity, while the effective viscosity of a neutrally buoyant suspension will be termed the suspension viscosity.

Brinkman compared his analytical results [30] with experimental data by Carman [33] for a column packed with particles and showed that not only was $\overline{\mu}^*$ not given by Einstein's result, but also that $\overline{\mu}^*$ could either be larger or smaller than μ, depending upon specific circumstances. Brinkman found that his theoretical results agreed better with Carman's experimental correlation for the choice $\overline{\mu}^* = \mu$, rather than (1.1-7). More recently [83], numerical results for the suspension viscosity, valid at larger particle concentrations, show that the suspension viscosity is larger than that predicted by (1.1-7). This would lead to even greater discrepancies between the results of Brinkman and Carman. More fundamentally, since Brinkman's basis for proposing (1.1-6) is purely empirical, no rational basis exists for determining $\overline{\mu}^*$ for a packed bed.

1.2 Current Objectives and Approach

This thesis proposes a technique involving a generalized Taylor series expansion for deriving the appropriate macroscale equations governing Stokes flow through a spatially periodic model of a porous medium together with the phenomenological coefficients appearing therein as a function of the microgeometry of the medium.

Chapter 2 describes earlier contributions in determining the Brinkman viscosity for a specific porous medium. In particular, Figure 2-1 shows a widespread disagreement as to the Brinkman viscosity of a random array of uniform sized spheres. The drawback to the random approach is that assumptions have to be made about the form of the macroscale description. Furthermore, it inherently relies on a volume average approach which may not produce *physical interpretations* of the averaged quantities.

Chapter 3 outlines the formulation of a generalized Taylor series expansion. The focus is on reorganizing the series into parts dependent upon a continuous local position vector, and parts dependent upon a discrete global position vector. As well, jump conditions are derived which are imposed upon the relevant microscale fields at each order of the expansion by the requirement of continuity of $\mathbf{v}$ and p across

contiguous cell faces.

Chapter 4 is devoted to applying the generalized Taylor series results of Chapter 3 to the specific problem of an arbitrary flow field within the intersticies of a spatially periodic model of a porous medium with with an arbitrary, but deterministic microscale geometry. Successive sections are devoted to solving a higher-order truncation of the generalized Taylor series, culminating in the central intermediate result that $\mathbf{v}$ and p can be expressed in a 'separation-of-variables' format involving *spatially periodic lattice functions* (functions determined uniquely by the unit cell geometry), multiplied by *constant arbitrary tensors* [cf. (4.6-32) and (4.6-33)]. This derivation is for an *arbitrary* microscale flow, with no assumptions being required as to scale separation.

Chapter 5 rigorously provides a means of interpreting the exact, general microscale solution, derived in Chapter 4, in terms of *physical*, macroscale variables. It is assumed, as usual, that three relevant length scales exist for the porous medium, namely a microscale ℓ, a mesoscale $\mathcal{L}$ [such that cell-face properties can be interpreted as macroscale differential properties, cf. Eqs. (5.2-3), (5.2-8) and (5.2-16)], and a macroscale L, obeying the strong inequality

$$L \gg \mathcal{L} \gg \ell.$$

When the macroscale velocity $\overline{\mathbf{v}}$ is determined at Taylor series orders greater than zero, the macroscale continuity condition is recovered from an auxiliary condition as

$$\overline{\boldsymbol{\nabla}} \cdot \overline{\mathbf{v}} = 0.$$

Moreover, because of the definitions of the macroscale velocity $\overline{\mathbf{v}}$ (5.2-9) and macroscale stress $\overline{\mathbf{P}}$ (5.2-11), Newton's laws of motion and continuum mechanical arguments furnish the macroscale linear momentum equation,

$$\overline{\boldsymbol{\nabla}} \cdot \overline{\mathbf{P}} + \overline{\mathbf{F}}^{(e)} = \mathbf{0},$$

with $\overline{\mathbf{F}}^{(e)}$ the net external volumetric body force density (required to hold the particles stationary). The macroscale pressure $\overline{p}$ then is simply proportional to the negative trace of $\overline{\mathbf{P}}$. This is in sharp contrast with volume averaging approaches (Afacan & Masliyah [6], Du Plessis & Masliyah [45], Lundgren [73], Slattery [103] and Whitaker [120]) that require assumptions be made as to a possible existence of a microscale pressure field or pressure gradient within the particle *interiors*. This is because definitions such as (5.2-9) and (5.2-11) are not derived. Similarly, the macroscale stress tensor is shown to satisfy the macroscale angular momentum equation

$$\overline{\mathbf{P}}_{\times} + \overline{\mathbf{N}}^{(e)} = \mathbf{0}$$

with $\overline{\mathbf{P}}_{\times}$ the macroscale stress pseudovector (related to the antisymmetric part of $\overline{\mathbf{P}}$) and $\overline{\mathbf{N}}^{(e)}$ the net external volumetric body couple density. Again, since the microscale stress is symmetric, volume averaging techniques will yield only symmetric macroscale stresses ($\overline{\mathbf{P}}_{\times} = \mathbf{0}$) even though, as a counterexample, a medium composed of asymmetric particles necessarily requires an external body couple density $\overline{\mathbf{N}}^{(e)}$ to keep the particles fixed in place.

Only terms up to and including $\overline{\boldsymbol{\nabla}}\,\overline{\boldsymbol{\nabla}}\overline{\mathbf{v}}$ in the taylor series expansion are computed, ultimately furnishing an equation of the form

$$\overline{\boldsymbol{\nabla}}\overline{p} = \overline{\mathbf{A}} \cdot \overline{\mathbf{v}} + \overline{\mathbf{B}} : \overline{\boldsymbol{\nabla}}\overline{\mathbf{v}} + \overline{\mathbf{C}} \vdots \overline{\boldsymbol{\nabla}}\,\overline{\boldsymbol{\nabla}}\overline{\mathbf{v}}$$

The phenomenological coefficents appearing above, consisting of the dyadic $\overline{\mathbf{A}}$, triadic $\overline{\mathbf{B}}$ and tetradic $\overline{\mathbf{C}}$ are uniquely determined from the solution of three cellular-level, inhomogeneous Stokes flow problems. Retention of higher-order terms such as $\overline{\boldsymbol{\nabla}}\,\overline{\boldsymbol{\nabla}}\,\overline{\boldsymbol{\nabla}}\,\overline{\mathbf{v}}$ does not affect these three coefficients. Accordingly, the above Brinkman-type equation possesses a general validity that transcends the truncation of the Taylor series expansion. A more fundamental form of the momentum equation is derived

$$\overline{\boldsymbol{\nabla}}\,\overline{p} = \overline{\mathbf{F}}^{(e)} + \overline{\boldsymbol{\nabla}} \cdot \left(\overline{\mathbf{T}}^{s} + \frac{1}{2}\boldsymbol{\epsilon} \cdot \overline{\mathbf{P}}_{\times} \right),$$

explicitly showing the contributions to the macroscale pressure drop from the external voumetric body force density $\overline{\mathbf{F}}^{(e)}$, symmetric deviatoric stress $\overline{\mathbf{T}}^{s}$ and stress pseudovector $\overline{\mathbf{P}}_{\times}$. In turn, the dependencies of these quantities upon the macroscale velocity $\overline{\mathbf{v}}$, vorticity $\overline{\boldsymbol{\omega}}$ and symmetric rate-of-strain dyadic $\overline{\mathbf{S}}$ are derived as

$$\begin{aligned}
\overline{\mathbf{F}}^{(e)} &= -\mu\mathbf{k}^{-1}\cdot\overline{\mathbf{v}} + \mu\overline{\boldsymbol{\nabla}}\cdot\left[\overline{\mathbf{f}}^{(l)}\cdot\overline{\mathbf{v}} + \overline{\mathbf{f}}^{(r)}\cdot\overline{\boldsymbol{\omega}} + \overline{\mathbf{f}}^{(s)}:\overline{\mathbf{S}}\right], \\
\overline{\mathbf{T}}^{s} &= \mu\left[\overline{\mathbf{K}}^{(l)}\cdot\overline{\mathbf{v}} + \overline{\mathbf{K}}^{(r)}\cdot\overline{\boldsymbol{\omega}} + \overline{\mathbf{K}}^{(s)}:\overline{\mathbf{S}}\right], \\
\overline{\mathbf{P}}_{\times} &= \mu\left[\overline{\mathbf{c}}^{(l)}\cdot\overline{\mathbf{v}} + \overline{\mathbf{c}}^{(r)}\cdot\overline{\boldsymbol{\omega}} + \overline{\mathbf{c}}^{(s)}:\overline{\mathbf{S}}\right]
\end{aligned}$$

with the phenomenological coefficients appearing therein uniquely determined from the same three cellular-level, inhomogeneous Stokes flow problems.

Finally, in Chapter 6, calculations of these coefficients for two-dimensional arrays of circular and elliptical cylinders is effected. Their dependence upon particle volume fraction and ellipse eccentricity is studied.

Chapter 2

Derivations and Uses of the Brinkman Equation

2.1 Introduction

Before formulating a rigorous theory for describing an exact, generalized microscale flow field and its macroscale interpretation, a brief account is presented here of previous work in both formulating and using the Brinkman equation.

2.2 Previous Derivations

Although the macroscale description (1.1-6) appears superficially to be a plausible extension of (1.1-4), no rigorous theoretical foundation exists that justifies its use.

The first steps toward validation of (1.1-6) were initiated by Beavers and coworkers [15, 16]. These researchers experimentally studied the laminar flow of a viscous fluid over a naturally permeable block and found that the mass efflux of a parallel Poiseuille flow was greatly enhanced over the corresponding rate observed for a comparable impermeable surface. A simple, linear-slip boundary condition using a nondimensional slip coefficient α was proposed; experimental α values for various materials lay in the range $0.1 < \alpha < 4.0$. This slip coefficient scheme was later justified by Saffman [93]. Subsequently, Neal & Nader [81] analytically solved this problem two ways: (i) using Darcy's equation within the medium together with a slip boundary condition on the free-stream side of the medium surface; (ii) using Brinkman's equation in the medium, together with matching velocities at the medium surface. They showed that these two methods were equivalent and that, in fact, the Brinkman viscosity and slip coefficient were related by $\overline{\mu}^*/\mu = \alpha^2$. Experimental values [15, 16] of $\overline{\mu}^*/\mu$ thereby ranged from 0.01 to 16.0.

Neal & Nader [81] concluded that although $\overline{\mu}^* \neq \mu$ in general, the choice of $\overline{\mu}^* = \mu$ was recommended since it was in keeping with established practice—stating specifically that

> "... it does not yet appear possible to accurately predict $\overline{\mu}^*/\mu$ for any given porous media."

Wiegel [122] provides a derivation of the macroscopic equations governing Stokes flow, but concentrates primarily on the Darcy term and assumes $\overline{\mu}^* = \mu$. Vafai & Tien [113] include boundary and inertial effects in their analysis, but also assume $\overline{\mu}^* = \mu$. Joseph *et al.* [67] include inertial and convective terms, but choose $\overline{\mu}^* = \mu$, arguing that

> "It is not appropriate to replace μ by an effective viscosity $\overline{\mu}^*$, as one does with suspensions, since the fluid in the porous medium retains its bulk

properties."

On the other hand, Ladd [71] assumes that all transport coefficients (e.g., self diffusivity, effective viscosity) are independent of whether the particle bed is fixed in space or constitutes a neutrally buoyant suspension.

Using a molecular-dynamics-like simulation (Stokesian dynamics), Durlofsky & Brady [46] conclude that the Brinkman equation is valid only when $\phi < 0.05$, but in their analysis they suppose $\overline{\mu}^* = \mu$.

Near macroscale boundaries, macroscale velocity and pressure gradients vary on a length scale of the order of the pore dimensions, at which scale a the continuum view of the porous medium becomes invalid. A method initially proposed for thermal transport processes [2, 34, 36] was later extended by Chang & Acrivos [35] to flow around a sphere immersed in a random array of fixed spheres. This method proposes that near macroscale surfaces one should replace $\overline{\mu}^*$ in (1.1-6) by a nonuniform Brinkman viscosity $\overline{\mu}_r^*$ which varies near macroscale surfaces according to the relation

$$\frac{\overline{\mu}_r^*}{\mu} = 1 + \left(\frac{\overline{\mu}^*}{\mu} - 1\right) \frac{\Psi(\overline{\mathbf{R}}, \phi)}{\phi}, \tag{2.2-1}$$

with $\overline{\mathbf{R}}$ is a macroscale position vector, Ψ the areal fraction of solids near the macroscale boundary, and $\overline{\mu}^*$ the Brinkman viscosity in the bulk medium. This equation possesses the property that the Brinkman viscosity reduces to the fluid viscosity near the macroscale boundary, and to that of the bulk Brinkman viscosity far from the macroscale boundary. Later, Sangani & Behl [96] numerically solved the problem of flow over a semi-infinite, spatially periodic array of spheres and compared results obtained for the slip coefficient with those obtained by the use of (1.1-6) with either a constant Brinkman viscosity or that given in (2.2-1). Better numerical agreement was obtained using (2.2-1); however, one must still determine $\overline{\mu}^*$. Sangani and coworkers [97, 96] utilized a previously developed method [35] used for random arrays to determine $\overline{\mu}^*$, and found that this method (as well as most self-consistent schemes) yielded $\overline{\mu}^*/\mu > 1$, even though better agreement with numerical calculations of the permeability was obtained only with the inequality $\overline{\mu}^*/\mu < 1$. For this reason, they

suggested retaining the relation $\overline{\mu}^* = \mu$.

A rigorous derivation of (1.1-6) should simultaneously furnish the effective properties of the porous medium, independently of the flow field. To date, this has not been achieved, although it has been accomplished for the separate cases of Darcy's equation and the rheological properties of neutrally-buoyant suspensions.

2.2.1 Darcy's Equation

In it's most general form, Darcy's equation (1.1-4) may be written as

$$\overline{\nabla}\overline{p} = -\mu \mathbf{k}^{-1} \cdot \overline{\mathbf{v}}, \tag{2.2-2}$$

where $\mathbf{k}$ is the dyadic permeability. One of the simpler ways to derive Darcy's equation (2.2-2) is to take a spatially periodic medium and subject it to a uniform macroscale pressure gradient. Details of this analysis may be found elsewhere (This actually corresponds to the zeroth-order flow field presented in Section 4.3).

Let the dyadic field $\widetilde{\mathbf{V}}^0(\mathbf{r})$ and vector field $\widetilde{\boldsymbol{\Pi}}^0(\mathbf{r})$ denote the solution of the cellular boundary-value problem

$$\nabla^2 \widetilde{\mathbf{V}}^0 - \boldsymbol{\nabla} \widetilde{\boldsymbol{\Pi}}^0 = \mathbf{I} \qquad \forall (\mathbf{r} \in \tau_f), \tag{2.2-3}$$

$$\boldsymbol{\nabla} \cdot \widetilde{\mathbf{V}}^0 = \mathbf{0} \qquad \forall (\mathbf{r} \in \tau_f), \tag{2.2-4}$$

with $\mathbf{I}$ the dyadic idemfactor, $\mathbf{r}$ a position vector defined within a unit cell, and τ_f the fluid (continuous) domain within a unit cell. Equations (2.2-3) and (2.2-4) are to be solved subject to the no-slip particle boundary condition,

$$\widetilde{\mathbf{V}}^0 = \mathbf{0} \qquad \forall (\mathbf{r} \in s_p), \tag{2.2-5}$$

and the requirement that $\widetilde{\mathbf{V}}^0$ and $\widetilde{\boldsymbol{\Pi}}^0$ be spatially periodic functions in a unit cell. Note that Equations (2.2-3)–(2.2-5) are functions only of the geometry of a unit cell.

The permeability is then defined as

$$\mathbf{k} \stackrel{\text{def}}{=} -\frac{1}{\tau_0} \int_{\tau_f} \widetilde{\mathbf{V}}^0 \, \mathrm{d}V, \tag{2.2-6}$$

where τ_0 is the volume of a unit cell, and $\mathrm{d}V$ is a differential volume element.

2.2.2 Suspension Rheology

Similar to the simple derivation of Darcy's equation shown previously, one may perform a similar analysis for a spatially periodic suspension. (See Adler and coworkers [3, 4], Zuzovsky *et al.* [125] and Nunan & Keller [83].) Subjecting a spatially periodic suspension to a macroscopic, homogeneous shear flow results in equations for the (configuration-specific) suspension viscosity which are only a function of the suspension geometry within a unit cell. Felderhof [52, 53, 54, 55] presents a theoretical derivation of the suspension viscosity of a random suspension.

Extensive reviews are provided by Brenner [20, 21, 22, 23], Adler *et al.* [5] and Jeffrey & Acrivos [66]. Recent calculations have been performed involving hard sphere (Clercx & Schram [43]), liquid/liquid (Miloh & Benveniste [77]), and liquid/vapor (Boshenyatov & Chernyshev [19] and Iguchi & Morita [65]) suspensions. Moreover, effects arising from aggregation/disaggregation (Potanin & Uriev [89]) and magnetofluids (Shen & Doi [101]) have also been studied.

2.2.3 Permeability

The permeability of porous media has been extensively calculated for various geometries. In general, results for the permeability of media composed of spheres are expressed in terms of the force acting on a single sphere in the array, namely

$$F = 6\pi\mu a U K, \tag{2.2-7}$$

where K is related to the permeability via the expression

$$\frac{k}{a^2} = \frac{2}{9\phi} K^{-1}. \tag{2.2-8}$$

Equations (2.2-7) and (2.2-8) apply for isotropic arrays of spheres. This is the case for most of the literature cited, the latter being concerned either with random arrays or square, spatially periodic arrays of spheres. The sole contribution addressing anisotropic permeabilities is that by Larson & Higdon [72], who computed the various permeability components of an array of ellipsoidal cylinders.

Results for spatially periodic cubic arrays of spheres were obtained initially by Hasimoto [60], and later by Zick & Homsy [124] and Sangani & Acrivos [95], who obtained

$$K^{-1} = 1 - 1.7601\phi^{\frac{1}{3}} + \phi - 1.5593\phi^2 + \ldots \qquad \text{(simple)}, \tag{2.2-9}$$

$$= 1 - 1.791\phi^{\frac{1}{3}} + \phi - 0.329\phi^2 + \ldots \qquad \text{(body-centered)}, \tag{2.2-10}$$

$$= 1 - 1.791\phi^{\frac{1}{3}} + \phi - 0.302\phi^2 + \ldots \qquad \text{(face-centered)}. \tag{2.2-11}$$

These expansions are valid for small concentrations. Comparable results [95] to $O(\phi^{10})$ exist. Additionally, Sangani & Acrivos [95] provide a direct substitution method, valid for all ϕ.

On the other hand, random arrays of spheres have been studied by Brinkman [30], Lundgren [73], Childress [42], Howells [63] and Buyevich & Shchelchkova [32], all of whom obtained

$$K^{-1} = \frac{\mu}{\overline{\mu}^*} \left\{ 1 + \frac{3}{4} \left[\phi - \left(8\phi - 3\phi^2 \right)^{\frac{1}{2}} \right] \right\}. \tag{2.2-12}$$

The central issue here is that one must have an expression for $\overline{\mu}^*/\mu$ as a function of ϕ. Accordingly, the goal becomes that of calculating both k and $\overline{\mu}^*$ *concurrently.*

Another common geometry studied is that of circular cylinders arrayed in a square lattice. Such two-dimensional arrays have been studied by Hasimoto [60] and Sangani

& Acrivos [94], who obtained

$$\frac{4\pi\mu U}{F'} = -\frac{1}{2}\ln\phi - 0.738 + \phi - 0.887\phi^2 + \ldots, \tag{2.2-13}$$

valid for small ϕ, with F' the drag per unit length of a cylinder in the array. Random arrays of cylinders were treated numerically by Sangani & Yao [97].

2.2.4 Brinkman Viscosity

Whereas general agreement exists regarding the *permeability* of a porous medium for a given geometry, the same cannot be said of the Brinkman viscosity. Experimental work on the latter subject is scarce, and the only experimental work performed to date to determine the Brinkman viscosity is that of Beavers and coworkers [15, 16] and more recently Givler & Altobelli [58]. Additionally, most theoretical evaluations of $\overline{\mu}^*$ have been directed at random arrays of spheres, with only a few contributions existing for other geometries.

Random Arrays of Spheres

Methods for calculating the Brinkman viscosity are based on a self-consistent field approach, in which each particle is regarded as being immersed in a fictitious medium.

i) (1970) Ooms *et al.* [84] used a previously developed averaging procedure, obtaining

$$\frac{\overline{\mu}^*}{\mu} = \frac{1}{1-\phi}, \tag{2.2-14}$$

or upon expansion about $\phi = 0$,

$$\frac{\overline{\mu}^*}{\mu} \simeq 1 + \phi + \phi^2 + O\left(\phi^3\right), \tag{2.2-15}$$

valid for low particle concentrations. This result was also obtained by Lundgren [73].

ii) (1972) Lundgren [73] extended statistical methods previously developed by Tam [107] and Saffman [93], to obtain

$$\frac{\overline{\mu}^*}{\mu} = \frac{4\pi}{3}\frac{\gamma}{\phi F(\gamma)}, \tag{2.2-16}$$

where

$$\begin{aligned} F(\gamma) &= -2\pi\sum_{j=1}^{\infty}(-1)^j(2j+1)^2 G_j(\gamma)^2 \\ &\quad -8\pi\sum_{j=1}^{\infty}(-1)^j(j+1)\left(\gamma G_j(\gamma)G_{j+1}(\gamma) + \frac{G_j(\gamma)}{\gamma H_j(\gamma)}\right) \\ &\quad +6\pi(1+\gamma)\left(\frac{\sinh\gamma}{\gamma}\right)^2, \end{aligned} \tag{2.2-17}$$

$$G_j(\gamma) = \left(\frac{\pi}{2\gamma}\right)^{\frac{1}{2}} I_{j+\frac{1}{2}}(\gamma), \qquad H_j(\gamma) = -\left(\frac{2}{\pi\gamma}\right)^{\frac{1}{2}} K_{j+\frac{1}{2}}(\gamma), \tag{2.2-18}$$

wherein I and K are respectively modified Bessel functions of the first and second kinds, and

$$\gamma \stackrel{\text{def}}{=} \frac{a}{\sqrt{k}}\left(\frac{\mu}{\overline{\mu}^*}\right)^{\frac{1}{2}} = \frac{\frac{9}{4}\phi + \frac{3}{4}(8\phi - 3\phi^2)^{\frac{1}{2}}}{1 - \frac{3}{2}\phi}, \tag{2.2-19}$$

with a the sphere radius. Lundgren [73] remarks that this expression may be valid only for small ϕ, as mutual impenetrability of the particles was neglected in the analysis. Note also the singular behavior at $\phi = 2/3$.

iii) (1978) Buyevich & Shchelchkova [32], using methods similar to Lundgren, obtained[1]

$$\frac{\overline{\mu}^*}{\mu} = \left[1 + \frac{9}{2}\frac{\phi}{\gamma^2}\left(e^\gamma - 1 - \gamma - \frac{1}{3}\gamma^2\right) - \frac{5}{2}\frac{\phi e^\gamma}{1+\gamma}\right]^{-1}, \tag{2.2-20}$$

[1]The last term in their [32] equation (5.35) appears to contain a typographical error, and should be multiplied by ϕ (ρ in that paper).

with γ given by (2.2-19). The expansion of (2.2-20) for small ϕ is

$$\frac{\overline{\mu}^*}{\mu} \simeq 1 + \frac{7}{4}\phi - \frac{9}{4\sqrt{2}}\phi^{\frac{3}{2}} + \frac{197}{32}\phi^2 + O\left(\phi^{\frac{5}{2}}\right). \tag{2.2-21}$$

Although Buyevich & Shchelchkova [32] include a term which they claim was overlooked by Lundgren, their Brinkman viscosity calculation now possesses a singularity at $\phi = 1/4$. Once again, this analysis neglects the mutual impenetrability of the particles.

iv) (1978) Freed & Muthukumar [57] use an effective medium approach to obtain[2]

$$\frac{\overline{\mu}^*}{\mu} = \frac{1 - 3\phi + \frac{9}{4}\phi^2}{1 - \frac{11}{2}\phi + \frac{363}{40}\phi^2 - \frac{549}{40}\phi^3 + \left(\frac{9}{8}\phi - \frac{189}{40}\phi^2\right)(8\phi - 3\phi^2)^{\frac{1}{2}}}, \tag{2.2-22}$$

or, for small ϕ,

$$\frac{\overline{\mu}^*}{\mu} \simeq 1 + \frac{5}{2}\phi - \frac{9}{2\sqrt{2}}\phi^{\frac{3}{2}} + \frac{277}{40}\phi^2 + O\left(\phi^{\frac{5}{2}}\right). \tag{2.2-23}$$

Here too, the effective viscosity becomes singular as $\phi \to 1/4$.

v) (1983) Koplik *et. al.* [70], arguing that the porous medium induces a viscosity renormalization, obtain two results for the Brinkman viscosity. By computing the energy dissipation caused by a sphere in an extensional flow field in a porous medium, they obtain

$$\frac{\overline{\mu}^*}{\mu} = 1 - \frac{1}{2}\phi, \tag{2.2-24}$$

whereas using a self-consistent method to determine both k and $\overline{\mu}^*$ simultaneously, they conclude that

$$\frac{\overline{\mu}^*}{\mu} \simeq 1 - \left(\frac{\phi}{10}\right)^{\frac{1}{3}} + \ldots. \tag{2.2-25}$$

[2]In their analysis [57], the penultimate term of Eq. (4.21) should be multiplied by a.

ϕ	Method A	Method B
0.1	1.30	1.30
0.2	1.76	1.79
0.3	2.56	2.69
0.4	3.50	4.88
0.5	5.96	13.5
0.6	9.20	42.3

Table 2.1: Values of $\overline{\mu}^*/\mu$ calculated by methods A and B [33,34].

In both (2.2-24) and (2.2-25) the effective viscosity is smaller than the interstitial fluid viscosity; from this fact, Koplik *et al.* drew the following conclusion:

> "... a reasonable *post hoc* explanation of our result is that once much of the force exerted by the porous medium is collected into the Darcy drag term, the remaining force exerted by the material due to gradients should be less than the same force exerted by pure fluid; in a sense, part of the Einstein contribution is already taken into account by the permeability term, a term absent in the case of suspensions."

vi) (1985) Kim & Russel [69] assumed pairwise-additive hydrodynamic interactions within an effective medium, obtaining

$$\frac{\overline{\mu}^*}{\mu} \simeq 1 + \frac{5}{2}\phi + \phi^2\left(\frac{81}{32}\log\phi + 21.041\right) + O\left(\phi^{\frac{5}{2}}\log\phi\right). \qquad (2.2\text{-}26)$$

vii) (1988) Chang & Acrivos [35, 36] use two methods, both based upon the application of (2.2-1) near the sphere. Method A is a self-consistent technique, whereas method B involves decomposing the velocity field around the sphere into a bulk flow and a disturbance. Results from both methods are presented in Table 2.1.

viii) (1989) Slobodov [104], using methods developed previously by Lundgren [73] and Tam [107], obtains

$$\frac{\overline{\mu}^*}{\mu} = \frac{75}{8}\left[\frac{\left\{\left(\frac{8}{9\phi}-\frac{1}{3}\right)^{\frac{1}{2}}-1\right\}\phi}{1-\phi}\right]^2, \tag{2.2-27}$$

or

$$\frac{\overline{\mu}^*}{\mu} \simeq \frac{25}{3}\phi - \frac{25}{\sqrt{2}}\phi^{\frac{3}{2}} + \frac{275}{12}\phi^2 + O\left(\phi^{\frac{5}{2}}\right). \tag{2.2-28}$$

The wide disparities between different authors in the ϕ-dependence of $\overline{\mu}^*/\mu$ is emphasized in Figure 2-1. It is evident that very little agreement exists between authors, even for very small ϕ. Indeed, it is unclear whether $\overline{\mu}^*$ should be larger or smaller than μ. Most theories predict $\overline{\mu}^* > \mu$, but experimental work [15, 16] and numerical computations [30, 96, 97] suggest that $\overline{\mu}^* < \mu$. Furthermore, since the permeability predicted for random media [30, 32, 42, 63, 73] is dependent on the value of $\overline{\mu}^*$ [cf. (2.2-12)], all these analyses yield different results for $\overline{\mu}^*$, despite the fact that they furnish the same equation for k, namely (2.2-12).

Other Geometries

Analyses of other geometries include random arrays of spheres with a given size distribution (Tam [107]), channels with periodic cross-bridging fibers (Tsay & Weinbaum [112]), and periodic arrays of circular (and ellipsoidal) cylinders (Larson & Higdon [72]).

Larson & Higdon [72] obtain numerical results for both the permeability and Brinkman viscosity. They also experimented with changing the aspect ratio of the cylinders, so that in one limiting case flow occurred across flat plates normal to the boundary, and in another flow occured across flat plates parallel to the interface. Suprisingly, they concluded that although the permeability was anisotropic, Brinkman's equation could not distinguish between the two types of flow (because of the scalar viscosity). They suggested that one should perhaps include terms propor-

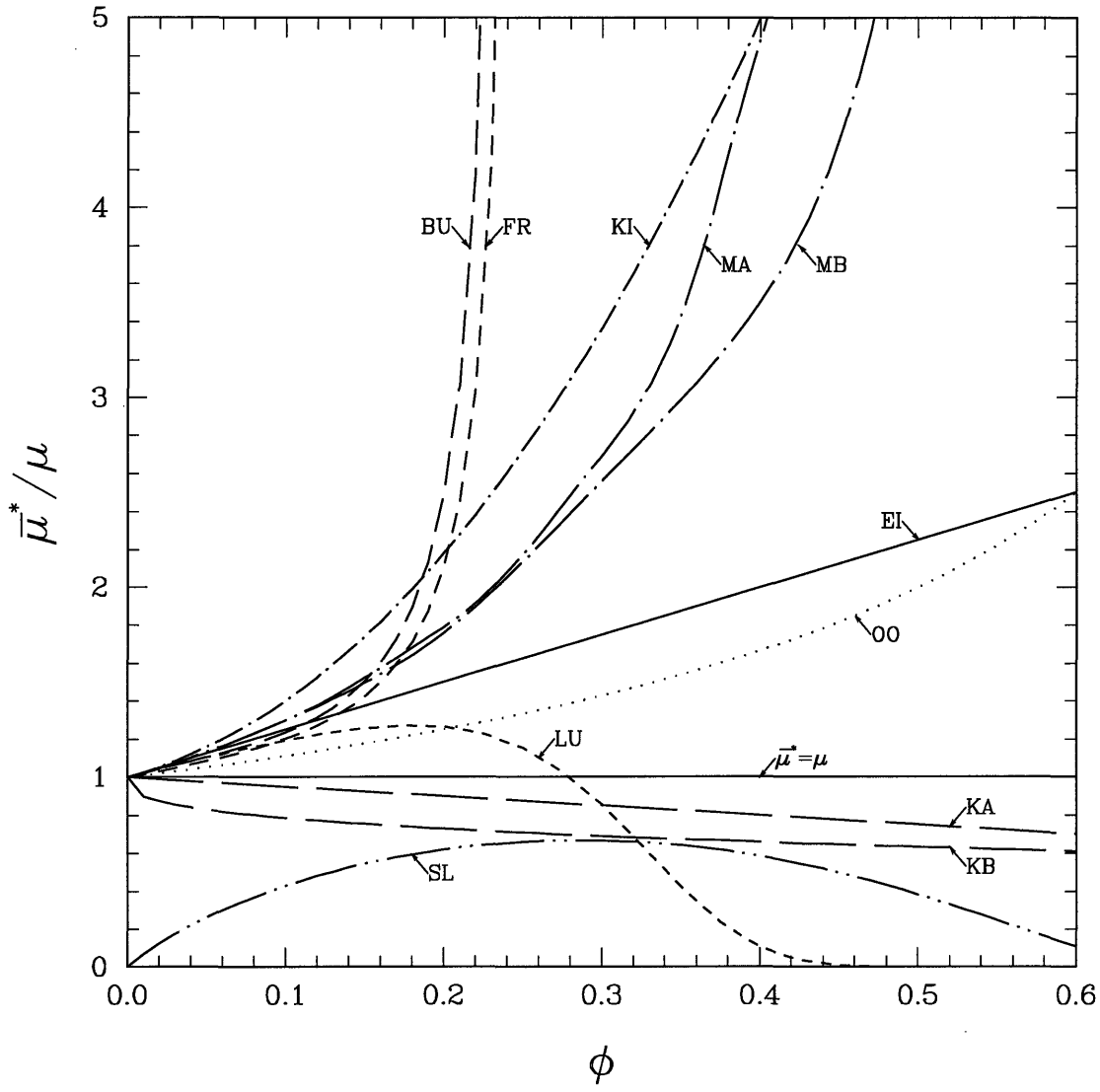

Figure 2-1: Theoretical predictions of the Brinkman viscosity of a random array of uniform size spheres. EI–Einstein; OO–Ooms *et al.*; LU–Lundgren; BU–Buyevich & Shchelchkova; FR–Freed & Muthukumar; KA,KB–Koplik *et al.*; KI–Kim & Russel; MA,MB–Chang & Acrivos (Methods A and B); SL–Slobodov.

tional to the velocity gradient in (1.1-6). It seems obvious that this type of media should not only exhibit an anisotropic, *tensorial* permeability, but also a *tensorial* Brinkman viscosity.

2.3 Applications of the Darcy-Brinkman Equation

The Brinkman equation finds application in many different fields. Initially, Brinkman was interested in modelling clusters of polymer molecules as porous spheres [29]. In a related context, polymers adsorbed to solid surfaces have been treated as a porous medium layer by Varoqui & Dejardin [115] and Anderson & Kim [7]. Flow in membranes with grafted polyelectrolyte brushes have been studied by Milner [76] and Misray & Varanasi [78]. In these applications to polymer systems, all authors supposed that $\overline{\mu}^* = \mu$.

The problem of flow in catalyst systems, where one encounters a porous medium composed of porous particles, each with a different permeability, was first treated by Brinkman [31]. Flow around a cylinder embedded in a porous medium (Pop & Cheng [88]) and flow relative to porous spheres (Neal *et al.* [80]) have also been studied, where the choice $\overline{\mu}^* = \mu$ was again made since it was "... in keeping with established practice."

Other flow systems studied via the Brinkman equation are: (i) flow of two immiscible fluids over a porous medium (Bhargava & Nirmal [18]); (ii) flow in a partially gel-filled channel, such as occurs in partially obstructed membranes and certain body tissues (Ethier & Kamm [51]); (iii) flow in a porous tube and shell system (Pangrle *et. al.* [85]); (iv) transport of solid spherical macromolecules in ordered and disordered media (Phillips *et al.* [86, 87]); (v) prediction of pressure drop and filtration efficiency in fibrous media (Spielman & Goren [105]); (vi) and instabilities of ferrofluids in porous media (Vaidyanathan *et al.* [114]). Here too, all these analyses are based on the assumption that $\overline{\mu}^* = \mu$.

Natural convection and the onset of instabilities in a fluid saturated porous medium have been studied for different geometries, most notably: (i) a medium bounded above and below by horizontal flat plates (Katto & Masuaka [68], Walker & Homsy [119], Chang & Jang [37]); (ii) a medium adjacent to a vertical flat plate (Cheng & Minkowycz [41], Hsu & Cheng [64]); (iii) a medium in a vertical enclosure

(Tong & Subramanian [111], Vasseur and coworkers [116, 117]); (iv) and a medium in an inclined slot (Vasseur *et al.* [118]). Chang & Jang [37] include not only the Darcy drag term (proportional to $\overline{\mathbf{v}}$) and a viscous Brinkman term (proportional to $\overline{\nabla}^2\overline{\mathbf{v}}$), but also contributions from convective terms (proportional to $\overline{\mathbf{v}} \cdot \overline{\nabla}\overline{\mathbf{v}}$) and inertial terms (proportional to $\overline{\mathbf{v}}|\overline{\mathbf{v}}|$) (Forchheimer [56] or Ergun [50]). They find *inter alia* that the greatest contribution to the heat flux arises from the viscous terms. This significant contribution was also noted by several other authors [64, 111, 116]. This suggests that the results would be highly dependent upon the choice of $\overline{\mu}^*$; yet all the above authors arbitrarily choose $\overline{\mu}^* = \mu$.

Other thermal systems studied that incorporate a Brinkman term include: (i) forced convection (Wooding [123], Cheng *et al.* [40], Nakayama *et al.* [79]); (ii) mixed convection (Hayes [61], Qin & Kaloni [90]); (iii) heat transfer in geothermal systems (Cheng [39]); (iv) freezing heat transfer in porous media (Sasaki *et al.* [98]); (v) and film condensation in porous media (Majumdar & Tien [74]). Once again, all of these studies assume that $\overline{\mu}^* = \mu$.

The sole application embodying the inequality $\overline{\mu}^* \neq \mu$ was an elementary stydy study by Berkowitz [17], involving the flow of fluid through a fracture bounded by a porous medium. He showed that the net flow rate through the fracture was very susceptible to the choice of $\overline{\mu}^*$.

One argument for using $\overline{\mu}^* = \mu$ results from the observation that in dilute systems, $\overline{\mu}^* \to \mu$, whereas in nondilute systems the decreasing permeability renders the Darcy term very much more significant than the Brinkman term. This argument is, however, incorrect for some of the systems listed previously. Another reason for the choice of $\overline{\mu}^* = \mu$ is simply that as of now, no rational way exists to determine $\overline{\mu}^*$ for a given medium geometry. Furthermore, those results already obtained are in wide disagreement (see Figure 2-1 on page 40).

Chapter 3

Generalized Taylor Series Expansion

3.1 Introduction

In general, it will be useful to expand any scalar or tensor field—itself functionally dependent upon an M-dimensional position vector—in a Taylor series about an arbitrary reference point such that there is a separation between the continuous local position vector and the discrete global position vector. This will be done by first examining a scalar function—dependent upon a one-dimensional position vector—subsequently building up to a more general expansion.

3.2 1-Dimensional Position Vector

Here we address scalar and tensor fields dependent upon but a single independent scalar position variable, X $(-\infty < X < \infty)$, say; that is, the fields depend functionally upon only one spatial dimension.

3.2.1 Scalar Fields: Continuous Derivative

Consider an arbitrary scalar function $f(X)$ of X. When $f(X)$ and all its derivatives $\mathrm{d}^m f(X)/\mathrm{d}X^m$ are finite at all positions X the function may be expressed in a convergent Taylor series about an arbitrary point X' (Figure 3-1a) as

$$f(X) = \sum_{m=0}^{\infty} \frac{1}{m!} \overline{f}^m(|X') \{X - X'\}^m , \tag{3.2-1}$$

where the functions $\overline{f}^m(|X')$ are defined as

$$\overline{f}^m(|X') \stackrel{\text{def}}{=} \left. \frac{\mathrm{d}^m f(X)}{\mathrm{d}X^m} \right|_{X=X'} . \tag{3.2-2}$$

As indicated by the arguments, the latter coefficients depend upon the position chosen for X' despite the fact that X' does not appear on the left-hand side of (3.2-1).

Examples of simple functions (having continuous derivatives at all points) are:

Exponential:

$$f(X) = \exp(X) \implies \overline{f}^m(|X') = \exp(X');$$

Trigonometric:

$$f(X) = \sin(X) \implies \overline{f}^m(|X') = \begin{cases} (-1)^{\frac{m}{2}} \sin(X') & m \text{ even}, \\ (-1)^{\frac{m-1}{2}} \cos(X') & m \text{ odd}; \end{cases}$$

Polynomial:

$$f(X) = \sum_{k=0}^{\infty} \frac{1}{k!} a_k X^k \implies \overline{f}^m(|X') = \sum_{k=0}^{\infty} \frac{1}{k!} a_{k+m} X'^k .$$

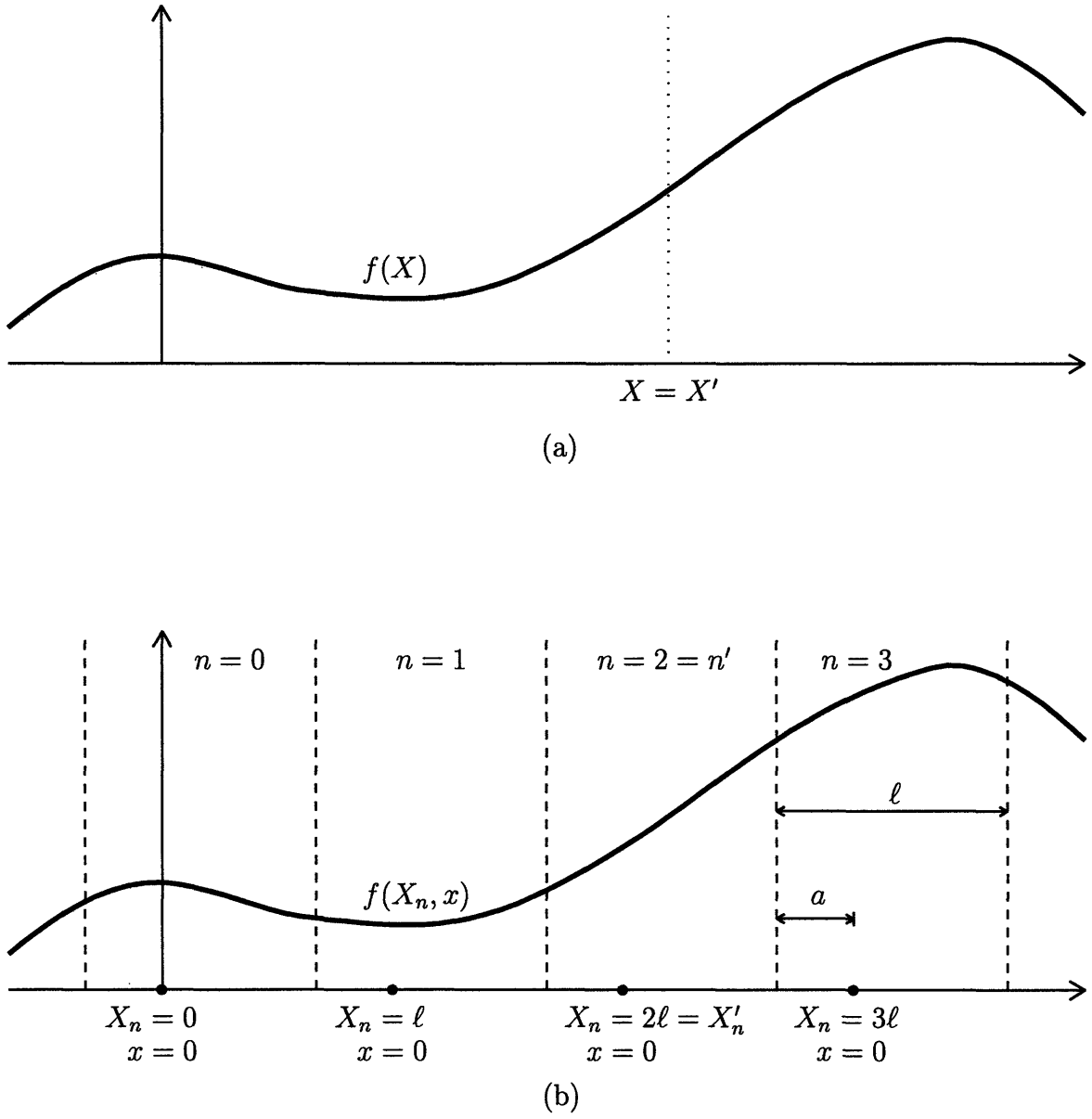

Figure 3-1: The arbitrary one dimensional scalar function $f(X)$ may be represented as: (a) a function of the continuous position variable X $(-\infty < X < \infty)$ and expanded in a Taylor series about the point $X = X'$; or (b) a function of the continuous local position x $(-a \leq x \leq \ell - a)$ and discrete global position $X_n = n\ell$ $(n = 0, \pm 1, \pm 2, \ldots)$ which in turn may be expanded in a Taylor series about the same point $X_n + x = X'$.

The latter are valid for all $m = 0, 1, 2, \ldots$.

3.2.2 Scalar Fields: Discrete Formulation

As shown in Figure 3-1b, the position variable X can be alternatively expressed as the sum of a continuous local position x and a discrete global position X_n as

$$X \stackrel{\text{def}}{=} X_n + x, \tag{3.2-3}$$

where x spans the range

$$-a \leq x \leq \ell - a, \tag{3.2-4}$$

and

$$X_n = n\ell \qquad \forall\, (n = 0, \pm 1, \pm 2, \ldots)\,. \tag{3.2-5}$$

The origin from which the local coordinate x is measured is chosen such that $x = 0$ corresponds to $X = X_n$.

In view of the above decomposition an arbitrary function $f(X)$ possesses the equivalent representation

$$f(X) \equiv f(X_n, x). \tag{3.2-6}$$

Now introduce into the Taylor series (3.2-1) the decomposition (3.2-3) to write

$$f(X_n, x) = \sum_{m=0}^{\infty} \frac{1}{m!} \overline{f}^m(|X')\,\{X_n + x - X'\}^m\,. \tag{3.2-7}$$

This equation may be rearranged into groups characterized by like powers of $X_n - X'$. This can be done via the identity

$$(a+b)^m \stackrel{\text{def}}{=} \sum_{j=0}^{m} \left(\begin{array}{c} m \\ j \end{array} \right) a^{m-j} b^j, \tag{3.2-8}$$

valid for any two scalars a and b with the binomial coefficients defined as

$$\begin{pmatrix} m \\ j \end{pmatrix} \stackrel{\text{def}}{=} \frac{m!}{(m-j)!j!}. \tag{3.2-9}$$

This enables (3.2-7) to be written as

$$f(X_n, x) = \sum_{m=0}^{\infty} \sum_{j=0}^{m} \frac{1}{m!} \begin{pmatrix} m \\ j \end{pmatrix} \overline{f}^m(|X')\, x^{m-j} \{X_n - X'\}^j . \tag{3.2-10}$$

The order of the double summation may be interchanged by the identity

$$\sum_{m=0}^{\infty} \sum_{j=0}^{m} A_{mj} = \sum_{j=0}^{\infty} \sum_{m=j}^{\infty} A_{mj}, \tag{3.2-11}$$

with A_{mj} the (m, j)th argument of the summation. Hence, upon reordering the inner summation, (3.2-10) becomes

$$f(X_n, x) = \sum_{j=0}^{\infty} \frac{1}{j!} \left[\sum_{m=0}^{\infty} \frac{1}{m!} \overline{f}^{j+m}(|X')\, x^m \right] \{X_n - X'\}^j . \tag{3.2-12}$$

This can be ultimately written as

$$f(X_n, x) = \sum_{m=0}^{\infty} \frac{1}{m!} f^m(x|X') \{X_n - X'\}^m \tag{3.2-13}$$

where the coefficents

$$f^m(x|X') \stackrel{\text{def}}{=} \sum_{j=0}^{\infty} \frac{1}{j!} \overline{f}^{m+j}(|X')\, x^j \tag{3.2-14}$$

are in general functions of the local position x as well as the choice of reference point X'. For the sample test functions given previously, this expansion gives:

Exponential:

$$f(X) = \exp(X) \implies f^m(x|X') = \exp(X' + x);$$

Trigonometric:

$$f(X) = \sin(X) \implies f^m(x|X') = \begin{cases} (-1)^{\frac{m}{2}} \sin(X'+x) & m \text{ even}, \\ (-1)^{\frac{m-1}{2}} \cos(X'+x) & m \text{ odd}; \end{cases}$$

Polynomial:

$$f(X) = \sum_{k=0}^{\infty} \frac{1}{k!} a_k X^k \implies f^m(x|X') = \sum_{k=0}^{\infty} \frac{1}{k!} a_{k+m} \{X'+x\}^k .$$

3.2.3 Scalar Fields: Continuity Conditions Imposed Upon $f^m(x|X')$

Because of the assumed continuity of $f(X)$, conditions pertaining to the continuity of $f^m(x|X')$ at points on the 'interface' between adjacent 'cells' may be derived. A point common to cells $n-1$ and n is $(X_{n-1}, \ell - a) \equiv (X_n, -a)$. Basically, at a point corresponding to an interface $(r = -a)$, we have that

$$f(X_n - \ell, x)\big|_{x=\ell-a} = f(X_n, x)\big|_{x=-a} , \tag{3.2-15}$$

wherein the left- and right-hand sides respectively refer to approaching the interface from the left and right. Substituting into the latter the explicit form of the Taylor series (3.2-13) yields

$$\sum_{m=0}^{\infty} \frac{1}{m!} f^m(-a|X') \{X_n - X'\}^m = \sum_{m=0}^{\infty} \frac{1}{m!} f^m(\ell - a|X') \{X_n - X' - \ell\}^m , \tag{3.2-16}$$

in which a common reference point X' has been used for both sides of (3.2-15). Next, regroup this equation into terms involving like powers of $X_n - X'$ by using (3.2-8) and (3.2-11) to rewrite (3.2-16) as

$$\begin{aligned} &\sum_{m=0}^{\infty} \frac{1}{m!} f^m(-a|X') \{X_n - X'\}^m \\ &= \sum_{m=0}^{\infty} \frac{1}{m!} \left[\sum_{j=0}^{\infty} \frac{1}{j!} f^{m+j}(\ell - a|X') \{-\ell\}^j \right] \{X_n - X'\}^m . \end{aligned} \tag{3.2-17}$$

Since both the current cell X_n of interest and the reference point X' are arbitrary, one may match all powers of $X_n - X'$ to obtain

$$f^m(-a|X') = \sum_{j=0}^{\infty} \frac{1}{j!} f^{m+j}(\ell - a|X') \{-\ell\}^j . \tag{3.2-18}$$

This expresses the value of f^m occuring on the left-hand boundary $x = -a$ of the cell in terms of the values of $f^m, f^{m+1}, f^{m+2}, \ldots$ occuring on the right-hand boundary $x = \ell - a$ of the cell. Now, define the jump in any function $F(x)$ as the difference between the value of the function at the right- and left-hand sides of the cell; explicitly,

$$\|F(x)\| \stackrel{\text{def}}{=} F(x)\big|_{x=\ell-a} - F(x)\big|_{x=-a} \tag{3.2-19}$$

such that (3.2-18) may be alternatively expressed as

$$\|f^m\| = \frac{\ell}{1!} f^{m+1}\Big|_{x=\ell-a} - \frac{\ell^2}{2!} f^{m+2}\Big|_{x=\ell-a} + \frac{\ell^3}{3!} f^{m+3}\Big|_{x=\ell-a} - \cdots \tag{3.2-20}$$

wherein the arguments $(x|X')$ have been suppressed. The ℓ appearing in the first term on the right hand side of (3.2-20) can be rewritten as $\ell = (\ell - a) + a$ giving the intermediate result

$$\begin{aligned} \|f^m\| \;=\; & \frac{\ell - a}{1!} f^{m+1}\Big|_{x=\ell-a} + \frac{a}{1!} f^{m+1}\Big|_{x=\ell-a} \\ & - \frac{\ell^2}{2!} f^{m+2}\Big|_{x=\ell-a} + \frac{\ell^3}{3!} f^{m+3}\Big|_{x=\ell-a} - \cdots . \end{aligned} \tag{3.2-21}$$

Next, replace m by $m + 1$ in (3.2-20) and substitute the result into the second term appearing on the right-hand side of (3.2-21) to obtain

$$\begin{aligned} \|f^m\| \;=\; & \frac{\ell - a}{1!} f^{m+1}\Big|_{x=\ell-a} + \frac{a}{1!} f^{m+1}\Big|_{x=-a} \\ & - \left(\frac{\ell^2}{2!} - \frac{\ell a}{1!}\right) f^{m+2}\Big|_{x=\ell-a} + \left(\frac{\ell^3}{3!} - \frac{\ell^2 a}{2!}\right) f^{m+3}\Big|_{x=\ell-a} - \cdots . \end{aligned} \tag{3.2-22}$$

But the first and second terms on the right-hand side of (3.2-22) correspond identically to the jump in the function $f^{m+1}x$ or

$$\begin{aligned} \|f^m\| &= \frac{1}{1!}\left\|f^{m+1}x\right\| \\ &\quad - \left(\frac{\ell^2}{2!} - \frac{\ell a}{1!}\right) f^{m+2}\Big|_{x=\ell-a} + \left(\frac{\ell^3}{3!} - \frac{\ell^2 a}{2!}\right) f^{m+3}\Big|_{x=\ell-a} - \cdots . \end{aligned} \tag{3.2-23}$$

This process of recursive substitution may be continued, eventually enabling (3.2-20) to be written in the form

$$\|f^m\| = \frac{1}{1!}\left\|f^{m+1}x\right\| - \frac{1}{2!}\left\|f^{m+2}x^2\right\| + \frac{1}{3!}\left\|f^{m+3}x^3\right\| - \cdots . \tag{3.2-24}$$

From (3.2-18) this furnishes the ultimate form

$$\|f^m(x|X')\| = -\sum_{j=1}^{\infty} \frac{(-1)^j}{j!}\left\|f^{m+j}(x|X')x^j\right\|, \tag{3.2-25}$$

expressing the jump in f^m in terms of the jumps in $f^{m+1}x, f^{m+2}x^2, \ldots$ and explicitly displaying the dependence of $f^m(x|X')$ upon both x and X'.

Finally, because $f(X)$ and all its derivatives have been assumed continuous and finite for all X, the expression (3.2-15) remains valid for any derivatives of $f(X_n, x)$ with respect to x when approached from either side. A similar procedure to that outlined previously then gives the general relation

$$\left\|\frac{\mathrm{d}^i f^m(x|X')}{\mathrm{d}x^i}\right\| = -\sum_{j=1}^{\infty} \frac{(-1)^j}{j!}\left\|\left[\frac{\mathrm{d}^i f^{m+j}(x|X')}{\mathrm{d}x^i}\right]x^j\right\| \tag{3.2-26}$$

$$= -\sum_{j=1}^{\infty} \frac{(-1)^j}{j!}\left\|\frac{\mathrm{d}^i}{\mathrm{d}x^i}\left[f^{m+j}(x|X')x^j\right]\right\| \tag{3.2-27}$$

valid for $m = 0, 1, 2, \ldots$ and $i = 0, 1, 2, \ldots$.

3.2.4 Tensor Fields

It is easy to extend the preceding results for a one-dimensional scalar field $f(X)$ to an Nth rank tensor field $\mathbf{f}(X)$ since the position vector is still one-dimensional. Thereby, (3.2-1) is replaced by

$$\mathbf{f}(X) = \sum_{m=0}^{\infty} \frac{1}{m!} \overline{\mathbf{f}}^m(|X') \{X - X'\}^n, \tag{3.2-28}$$

where

$$\overline{\mathbf{f}}^m(|X') \stackrel{\text{def}}{=} \left. \frac{\mathrm{d}^m \mathbf{f}(X)}{\mathrm{d}X^m} \right|_{X=X'}. \tag{3.2-29}$$

In terms of the decomposition of X into X_n and x, the Taylor series becomes

$$\mathbf{f}(X_n, x) = \sum_{m=0}^{\infty} \frac{1}{m!} \mathbf{f}^m(x|X') \{X_n - X'\}^m, \tag{3.2-30}$$

wherein

$$\mathbf{f}^m(x|X') \stackrel{\text{def}}{=} \sum_{j=0}^{\infty} \frac{1}{j!} \overline{\mathbf{f}}^{m+j}(|X')\, x^j. \tag{3.2-31}$$

Finally, the continuity of $\mathbf{f}(X)$ and its derivatives across cell faces results in (3.2-26) and (3.2-27) adopting the respective forms

$$\left\| \frac{\mathrm{d}^i \mathbf{f}^m(x|X')}{\mathrm{d}x^i} \right\| = -\sum_{j=1}^{\infty} \frac{(-1)^j}{j!} \left\| \left[\frac{\mathrm{d}^i \mathbf{f}^{m+j}(x|X')}{\mathrm{d}x^i} \right] x^j \right\| \tag{3.2-32}$$

$$= -\sum_{j=1}^{\infty} \frac{(-1)^j}{j!} \left\| \frac{\mathrm{d}^i}{\mathrm{d}x^i} \left[\mathbf{f}^{m+j}(x|X') x^j \right] \right\|. \tag{3.2-33}$$

3.3 M-Dimensional Position Vector

Next, we consider scalar and tensor fields dependent upon M independent scalar position variables $(X_1, X_2, \ldots, X_M)$ characterized by the position vector

$$\mathbf{R} \equiv \mathbf{R}(X_1, X_2, \ldots, X_M). \tag{3.3-1}$$

[These independent position variables are not to be confused with the one-dimensional discrete position vector X_n. The M-dimensional counterpart to X_n, namely $\mathbf{R_n}$, will be developed later.]

3.3.1 Scalar Fields: Continuous

Consider a Taylor series expansion of a scalar function $f(\mathbf{R})$ where our attention is restricted to the class of function in which $f(\mathbf{R})$ and all of its derivatives

$$\mathrm{d}^m f(\mathbf{R})/\mathrm{d}\mathbf{R}^m \equiv \boldsymbol{\nabla}^m f(\mathbf{R}), \tag{3.3-2}$$

are finite at all positions $\mathbf{R}$, wherein the gradient operator is defined as

$$\boldsymbol{\nabla} \stackrel{\text{def}}{=} \frac{\partial}{\partial \mathbf{R}}, \tag{3.3-3}$$

and the notation $\mathbf{a}^m$ (or $\boldsymbol{\nabla}^m$) for any vector $\mathbf{a}$ represents the mth rank tensor $\mathbf{aa}\ldots\mathbf{a}$, where $\mathbf{a}$ is repeated m times. The function $f(\mathbf{R})$ may then be expanded in a convergent Taylor series about an arbitrary point $\mathbf{R}'$ as

$$f(\mathbf{R}) = \sum_{m=0}^{\infty} \frac{1}{m!} \overline{\mathbf{f}}^m(|\mathbf{R}'|) \{\cdot\}^m \{\mathbf{R} - \mathbf{R}'\}^m \tag{3.3-4}$$

$$= \overline{f}^0(|\mathbf{R}'|) + \overline{\mathbf{f}}^1(|\mathbf{R}'|) \cdot \{\mathbf{R} - \mathbf{R}'\} + \frac{1}{2!}\overline{\mathbf{f}}^2(|\mathbf{R}'|) : \{\mathbf{R} - \mathbf{R}'\}^2 + \frac{1}{3!}\overline{\mathbf{f}}^3(|\mathbf{R}'|) \vdots \{\mathbf{R} - \mathbf{R}'\}^3 + \cdots. \tag{3.3-5}$$

The multiple-dot notation $\{\cdot\}^m$ appearing as the operator in the expression $\mathbf{A}\{\cdot\}^m\mathbf{B}$, involving any two tensors $\mathbf{A}$ and $\mathbf{B}$ (each of rank greater than m), represents the contraction between the last m indices of $\mathbf{A} \equiv A_{a_1a_2\ldots a_p}$ $(p \geq m)$ and the first m indices of $\mathbf{B} \equiv B_{b_1b_2\ldots b_q}$ $(q \geq m)$ in the order specified by the 'nesting convention' [38, 75]. This operation can be expressed in summation convention notation as

$$\left[\mathbf{A}\{\cdot\}^0\mathbf{B}\right]_{a_1a_2\ldots a_pb_1b_2\ldots b_q} \equiv A_{a_1a_2\ldots a_p}B_{b_1b_2\ldots b_q},$$

$$\left[\mathbf{A}\{\cdot\}^1\mathbf{B}\right]_{a_1a_2\ldots a_{p-1}b_2b_3\ldots b_q} \equiv A_{a_1a_2\ldots a_{p-1}c_1}B_{c_1b_2b_3\ldots b_q},$$

$$\left[\mathbf{A}\{\cdot\}^2\mathbf{B}\right]_{a_1a_2\ldots a_{p-2}b_3b_4\ldots b_q} \equiv A_{a_1a_2\ldots a_{p-2}c_2c_1}B_{c_1c_2b_3b_4\ldots b_q}$$

and, in general,

$$[\mathbf{A}\{\cdot\}^m\mathbf{B}]_{a_1a_2\ldots a_{p-m}b_{m+1}b_{m+2}\ldots b_q} \equiv A_{a_1a_2\ldots a_{p-m}c_m\ldots c_1}B_{c_1\ldots c_mb_{m+1}b_{m+2}\ldots b_q}. \tag{3.3-6}$$

In the Taylor series (3.3-4) the quantity $\overline{\mathbf{f}}^m(|\mathbf{R}')$ is simply the mth derivative of $f(\mathbf{R})$ with respect to $\mathbf{R}$, evaluated at the point $\mathbf{R}'$. As indicated by the argument, $\overline{\mathbf{f}}^m(|\mathbf{R}')$ depends upon the choice of reference position $\mathbf{R}'$ and is defined as

$$\overline{\mathbf{f}}^m(|\mathbf{R}') \stackrel{\text{def}}{=} [\boldsymbol{\nabla}^m f(\mathbf{R})]|_{\mathbf{R}=\mathbf{R}'} \tag{3.3-7}$$

or, alternatively,

$$\overline{f}^m_{i_1i_2\ldots i_m}(|\mathbf{R}') = [\nabla_{i_1}\nabla_{i_2}\ldots\nabla_{i_m}f(\mathbf{R})]|_{\mathbf{R}=\mathbf{R}'}. \tag{3.3-8}$$

From these definitions, it is obvious that $\overline{\mathbf{f}}^m(|\mathbf{R}')$ is symmetric with respect to all its m indices. Furthermore, $\overline{f}^0$, $\overline{\mathbf{f}}^1$ and $\overline{\mathbf{f}}^2$ respectively represent a scalar, vector and dyadic function.

For a simple function (possessing continuous derivatives at all points) the $\overline{\mathbf{f}}^m$'s are:

Exponential:

$$
\begin{aligned}
f(\mathbf{R}) = \exp(\mathbf{R}\cdot\mathbf{R}) \Longrightarrow \quad & \overline{f}^{0}(|\mathbf{R}') = \exp(\mathbf{R}'\cdot\mathbf{R}'), \\
& \overline{\mathbf{f}}^{1}(|\mathbf{R}') = 2\mathbf{R}'\exp(\mathbf{R}'\cdot\mathbf{R}'), \\
& \overline{\mathbf{f}}^{2}(|\mathbf{R}') = 2\left[\mathbf{I} + 2\mathbf{R}'\mathbf{R}'\right]\exp(\mathbf{R}'\cdot\mathbf{R}'), \\
& \overline{\mathbf{f}}^{3}(|\mathbf{R}') = 4\left[\mathbf{I}\mathbf{R}' + (\mathbf{I}\mathbf{R}')^{\dagger} + \mathbf{R}'\mathbf{I} + 2\mathbf{R}'\mathbf{R}'\mathbf{R}'\right]\exp(\mathbf{R}'\cdot\mathbf{R}').
\end{aligned}
$$

3.3.2 Scalar Fields: Discrete

Alternatively, as outlined in Appendix B, the continuous position vector $\mathbf{R}$ can be expressed as the sum of a discrete global position vector $\mathbf{R_n}$ and a continuous local position vector $\mathbf{r}$ [cf. (B.0-1)], namely

$$
\mathbf{R} = \mathbf{R_n} + \mathbf{r}, \tag{3.3-9}
$$

similar to the decomposition (3.2-3). An arbitrary function then has the equivalent expression

$$
f(\mathbf{R}) \equiv f(\mathbf{R_n}, \mathbf{r}). \tag{3.3-10}
$$

Introduce the decomposition (3.3-9) into the Taylor series (3.3-4) to write

$$
f(\mathbf{R_n}, \mathbf{r}) = \sum_{m=0}^{\infty} \frac{1}{m!}\overline{\mathbf{f}}^{m}(|\mathbf{R}')\{\cdot\}^{m}\{\mathbf{R} + \mathbf{r} - \mathbf{R}'\}^{m}. \tag{3.3-11}
$$

Collect like powers of $\mathbf{R_n} - \mathbf{R}'$ by making use of the following identity for any two vectors $\mathbf{a}$ and $\mathbf{b}$:

$$
(\mathbf{a} + \mathbf{b})^{m} \stackrel{\text{def}}{=} \sum_{j=0}^{m} \begin{pmatrix} m \\ j \end{pmatrix} \left[\!\!\left[\mathbf{a}^{m-j}\mathbf{b}^{j} \right]\!\!\right]^{s}. \tag{3.3-12}
$$

This is similar to its scalar counterpart (3.2-8), with the normalized permutation symmetrization operator $\left[\!\!\left[\mathbf{A} \right]\!\!\right]^{s}$ defined as [92]

$$
\left[\!\!\left[A_{i_1 i_2 \ldots i_{n-1} i_n} \right]\!\!\right]^{s} \stackrel{\text{def}}{=} \frac{1}{n!}\left(A_{i_1 i_2 \ldots i_{n-1} i_n} + A_{i_2 i_1 \ldots i_{n-1} i_n} + \cdots + A_{i_1 i_2 \ldots i_n i_{n-1}}\right). \tag{3.3-13}
$$

Equation (3.3-11) may then be rewritten as

$$f(\mathbf{R_n},\mathbf{r}) = \sum_{j=0}^{\infty} \frac{1}{j!} \left[\sum_{m=0}^{\infty} \frac{1}{m!} \overline{\mathbf{f}}^{j+m}(|\mathbf{R}') \{\cdot\}^m \mathbf{r}^m \right] \{\cdot\}^j \{\mathbf{R_n} - \mathbf{R}'\}^j \tag{3.3-14}$$

where the symmetry operator has been dropped because of the symmetry of the tensors $\overline{\mathbf{f}}^m(|\mathbf{R}')$. The previous equation may be ultimately written as

$$f(\mathbf{R_n},\mathbf{r}) = \sum_{m=0}^{\infty} \frac{1}{m!} \mathbf{f}^m(\mathbf{r}|\mathbf{R}') \{\cdot\}^m \{\mathbf{R_n} - \mathbf{R}'\}^m \tag{3.3-15}$$

where the tensors $\mathbf{f}^m(\mathbf{r}|\mathbf{R}')$ are defined as

$$\mathbf{f}^m(\mathbf{r}|\mathbf{R}') \stackrel{\text{def}}{=} \sum_{j=0}^{\infty} \frac{1}{j!} \overline{\mathbf{f}}^{m+j}(|\mathbf{R}') \{\cdot\}^j \mathbf{r}^j \tag{3.3-16}$$

and are themselves fully symmetric with respect to all their m indices.

3.3.3 Scalar Fields: Continuity Conditions Imposed Upon $\mathbf{f}^m(\mathbf{r}|\mathbf{R}')$

Once again, it will prove useful to derive some continuity conditions imposed upon the $\mathbf{f}^m(\mathbf{r}|\mathbf{R}')$'s given the assumed continuity of $f(\mathbf{R})$ across the cell faces $\partial\tau_0$. Continuity of $f(\mathbf{R_n},\mathbf{r})$ requires that

$$f(\mathbf{R_n} - \mathbf{l}_k, \mathbf{r} + \mathbf{l}_k) = f(\mathbf{R_n},\mathbf{r}) \qquad \forall\,(\mathbf{r} \in \partial\tau_0; k = 1,2,\ldots,M)\,, \tag{3.3-17}$$

where the $\mathbf{l}_k$'s are the lattice vectors (see Appendix B). Substitute the Taylor series (3.3-15) into the equality (3.3-17) to obtain

$$\sum_{m=0}^{\infty} \frac{1}{m!} \mathbf{f}^m(\mathbf{r}|\mathbf{R}') \{\cdot\}^m \{\mathbf{R_n} - \mathbf{R}'\}^m = \sum_{m=0}^{\infty} \frac{1}{m!} \mathbf{f}^m(\mathbf{r} + \mathbf{l}_k|\mathbf{R}') \{\cdot\}^m \{\mathbf{R_n} - \mathbf{R}' - \mathbf{l}_k\}^m\,, \tag{3.3-18}$$

assumed to hold at all points lying on the cell surface and for all lattice vectors. The next step entails collecting together terms involving like powers of $\mathbf{R_n} - \mathbf{R}'$. Towards

this end, equation (3.3-18) may be rewritten by using (3.3-12) and (3.2-11) to obtain

$$\sum_{m=0}^{\infty} \frac{1}{m!} \mathbf{f}^m(\mathbf{r}|\mathbf{R}') \{\cdot\}^m \{\mathbf{R_n} - \mathbf{R}'\}^m$$
$$= \sum_{m=0}^{\infty} \frac{1}{m!} \left[\sum_{j=0}^{\infty} \frac{1}{j!} \mathbf{f}^{m+j}(\mathbf{r} + \mathbf{l}_k|\mathbf{R}') \{\cdot\}^j \{-\mathbf{l}_k\}^j \right] \{\cdot\}^m \{\mathbf{R_n} - \mathbf{R}'\}^m , \quad (3.3\text{-}19)$$

where the symmetry operator appearing in (3.3-12) has been dropped because of the symmetry of the tensors $\mathbf{f}^m(\mathbf{r}|\mathbf{R}')$. Since the vector $\mathbf{R_n} - \mathbf{R}'$ is arbitrary, this equation must be satisfied for all powers of $\mathbf{R_n} - \mathbf{R}'$. This leads to the following expression [similar to (3.2-18) for the one-dimensional position vector]:

$$\mathbf{f}^m(\mathbf{r}|\mathbf{R}') = \sum_{j=0}^{\infty} \frac{1}{j!} \mathbf{f}^{m+j}(\mathbf{r} + \mathbf{l}_k|\mathbf{R}') \{\cdot\}^j \{-\mathbf{l}_k\}^j , \quad (3.3\text{-}20)$$

valid for $\mathbf{r} \in \partial\tau_0$. Equation (3.3-20) relates the value of $\mathbf{f}^m$ on the cell face at $\mathbf{r}$ to the values of $\mathbf{f}^m, \mathbf{f}^{m+1}, \mathbf{f}^{m+2}, \ldots$ on the opposite cell face at $\mathbf{r} + \mathbf{l}_k$ for all cell faces $k = 1, 2, \ldots, M$. The jump condition (3.2-19) can be extended for any scalar function $F(\mathbf{r})$ to represent the difference between the value of the function on opposite cell faces as

$$\|F(\mathbf{r})\| \stackrel{\text{def}}{=} F(\mathbf{r} + \mathbf{l}_k) - F(\mathbf{r}) \qquad \forall (\mathbf{r} \in \partial\tau_0; k = 1, 2, \ldots, M) . \quad (3.3\text{-}21)$$

Following a similar procedure to that outlined in the one-dimensional theory, recursive substitution of (3.3-20) into itself along with use of the definition of the jump (3.3-21) and the symmetry of the tensors $\mathbf{f}^m(\mathbf{r}|\mathbf{R}'_\mathbf{n})$, ultimately leads to the expression

$$\|\mathbf{f}^m(\mathbf{r}|\mathbf{R}')\| = -\sum_{j=1}^{\infty} \frac{(-1)^j}{j!} \left\| \mathbf{f}^{m+j}(\mathbf{r}|\mathbf{R}') \{\cdot\}^j \mathbf{r}^j \right\| , \quad (3.3\text{-}22)$$

relating the jump in $\mathbf{f}^m$ to the jumps in $\mathbf{f}^{m+1}, \mathbf{f}^{m+2}, \ldots$ together with the continuous local position vector $\mathbf{r}$. Finally, because $f(\mathbf{R})$ and its derivatives are assumed continuous and finite at all points $\mathbf{R}$, equation (3.3-17) holds for all the derivatives of $f(\mathbf{R_n}, \mathbf{r})$ with respect to $\mathbf{r}$ when approached from opposite sides of a given cell face.

This enables (3.3-22) to take on the more general form

$$\left\|\boldsymbol{\nabla}^i \mathbf{f}^m(\mathbf{r}|\mathbf{R}')\right\| = -\sum_{j=1}^{\infty} \frac{(-1)^j}{j!} \left\|\left[\boldsymbol{\nabla}^i \mathbf{f}^{m+j}(\mathbf{r}|\mathbf{R}')\right] \{\cdot\}^j \mathbf{r}^j\right\| \tag{3.3-23}$$

$$= -\sum_{j=1}^{\infty} \frac{(-1)^j}{j!} \left\|\boldsymbol{\nabla}^i \left[\mathbf{f}^{m+j}(\mathbf{r}|\mathbf{R}') \{\cdot\}^j \mathbf{r}^j\right]\right\|, \tag{3.3-24}$$

valid for all $\mathbf{r} \in \partial\tau_0$, $i = 0, 1, 2, \ldots$ and $m = 0, 1, 2, \ldots$. The gradient operator here is, of course, $\boldsymbol{\nabla} = \partial/\partial\mathbf{r}$. The latter is equivalent to (3.3-3) for all points not on the surface ($\mathbf{r} \ni \partial\tau_0$), but the jump operator itself involves taking the limit as the position vector $\mathbf{r}$ approaches a cell face from opposite sides, so that no ambiguity exists in the choice of notation.

3.3.4 Tensor Fields

Finally, the previous results for a scalar function are extended to the most general case of an Nth rank tensor field $\mathbf{f}(\mathbf{R})$ depending upon the M-dimensional position vector $\mathbf{R}$. The function $\mathbf{f}(\mathbf{R})$ can be substituted for $f(\mathbf{R})$ but care must be taken in preserving the right indices of $\mathbf{f}(\mathbf{R})$ throughout the many dot products. The continuous Taylor series (3.3-4) can be written as

$$\mathbf{f}(\mathbf{R}) = \sum_{m=0}^{\infty} \frac{1}{m!} \overline{\mathbf{f}}^m(|\mathbf{R}') \{\cdot\}^m \{\mathbf{R} - \mathbf{R}'\}^m \tag{3.3-25}$$

$$= \overline{\mathbf{f}}^0(|\mathbf{R}') + \overline{\mathbf{f}}^1(|\mathbf{R}') \cdot \{\mathbf{R} - \mathbf{R}'\} + \frac{1}{2!}\overline{\mathbf{f}}^2(|\mathbf{R}') : \{\mathbf{R} - \mathbf{R}'\}^2 + \frac{1}{3!}\overline{\mathbf{f}}^3(|\mathbf{R}') \vdots \{\mathbf{R} - \mathbf{R}'\}^3 + \cdots \tag{3.3-26}$$

and if $f_{i_1 i_2 \ldots i_N}(\mathbf{R})$ represents $\mathbf{f}(\mathbf{R})$ written in component form where $i_1 i_2 \ldots i_N$ represent the N indices of $\mathbf{f}(\mathbf{R})$, then the tensors $\overline{\mathbf{f}}^m(|\mathbf{R}')$ are given as

$$\overline{f}^m_{i_1 i_2 \ldots i_N j_1 j_2 \ldots j_m}(|\mathbf{R}') \stackrel{\text{def}}{=} \left[\nabla_{j_1} \nabla_{j_2} \ldots \nabla_{j_m} f_{i_1 i_2 \ldots i_N}(\mathbf{R})\right]\Big|_{\mathbf{R}=\mathbf{R}'}, \tag{3.3-27}$$

where $\overline{\mathbf{f}}^m(|\mathbf{R}')$ represents the mth derivative of $\mathbf{f}(\mathbf{R})$ with respect to $\mathbf{R}$, evaluated at the arbitrary reference point $\mathbf{R}'$. [1] Notice that the tensor $\overline{\mathbf{f}}^m(|\mathbf{R}')$ is of rank $N+m$; furthermore, this tensor is symmetric with respect to its *last* m indices.

The decomposition (3.3-9), followed by forming derivatives of $\mathbf{f}(\mathbf{R_n}, \mathbf{r})$ with respect to $\mathbf{R_n}$, furnishes the Taylor series analog to (3.3-15), but now with the Nth rank tensor $\mathbf{f}(\mathbf{R_n}, \mathbf{r})$ appearing in place of the scalar field $f(\mathbf{R_n}, \mathbf{r})$; explicitly,

$$\mathbf{f}(\mathbf{R_n}, \mathbf{r}) = \sum_{m=0}^{\infty} \frac{1}{m!} \mathbf{f}^m(\mathbf{r}|\mathbf{R}') \{\cdot\}^m \{\mathbf{R_n} - \mathbf{R}'\}^m, \tag{3.3-28}$$

where the tensor $\mathbf{f}^m(\mathbf{r}|\mathbf{R}'_\mathbf{n})$ is defined as

$$\mathbf{f}^m(\mathbf{r}|\mathbf{R}') \stackrel{\text{def}}{=} \sum_{j=0}^{\infty} \frac{1}{j!} \overline{\mathbf{f}}^{m+j}(|\mathbf{R}') \{\cdot\}^j \mathbf{r}^j \tag{3.3-29}$$

and is of rank $N+m$ and symmetric with respect to its *last* m indices. Furthermore, the general continuity conditions imposed upon the tensor $\mathbf{f}^m(\mathbf{r}|\mathbf{R}')$—as a result of the implied continuity of $\mathbf{f}(\mathbf{R})$ and its derivatives across cell faces—can be expressed as

$$\left\| \boldsymbol{\nabla}^i \mathbf{f}^m(\mathbf{r}|\mathbf{R}') \right\| = -\sum_{j=1}^{\infty} \frac{(-1)^j}{j!} \left\| \left[\boldsymbol{\nabla}^i \mathbf{f}^{m+j}(\mathbf{r}|\mathbf{R}') \right] \{\cdot\}^j \mathbf{r}^j \right\| \tag{3.3-30}$$

$$= -\sum_{j=1}^{\infty} \frac{(-1)^j}{j!} \left\| \boldsymbol{\nabla}^i \left[\mathbf{f}^{m+j}(\mathbf{r}|\mathbf{R}') \{\cdot\}^j \mathbf{r}^j \right] \right\|, \tag{3.3-31}$$

valid for all $\mathbf{r} \in \partial\tau_0$, $i = 0, 1, 2, \ldots$ and $m = 0, 1, 2, \ldots$.

[1] The indices of $\mathbf{f}(\mathbf{R})$ are preserved at the *front* of $\overline{\mathbf{f}}^m(|\mathbf{R}')$ such that the tensor $\{\mathbf{R} - \mathbf{R}'\}^m$ is *post*-dotted into the tensor $\overline{\mathbf{f}}^m(|\mathbf{R}')$, as in (3.3-25).

3.4 Spatially Periodic Functions

The most general results, namely (3.3-30) or (3.3-31) will be used in subsequent sections to extract the jump conditions imposed upon the coefficients of the velocity and pressure fields when expanded in a Taylor series. Functions that are independent of the discrete position variable $\mathbf{R_n}$ will be termed spatially periodic:

$$\mathbf{F}(\mathbf{R}) \equiv \mathbf{F}(\mathbf{r}). \tag{3.4-1}$$

Furthermore, if this spatially periodic function is continuous and smooth everywhere, then it and all its derivatives will be single valued everywhere. Such a function will be termed *fully* spatially periodic and identified by a tilde:

$$\mathbf{F}(\mathbf{R}) \equiv \mathbf{F}(\mathbf{r}) \equiv \widetilde{\mathbf{F}}(\mathbf{R}) \equiv \widetilde{\mathbf{F}}(\mathbf{r}). \tag{3.4-2}$$

Finally, because of the unique value of $\widetilde{\mathbf{F}}(\mathbf{r})$ and all its derivatives at all points in space (including points lying on cell boundaries), the jump in this function and all of its derivatives is identically zero:

$$\left\| \boldsymbol{\nabla}^i \widetilde{\mathbf{F}}(\mathbf{r}) \right\| = \mathbf{0} \qquad \forall\, (i = 0, 1, 2, \ldots)\,. \tag{3.4-3}$$

This property can, in fact, be thought of as defining a *fully* spatially periodic function.

Chapter 4

An Exact Microscale Solution for Generalized Flow through Porous Media

4.1 Introduction

In this chapter, creeping flow in a spatially periodic model of a porous medium is studied. The geometry of each cell is assumed known *a priori* and sequential solutions representing increasing orders of flow complexity are developed, culmulating in a general solution for an entirely arbitrary mean flow. This solution [cf. (4.6-39) and (4.6-40)] is composed of: (i) fully spatially periodic functions determined from characteristic cell problems [cf. (4.6-41)] and uniquely defined *entirely* by the cell geometry; (ii) an arbitrary scalar function and its derivatives. In effect, item (i) pertains to the *micro*scale flow, whereas item (ii) pertains to the *macro*scale or mean, Darcy-scale flow.

4.2 Basic Theory

Here, generalized Taylor series expansions (in the discrete vector $\mathbf{R_n}$) are developed for the microscale velocity and pressure fields. Equations satisfied by these fields, corresponding to successive powers of $\mathbf{R_n}$, are subsequently established. The velocity and the pressure are assumed continuous and smooth at all fluid points $\mathbf{R}$. The generic results of Chapter 3, pertaining to the expansion of an arbitrary but smooth function (3.3-28), as well as the jump conditions imposed on the functions appearing in these series (3.3-30) or (3.3-31), will be used.

4.2.1 Steady-state Stokes Equations

Attention will be restricted to steady, incompressible, creeping flows, for which the equations satisfied by the velocity and pressure fields $\mathbf{v}(\mathbf{R})$ and $p(\mathbf{R})$ at all points $\mathbf{R}$ within the fluid domain are

$$\mu\nabla^2\mathbf{v} - \boldsymbol{\nabla}p = \mathbf{0}, \tag{4.2-1}$$

$$\boldsymbol{\nabla}\cdot\mathbf{v} = 0, \tag{4.2-2}$$

subject to the usual no-slip boundary condition on the partice surfaces:

$$\mathbf{v} = \mathbf{0} \qquad \forall\,(\mathbf{R} \in s_p)\,, \tag{4.2-3}$$

with the gradient operator defined as $\boldsymbol{\nabla} = \partial/\partial\mathbf{R}$, as in (3.3-3). The next step involves expanding these fields in a Taylor series, subsequently determining from the creeping flow and continuity equations the differential equations satisfied by the Taylor series coefficients appearing in these expansions.

4.2.2 General Taylor Series Expansion for the Velocity and Pressure Fields

In any spatially periodic geometric model porous medium, the velocity and pressure fields at any point $\mathbf{R}$ within the interstitial fluid possess the equivalent representations

$$\mathbf{v}(\mathbf{R}) \equiv \mathbf{v}(\mathbf{R_n}, \mathbf{r}) \tag{4.2-4}$$

and

$$p(\mathbf{R}) \equiv p(\mathbf{R_n}, \mathbf{r}). \tag{4.2-5}$$

Because of their assumed smoothness, these fields can be expanded in the discrete form of a Taylor series about an arbitrary point (denoted by the position $\mathbf{R}'$). From (3.3-28) we obtain

$$\begin{aligned} \mathbf{v}(\mathbf{R_n}, \mathbf{r}) &= \sum_{m=0}^{\infty} \frac{1}{m!} \mathbf{v}^m(\mathbf{r}|\mathbf{R}') \{\cdot\}^m \{\mathbf{R_n} - \mathbf{R}'\}^m \qquad (4.2\text{-}6) \\ &\equiv \mathbf{v}^0(\mathbf{r}|\mathbf{R}') + \mathbf{v}^1(\mathbf{r}|\mathbf{R}') \cdot \{\mathbf{R_n} - \mathbf{R}'\} \\ &\quad + \frac{1}{2!} \mathbf{v}^2(\mathbf{r}|\mathbf{R}') : \{\mathbf{R_n} - \mathbf{R}'\}^2 + \frac{1}{3!} \mathbf{v}^3(\mathbf{r}|\mathbf{R}') \vdots \{\mathbf{R_n} - \mathbf{R}'\}^3 + \cdots \end{aligned}$$

and

$$\begin{aligned} p(\mathbf{R_n}, \mathbf{r}) &= \sum_{m=0}^{\infty} \frac{1}{m!} \mathbf{p}^m(\mathbf{r}|\mathbf{R}') \{\cdot\}^m \{\mathbf{R_n} - \mathbf{R}'\}^m \qquad (4.2\text{-}7) \\ &\equiv p^0(\mathbf{r}|\mathbf{R}') + \mathbf{p}^1(\mathbf{r}|\mathbf{R}') \cdot \{\mathbf{R_n} - \mathbf{R}'\} \\ &\quad + \frac{1}{2!} \mathbf{p}^2(\mathbf{r}|\mathbf{R}') : \{\mathbf{R_n} - \mathbf{R}'\}^2 + \frac{1}{3!} \mathbf{p}^3(\mathbf{r}|\mathbf{R}') \vdots \{\mathbf{R_n} - \mathbf{R}'\}^3 + \cdots . \end{aligned}$$

The definitions of the tensors $\mathbf{v}^m(\mathbf{r}|\mathbf{R}')$ and $\mathbf{p}^m(\mathbf{r}|\mathbf{R}')$ of respective ranks $m+1$ and m follow directly from (3.3-29) as

$$\mathbf{v}^m(\mathbf{r}|\mathbf{R}') \stackrel{\text{def}}{=} \sum_{j=0}^{\infty} \frac{1}{j!} \overline{\mathbf{v}}^{m+j}(|\mathbf{R}') \{\cdot\}^j \mathbf{r}^j \tag{4.2-8}$$

and

$$\mathbf{p}^m(\mathbf{r}|\mathbf{R}') \stackrel{\text{def}}{=} \sum_{j=0}^{\infty} \frac{1}{j!} \overline{\mathbf{p}}^{m+j}(|\mathbf{R}') \{\cdot\}^j \mathbf{r}^j \tag{4.2-9}$$

where the functions $\overline{\mathbf{v}}^m(|\mathbf{R}')$ and $\overline{\mathbf{p}}^m(|\mathbf{R}')$ are given as

$$\overline{v}^m_{i_1 j_1 j_2 \ldots j_m}(|\mathbf{R}') \stackrel{\text{def}}{=} [\nabla_{j_1} \nabla_{j_2} \ldots \nabla_{j_m} v_{i_1}(\mathbf{R})]|_{\mathbf{R}=\mathbf{R}'} \tag{4.2-10}$$

$$\overline{p}^m_{j_1 j_2 \ldots j_m}(|\mathbf{R}') \stackrel{\text{def}}{=} [\nabla_{j_1} \nabla_{j_2} \ldots \nabla_{j_m} p(\mathbf{R})]|_{\mathbf{R}=\mathbf{R}'} \tag{4.2-11}$$

represent the mth derivative of the velocity and pressure fields with respect to the position vector $\mathbf{R}$, evaluated at the reference point $\mathbf{R}'$. Note in the former that the tensorial index representing the vector $\mathbf{v}(\mathbf{R})$ constitutes the leading tensorial index of the $m+1$ rank tensors $\overline{\mathbf{v}}^m(|\mathbf{R}')$ and $\mathbf{v}^m(\mathbf{r}|\mathbf{R}')$. As noted by their arguments, the tensors $\mathbf{v}^m$ and $\mathbf{p}^m$ depend upon the local position $\mathbf{r}$ and the reference point $\mathbf{R}'$. From these definitions it is obvious that the tensor $\mathbf{v}^m(\mathbf{r}|\mathbf{R}')$ is symmetric with respect to its last m indices whereas $\mathbf{p}^m(\mathbf{r}|\mathbf{R}')$ is symmetric with respect to all its m indices. The respective tensors $\mathbf{v}^0$, $\mathbf{v}^1$ and $\mathbf{v}^2$ represent vector, dyadic and triadic fields, whereas p^0, $\mathbf{p}^1$ and $\mathbf{p}^2$ respectively represent scalar, vector and dyadic fields.

4.2.3 mth-order Equations: The Fluid Domain, τ_f

Substitute (4.2-6) and (4.2-7) into (4.2-1) to (4.2-3) and note that $\mathbf{R_n} - \mathbf{R}'$ is constant and arbitrary within the fluid region $\mathbf{r}$ of a cell. As such, the resulting expressions must match at all orders of $\mathbf{R_n} - \mathbf{R}'$. This ultimately furnishes the equations for $\mathbf{v}^m(\mathbf{r}|\mathbf{R}')$ and $\mathbf{p}^m(\mathbf{r}|\mathbf{R}')$, namely

$$\mu \nabla^2 \mathbf{v}^m - \boldsymbol{\nabla} \mathbf{p}^m = \mathbf{0}, \tag{4.2-12}$$

$$\boldsymbol{\nabla} \cdot \mathbf{v}^m = \mathbf{0} \tag{4.2-13}$$

and

$$\mathbf{v}^m = \mathbf{0} \qquad \forall (\mathbf{r} \in s_p). \tag{4.2-14}$$

These equations apply for each $m = 0, 1, 2, \ldots$, for all cells and for all $\mathbf{r} \in \tau_f$ except for the set of points of zero measure lying on the cell faces ($\mathbf{r} \ni \partial\tau_0$). The interpretation of the gradient operator in equations (4.2-12) to (4.2-14) is that, within a given cell, the discrete vector $\mathbf{R_n}$ is a constant and thus derivatives with respect to $\mathbf{R}$ are equivalent to derivatives with respect to $\mathbf{r}$:

$$\boldsymbol{\nabla} \equiv \frac{\partial}{\partial \mathbf{r}} \qquad \forall\, (\mathbf{r} \ni \partial\tau_0)\,. \tag{4.2-15}$$

Cell boundaries must be treated separately, since ambiguity exists as to what is meant by $\partial/\partial\mathbf{r}$ on a cell surface owing to the fact that the boundary is common to contiguous cells.

4.2.4 mth-order Equations: The Boundary $\partial\tau_0$ of a Cell

Since the velocity and pressure (and their derivatives) are assumed to be continuous, each must have a unique value when approached from opposite sides of a common cell face, i.e.,

$$\left[\boldsymbol{\nabla}^i \mathbf{v}(\mathbf{R_n}, \mathbf{r})\right]\Big|_{\mathbf{R_n},\mathbf{r}} = \left[\boldsymbol{\nabla}^i \mathbf{v}(\mathbf{R_n}, \mathbf{r})\right]\Big|_{\mathbf{R_n}-\mathbf{l}_k,\mathbf{r}+\mathbf{l}_k} \qquad \forall \begin{pmatrix} \mathbf{r} \in \partial\tau_0; \\ k = 1, 2, 3; \\ i = 0, 1, 2, \ldots \end{pmatrix} \tag{4.2-16}$$

and

$$\left[\boldsymbol{\nabla}^i p(\mathbf{R_n}, \mathbf{r})\right]\Big|_{\mathbf{R_n},\mathbf{r}} = \left[\boldsymbol{\nabla}^i p(\mathbf{R_n}, \mathbf{r})\right]\Big|_{\mathbf{R_n}-\mathbf{l}_k,\mathbf{r}+\mathbf{l}_k} \qquad \forall \begin{pmatrix} \mathbf{r} \in \partial\tau_0; \\ k = 1, 2, 3; \\ i = 0, 1, 2, \ldots \end{pmatrix}, \tag{4.2-17}$$

similar to (3.3-17). Writing (3.3-31) in terms of $\mathbf{v}^m(\mathbf{r}|\mathbf{R}')$ gives

$$\left\|\boldsymbol{\nabla}^i \mathbf{v}^m(\mathbf{r}|\mathbf{R}')\right\| \;=\; -\sum_{j=1}^{\infty} \frac{(-1)^j}{j!} \left\|\left[\boldsymbol{\nabla}^i \mathbf{v}^{m+j}(\mathbf{r}|\mathbf{R}')\right] \{\cdot\}^j\, \mathbf{r}^j\right\| \tag{4.2-18}$$

$$\equiv -\sum_{j=1}^{\infty} \frac{(-1)^j}{j!} \left\| \boldsymbol{\nabla}^i \left[\mathbf{v}^{m+j}(\mathbf{r}|\mathbf{R}') \{\cdot\}^j \mathbf{r}^j \right] \right\|. \qquad (4.2\text{-}19)$$

Similarily, the jump conditions imposed upon $\mathbf{p}^m(\mathbf{r}|\mathbf{R}')$ are

$$\left\| \boldsymbol{\nabla}^i \mathbf{p}^m(\mathbf{r}|\mathbf{R}') \right\| = -\sum_{j=1}^{\infty} \frac{(-1)^j}{j!} \left\| \left[\boldsymbol{\nabla}^i \mathbf{p}^{m+j}(\mathbf{r}|\mathbf{R}') \right] \{\cdot\}^j \mathbf{r}^j \right\| \qquad (4.2\text{-}20)$$

$$\equiv -\sum_{j=1}^{\infty} \frac{(-1)^j}{j!} \left\| \boldsymbol{\nabla}^i \left[\mathbf{p}^{m+j}(\mathbf{r}|\mathbf{R}') \{\cdot\}^j \mathbf{r}^j \right] \right\|. \qquad (4.2\text{-}21)$$

The latter pairs of $\left\| \boldsymbol{\nabla}^i \mathbf{v}^m \right\|$ and $\left\| \boldsymbol{\nabla}^i \mathbf{p}^m \right\|$ equations are valid for all $\mathbf{r} \in \partial\tau_0$ and at each $i = 0, 1, 2, \ldots$ and $m = 0, 1, 2, \ldots$. Whereas equations (4.2-12) to (4.2-14) describe how $\mathbf{v}^m(\mathbf{r}|\mathbf{R}')$ and $\mathbf{p}^m(\mathbf{r}|\mathbf{R}')$ vary within the local fluid domain $\mathbf{r} \in \tau_f$ of each cell, the latter pairs of velocity/pressure equations describe how these fields vary from cell to cell as $\mathbf{n}$ changes.

In what follows, the discrete series (4.2-6) for the velocity field (and comparable series for the pressure field) will be successively truncated at terms of ever-increasing order in the index m. The successive solutions for the fields $\mathbf{v}^m(\mathbf{r}|\mathbf{R}')$ and $\mathbf{p}^m(\mathbf{r}|\mathbf{R}')$ will be determined, ultimately deriving—by induction—a general solution for the original, untruncated series.

4.3 Truncated Zeroth-order Microscale Flow

In this section, the discrete form Taylor series expansion (4.2-6) for $\mathbf{v}(\mathbf{R})$ will be truncated so that only the leading term, $\mathbf{v}^0(\mathbf{r}|\mathbf{R}')$, remains.

4.3.1 Microscale Velocity, $\mathbf{v}(\mathbf{R})$

Arbitrarily choose

$$\mathbf{v}^1(\mathbf{r}|\mathbf{R}') = \mathbf{v}^2(\mathbf{r}|\mathbf{R}') = \cdots = \mathbf{0} \tag{4.3-1}$$

in the discrete Taylor series (4.2-6), so that attention is focused only on the flow field

$$\mathbf{v}\left(\mathbf{R_n}, \mathbf{r}\right) = \mathbf{v}^0(\mathbf{r}|\mathbf{R}'), \tag{4.3-2}$$

where *physical* significance remains to be established. The choice (4.3-1) combined with the jump restrictions [embodied in (4.2-18) or (4.2-19) with $m = 0$] imposed upon $\mathbf{v}^0(\mathbf{r}|\mathbf{R}')$ as a result of the continuous nature of $\mathbf{v}(\mathbf{R})$ and all its derivatives at every point in the fluid shows that the function $\mathbf{v}^0(\mathbf{r}|\mathbf{R}')$ must satisfy

$$\left\| \boldsymbol{\nabla}^i \mathbf{v}^0(\mathbf{r}|\mathbf{R_n}) \right\| = \mathbf{0} \qquad \forall\,(i = 0, 1, 2, \ldots)\,. \tag{4.3-3}$$

Recall from (3.4-3) that this is what constitutes a *fully* spatially periodic function—one in which the function and all its derivatives are spatially periodic and continuous at all points in the fluid; accordingly, we may write

$$\mathbf{v}^0(\mathbf{r}|\mathbf{R}') \equiv \tilde{\mathbf{v}}^0(\mathbf{r}|\mathbf{R}'), \tag{4.3-4}$$

where the tilde serves as a reminder that the function to which it is affixed is fully spatially periodic.

In combination, the forms of the tensors $\mathbf{v}^m(\mathbf{r}|\mathbf{R}')$ are

$$\mathbf{v}^m = \begin{cases} \widetilde{\mathbf{v}}^0 & (m=0), \\ \\ \mathbf{0} & \forall (m=1,2,3,\ldots), \end{cases} \tag{4.3-5}$$

in which the arguments $(\mathbf{r}|\mathbf{R}')$ have been suppressed. Hence, from (4.3-2), $\mathbf{v}(\mathbf{R})$ is of the form

$$\mathbf{v}\left(\mathbf{R_n}, \mathbf{r}\right) = \widetilde{\mathbf{v}}^0(\mathbf{r}|\mathbf{R}'). \tag{4.3-6}$$

It is of course intuitively clear that the velocity field, having been assumed independent of $\mathbf{R_n}$ as in (4.3-2), is necessarily spatially periodic, as in (4.3-6), and so the conclusion may appear trivial. However, when dealing with higher-order flows, where intuition may be lacking, the procedure outlined here serves to systematically establish the requisite forms of the tensors $\mathbf{v}^m(\mathbf{r}|\mathbf{R}')$.

4.3.2 Microscale Pressure, $p(\mathbf{R})$

Equations (4.2-12) and the form of the tensors $\mathbf{v}^m(\mathbf{r}|\mathbf{R}')$ [see equation (4.3-5)] give

$$\boldsymbol{\nabla}\mathbf{p}^1 = \boldsymbol{\nabla}\mathbf{p}^2 = \cdots = \mathbf{0}. \tag{4.3-7}$$

This shows that the tensors $\mathbf{p}^m(\mathbf{r}|\mathbf{R}')$ for $m = 1, 2, 3, \ldots$ are all, *at most*, constants (dependent of course upon the choice of reference point $\mathbf{R}'$). As such, we may write

$$\mathbf{p}^m(\mathbf{r}|\mathbf{R}') = \overline{\boldsymbol{\Psi}}^m(|\mathbf{R}') \qquad \forall\,(m=1,2,3,\ldots)\,. \tag{4.3-8}$$

Next, write jump condition (4.2-20) for $m \geq 1$ and $i = 0$. [The case $i \geq 1$ when $m \geq 1$ with the form (4.3-8) yields $\mathbf{0} = \mathbf{0}$, which is of course always satisfied.] Subsequent use of (4.3-8) yields

$$\mathbf{0} = -\sum_{j=1}^{\infty} \frac{(-1)^j}{j!} \overline{\boldsymbol{\Psi}}^{m+j}(|\mathbf{R}')\,\{\cdot\}^j \left\|\mathbf{r}^j\right\| \qquad \forall\,(m=1,2,3,\ldots)\,. \tag{4.3-9}$$

Since the latter must hold for all $\mathbf{r}$ and for all values of m indicated, this necessitates that

$$\overline{\boldsymbol{\Psi}}^m(|\mathbf{R}') = \mathbf{0} \qquad \forall\,(m = 2, 3, 4, \ldots)\,. \tag{4.3-10}$$

The jump conditon (4.2-21) for $m = 0$, together with (4.3-8) and (4.3-10), requires that

$$\left\|\boldsymbol{\nabla}^i p^0(\mathbf{r}|\mathbf{R}')\right\| = \left\|\boldsymbol{\nabla}^i \left[\overline{\boldsymbol{\Psi}}^1(|\mathbf{R}') \cdot \mathbf{r}\right]\right\| \qquad \forall\,(i = 0, 1, 2, \ldots)\,. \tag{4.3-11}$$

In conjunction with (3.4-3), the preceding relation requires that $p^0(\mathbf{r}|\mathbf{R}')$ be of the form

$$p^0(\mathbf{r}|\mathbf{R}') = \tilde{p}^0(\mathbf{r}|\mathbf{R}') + \overline{\boldsymbol{\Psi}}^1(|\mathbf{R}') \cdot \mathbf{r} \tag{4.3-12}$$

where, by definition, the jump in $\tilde{p}^0(\mathbf{r}|\mathbf{R}')$ as well as in all of its derivatives is identically zero. From (4.3-12), (4.3-8) and (4.3-10) it is apparent that the tensor $\mathbf{p}^m(\mathbf{r}|\mathbf{R}')$ is of the form

$$\mathbf{p}^m = \begin{cases} \tilde{p}^0 + \overline{\boldsymbol{\Psi}}^1 \cdot \mathbf{r} & (m = 0), \\ \\ \overline{\boldsymbol{\Psi}}^1 & (m = 1), \\ \\ \mathbf{0} & \forall (m = 2, 3, 4, \ldots), \end{cases} \tag{4.3-13}$$

wherein the arguments $(\mathbf{r}|\mathbf{R}')$ and $(|\mathbf{R}')$ have been suppressed. The preceding constitutes the counterpart of (4.3-5).

Substitute (4.3-13) into the discrete form of the Taylor series (4.2-6) for $p(\mathbf{R})$ to ultimately obtain the following form of the microscale pressure field:

$$p(\mathbf{R_n}, \mathbf{r}) = \tilde{p}^0(\mathbf{r}|\mathbf{R}') + \overline{\boldsymbol{\Psi}}^1(|\mathbf{R}') \cdot \{\mathbf{R} - \mathbf{R}'\}\,. \tag{4.3-14}$$

This shows that the microscale pressure field is composed of a spatially periodic part and a part that grows linearly with $\mathbf{R}$. [This form of $p(\mathbf{R})$ could have been obtained more straightforwardly by noting that since the microscale velocity field is spatially periodic, as in (4.3-6), it follows directly from (4.2-1) that the microscale

pressure gradient is also spatially periodic. In turn, the latter fact implies the result (4.3-14). However, the general utility of this scheme for choosing a specific $\mathbf{v}(\mathbf{R})$ and determining therefrom the resulting form of $p(\mathbf{R})$ will be manifest when dealing with more complex flows.]

Basically $\mathbf{v}(\mathbf{R})$ and $p(\mathbf{R})$ for this zeroth-order flow field have been expressed in terms of fully spatially periodic functions, namely $\tilde{\mathbf{v}}^0(\mathbf{r}|\mathbf{R}')$, $\tilde{p}^0(\mathbf{r}|\mathbf{R}')$, and an arbitrary constant vector, $\overline{\mathbf{\Psi}}^1(|\mathbf{R}')$. The next step involves removing the dependence of $\tilde{\mathbf{v}}^0(\mathbf{r}|\mathbf{R}')$ and $\tilde{p}^0(\mathbf{r}|\mathbf{R}')$ upon the choice of reference point, $\mathbf{R}'$. This will ultimately show [cf. (4.3-50) and (4.3-51)] that $\mathbf{v}(\mathbf{R})$ and $p(\mathbf{R})$ can be expressed as a sum of three components: (i) fully spatially periodic functions, depending only upon *unit cell geometry*; (ii) constants, dependent upon reference point $\mathbf{R}'$; and (iii) powers of $\mathbf{R} - \mathbf{R}'$. Again, the utility of this general procedure will be evident in subsequent sections.

4.3.3 Solution of $\tilde{\mathbf{v}}^0(\mathbf{r}|\mathbf{R}')$, $\tilde{p}^0(\mathbf{r}|\mathbf{R}')$

Set $m = 0$ in Eqs. (4.2-12) to (4.2-14) and substitute into these the respective 'decompositions' of $\mathbf{v}^0(\mathbf{r}|\mathbf{R}')$ and $p^0(\mathbf{r}|\mathbf{R}')$ appearing in (4.3-5) and (4.3-13) to obtain

$$\mu\nabla^2\tilde{\mathbf{v}}^0 - \boldsymbol{\nabla}\tilde{p}^0 = \overline{\mathbf{\Psi}}^1, \tag{4.3-15}$$

$$\boldsymbol{\nabla}\cdot\tilde{\mathbf{v}}^0 = 0, \tag{4.3-16}$$

$$\tilde{\mathbf{v}}^0 = \mathbf{0} \qquad \forall(\mathbf{r}\in s_p)\,. \tag{4.3-17}$$

As the problem defined by (4.3-15) to (4.3-17) is linear, the unknown constant vector $\overline{\mathbf{\Psi}}^1(|\mathbf{R}')$ and the viscosity μ may be removed from the problem by defining the dyadic 'velocity' field $\widetilde{\mathbf{V}}^0(\mathbf{r})$ and the vector 'pressure' field $\widetilde{\mathbf{\Pi}}^0(\mathbf{r})$ as

$$\mu\tilde{\mathbf{v}}^0(\mathbf{r}|\mathbf{R}') \overset{\text{def}}{=} \widetilde{\mathbf{V}}^0(\mathbf{r})\cdot\overline{\mathbf{\Psi}}^1(|\mathbf{R}'), \tag{4.3-18}$$

$$\tilde{p}^0(\mathbf{r}|\mathbf{R}') \overset{\text{def}}{=} \overline{\Psi}^0(|\mathbf{R}') + \widetilde{\mathbf{\Pi}}^0(\mathbf{r})\cdot\overline{\mathbf{\Psi}}^1(|\mathbf{R}'), \tag{4.3-19}$$

where the scalar constant $\overline{\Psi}^0(|\mathbf{R}')$ is included to remove the arbitrary constant which would otherwise appear in $\tilde{p}^0(\mathbf{r}|\mathbf{R}')$, as implied by (4.3-15). Define $\overline{\Psi}^0(|\mathbf{R}')$ as

$$\overline{\Psi}^0(|\mathbf{R}') \stackrel{\text{def}}{=} \left\langle \tilde{p}^0(\mathbf{r}|\mathbf{R}') \right\rangle, \tag{4.3-20}$$

with the interstitial average of any function $\mathbf{F}(\mathbf{r})$ defined as

$$\langle \mathbf{F}(\mathbf{r}) \rangle \stackrel{\text{def}}{=} \frac{1}{\tau_f} \int_{\tau_f} \mathbf{F}(\mathbf{r})\, \mathrm{d}^3\mathbf{r}, \tag{4.3-21}$$

in which $\mathrm{d}^3\mathbf{r}$ denotes a volume element in the local space domain, $\mathbf{r} \in \tau_0$. The choice of the zero-order constant in (4.3-20) implies that $\widetilde{\mathbf{\Pi}}^0(\mathbf{r})$ is normalized as

$$\left\langle \widetilde{\mathbf{\Pi}}^0(\mathbf{r}) \right\rangle = \mathbf{0}. \tag{4.3-22}$$

The 'separation-of-variables' relations (4.3-18) and (4.3-19) are of course subject to *a posteriori* verification. Explicitly, if the constants $\overline{\Psi}^0(|\mathbf{R}')$ and $\overline{\Psi}^1(|\mathbf{R}')$ can be removed from equations (4.3-15) to (4.3-17) by the proposed forms (4.3-18) and (4.3-19), then this will prove that the fields $\widetilde{\mathbf{V}}^0(\mathbf{r})$ and $\widetilde{\mathbf{\Pi}}^0(\mathbf{r})$ are indeed independent of the choice of reference point $\mathbf{R}'$.

Substitute the definitions (4.3-18) and (4.3-19) into (4.3-15) to (4.3-17) to obtain

$$\left(\nabla^2\widetilde{\mathbf{V}}^0 - \boldsymbol{\nabla}\widetilde{\mathbf{\Pi}}^0 - \mathbf{I}\right) \cdot \overline{\mathbf{\Psi}}^1 = \mathbf{0}, \tag{4.3-23}$$

$$\left(\boldsymbol{\nabla} \cdot \widetilde{\mathbf{V}}^0\right) \cdot \overline{\mathbf{\Psi}}^1 = \mathbf{0}, \tag{4.3-24}$$

$$\widetilde{\mathbf{V}}^0 \cdot \overline{\mathbf{\Psi}}^1 = \mathbf{0} \qquad \forall\, (\mathbf{r} \in s_p)\,. \tag{4.3-25}$$

As $\overline{\mathbf{\Psi}}^1(|\mathbf{R}')$ is an arbitrary vector, the equality of the terms that it dot multiplies must be identically zero. Thus we obtain the characteristic 'unit cell' problem:

$$\nabla^2\widetilde{\mathbf{V}}^0 - \boldsymbol{\nabla}\widetilde{\mathbf{\Pi}}^0 = \mathbf{I}, \tag{4.3-26}$$

$$\boldsymbol{\nabla} \cdot \widetilde{\mathbf{V}}^0 = \mathbf{0}, \tag{4.3-27}$$

$$\widetilde{\mathbf{V}}^0 = \mathbf{0} \qquad \forall\, (\mathbf{r} \in s_p)\,, \tag{4.3-28}$$

subject to the normalization condition

$$\left\langle \widetilde{\mathbf{\Pi}}^0(\mathbf{r}) \right\rangle = \mathbf{0}, \tag{4.3-29}$$

wherein the appearance of the tilde implies that the functions $\widetilde{\mathbf{V}}^0(\mathbf{r})$ and $\widetilde{\mathbf{\Pi}}^0(\mathbf{r})$ are fully spatially periodic. Equations (4.3-26) to (4.3-29) will be termed the $\mathcal{O}(0)$ (i.e. zero order) *cell problem.* This unit cell problem is devoid of both the arbitrary constants $[\overline{\Psi}^0(|\mathbf{R}'), \overline{\mathbf{\Psi}}^1(|\mathbf{R}')]$ as well as the fluid rheology (characterized by μ). Consequently, the spatially periodic fields $\widetilde{\mathbf{V}}^0(\mathbf{r})$ and $\widetilde{\mathbf{\Pi}}^0(\mathbf{r})$ are determined from and are solely functions of the given geometry of the unit cell, i.e. of $\mathbf{r}$.

4.3.4 Uniqueness of $\widetilde{\mathbf{V}}^0(\mathbf{r})$, $\widetilde{\mathbf{\Pi}}^0(\mathbf{r})$

To demonstrate uniqueness, assume that there exist at least two different solutions $\left(\widetilde{\mathbf{V}}', \widetilde{\mathbf{\Pi}}'\right)$ and $\left(\widetilde{\mathbf{V}}'', \widetilde{\mathbf{\Pi}}''\right)$ of the system of equations (4.3-26) to (4.3-29). Uniqueness will be proved by showing that the pair of quantities $\left(\widetilde{\mathbf{V}}, \widetilde{\mathbf{\Pi}}\right)$ defined as

$$\widetilde{\mathbf{V}}(\mathbf{r}) \stackrel{\text{def}}{=} \widetilde{\mathbf{V}}'(\mathbf{r}) - \widetilde{\mathbf{V}}''(\mathbf{r}) \tag{4.3-30}$$

and

$$\widetilde{\mathbf{\Pi}}(\mathbf{r}) \stackrel{\text{def}}{=} \widetilde{\mathbf{\Pi}}'(\mathbf{r}) - \widetilde{\mathbf{\Pi}}''(\mathbf{r}) \tag{4.3-31}$$

are zero for all $\mathbf{r} \in \tau_f$:

$$\widetilde{\mathbf{V}}(\mathbf{r}) = \mathbf{0}, \tag{4.3-32}$$

$$\widetilde{\mathbf{\Pi}}(\mathbf{r}) = \mathbf{0}. \tag{4.3-33}$$

As the primed and double-primed fields each satisfy (4.3-26) to (4.3-29), it follows from the linearity of these equations that $\left(\widetilde{\mathbf{V}}, \widetilde{\mathbf{\Pi}}\right)$ satisfy

$$\nabla^2 \widetilde{\mathbf{V}} = \boldsymbol{\nabla} \widetilde{\mathbf{\Pi}}, \tag{4.3-34}$$

$$\boldsymbol{\nabla} \cdot \widetilde{\mathbf{V}} = \mathbf{0}, \tag{4.3-35}$$

$$\widetilde{\mathbf{V}} = \mathbf{0} \qquad \forall (\mathbf{r} \in s_p), \tag{4.3-36}$$

$$\left\langle \widetilde{\boldsymbol{\Pi}} \right\rangle = \mathbf{0}. \tag{4.3-37}$$

Double-dot multiply (4.3-34) by $\widetilde{\mathbf{V}}^{\dagger}$ and use the Cartesian tensor identities

$$\tilde{V}_{ij}\nabla_i\tilde{\Pi}_j = \nabla_i\left(\tilde{V}_{ij}\tilde{\Pi}_j\right) - \left(\nabla_i\tilde{V}_{ij}\right)\tilde{\Pi}_j$$

and

$$\tilde{V}_{ij}\nabla_l\nabla_l\tilde{V}_{ij} = \nabla_l\left[\left(\nabla_l\tilde{V}_{ij}\right)\tilde{V}_{ij}\right] - \left(\nabla_l\tilde{V}_{ij}\right)\left(\nabla_l\tilde{V}_{ij}\right)$$

in conjunction with (4.3-35) to obtain

$$\left(\nabla_l\tilde{V}_{ij}\right)\left(\nabla_l\tilde{V}_{ij}\right) = \nabla_l\left[\left(\nabla_l\tilde{V}_{ij}\right)\tilde{V}_{ij}\right] - \nabla_i\left(\tilde{V}_{ij}\tilde{\Pi}_j\right).$$

Integrate this over τ_f and use the divergence theorem to obtain

$$\int_{\tau_f}\left(\nabla_l\tilde{V}_{ij}\right)\left(\nabla_l\tilde{V}_{ij}\right)\mathrm{d}^3\mathbf{r} = \oint_{\partial\tau_0+s_p}\mathrm{d}S_l\left(\nabla_l\tilde{V}_{ij}\right)\tilde{V}_{ij} - \oint_{\partial\tau_0+s_p}\mathrm{d}S_i\tilde{V}_{ij}\tilde{\Pi}_j. \tag{4.3-38}$$

The surface integrals over s_p vanish as a consequence of (4.3-36) while the integrals over $\partial\tau_0$ may be rewritten using the identity [28]

$$\int_{\partial\tau_0}\mathrm{d}\mathbf{S}\cdot\mathbf{A} = \sum_{j=1}^{3}\int_{s+j}\mathrm{d}\mathbf{S}\cdot\|\mathbf{A}\|, \tag{4.3-39}$$

valid for any tensor function $\mathbf{A}$. The jump conditions implied by the fact that $\widetilde{\mathbf{V}}(\mathbf{r})$ and $\widetilde{\boldsymbol{\Pi}}(\mathbf{r})$ are fully spatially periodic (3.4-3) necessitate that the surface integrals over $\partial\tau_0$ appearing in (4.3-38) are identically zero. Consequently,

$$\int_{\tau_f}\left(\nabla_l\tilde{V}_{ij}\right)\left(\nabla_l\tilde{V}_{ij}\right)\mathrm{d}^3\mathbf{r} = 0. \tag{4.3-40}$$

As a consequence of the quadratic, nonnegative nature of the integrand at each

point $\mathbf{r}$, it is necessarily true that

$$\left(\nabla_l \widetilde{V}_{ij}\right)\left(\nabla_l \widetilde{V}_{ij}\right) \geq 0,$$

whence it follows that

$$\boldsymbol{\nabla}\widetilde{\mathbf{V}} = \mathbf{0} \qquad \forall\left(\mathbf{r} \in \tau_f\right).$$

This, in turn, requires that $\widetilde{\mathbf{V}}(\mathbf{r})$ be at most a constant. However, from the boundary condition (4.3-36) this constant must be identically zero, thereby demonstrating the validity of (4.3-32). Furthermore, it now follows from (4.3-34) that

$$\boldsymbol{\nabla}\widetilde{\boldsymbol{\Pi}} = \mathbf{0} \qquad \forall\left(\mathbf{r} \in \tau_f\right).$$

From (4.3-37) this demonstrates the validity of (4.3-33), whence the uniqueness of $\widetilde{\mathbf{V}}^0(\mathbf{r})$ and $\widetilde{\boldsymbol{\Pi}}^0(\mathbf{r})$ is established. (Q.E.D.)

4.3.5 Negativity and Symmetry of $\overline{\mathbf{V}}^0$

The dyadic coefficient

$$\overline{\mathbf{V}}^0 \stackrel{\text{def}}{=} \frac{1}{\tau_0}\oint_{\partial\tau_0} \mathbf{r}\mathrm{d}\mathbf{S}\cdot\widetilde{\mathbf{V}}^0(\mathbf{r}) \tag{4.3-41}$$

will subsequently appear in the macroscale formulation [cf. (5.3-6)] of our flow problem. Application of the divergence theorem, followed by differentiation by parts, together with the vanishing (4.3-28) of $\widetilde{\mathbf{V}}^0(\mathbf{r})$ on the paricle surfaces and the fact (4.3-27) that $\widetilde{\mathbf{V}}^0(\mathbf{r})$ is divergence free, leads to the equivalent expression

$$\begin{aligned}\overline{\mathbf{V}}^0 &= \frac{1}{\tau_0}\int_{\tau_f}\widetilde{\mathbf{V}}^0(\mathbf{r})\,\mathrm{d}^3\mathbf{r} \\ &\equiv \frac{\tau_f}{\tau_0}\left\langle\widetilde{\mathbf{V}}^0(\mathbf{r})\right\rangle.\end{aligned} \tag{4.3-42}$$

The utility of this expression is that since $\overline{\mathbf{V}}^0$ is expressible as the integral of a spatially periodic function over the domain τ_f, it is then a *lattice constant*; that is, it depends

only upon the lattice configuration, but not upon the particular choice made for the manner in which the spatially periodic geometry is decomposed into unit cells [28].

To determine the properties of $\overline{\mathbf{V}}^0$ defined in (4.3-41), first pre-dot (4.3-26) by $\widetilde{\mathbf{V}}^{0\dagger}$ to obtain

$$\tilde{V}^0_{ki}\nabla_l\nabla_l\tilde{V}^0_{kj} - \tilde{V}^0_{ki}\nabla_k\tilde{\Pi}^0_j - \tilde{V}^0_{ji} = 0.$$

With use of (4.3-27) the previous equation may be rewritten as

$$\nabla_l\left(\tilde{V}^0_{ki}\nabla_l\tilde{V}^0_{kj}\right) - \left(\nabla_l\tilde{V}^0_{ki}\right)\left(\nabla_l\tilde{V}^0_{kj}\right) - \nabla_l\left(\tilde{V}^0_{li}\tilde{\Pi}^0_j\right) - \tilde{V}_{ji} = 0.$$

Integrate the latter over the fluid domain τ_f, use (4.3-42), and rearrange the resulting expression, thereby obtaining

$$-\frac{1}{\tau_0}\int_{\tau_f}\left(\nabla_l\tilde{V}^0_{ki}\right)\left(\nabla_l\tilde{V}^0_{kj}\right)\,\mathrm{d}^3\mathbf{r} = \frac{1}{\tau_0}\int_{\tau_f}\nabla_l\left(\tilde{V}^0_{li}\tilde{\Pi}^0_j - \tilde{V}^0_{ki}\nabla_l\tilde{V}^0_{kj}\right)\,\mathrm{d}^3\mathbf{r} + \overline{V}^0_{ji}.$$

The first term on the right-hand side may be converted into a surface integral over both $\partial\tau_0$ and s_p. The integral over s_p will vanish as a consequence of the no-slip condition (4.3-36) while the integral over $\partial\tau_0$ will vanish as a result of the spatially periodic nature of the integrand. This provides an alternate definition of $\overline{\mathbf{V}}^0$, namely

$$\overline{V}^0_{ij} = -\frac{1}{\tau_0}\int_{\tau_f}\left(\nabla_l V^0_{kj}\right)\left(\nabla_l V^0_{ki}\right)\,\mathrm{d}^3\mathbf{r}. \tag{4.3-43}$$

Since the right-hand side of (4.3-43) is obviously invariant upon exchanging i and j, it follows that $\overline{\mathbf{V}}^0$ is symmetric:

$$\overline{\mathbf{V}}^{0\dagger} = \overline{\mathbf{V}}^0. \tag{4.3-44}$$

Pre- and post-dotting (4.3-43) by an arbitrary constant vector $\boldsymbol{\chi}$ yields

$$\chi_i\overline{V}^0_{ij}\chi_j = -\frac{1}{\tau_0}\int_{\tau_f}\left(\chi_j\nabla_l V^0_{kj}\right)\left(\chi_i\nabla_l V^0_{ki}\right)\,\mathrm{d}^3\mathbf{r}.$$

As a consequence of the nonnegative nature of the integrand at each point $\mathbf{r}$, it follows that

$$-\boldsymbol{\chi}\cdot\overline{\mathbf{V}}^{0}\cdot\boldsymbol{\chi}\geq 0 \qquad \forall(\boldsymbol{\chi}), \tag{4.3-45}$$

whence $\overline{\mathbf{V}}^{0}$ is a negative-definite dyadic. This property implies, *inter alia*, that the determinant as well as the inverse of $\overline{\mathbf{V}}^{0}$ are both well defined. Ultimately, it will be shown that $-\overline{\mathbf{V}}^{0}$ physically represents the permeability dyadic $\mathbf{k}$ of the medium.

4.3.6 Dependence of $\overline{\Psi}^{0}(|\mathbf{R}')$ and $\overline{\mathbf{\Psi}}^{1}(|\mathbf{R}')$ Upon Choice of Reference Point

From (4.3-6) and (4.3-18) the exact microscale velocity field for the present zeroth-order flow field is

$$\mu\mathbf{v}(\mathbf{R_n},\mathbf{r})=\widetilde{\mathbf{V}}^{0}(\mathbf{r})\cdot\overline{\mathbf{\Psi}}^{1}(|\mathbf{R}'), \tag{4.3-46}$$

while from (4.3-14) and (4.3-19) the corresponding microscale pressure field is

$$p(\mathbf{R_n},\mathbf{r})=\overline{\Psi}^{0}(|\mathbf{R}')+\overline{\mathbf{\Psi}}^{1}(|\mathbf{R}')\cdot\{\mathbf{R}-\mathbf{R}'\}+\widetilde{\mathbf{\Pi}}^{0}(\mathbf{r})\cdot\overline{\mathbf{\Psi}}^{1}(|\mathbf{R}'). \tag{4.3-47}$$

As the microscale flow fields $\mathbf{v}(\mathbf{R})\equiv\mathbf{v}(\mathbf{R_n},\mathbf{r})$ and $p(\mathbf{R})\equiv p(\mathbf{R_n},\mathbf{r})$ are both independent of the choice of reference point $\mathbf{R}'$, a different choice of reference point, say $\mathbf{R}''$, necessarily yields the identical fields $\mathbf{v}$ and p. Equate the velocity and pressure fields for a given flow $(\mathbf{v},p)$ characterized by the constants $\left\{\overline{\Psi}^{0}(|\mathbf{R}'),\overline{\mathbf{\Psi}}^{1}(|\mathbf{R}')\right\}$ with the identical velocity and pressure fields characterized by the different set of constants $\left\{\overline{\Psi}^{0}(|\mathbf{R}''),\overline{\mathbf{\Psi}}^{1}(|\mathbf{R}'')\right\}$ arising from the choice of $\mathbf{R}''$ as the reference point. In this context, equality of the velocity fields yields

$$\widetilde{\mathbf{V}}^{0}(\mathbf{r})\cdot\overline{\mathbf{\Psi}}^{1}(|\mathbf{R}')=\widetilde{\mathbf{V}}^{0}(\mathbf{r})\cdot\overline{\mathbf{\Psi}}^{1}(|\mathbf{R}''),$$

whereas equality of the pressure fields gives

$$\overline{\Psi}^{0}(|\mathbf{R}')+\overline{\mathbf{\Psi}}^{1}(|\mathbf{R}')\cdot\{\mathbf{R}-\mathbf{R}'\}+\widetilde{\mathbf{\Pi}}^{0}(\mathbf{r})\cdot\overline{\mathbf{\Psi}}^{1}(|\mathbf{R}')$$

$$= \quad \overline{\Psi}^0(|\mathbf{R}'') + \overline{\Psi}^1(|\mathbf{R}'') \cdot \{\mathbf{R} - \mathbf{R}''\} + \widetilde{\Pi}^0(\mathbf{r}) \cdot \overline{\Psi}^1(|\mathbf{R}'').$$

Since these expressions must match for all choices of $\mathbf{R}$, it follows that

$$\overline{\Psi}^1(|\mathbf{R}'') = \overline{\Psi}^1(|\mathbf{R}') = \overline{\Psi}^1, \text{ say} \tag{4.3-48}$$

and

$$\overline{\Psi}^0(|\mathbf{R}'') = \overline{\Psi}^0(|\mathbf{R}') + \overline{\Psi}^1 \cdot \{\mathbf{R}'' - \mathbf{R}'\}, \tag{4.3-49}$$

expressing the changes in the value of these constants with different choices of reference point. This also shows that the choice of reference point is somewhat arbitrary, since knowledge of these constants for one particular reference point implies that they are known for any other choice of reference point. Furthermore, for this zeroth-order flow field the vector $\overline{\Psi}^1$ is a true constant, independent of reference point.

4.3.7 Summary of Truncated Zeroth-order Flow

The zeroth-order microscale velocity field—initially defined by truncating the discrele Taylor series (4.2-6) at one term—can be expressed via (4.3-6), (4.3-18) and (4.3-48) in the form

$$\mu \mathbf{v}(\mathbf{R}) = \widetilde{\mathbf{V}}^0(\mathbf{r}) \cdot \overline{\Psi}^1, \tag{4.3-50}$$

whereas the corresponding microscale pressure field can be obtained from (4.3-14), (4.3-19) and (4.3-18) as

$$p(\mathbf{R}) = \overline{\Psi}^0(|\mathbf{R}') + \overline{\Psi}^1 \cdot \{\mathbf{R} - \mathbf{R}'\} + \widetilde{\Pi}^0(\mathbf{r}) \cdot \overline{\Psi}^1. \tag{4.3-51}$$

The preceding pair of relations correspond to a spatially periodic flow field, with the pressure varying linearly on the macroscale $\mathbf{R_n}$. All the microscale details of the flow are contained in the fully spatially periodic functions $\widetilde{\mathbf{V}}^0(\mathbf{r})$ and $\widetilde{\Pi}^0(\mathbf{r})$, which form the $\mathcal{O}(0)$ *cell problem.* Expicitly from (4.3-26) to (4.3-29):

$\mathcal{O}(0)$ *cell problem:*

$$
\begin{aligned}
\nabla^2\widetilde{\mathbf{V}}^0 - \boldsymbol{\nabla}\widetilde{\boldsymbol{\Pi}}^0 &= \mathbf{I}, \\
\boldsymbol{\nabla}\cdot\widetilde{\mathbf{V}}^0 &= \mathbf{0}, \\
\widetilde{\mathbf{V}}^0 &= \mathbf{0} \qquad \forall\left(\mathbf{r}\in s_p\right), \\
\left\langle\widetilde{\boldsymbol{\Pi}}^0\right\rangle &= \mathbf{0}.
\end{aligned}
\tag{4.3-52}
$$

This zero-order problem uniquely defines the fields $\left(\widetilde{\mathbf{V}},\widetilde{\boldsymbol{\Pi}}\right)$ which are determined entirely from the geometry of the unit cell (independently of the arbitrary choice of cell shape); that is, they are 'lattice fields'. All the macroscale details are embodied within the constants $\overline{\Psi}^0(|\mathbf{R}')$ and $\overline{\boldsymbol{\Psi}}^1$, wherein the dependence of $\overline{\Psi}^0(|\mathbf{R}')$ upon the choice of reference point is given by Eq. (4.3-49) as

$$
\overline{\Psi}^0(|\mathbf{R}'') = \overline{\Psi}^0(|\mathbf{R}') + \overline{\boldsymbol{\Psi}}^1\cdot\{\mathbf{R}''-\mathbf{R}'\}\,. \tag{4.3-53}
$$

4.4 Truncated First-order Microscale Flow

In this subsection we truncate the discrete Taylor series (4.2-6) for $\mathbf{v}(\mathbf{R})$ at two terms and determine the corresponding form of the pressure field.

4.4.1 Microscale Velocity, $\mathbf{v}(\mathbf{R})$

Retain only the first two tensors in (4.2-6) by setting

$$\mathbf{v}^m(\mathbf{r}|\mathbf{R}') = \mathbf{0} \qquad \forall\,(m = 2, 3, 4, \ldots) \tag{4.4-1}$$

such that the discrete form of the Taylor series yields the microscale velocity field

$$\mathbf{v}\left(\mathbf{R_n}, \mathbf{r}\right) = \mathbf{v}^0(\mathbf{r}|\mathbf{R}') + \mathbf{v}^1(\mathbf{r}|\mathbf{R}') \cdot \{\mathbf{R_n} - \mathbf{R}'\}\,. \tag{4.4-2}$$

Use the jump condition imposed upon $\mathbf{v}^1(\mathbf{r}|\mathbf{R}')$ by setting $m = 1$ in (4.2-18), along with the choice (4.4-1), and write

$$\left\|\boldsymbol{\nabla}^i \mathbf{v}^1(\mathbf{r}|\mathbf{R}')\right\| = \mathbf{0} \qquad \forall\,(i = 0, 1, 2, \ldots)\,. \tag{4.4-3}$$

The latter immediately implies as a consequence of (3.4-3) that this first-order field is *fully* spatially periodic:

$$\mathbf{v}^1(\mathbf{r}|\mathbf{R}') = \widetilde{\mathbf{v}}^1(\mathbf{r}|\mathbf{R}'). \tag{4.4-4}$$

Now determine the form of $\mathbf{v}^0(\mathbf{r}|\mathbf{R}')$ by setting $m = 0$ in the jump condition (4.2-19) and combine this with the choice (4.4-1) and (4.4-4) to obtain

$$\left\|\boldsymbol{\nabla}^i \mathbf{v}^0(\mathbf{r}|\mathbf{R}')\right\| = \left\|\boldsymbol{\nabla}^i \left[\widetilde{\mathbf{v}}^1(\mathbf{r}|\mathbf{R}') \cdot \mathbf{r}\right]\right\| \qquad \forall\,(i = 0, 1, 2, \ldots)\,, \tag{4.4-5}$$

which again implies that $\mathbf{v}^0(\mathbf{r}|\mathbf{R}')$ is of the form

$$\mathbf{v}^0(\mathbf{r}|\mathbf{R}') = \widetilde{\mathbf{v}}^0(\mathbf{r}|\mathbf{R}') + \widetilde{\mathbf{v}}^1(\mathbf{r}|\mathbf{R}') \cdot \mathbf{r} \tag{4.4-6}$$

and consists of both a *fully* spatially periodic part and a second *fully* spatially periodic part multiplied by $\mathbf{r}$.

For this first order flow, Eqs. (4.4-2), (4.4-4) and (4.4-6) show that the tensor $\mathbf{v}^m(\mathbf{r}|\mathbf{R}')$ is of the form

$$\mathbf{v}^m = \begin{cases} \tilde{\mathbf{v}}^0 + \tilde{\mathbf{v}}^1 \cdot \mathbf{r} & (m = 0), \\ \tilde{\mathbf{v}}^1 & (m = 1), \\ \mathbf{0} & \forall (m = 2, 3, 4, \ldots). \end{cases} \tag{4.4-7}$$

Accordingly, the first-order microscale velocity field (4.4-2) may be rewritten as

$$\mathbf{v}(\mathbf{R_n}, \mathbf{r}) = \tilde{\mathbf{v}}^0(\mathbf{r}|\mathbf{R}') + \tilde{\mathbf{v}}^1(\mathbf{r}|\mathbf{R}') \cdot \{\mathbf{R} - \mathbf{R}'\}, \tag{4.4-8}$$

where it is important to note that the last term on the right-hand side is dotted by $\mathbf{R}$ and not $\mathbf{R_n}$ as in (4.4-2). Comparing (4.4-8) to (4.3-6) it is apparent that the form of this first-order flow is composed of a fully spatially periodic part $\tilde{\mathbf{v}}^0$ and a second fully spatially periodic piece multiplied by the continuous position vector $\mathbf{R}$. However, the functions $\tilde{\mathbf{v}}^0$ appearing in both (4.3-6) and (4.4-8) are *not* the same [cf. (4.3-18) and (4.4-33)].

4.4.2 Microscale Pressure, $p(\mathbf{R})$

Similar to (4.3-7), Eqs. (4.2-12) and (4.4-7) combine to give

$$\boldsymbol{\nabla} \mathbf{p}^m = \mathbf{0} \qquad \forall (m = 2, 3, 4, \ldots), \tag{4.4-9}$$

implying that for $m \geq 2$ these tensors are at most constants:

$$\mathbf{p}^m(\mathbf{r}|\mathbf{R}') = \overline{\boldsymbol{\Psi}}^m(|\mathbf{R}') \qquad \forall (m = 2, 3, 4, \ldots). \tag{4.4-10}$$

Use of the jump condition (4.2-20) for $m \geq 2$ and $i = 0$ (note that the cases $i \geq 1$ and $m \geq 2$ yield the trivial solution $\mathbf{0} = \mathbf{0}$) in conjunction with the above shows that

$$\overline{\Psi}^m(|\mathbf{R}') = \mathbf{0} \qquad \forall\,(m = 3, 4, 5, \ldots)\,. \tag{4.4-11}$$

Write the jump condition (4.2-21) for $m = 1$ and use (4.4-10) and (4.4-11) to obtain

$$\left\|\boldsymbol{\nabla}^i \mathbf{p}^1(\mathbf{r}|\mathbf{R}')\right\| = \left\|\boldsymbol{\nabla}^i \left[\overline{\Psi}^2(|\mathbf{R}') \cdot \mathbf{r}\right]\right\| \qquad \forall\,(i = 0, 1, 2, \ldots)\,, \tag{4.4-12}$$

implying that $\mathbf{p}^1(\mathbf{r}|\mathbf{R}')$ is of the form

$$\mathbf{p}^1(\mathbf{r}|\mathbf{R}') = \tilde{\mathbf{p}}^1(\mathbf{r}|\mathbf{R}') + \overline{\Psi}^2(|\mathbf{R}') \cdot \mathbf{r}. \tag{4.4-13}$$

Next, set $m = 0$ in (4.2-21) and use (4.4-10), (4.4-11) and (4.4-13) to derive the expression

$$\left\|\boldsymbol{\nabla}^i p^0\right\| = \left\|\boldsymbol{\nabla}^i \left[\tilde{\mathbf{p}}^1 \cdot \mathbf{r}\right]\right\| + \frac{1}{2}\left\|\boldsymbol{\nabla}^i \left[\overline{\Psi}^2 : \mathbf{rr}\right]\right\| \qquad \forall\,(i = 0, 1, 2, \ldots)\,. \tag{4.4-14}$$

In this expression the explicit dependence of the various terms upon $\mathbf{r}$ and $\mathbf{R}'$ has been suppressed. The preceding equation implies that $p^0(\mathbf{r}|\mathbf{R}')$ is of the form

$$p^0(\mathbf{r}|\mathbf{R}') = \tilde{p}^0(\mathbf{r}|\mathbf{R}') + \tilde{\mathbf{p}}^1(\mathbf{r}|\mathbf{R}') \cdot \mathbf{r} + \frac{1}{2}\overline{\Psi}^2(|\mathbf{R}') : \mathbf{rr}. \tag{4.4-15}$$

Ultimately, from (4.4-10), (4.4-11), (4.4-13) and (4.4-15) the tensor $\mathbf{p}^m(\mathbf{r}|\mathbf{R}')$ is

found to be

$$\mathbf{p}^m = \begin{cases} \tilde{p}^0 + \tilde{\mathbf{p}}^1 \cdot \mathbf{r} + \frac{1}{2}\overline{\Psi}^2 : \mathbf{rr} & (m=0), \\ \tilde{\mathbf{p}}^1 + \overline{\Psi}^2 \cdot \mathbf{r} & (m=1), \\ \overline{\Psi}^2 & (m=2), \\ \mathbf{0} & \forall (m = 3,4,5,\ldots). \end{cases} \tag{4.4-16}$$

This constitutes the counterpart of (4.4-7). Moreover, the microscale pressure field for the present truncated first-order flow may be written as

$$p(\mathbf{R_n}, \mathbf{r}) = \tilde{p}^0(\mathbf{r}|\mathbf{R}') + \tilde{\mathbf{p}}^1(\mathbf{r}|\mathbf{R}') \cdot \{\mathbf{R} - \mathbf{R}'\} + \frac{1}{2}\overline{\Psi}^2(|\mathbf{R}') : \{\mathbf{R} - \mathbf{R}'\}^2 . \tag{4.4-17}$$

It follows from the definition of $\mathbf{p}^m(\mathbf{r}|\mathbf{R}')$ [see (4.2-9)] that the dyadic $\overline{\Psi}^2(|\mathbf{R}')$ is symmetric. As was the case with the truncated zeroth-order flow problem, we wish to separate out from $\tilde{\mathbf{v}}^m(\mathbf{r}|\mathbf{R}')$ and $\tilde{\mathbf{p}}^m(\mathbf{r}|\mathbf{R}')$ their explicit dependence upon the choice of reference point $\mathbf{R}'$. By so doing, the decomposition is thereby separated into its microscale and macroscale elements.

4.4.3 Solution of $\tilde{\mathbf{v}}^1(\mathbf{r}|\mathbf{R}')$ and $\tilde{\mathbf{p}}^1(\mathbf{r}|\mathbf{R}')$

Set $m = 1$ in Eqs. (4.2-12) to (4.2-14) and introduce the forms of $\mathbf{v}^1(\mathbf{r}|\mathbf{R}')$ and $\mathbf{p}^1(\mathbf{r}|\mathbf{R}')$ as in (4.4-7) and (4.4-16):

$$\mu\nabla^2\tilde{\mathbf{v}}^1 - \boldsymbol{\nabla}\tilde{\mathbf{p}}^1 = \overline{\Psi}^2, \tag{4.4-18}$$

$$\boldsymbol{\nabla} \cdot \tilde{\mathbf{v}}^1 = \mathbf{0}, \tag{4.4-19}$$

$$\tilde{\mathbf{v}}^1 = \mathbf{0} \qquad \forall (\mathbf{r} \in s_p) . \tag{4.4-20}$$

The symmetry of $\overline{\Psi}^2(|\mathbf{R}')$ has been employed in deriving (4.4-18). As in the truncated zeroth-order flow problem, the goal is to remove from these equations their dependence upon $\overline{\Psi}^2(|\mathbf{R}')$. At first thought one might suppose (since these equations are linear

in the dyadic $\overline{\Psi}^2$) that the dyadic $\tilde{\mathbf{v}}^1$ is necessarily of the form $\tilde{\mathbf{v}}^1 = \mathbf{A} : \overline{\Psi}^2$, where $\mathbf{A}$ is a 4th rank tensor (together with a similar decoupling for $\tilde{\mathbf{p}}^1$). However, the problem is even simpler since the dyadic equations (4.4-18) to (4.4-20) uncouple with respect to the last tensoral index. Explicitly, if one defines: (i) the vector $\mathbf{F}^j$ as the jth column of the dyadic ('matrix') $\tilde{\mathbf{v}}^1$

$$F_i^j \stackrel{\text{def}}{=} \tilde{v}_{ij}^1 \; ;$$

(ii) the scalar f^j as the jth component of vector $\tilde{\mathbf{p}}^1$

$$f^j \stackrel{\text{def}}{=} \tilde{p}_j^1 \; ;$$

(iii) and the vector $\overline{\mathbf{G}}^j$ as the jth column of the dyadic $\overline{\Psi}^2$

$$\overline{G}_i^j \stackrel{\text{def}}{=} \overline{\Psi}_{ij}^2 \; ,$$

then Eqs. (4.4-18) to (4.4-20) may be rewritten in terms of $\mathbf{F}^j$, f^j and $\overline{\mathbf{G}}^j$. The resulting equations, namely

$$\begin{aligned} \mu\nabla^2\mathbf{F}^j - \boldsymbol{\nabla} f^j &= \overline{\mathbf{G}}^j, \\ \boldsymbol{\nabla}\cdot\mathbf{F}^j &= 0, \\ \mathbf{F}^j &= \mathbf{0} \qquad \forall\,(\mathbf{r}\in s_p)\,, \end{aligned}$$

valid for $j = 1, 2, \ldots, M$, are identical to those governing $\tilde{\mathbf{v}}^0$ and $\tilde{p}^0$ of the truncated zeroth-order flow, namely Eqs. (4.3-15) to (4.3-17). Ultimately, as in (4.3-18) and (4.3-19), this enables the dyadic field $\tilde{\mathbf{v}}^1(\mathbf{r}|\mathbf{R}')$ and the vector field $\tilde{\mathbf{p}}^1(\mathbf{r}|\mathbf{R}')$ to be written in the respective forms

$$\mu\tilde{\mathbf{v}}^1(\mathbf{r}|\mathbf{R}') = \widetilde{\mathbf{V}}^0(\mathbf{r})\cdot\overline{\Psi}^2(|\mathbf{R}'), \tag{4.4-21}$$

$$\tilde{\mathbf{p}}^1(\mathbf{r}|\mathbf{R}') = \overline{\Psi}^1(|\mathbf{R}') + \widetilde{\Pi}^0(\mathbf{r})\cdot\overline{\Psi}^2(|\mathbf{R}'), \tag{4.4-22}$$

where $\widetilde{\mathbf{V}}^0(\mathbf{r})$ and $\widetilde{\mathbf{\Pi}}^0(\mathbf{r})$ are the solutions of the $\mathcal{O}(0)$ *cell problem* (4.3-52). The constant vector $\overline{\mathbf{\Psi}}^1(|\mathbf{R}')$, defined as

$$\overline{\mathbf{\Psi}}^1(|\mathbf{R}') \stackrel{\text{def}}{=} \left\langle \tilde{\mathbf{p}}^1(\mathbf{r}|\mathbf{R}') \right\rangle, \tag{4.4-23}$$

has been included to remove the arbitrary constant vector from $\tilde{\mathbf{p}}^1(\mathbf{r}|\mathbf{R}')$.

4.4.4 First Auxiliary Condition

Essentially, (4.4-8) is equivalent to a macroscale shearing motion. As such, there exists a restriction imposed upon $\tilde{\mathbf{v}}^1(\mathbf{r}|\mathbf{R}')$ owing to fluid incompressibility. This auxiliary condition can be quantified by setting $m = 0$ in (4.2-13) and integrating over the fluid domain:

$$\frac{1}{\tau_0} \int_{\tau_f} \boldsymbol{\nabla} \cdot \mathbf{v}^0 \, \mathrm{d}^3\mathbf{r} = 0.$$

In the latter use the divergence theorem together with the facts that: (i) $\mathbf{v}^0$ vanishes on s_p (4.2-14); (ii) $\mathbf{v}^0$ is given by (4.4-6); (iii) surface integrals of spatially periodic functions over $\partial\tau_0$ vanish. This yields

$$\frac{1}{\tau_0} \oint_{\partial\tau_0} \mathrm{d}\mathbf{S} \cdot \tilde{\mathbf{v}}^1 \cdot \mathbf{r} = 0. \tag{4.4-24}$$

Equivalently, from (4.4-21),

$$\frac{1}{\tau_0} \oint_{\partial\tau_0} \mathrm{d}\mathbf{S} \cdot \left(\widetilde{\mathbf{V}}^0 \cdot \overline{\mathbf{\Psi}}^2 \right) \cdot \mathbf{r} = 0,$$

which may be rewritten as

$$\left(\frac{1}{\tau_0} \oint \mathbf{r} \mathrm{d}\mathbf{S} \cdot \widetilde{\mathbf{V}}^0 \right) : \overline{\mathbf{\Psi}}^2 = 0.$$

However, the term in parentheses is simply the truncated zeroth-order dyadic $\overline{\mathbf{V}}^0$ given by (4.3-41). Consequently,

$$\overline{\mathbf{V}}^0 : \overline{\mathbf{\Psi}}^2 = 0 \tag{4.4-25}$$

or

$$\left\langle \widetilde{\mathbf{V}}^0(\mathbf{r}) \right\rangle : \overline{\mathbf{\Psi}}^2(|\mathbf{R}') = 0. \tag{4.4-26}$$

Hereafter, the restriction (4.4-25) or (4.4-26) will be termed *auxiliary condition* #1.

Since $\overline{\mathbf{V}}^0$ is not singular, but is rather a negative-definite dyadic, Eq. (4.4-25) places a restriction upon the choice of the symmetric dyadic $\overline{\mathbf{\Psi}}^2(|\mathbf{R}')$ for incompressibility to be retained. This is similar to the restriction imposed upon the velocity gradient dyadic $\mathbf{G}$ for an arbitrary shear flow, $\mathbf{v} = \mathbf{G} \cdot \mathbf{R}$, requiring that $\mathbf{I} : \mathbf{G} = 0$ in order that the incompressibility condition $\boldsymbol{\nabla} \cdot \mathbf{v} = 0$ be satisfied.

4.4.5 Solution of $\tilde{\mathbf{v}}^0(r|\mathbf{R}')$ and $\tilde{p}^0(\mathbf{r}|\mathbf{R}')$

Combine $\mathbf{v}^0(\mathbf{r}|\mathbf{R}')$ and $p^0(\mathbf{r}|\mathbf{R}')$ given in (4.4-7) and (4.4-16) with the solutions $\tilde{\mathbf{v}}^1(\mathbf{r}|\mathbf{R}')$ and $\tilde{\mathbf{p}}^1(\mathbf{r}|\mathbf{R}')$ appearing in (4.4-21) and (4.4-22) to obtain the alternative expressions

$$\mu \mathbf{v}^0 = \mu \tilde{\mathbf{v}}^0 + \widetilde{\mathbf{V}}^0 \cdot \overline{\mathbf{\Psi}}^2 \cdot \mathbf{r}, \tag{4.4-27}$$

$$p^0 = \tilde{p}^0 + \overline{\mathbf{\Psi}}^1 \cdot \mathbf{r} + \widetilde{\mathbf{\Pi}}^0 \cdot \overline{\mathbf{\Psi}}^2 \cdot \mathbf{r} + \frac{1}{2} \overline{\mathbf{\Psi}}^2 : \mathbf{rr}. \tag{4.4-28}$$

Set $m = 0$ in (4.2-12) to (4.2-14) and use the previous two equations to derive the following intermediate equations governing the fully spatially periodic fields $\tilde{\mathbf{v}}^0(\mathbf{r}|\mathbf{R}')$ and $\tilde{p}^0(\mathbf{r}|\mathbf{R}')$:

$$\mu \nabla^2 \tilde{\mathbf{v}}^0 - \boldsymbol{\nabla} \tilde{p}^0 = \overline{\mathbf{\Psi}}^1 + \left[\mathbf{I} \widetilde{\mathbf{\Pi}}^0 - 2^{\dagger} \left(\boldsymbol{\nabla} \widetilde{\mathbf{V}}^0 \right) \right] : \overline{\mathbf{\Psi}}^2 - \left[\nabla^2 \widetilde{\mathbf{V}}^0 - \boldsymbol{\nabla} \widetilde{\mathbf{\Pi}}^0 - \mathbf{I} \right] \cdot \overline{\mathbf{\Psi}}^2 \cdot \mathbf{r},$$

$$\mu \boldsymbol{\nabla} \cdot \tilde{\mathbf{v}}^0 = -\widetilde{\mathbf{V}}^0 : \overline{\boldsymbol{\Psi}}^2 - \left[\boldsymbol{\nabla} \cdot \widetilde{\mathbf{V}}^0\right] \cdot \overline{\boldsymbol{\Psi}}^2 \cdot \mathbf{r},$$

$$\mu \tilde{\mathbf{v}}^0 = -\widetilde{\mathbf{V}}^0 \cdot \overline{\boldsymbol{\Psi}}^2 \cdot \mathbf{r} \qquad \forall (\mathbf{r} \in s_p).$$

In light of the $\mathcal{O}(0)$ *cell problem* (4.3-52) and the fact that $\overline{\boldsymbol{\Psi}}^2(|\mathbf{R}')$ is a symmetric dyadic, these governing equations may be rewritten without any loss of generality as

$$\mu \nabla^2 \tilde{\mathbf{v}}^0 - \boldsymbol{\nabla} \tilde{p}^0 = \overline{\boldsymbol{\Psi}}^1 + \left[\!\!\left[\mathbf{I}\widetilde{\boldsymbol{\Pi}}^0 - 2^{\dagger}\left(\boldsymbol{\nabla}\widetilde{\mathbf{V}}^0\right) \right]\!\!\right]^{s2} : \overline{\boldsymbol{\Psi}}^2, \tag{4.4-29}$$

$$\mu \boldsymbol{\nabla} \cdot \tilde{\mathbf{v}}^0 = -\left[\!\!\left[\widetilde{\mathbf{V}}^0 \right]\!\!\right]^{s} : \overline{\boldsymbol{\Psi}}^2, \tag{4.4-30}$$

$$\mu \tilde{\mathbf{v}}^0 = \mathbf{0} \qquad \forall (\mathbf{r} \in s_p). \tag{4.4-31}$$

Notationally, $\left[\!\!\left[\mathbf{A} \right]\!\!\right]^{sn}$ is the symmetrization operator defined in (3.3-13) but only with respect to the *last n* indices of the general tensor $\mathbf{A}$. It is obvious that integrating the continuity condition (4.4-30) over the fluid domain and using the divergence theorem along with the other properties of $\tilde{\mathbf{v}}^0(\mathbf{r}|\mathbf{R}')$ reproduces *auxiliary condition* #1, namely Eqs. (4.4-25) or (4.4-26), restricting the value of $\overline{\boldsymbol{\Psi}}^2(|\mathbf{R}')$.

As Eqs. (4.4-29) to (4.4-31) are linear in $\overline{\boldsymbol{\Psi}}^1(|\mathbf{R}')$ and $\overline{\boldsymbol{\Psi}}^2(|\mathbf{R}')$, the latter constants can be removed from the governing equations. In particular the vector $\overline{\boldsymbol{\Psi}}^1(|\mathbf{R}')$ may be removed in exactly the same manner as in the truncated zeroth-order flow problem via the decompositions (4.3-18) and (4.3-19). In a similar manner, one might envision removing the dyadic $\overline{\boldsymbol{\Psi}}^2(|\mathbf{R}')$ by supposing its dependence upon $\tilde{\mathbf{v}}^0(\mathbf{r}|\mathbf{R}')$ to be of the form $\tilde{\mathbf{v}}^0 = \widetilde{\mathbf{A}} : \overline{\boldsymbol{\Psi}}^2$, with $\widetilde{\mathbf{A}}(\mathbf{r})$ a third rank tensor field. Unfortunately, this would lead to (4.4-30) adopting the form $\boldsymbol{\nabla} \cdot \widetilde{\mathbf{A}} = -\widetilde{\mathbf{V}}^0$, which upon integrating this continuity condition over the fluid volume τ_f and recognizing (4.3-42) would lead to the inconsistent requirement that $\overline{\mathbf{V}}^0 = \mathbf{0}$. This error arises because $\overline{\boldsymbol{\Psi}}^2(|\mathbf{R}')$ is not a totally arbitrary dyadic, but rather must obey *auxiliary condition* #1, Eqs. (4.4-25) or (4.4-26).

This problem may be rectified by rewriting (4.4-30) as

$$\mu\boldsymbol{\nabla}\cdot\tilde{\mathbf{v}}^0 = -\Big[\!\Big[\,\widetilde{\mathbf{V}}^0 - \big\langle\widetilde{\mathbf{V}}^0\big\rangle\,\Big]\!\Big]^s : \overline{\boldsymbol{\Psi}}^2, \tag{4.4-32}$$

without loss of generality. This *ansatz* removes the difficulty described previously, enabling us to postulate a solution of Eqs. (4.4-29), (4.4-31) and (4.4-32) of the form

$$\begin{aligned}\mu\tilde{\mathbf{v}}^0(\mathbf{r}|\mathbf{R}') \;&\stackrel{\text{def}}{=}\; \widetilde{\mathbf{V}}^0(\mathbf{r})\cdot\overline{\boldsymbol{\Psi}}^1(|\mathbf{R}') \\ &\quad +\widetilde{\mathbf{V}}^1(\mathbf{r}) : \overline{\boldsymbol{\Psi}}^2(|\mathbf{R}'),\end{aligned} \tag{4.4-33}$$

$$\begin{aligned}\tilde{p}^0(\mathbf{r}|\mathbf{R}'_{\mathbf{n}}) \;&\stackrel{\text{def}}{=}\; \overline{\Psi}^0(|\mathbf{R}') + \widetilde{\boldsymbol{\Pi}}^0(\mathbf{r})\cdot\overline{\boldsymbol{\Psi}}^1(|\mathbf{R}') \\ &\quad +\widetilde{\boldsymbol{\Pi}}^1(\mathbf{r}) : \overline{\boldsymbol{\Psi}}^2(|\mathbf{R}').\end{aligned} \tag{4.4-34}$$

Appearing in these expressions are the triadic field $\widetilde{\mathbf{V}}^1(\mathbf{r})$ and the dyadic field $\widetilde{\boldsymbol{\Pi}}^1(\mathbf{r})$, with

$$\overline{\Psi}^0(|\mathbf{R}') \stackrel{\text{def}}{=} \big\langle\tilde{p}^0(\mathbf{r}|\mathbf{R}')\big\rangle \tag{4.4-35}$$

included to remove the arbitrary constant in $\tilde{p}^0(\mathbf{r}|\mathbf{R}')$. The characteristic problem satisfied by $\widetilde{\mathbf{V}}^1(\mathbf{r})$ and $\widetilde{\boldsymbol{\Pi}}^1(\mathbf{r})$ is then

$$\nabla^2\widetilde{\mathbf{V}}^1 - \boldsymbol{\nabla}\widetilde{\boldsymbol{\Pi}}^1 \;=\; \Big[\!\Big[\,\mathbf{I}\widetilde{\boldsymbol{\Pi}}^0 - 2^\dagger\big(\boldsymbol{\nabla}\widetilde{\mathbf{V}}^0\big)\,\Big]\!\Big]^{s2}, \tag{4.4-36}$$

$$\boldsymbol{\nabla}\cdot\widetilde{\mathbf{V}}^1 \;=\; -\Big[\!\Big[\,\widetilde{\mathbf{V}}^0 - \big\langle\widetilde{\mathbf{V}}^0\big\rangle\,\Big]\!\Big]^s, \tag{4.4-37}$$

$$\widetilde{\mathbf{V}}^1 \;=\; \mathbf{0} \qquad \forall\,(\mathbf{r}\in s_p)\,, \tag{4.4-38}$$

together with the normalization condition

$$\big\langle\widetilde{\boldsymbol{\Pi}}^1\big\rangle = \mathbf{0} \tag{4.4-39}$$

and the fact that these fields are *fully* spatially periodic.

Equations (4.4-36) to (4.4-39) constitute the $\mathcal{O}(1)$ *cell problem.* This problem is devoid of all arbitrary constants and fluid rheology. As such, the fields $\widetilde{\mathbf{V}}^1(\mathbf{r})$ and $\widetilde{\mathbf{\Pi}}^1(\mathbf{r})$ are uniquely defined by the unit cell geometry. Furthermore, the form of the inhomogeneous, forcing terms on the right-hand sides of (4.4-36) and (4.4-37) is such that the triadic field $\widetilde{\mathbf{V}}^1(\mathbf{r})$ is symmetric with respect to its *last* two indices, while the dyadic field $\widetilde{\mathbf{\Pi}}^1(\mathbf{r})$ is symmetric with respect to *all* its indices.

4.4.6 Uniqueness of $\widetilde{\mathbf{V}}^1(\mathbf{r})$ and $\widetilde{\mathbf{\Pi}}^1(\mathbf{r})$

As in §4.3.4, uniqueness will be proved by first assuming that there exist at least two solutions, $\left(\widetilde{\mathbf{V}}', \widetilde{\mathbf{\Pi}}'\right)$ and $\left(\widetilde{\mathbf{V}}'', \widetilde{\mathbf{\Pi}}''\right)$, of the system of equations (4.4-36) to (4.4-39). Uniqueness is demonstrated by proving that the quantities $\left(\widetilde{\mathbf{V}}, \widetilde{\mathbf{\Pi}}\right)$ defined as

$$\widetilde{\mathbf{V}} \stackrel{\text{def}}{=} \widetilde{\mathbf{V}}' - \widetilde{\mathbf{V}}'', \tag{4.4-40}$$

$$\widetilde{\mathbf{\Pi}} \stackrel{\text{def}}{=} \widetilde{\mathbf{\Pi}}' - \widetilde{\mathbf{\Pi}}'' \tag{4.4-41}$$

vanish identically:

$$\widetilde{\mathbf{V}} = \mathbf{0}, \tag{4.4-42}$$

$$\widetilde{\mathbf{\Pi}} = \mathbf{0}. \tag{4.4-43}$$

As the primed and double-primed fields each satisfy (4.4-36) to (4.4-39), and the uniqueness of $\widetilde{\mathbf{V}}^0$ and $\widetilde{\mathbf{\Pi}}^0$ (and of course $\left\langle \widetilde{\mathbf{V}}^0 \right\rangle$) was shown in §4.3.4, it follows from the linearity of these equations that $\left(\widetilde{\mathbf{V}}, \widetilde{\mathbf{\Pi}}\right)$ satisfy the system of equations

$$\nabla^2 \widetilde{\mathbf{V}} = \boldsymbol{\nabla} \widetilde{\mathbf{\Pi}}, \tag{4.4-44}$$

$$\boldsymbol{\nabla} \cdot \widetilde{\mathbf{V}} = \mathbf{0}, \tag{4.4-45}$$

$$\widetilde{\mathbf{V}} = \mathbf{0} \qquad \forall \left(\mathbf{r} \in s_p\right), \tag{4.4-46}$$

$$\left\langle \widetilde{\mathbf{\Pi}} \right\rangle = \mathbf{0}. \tag{4.4-47}$$

As in §4.3.4, triple-dot multiply (4.4-44) by $\widetilde{\mathbf{V}}$ (contracting equivalent indices),

employ differentiation by parts, utilize (4.4-45), integrate the result over τ_f, use the divergence theorem, apply (4.4-46) to the integral over s_p, and finally observe that surface integrals of spatially periodic functions over $\partial\tau_0$ vanish. These arguments eventually yield

$$\int_{\tau_f} \left(\nabla_l \tilde{V}_{ijk}\right)\left(\nabla_l \tilde{V}_{ijk}\right)\, \mathrm{d}^3\mathbf{r} = 0. \tag{4.4-48}$$

As a consequence of the nonnegative nature of this quadratic integrand at each point $\mathbf{r} \in \tau_f$, the tetradic quantity $\boldsymbol{\nabla}\widetilde{\mathbf{V}}$ must itself be identically zero, implying that $\widetilde{\mathbf{V}}$ is at most a constant. But from (4.4-46) the value of this constant must be identically zero, thereby proving (4.4-42). It then follows from (4.4-42) and (4.4-44) that $\boldsymbol{\nabla}\widetilde{\boldsymbol{\Pi}} = \mathbf{0}$ at all points $\mathbf{r} \in \tau_f$, implying $\widetilde{\boldsymbol{\Pi}}$ is at most a constant. However, from (4.4-47) this constant is identically zero, thereby proving (4.4-43). (Q.E.D.)

4.4.7 Dependence of $\overline{\boldsymbol{\Psi}}^m(|\mathbf{R}')$ upon the Choice of Reference Point

Upon combining Eqs. (4.4-8), (4.4-21) and (4.4-33), the exact microscale velocity field describing this truncated first-order flow field is

$$\begin{aligned} \mu\mathbf{v}(\mathbf{R_n}, \mathbf{r}) &= \widetilde{\mathbf{V}}^0(\mathbf{r}) \cdot \left[\overline{\boldsymbol{\Psi}}^1(|\mathbf{R}') + \overline{\boldsymbol{\Psi}}^2(|\mathbf{R}') \cdot \{\mathbf{R} - \mathbf{R}'\}\right] \\ &\quad + \widetilde{\mathbf{V}}^1(\mathbf{r}) : \overline{\boldsymbol{\Psi}}^2(|\mathbf{R}'). \end{aligned} \tag{4.4-49}$$

Substitution of (4.4-22) and (4.4-34) into (4.4-17) yields the corresponding microscale pressure field, namely

$$\begin{aligned} p(\mathbf{R_n}, \mathbf{r}) &= \overline{\boldsymbol{\Psi}}^0(|\mathbf{R}') + \overline{\boldsymbol{\Psi}}^1(|\mathbf{R}') \cdot \{\mathbf{R} - \mathbf{R}'\} + \frac{1}{2}\overline{\boldsymbol{\Psi}}^2(|\mathbf{R}') : \{\mathbf{R} - \mathbf{R}'\}^2 \\ &\quad + \widetilde{\boldsymbol{\Pi}}^0(\mathbf{r}) \cdot \left[\overline{\boldsymbol{\Psi}}^1(|\mathbf{R}') + \overline{\boldsymbol{\Psi}}^2(|\mathbf{R}') \cdot \{\mathbf{R} - \mathbf{R}'\}\right] \\ &\quad + \widetilde{\boldsymbol{\Pi}}^1(\mathbf{r}) : \overline{\boldsymbol{\Psi}}^2(|\mathbf{R}'). \end{aligned} \tag{4.4-50}$$

These microscale fields are independent of the choice of reference point $\mathbf{R}'$. As such, the set of constants $\left\{\overline{\boldsymbol{\Psi}}^0(|\mathbf{R}'), \overline{\boldsymbol{\Psi}}^1(|\mathbf{R}'), \overline{\boldsymbol{\Psi}}^2(|\mathbf{R}')\right\}$ based upon a reference point

$\mathbf{R}'$ are related to those based upon a different reference point $\mathbf{R}''$, namely $\left\{\overline{\Psi}^0(|\mathbf{R}'), \overline{\Psi}^1(|\mathbf{R}'), \overline{\Psi}^2(|\mathbf{R}')\right\}$. Their exact interrelations can be found by equating the velocity and pressure fields written with respect to each of these two alternative choices of reference points, and subsequently matching the results for all orders of $\mathbf{R}$. The final result is the trio of relations

$$\overline{\Psi}^2(|\mathbf{R}'') = \overline{\Psi}^2(|\mathbf{R}') = \overline{\Psi}^2, \text{ say,} \tag{4.4-51}$$

$$\overline{\Psi}^1(|\mathbf{R}'') = \overline{\Psi}^1(|\mathbf{R}') + \overline{\Psi}^2 \cdot \{\mathbf{R}'' - \mathbf{R}'\}, \tag{4.4-52}$$

$$\overline{\Psi}^0(|\mathbf{R}'') = \overline{\Psi}^0(|\mathbf{R}') + \overline{\Psi}^1(|\mathbf{R}') \cdot \{\mathbf{R}'' - \mathbf{R}'\} + \frac{1}{2}\overline{\Psi}^2 : \{\mathbf{R}'' - \mathbf{R}'\}^2, \tag{4.4-53}$$

expressing the value of these constants with respect to the reference point $\mathbf{R}''$ in terms of their values with respect to the reference point $\mathbf{R}'$.

4.4.8 Summary of Truncated First-order Flow

The first-order microscale velocity and pressure fields—defined by appropriately truncating the discrete form of the Taylor series (4.2-6) for the velocity at two terms—are given by (4.4-49) and (4.4-50) as

$$\mu \mathbf{v}(\mathbf{R}) = \widetilde{\mathbf{V}}^0(\mathbf{r}) \cdot \left[\overline{\Psi}^1(|\mathbf{R}') + \overline{\Psi}^2 \cdot \{\mathbf{R} - \mathbf{R}'\}\right] + \widetilde{\mathbf{V}}^1(\mathbf{r}) : \overline{\Psi}^2 \tag{4.4-54}$$

and

$$\begin{aligned} p(\mathbf{R}) = {} & \overline{\Psi}^0(|\mathbf{R}') + \overline{\Psi}^1(|\mathbf{R}') \cdot \{\mathbf{R} - \mathbf{R}'\} + \frac{1}{2}\overline{\Psi}^2 : \{\mathbf{R} - \mathbf{R}'\}^2 \\ & + \widetilde{\Pi}^0(\mathbf{r}) \cdot \left[\overline{\Psi}^1(|\mathbf{R}') + \overline{\Psi}^2 \cdot \{\mathbf{R} - \mathbf{R}'\}\right] + \widetilde{\Pi}^1(\mathbf{r}) : \overline{\Psi}^2. \end{aligned} \tag{4.4-55}$$

All microscale flow characteristics are implicitly contained in the fields $\left\{\widetilde{\mathbf{V}}^0(\mathbf{r}), \widetilde{\Pi}^0(\mathbf{r})\right\}$ and $\left\{\widetilde{\mathbf{V}}^1(\mathbf{r}), \widetilde{\Pi}^1(\mathbf{r})\right\}$, with the former fields constituting the $\mathcal{O}(0)$ *cell problem* defined in (4.3-52) and the latter fields the $\mathcal{O}(1)$ *cell problem* defined in Eqs. (4.4-36) to

(4.4-39):

$\mathcal{O}(1)$ *Cell Problem:* (4.4-56)

$$\nabla^2\widetilde{\mathbf{V}}^1 - \boldsymbol{\nabla}\widetilde{\boldsymbol{\Pi}}^1 = \left[\!\left[\mathbf{I}\widetilde{\Pi}^0 - 2^{\dagger}\left(\boldsymbol{\nabla}\widetilde{\mathbf{V}}^0\right) \right]\!\right]^{s2},$$

$$\boldsymbol{\nabla}\cdot\widetilde{\mathbf{V}}^1 = -\left[\!\left[\widetilde{\mathbf{V}}^0 - \left\langle\widetilde{\mathbf{V}}^0\right\rangle \right]\!\right]^{s},$$

$$\widetilde{\mathbf{V}}^1 = \mathbf{0} \qquad \forall\left(\mathbf{r}\in s_p\right),$$

$$\left\langle\widetilde{\boldsymbol{\Pi}}^1\right\rangle = \mathbf{0}.$$

This problem posed by these equations is uniquely determined from the unit cell geometry. All macroscale details are embedded in the constants $\overline{\Psi}^0(|\mathbf{R}')$, $\overline{\boldsymbol{\Psi}}^1(|\mathbf{R}')$ and $\overline{\boldsymbol{\Psi}}^2$. It is apparent that setting $\overline{\boldsymbol{\Psi}}^2 = \mathbf{0}$ in (4.4-54) and (4.4-55) reduces these to (4.3-50) and (4.3-51) respectively; that is, the zeroth-order flow solution is recovered. Consequently, this higher-order flow is determined entirely by the value of $\overline{\boldsymbol{\Psi}}^2$. This constant symmetric dyadic is not entirely arbitrary, but rather is restricted by *auxiliary condition* #1 given by (4.4-26):

$$\left\langle\widetilde{\mathbf{V}}^0\right\rangle : \overline{\boldsymbol{\Psi}}^2 = 0. \tag{4.4-57}$$

The explicit dependence of $\overline{\Psi}^0(|\mathbf{R}')$ and $\overline{\boldsymbol{\Psi}}^1(|\mathbf{R}')$ upon the choice of reference point is given by Eqs. (4.4-52) and (4.4-53) as

$$\overline{\boldsymbol{\Psi}}^1(|\mathbf{R}'') = \overline{\boldsymbol{\Psi}}^1(|\mathbf{R}') + \overline{\boldsymbol{\Psi}}^2\cdot\{\mathbf{R}''-\mathbf{R}'\}, \tag{4.4-58}$$

$$\overline{\Psi}^0(|\mathbf{R}'') = \overline{\Psi}^0(|\mathbf{R}') + \overline{\boldsymbol{\Psi}}^1(|\mathbf{R}')\cdot\{\mathbf{R}''-\mathbf{R}'\} + \frac{1}{2}\overline{\boldsymbol{\Psi}}^2 : \{\mathbf{R}''-\mathbf{R}'\}^2. \tag{4.4-59}$$

4.5 Truncated Second-order Microscale Flow

Second-order flow entails truncating the discrete form of the Taylor series (4.2-6) for $\mathbf{v}(\mathbf{R})$ at three terms and determining the corresponding pressure field.

4.5.1 Microscale Velocity, $\mathbf{v}(\mathbf{R})$

Retain only the first three tensors $\mathbf{v}^m(\mathbf{r}|\mathbf{R}')$ in the expansion (4.2-6) by setting

$$\mathbf{v}^m(\mathbf{r}|\mathbf{R}') = \mathbf{0} \qquad \forall\,(m = 3, 4, 5, \ldots) \tag{4.5-1}$$

to obtain

$$\mathbf{v}\left(\mathbf{R_n}, \mathbf{r}\right) = \mathbf{v}^0(\mathbf{r}|\mathbf{R}') + \mathbf{v}^1(\mathbf{r}|\mathbf{R}') \cdot \{\mathbf{R_n} - \mathbf{R}'\} + \frac{1}{2}\mathbf{v}^2(\mathbf{r}|\mathbf{R}') : \{\mathbf{R_n} - \mathbf{R}'\}^2 . \tag{4.5-2}$$

As in §§4.3.1 and 4.4.1, set $m = 2$ in the boundary condition (4.2-19) and use (4.5-2) to determine the form of the triadic $\mathbf{v}^2(\mathbf{r}|\mathbf{R}')$. Next, proceeding downward recursively, set $m = 1$ and $m = 0$ in (4.2-19) to determine the respective forms of the dyadic $\mathbf{v}^1(\mathbf{r}|\mathbf{R}')$ and the vector $\mathbf{v}^0(\mathbf{r}|\mathbf{R}')$. This procedure shows that the tensors $\mathbf{v}^m(\mathbf{r}|\mathbf{R}')$ for this truncated second-order flow field are given by

$$\mathbf{v}^m = \begin{cases} \widetilde{\mathbf{v}}^0 + \widetilde{\mathbf{v}}^1 \cdot \mathbf{r} + \frac{1}{2}\widetilde{\mathbf{v}}^2 : \mathbf{rr} & (m = 0), \\ \widetilde{\mathbf{v}}^1 + \widetilde{\mathbf{v}}^2 \cdot \mathbf{r} & (m = 1), \\ \widetilde{\mathbf{v}}^2 & (m = 2), \\ \mathbf{0} & \forall (m = 3, 4, 5, \ldots). \end{cases} \tag{4.5-3}$$

Consequently, the second-order microscale velocity (4.5-2) may be rewritten as

$$\mathbf{v}\left(\mathbf{R_n}, \mathbf{r}\right) = \widetilde{\mathbf{v}}^0(\mathbf{r}|\mathbf{R}') + \widetilde{\mathbf{v}}^1(\mathbf{r}|\mathbf{R}') \cdot \{\mathbf{R} - \mathbf{R}'\} + \frac{1}{2}\widetilde{\mathbf{v}}^2(\mathbf{r}|\mathbf{R}') : \{\mathbf{R} - \mathbf{R}'\}^2 . \tag{4.5-4}$$

Equations (4.5-3) and (4.5-4) are the functional counterparts of the truncated zeroth-order velocity field (4.3-5), (4.3-6) and the truncated first-order velocity field (4.4-7), (4.4-8). Again, the functions $\tilde{\mathbf{v}}^0(\mathbf{r}|\mathbf{R}')$ and $\tilde{\mathbf{v}}^1(\mathbf{r}|\mathbf{R}')$ appearing here are different than those for the lower-order truncations.

4.5.2 Microscale Pressure, $p(\mathbf{R})$

Again, as in §§4.3.2 and 4.4.2, set $m = 3, 4, 5, \ldots$ in (4.2-12), (4.5-3) and in the jump conditon (4.2-20) to determine the form of the higher order tensors $\mathbf{p}^m(\mathbf{r}|\mathbf{R}')$. Then work backwards, setting $m = 2, 1, 0$, determining therefrom the form of $\mathbf{p}^m(\mathbf{r}|\mathbf{R}')$ for each m. This procedure ultimately yields

$$\mathbf{p}^m = \begin{cases} \tilde{p}^0 + \tilde{\mathbf{p}}^1 \cdot \mathbf{r} + \frac{1}{2}\tilde{\mathbf{p}}^2 : \mathbf{rr} + \frac{1}{6}\overline{\mathbf{\Psi}}^3 \vdots \mathbf{rrr} & (m = 0), \\ \tilde{\mathbf{p}}^1 + \tilde{\mathbf{p}}^2 \cdot \mathbf{r} + \frac{1}{2}\overline{\mathbf{\Psi}}^3 : \mathbf{rr} & (m = 1), \\ \tilde{\mathbf{p}}^2 + \overline{\mathbf{\Psi}}^3 \cdot \mathbf{r} & (m = 2), \\ \overline{\mathbf{\Psi}}^3 & (m = 3), \\ \mathbf{0} & \forall (m = 4, 5, 6, \ldots), \end{cases} \tag{4.5-5}$$

where $\overline{\mathbf{\Psi}}^3(|\mathbf{R}')$ is an arbitrary, fully symmetric triadic. This is the counterpart of (4.5-3). Additionally, the microscale pressure field for this truncated second-order flow may be written as

$$\begin{aligned} p(\mathbf{R_n}, \mathbf{r}) &= \tilde{p}^0(\mathbf{r}|\mathbf{R}') + \tilde{\mathbf{p}}^1(\mathbf{r}|\mathbf{R}') \cdot \{\mathbf{R} - \mathbf{R}'\} \\ &\quad + \frac{1}{2}\tilde{\mathbf{p}}^2(\mathbf{r}|\mathbf{R}') : \{\mathbf{R} - \mathbf{R}'\}^2 + \frac{1}{6}\overline{\mathbf{\Psi}}^3(|\mathbf{R}') \vdots \{\mathbf{R} - \mathbf{R}'\}^3, \end{aligned} \tag{4.5-6}$$

where once again, the functions $\tilde{p}^0(\mathbf{r}|\mathbf{R}')$ and $\tilde{\mathbf{p}}^1(\mathbf{r}|\mathbf{R}')$ differ from those appearing in the lower-order flows.

4.5.3 Solution of $\tilde{\mathbf{v}}^2(\mathbf{r}|\mathbf{R}')$ and $\tilde{\mathbf{p}}^2(\mathbf{r}|\mathbf{R}')$

Set $m = 2$ in Eqs. (4.2-12) to (4.2-14) and use the forms of $\tilde{\mathbf{v}}^2(\mathbf{r}|\mathbf{R}'_\mathbf{n})$ and $\tilde{\mathbf{p}}^2(\mathbf{r}|\mathbf{R}'_\mathbf{n})$ given in (4.5-3) and (4.5-5) to obtain

$$\mu\nabla^2\tilde{\mathbf{v}}^2 - \boldsymbol{\nabla}\tilde{\mathbf{p}}^2 = \overline{\boldsymbol{\Psi}}^3, \tag{4.5-7}$$

$$\boldsymbol{\nabla}\cdot\tilde{\mathbf{v}}^2 = \mathbf{0}, \tag{4.5-8}$$

$$\tilde{\mathbf{v}}^2 = \mathbf{0} \qquad \forall\,(\mathbf{r}\in s_p)\,, \tag{4.5-9}$$

wherein the symmetry of $\overline{\boldsymbol{\Psi}}^3(|\mathbf{R}')$ has been used in deriving (4.5-7). Once again, owing to the fact that these equations are linearly independent with respect to their last two indices, the technique subsequently used to remove $\overline{\boldsymbol{\Psi}}^3(|\mathbf{R}')$ from the previous equations is identical to the procedure outlined in §4.4.3. As such, the solution of the preceding trio of equations is

$$\mu\tilde{\mathbf{v}}^2(\mathbf{r}|\mathbf{R}') = \widetilde{\mathbf{V}}^0(\mathbf{r})\cdot\overline{\boldsymbol{\Psi}}^3(|\mathbf{R}'), \tag{4.5-10}$$

$$\tilde{\mathbf{p}}^2(\mathbf{r}|\mathbf{R}') = \overline{\boldsymbol{\Psi}}^2(|\mathbf{R}') + \widetilde{\boldsymbol{\Pi}}^0(\mathbf{r})\cdot\overline{\boldsymbol{\Psi}}^3(|\mathbf{R}'), \tag{4.5-11}$$

in which $\widetilde{\mathbf{V}}^0(\mathbf{r})$ and $\widetilde{\boldsymbol{\Pi}}^0(\mathbf{r})$ are the solutions of the $\mathcal{O}(0)$ *cell problem* (4.3-52). The constant symmetric dyadic $\overline{\boldsymbol{\Psi}}^2(|\mathbf{R}')$ which has been introduced is defined

$$\overline{\boldsymbol{\Psi}}^2(|\mathbf{R}') \stackrel{\text{def}}{=} \left\langle\tilde{\mathbf{p}}^2(\mathbf{r}|\mathbf{R}')\right\rangle. \tag{4.5-12}$$

4.5.4 Second Auxiliary Condition

In what follows, restrictions are placed on the values of $\tilde{\mathbf{v}}^2(\mathbf{r}|\mathbf{R}')$ such that the incompressibility condition is satisfied. *Auxiliary condition* #2 [cf. (4.5-14)] may then be

established from (4.2-13) and (4.5-3).

Set $m = 1$ in (4.2-13) and integrate over the fluid domain to obtain

$$\frac{1}{\tau_0}\int_{\tau_f} \boldsymbol{\nabla}\cdot\mathbf{v}^1\,\mathrm{d}^3\mathbf{r} = \mathbf{0}.$$

Use the divergence theorem together with (4.2-14) and (4.5-3) yields

$$\frac{1}{\tau_0}\oint_{\partial\tau_0} \mathrm{d}\mathbf{S}\cdot\tilde{\mathbf{v}}^2\cdot\mathbf{r} = \mathbf{0}. \tag{4.5-13}$$

Substitute (4.5-10) into the previous equation and rewrite the resulting expression as

$$\left(\frac{1}{\tau_0}\oint_{\partial\tau_0} \mathbf{r}\mathrm{d}\mathbf{S}\cdot\widetilde{\mathbf{V}}^0\right) : \overline{\boldsymbol{\Psi}}^3 = \mathbf{0}$$

upon recognizing the symmetry of $\overline{\boldsymbol{\Psi}}^3(|\mathbf{R}')$. The term in parentheses appearing above is simply the zeroth-order dyadic $\overline{\mathbf{V}}^0$ (4.3-41), whereupon we obtain *auxiliary condition #2*:

$$\overline{\mathbf{V}}^0 : \overline{\boldsymbol{\Psi}}^3 = \mathbf{0} \tag{4.5-14}$$

or

$$\left\langle\widetilde{\mathbf{V}}^0(\mathbf{r})\right\rangle : \overline{\boldsymbol{\Psi}}^3(|\mathbf{R}') = \mathbf{0}. \tag{4.5-15}$$

This condition shows that $\overline{\boldsymbol{\Psi}}^3(|\mathbf{R}')$ itself is not a totally arbitrary constant symmetric triadic, but rather must satisfy (4.5-14) or (4.5-15) for the requirement of incompressibility to be preserved.

4.5.5 Solution of $\tilde{\mathbf{v}}^1(\mathbf{r}|\mathbf{R}')$ and $\tilde{\mathbf{p}}^1(\mathbf{r}|\mathbf{R}')$

Combine the forms of $\mathbf{v}^1(\mathbf{r}|\mathbf{R}')$ and $\mathbf{p}^1(\mathbf{r}|\mathbf{R}')$ given in Eqs. (4.5-3) and (4.5-5) with the solutions of $\tilde{\mathbf{v}}^2(\mathbf{r}|\mathbf{R}')$ and $\tilde{\mathbf{p}}^2(\mathbf{r}|\mathbf{R}')$ from (4.5-10) and (4.5-11) to derive

$$\mu\mathbf{v}^1 = \mu\tilde{\mathbf{v}}^1 + \widetilde{\mathbf{V}}^0\cdot\overline{\boldsymbol{\Psi}}^3\cdot\mathbf{r}, \tag{4.5-16}$$

$$\mathbf{p}^1 = \tilde{\mathbf{p}}^1 + \overline{\boldsymbol{\Psi}}^2 \cdot \mathbf{r} + \widetilde{\boldsymbol{\Pi}}^0 \cdot \overline{\boldsymbol{\Psi}}^3 \cdot \mathbf{r} + \frac{1}{2}\overline{\boldsymbol{\Psi}}^3 : \mathbf{rr}. \tag{4.5-17}$$

Set $m = 1$ in Eqs. (4.2-12) to (4.2-14) and substitute into (4.5-16) and (4.5-17) the forms of $\mathbf{v}^1(\mathbf{r}|\mathbf{R}')$ and $\mathbf{p}^1(\mathbf{r}|\mathbf{R}')$, thereby obtaining the following system of equations governing the fully spatially periodic dyadic field $\tilde{\mathbf{v}}^1(\mathbf{r}|\mathbf{R}')$ and vector field $\tilde{\mathbf{p}}^1(\mathbf{r}|\mathbf{R}')$:

$$\mu\nabla^2\tilde{\mathbf{v}}^1 - \boldsymbol{\nabla}\tilde{\mathbf{p}}^1 = \overline{\boldsymbol{\Psi}}^2 + \left[\mathbf{I}\widetilde{\boldsymbol{\Pi}}^0 - 2^\dagger\left(\boldsymbol{\nabla}\widetilde{\mathbf{V}}^0\right)\right] : \overline{\boldsymbol{\Psi}}^3 - \left[\nabla^2\widetilde{\mathbf{V}}^0 - \boldsymbol{\nabla}\boldsymbol{\Pi}^0 - \mathbf{I}\right] \cdot \overline{\boldsymbol{\Psi}}^3 \cdot \mathbf{r},$$

$$\mu\boldsymbol{\nabla} \cdot \tilde{\mathbf{v}}^1 = -\widetilde{\mathbf{V}}^0 : \overline{\boldsymbol{\Psi}}^3 - \left[\boldsymbol{\nabla} \cdot \widetilde{\mathbf{V}}^0\right] \cdot \overline{\boldsymbol{\Psi}}^3 \cdot \mathbf{r},$$

$$\mu\tilde{\mathbf{v}}^1 = -\widetilde{\mathbf{V}}^0 \cdot \overline{\boldsymbol{\Psi}}^3 \cdot \mathbf{r} \qquad \forall\left(\mathbf{r} \in s_p\right),$$

in which the fully symmetric properties of the dyadic $\overline{\boldsymbol{\Psi}}^2(|\mathbf{R}')$ and triadic $\overline{\boldsymbol{\Psi}}^3(|\mathbf{R}')$ have been exploited. These symmetry conditions, together with the $\mathcal{O}(0)$ *cell problem* defined by Eqs. (4.3-52), can be used to rewrite these governing equations in the equivalent form

$$\mu\nabla^2\tilde{\mathbf{v}}^1 - \boldsymbol{\nabla}\tilde{\mathbf{p}}^1 = \overline{\boldsymbol{\Psi}}^2 + \left[\!\!\left[\, \mathbf{I}\widetilde{\boldsymbol{\Pi}}^0 - 2^\dagger\left(\boldsymbol{\nabla}\widetilde{\mathbf{V}}^0\right) \,\right]\!\!\right]^{s2} : \overline{\boldsymbol{\Psi}}^3, \tag{4.5-18}$$

$$\mu\boldsymbol{\nabla} \cdot \tilde{\mathbf{v}}^1 = -\left[\!\!\left[\, \widetilde{\mathbf{V}}^0 \,\right]\!\!\right]^{s} : \overline{\boldsymbol{\Psi}}^3, \tag{4.5-19}$$

$$\mu\tilde{\mathbf{v}}^1 = \mathbf{0} \qquad \forall\left(\mathbf{r} \in s_p\right). \tag{4.5-20}$$

Obviously, integrating the continuity conditon (4.5-19) over the fluid domain, followed by use of the divergence theorem, the no-slip condition (4.5-20) and the spatially periodic nature of $\tilde{\mathbf{v}}^1(\mathbf{r}|\mathbf{R}')$, leads directly to *auxiliary condition* #2 [Eqs. (4.5-14) or (4.5-15)] restricting the value chosen for the fully symmetric triadic $\overline{\boldsymbol{\Psi}}^3(|\mathbf{R}')$.

As in §4.4.5, although Eqs. (4.5-18) to (4.5-20) are linear in $\overline{\boldsymbol{\Psi}}^2(|\mathbf{R}')$ and $\overline{\boldsymbol{\Psi}}^3(|\mathbf{R}')$, it is this restriction placed upon $\overline{\boldsymbol{\Psi}}^3(|\mathbf{R}')$ which requires consideration when removing

the dependence of $\tilde{\mathbf{v}}^1(\mathbf{r}|\mathbf{R}')$ and $\tilde{\mathbf{p}}^1(\mathbf{r}|\mathbf{R}')$ upon these constant tensors. In light of (4.5-15), the continuity condition (4.5-19) is replaced by the equivalent expression

$$\mu\boldsymbol{\nabla}\cdot\tilde{\mathbf{v}}^1 = -\left[\!\left[\,\widetilde{\mathbf{V}}^0 - \left\langle\widetilde{\mathbf{V}}^0\right\rangle\,\right]\!\right]^s : \overline{\boldsymbol{\Psi}}^3, \tag{4.5-21}$$

and the solutions $\tilde{\mathbf{v}}^1(\mathbf{r}|\mathbf{R}')$ and $\tilde{\mathbf{p}}^1(\mathbf{r}|\mathbf{R}')$ may be written as

$$\mu\tilde{\mathbf{v}}^1(\mathbf{r}|\mathbf{R}') = \widetilde{\mathbf{V}}^0(\mathbf{r})\cdot\overline{\boldsymbol{\Psi}}^2(|\mathbf{R}') + \widetilde{\mathbf{V}}^1(\mathbf{r}) : \overline{\boldsymbol{\Psi}}^3(|\mathbf{R}'), \tag{4.5-22}$$

$$\tilde{\mathbf{p}}^1(\mathbf{r}|\mathbf{R}') = \overline{\boldsymbol{\Psi}}^1(|\mathbf{R}') + \widetilde{\boldsymbol{\Pi}}^0(\mathbf{r})\cdot\overline{\boldsymbol{\Psi}}^2(|\mathbf{R}') + \widetilde{\boldsymbol{\Pi}}^1(\mathbf{r}) : \overline{\boldsymbol{\Psi}}^3(|\mathbf{R}'), \tag{4.5-23}$$

with the constant vector $\overline{\boldsymbol{\Psi}}^1(|\mathbf{R}')$ defined as

$$\overline{\boldsymbol{\Psi}}^1(|\mathbf{R}') \stackrel{\text{def}}{=} \left\langle\tilde{\mathbf{p}}^1(\mathbf{r}|\mathbf{R}')\right\rangle. \tag{4.5-24}$$

This solution clearly depends upon knowledge of the solutions of the $\mathcal{O}(0)$ *cell problem* (4.3-52) for $\left[\widetilde{\mathbf{V}}^0(\mathbf{r}), \widetilde{\boldsymbol{\Pi}}^0(\mathbf{r})\right]$, the $\mathcal{O}(1)$ *cell problem* (4.4-56) for $\left[\widetilde{\mathbf{V}}^1(\mathbf{r}), \widetilde{\boldsymbol{\Pi}}^1(\mathbf{r})\right]$ and the constants $\overline{\boldsymbol{\Psi}}^1(|\mathbf{R}')$, $\overline{\boldsymbol{\Psi}}^2(|\mathbf{R}')$ and $\overline{\boldsymbol{\Psi}}^3(|\mathbf{R}')$.

4.5.6 First Auxiliary Condition

Further restrictions need to be imposed upon the fields $\tilde{\mathbf{v}}^1(\mathbf{r}|\mathbf{R}')$ and $\tilde{\mathbf{v}}^2(\mathbf{r}|\mathbf{R}')$ to assure that fluid incompressibility is always satisfied. To establish these restrictions, set $m = 0$ in (4.2-13) and integrate over the fluid domain τ_f to obtain

$$\left\langle\boldsymbol{\nabla}\cdot\mathbf{v}^0\right\rangle = 0.$$

Subsequent use of the divergence theorem, together with the no-slip condition (4.2-14), the form of $\mathbf{v}^0(\mathbf{r}|\mathbf{R}')$ suggested in (4.5-3) and the fact that spatially periodic

functions integrate to zero over the surface of a cell $\partial\tau_0$ furnishes the requirement

$$\frac{1}{\tau_f}\oint_{\partial\tau_0} d\mathbf{S}\cdot\left[\tilde{\mathbf{v}}^1\cdot\mathbf{r}+\frac{1}{2}\tilde{\mathbf{v}}^2:\mathbf{rr}\right]=0. \tag{4.5-25}$$

Re-use of the divergence theorem and the no-slip conditions (4.4-31) and (4.5-20) reduce the above to the form

$$\left\langle\boldsymbol{\nabla}\cdot\left[\tilde{\mathbf{v}}^1\cdot\mathbf{r}+\frac{1}{2}\tilde{\mathbf{v}}^2:\mathbf{rr}\right]\right\rangle=0.$$

Perform the divergence operations in the latter to obtain

$$\left\langle\left[\boldsymbol{\nabla}\cdot\tilde{\mathbf{v}}^1\right]\cdot\mathbf{r}+\mathbf{I}:\tilde{\mathbf{v}}^1+\frac{1}{2}\left[\boldsymbol{\nabla}\cdot\tilde{\mathbf{v}}^2\right]:\mathbf{rr}+\mathbf{I}:\tilde{\mathbf{v}}^2\cdot\mathbf{r}\right\rangle=0$$

and subsequently use the forms of $\tilde{\mathbf{v}}^1(\mathbf{r}|\mathbf{R}')$ and $\tilde{\mathbf{v}}^2(\mathbf{r}|\mathbf{R}')$ established in (4.5-22) and (4.5-10) to derive

$$\left\langle\left[\boldsymbol{\nabla}\cdot\widetilde{\mathbf{V}}^0\right]\cdot\left[\overline{\boldsymbol{\Psi}}^2\cdot\mathbf{r}+\frac{1}{2}\overline{\boldsymbol{\Psi}}^3:\mathbf{rr}\right]+\left[\boldsymbol{\nabla}\cdot\widetilde{\mathbf{V}}^1+\widetilde{\mathbf{V}}^0\right]:\overline{\boldsymbol{\Psi}}^3\cdot\mathbf{r}+\widetilde{\mathbf{V}}^0:\overline{\boldsymbol{\Psi}}^2+\widetilde{\mathbf{V}}^1:\overline{\boldsymbol{\Psi}}^3\right\rangle=0.$$

This result may be simplified by using the continuity conditions imposed upon $\widetilde{\mathbf{V}}^0(\mathbf{r})$ and $\widetilde{\mathbf{V}}^1(\mathbf{r})$ given in the cell problems (4.3-52) and (4.4-56):

$$\left\langle\widetilde{\mathbf{V}}^0\right\rangle:\overline{\boldsymbol{\Psi}}^3\cdot\langle\mathbf{r}\rangle+\left\langle\widetilde{\mathbf{V}}^0\right\rangle:\overline{\boldsymbol{\Psi}}^2+\left\langle\widetilde{\mathbf{V}}^1\right\rangle:\overline{\boldsymbol{\Psi}}^3=0.$$

Upon recognizing that the first term on the left-hand side of the above is identically zero as a result of *auxiliary condition* #2 (4.5-15), one obtains the ultimate result

$$\left\langle\widetilde{\mathbf{V}}^0(\mathbf{r})\right\rangle:\overline{\boldsymbol{\Psi}}^2(|\mathbf{R}')+\left\langle\widetilde{\mathbf{V}}^1(\mathbf{r})\right\rangle:\overline{\boldsymbol{\Psi}}^3(|\mathbf{R}')=0, \tag{4.5-26}$$

where the symmetry of the tensors $\overline{\boldsymbol{\Psi}}^2(|\mathbf{R}')$ and $\overline{\boldsymbol{\Psi}}^3(|\mathbf{R}')$ has again been utilized. This is *auxiliary condition* #1, restricting the choice of $\overline{\boldsymbol{\Psi}}^2(|\mathbf{R}')$ and $\overline{\boldsymbol{\Psi}}^3(|\mathbf{R}')$ such that the indicated sum is satisfied. Notice that the choice of $\overline{\boldsymbol{\Psi}}^3(|\mathbf{R}')=\mathbf{0}$ automatically satisfies *auxilliary condition* #2 (4.5-15) and, furthermore, that *auxiliary condition*

#1 becomes identical to that calculated for the first-order flow field (4.4-26).

4.5.7 Solution of $\tilde{\mathbf{v}}^0(\mathbf{r}|\mathbf{R}')$ and $\tilde{p}^0(\mathbf{r}|\mathbf{R}')$

Substitute (4.5-10), (4.5-11), (4.5-22) and (4.5-23) into (4.5-3) and (4.5-5) and use the symmetry of the constants $\overline{\boldsymbol{\Psi}}^m(|\mathbf{R}')$ to obtain

$$\mu\mathbf{v}^0 = \mu\tilde{\mathbf{v}}^0 + \widetilde{\mathbf{V}}^0\cdot\overline{\boldsymbol{\Psi}}^2\cdot\mathbf{r} + \left[\widetilde{\mathbf{V}}^1\mathbf{r} + \frac{1}{2}\widetilde{\mathbf{V}}^0\mathbf{rr}\right]\vdots\overline{\boldsymbol{\Psi}}^3, \tag{4.5-27}$$

$$p^0 = \tilde{p}^0 + \overline{\boldsymbol{\Psi}}^1\cdot\mathbf{r} + \left[\widetilde{\boldsymbol{\Pi}}^0\mathbf{r} + \frac{1}{2}\mathbf{rr}\right] : \overline{\boldsymbol{\Psi}}^2 + \left[\widetilde{\boldsymbol{\Pi}}^1\mathbf{r} + \frac{1}{2}\widetilde{\boldsymbol{\Pi}}^0\mathbf{rr} + \frac{1}{6}\mathbf{rrr}\right]\vdots\overline{\boldsymbol{\Psi}}^3. \tag{4.5-28}$$

Set $m = 0$ in Eqs. (4.2-12) to (4.2-14) and substitute the previous equations into the resulting expressions to obtain the following system of equations governing the fully spatially periodic vector field $\tilde{\mathbf{v}}^0(\mathbf{r}|\mathbf{R}')$ and scalar field $\tilde{p}^0(\mathbf{r}|\mathbf{R}')$:

$$\begin{aligned}
\mu\nabla^2\tilde{\mathbf{v}}^0 - \boldsymbol{\nabla}\tilde{p}^0 = {} & \overline{\boldsymbol{\Psi}}^1 - \left[\nabla^2\widetilde{\mathbf{V}}^0 - \boldsymbol{\nabla}\widetilde{\boldsymbol{\Pi}}^0 - \mathbf{I}\right]\cdot\left[\overline{\boldsymbol{\Psi}}^2\cdot\mathbf{r} + \frac{1}{2}\overline{\boldsymbol{\Psi}}^3 : \mathbf{rr}\right] \\
& - \left[\nabla^2\widetilde{\mathbf{V}}^1 - \boldsymbol{\nabla}\widetilde{\boldsymbol{\Pi}}^1 - \mathbf{I}\widetilde{\boldsymbol{\Pi}}^0 + 2^\dagger\left(\boldsymbol{\nabla}\widetilde{\mathbf{V}}^0\right)\right] : \overline{\boldsymbol{\Psi}}^3\cdot\mathbf{r} \\
& + \left[\mathbf{I}\widetilde{\boldsymbol{\Pi}}^0 - 2^\dagger\left(\boldsymbol{\nabla}\widetilde{\mathbf{V}}^0\right)\right] : \overline{\boldsymbol{\Psi}}^2 \\
& + \left[\mathbf{I}\widetilde{\boldsymbol{\Pi}}^1 - 2^\dagger\left(\boldsymbol{\nabla}\widetilde{\mathbf{V}}^1\right) - \widetilde{\mathbf{V}}^0\mathbf{I}\right]\vdots\overline{\boldsymbol{\Psi}}^3,
\end{aligned}$$

$$\begin{aligned}
\mu\boldsymbol{\nabla}\cdot\tilde{\mathbf{v}}^0 = {} & -\left[\boldsymbol{\nabla}\cdot\widetilde{\mathbf{V}}^0\right]\cdot\left[\overline{\boldsymbol{\Psi}}^2\cdot\mathbf{r} + \frac{1}{2}\overline{\boldsymbol{\Psi}}^3 : \mathbf{rr}\right] \\
& - \left[\boldsymbol{\nabla}\cdot\widetilde{\mathbf{V}}^1 + \widetilde{\mathbf{V}}^0\right] : \overline{\boldsymbol{\Psi}}^3\cdot\mathbf{r} \\
& - \widetilde{\mathbf{V}}^0 : \overline{\boldsymbol{\Psi}}^2 - \widetilde{\mathbf{V}}^1\vdots\overline{\boldsymbol{\Psi}}^3,
\end{aligned}$$

$$\mu\mathbf{v}^0 = -\widetilde{\mathbf{V}}^0\cdot\overline{\boldsymbol{\Psi}}^2\cdot\mathbf{r} - \left[\widetilde{\mathbf{V}}^1\mathbf{r} + \frac{1}{2}\widetilde{\mathbf{V}}^0\mathbf{rr}\right]\vdots\overline{\boldsymbol{\Psi}}^3 \qquad \forall\left(\mathbf{r}\in s_p\right).$$

The symmetry conditions imposed on the tensors $\overline{\boldsymbol{\Psi}}^m(|\mathbf{R}')$, in conjunction with the $\mathcal{O}(0)$ *cell problem* (4.3-52), the $\mathcal{O}(1)$ *cell problem* (4.4-56), and *auxiliary condition*

#2 defined in (4.5-15), enable the preceding equations for $\tilde{\mathbf{v}}^0(\mathbf{r}|\mathbf{R}')$ and $\tilde{p}^0(\mathbf{r}|\mathbf{R}')$ to be rewritten as

$$\begin{aligned}\mu\nabla^2\tilde{\mathbf{v}}^0 - \boldsymbol{\nabla}\tilde{p}^0 &= \overline{\boldsymbol{\Psi}}^1 + \Big[\!\Big[\mathbf{I}\widetilde{\boldsymbol{\Pi}}^0 - 2^\dagger\big(\boldsymbol{\nabla}\widetilde{\mathbf{V}}^0\big) \Big]\!\Big]^{s2} : \overline{\boldsymbol{\Psi}}^2 \\ &\quad + \Big[\!\Big[\mathbf{I}\widetilde{\boldsymbol{\Pi}}^1 - 2^\dagger\big(\boldsymbol{\nabla}\widetilde{\mathbf{V}}^1\big) - \widetilde{\mathbf{V}}^0\mathbf{I} \Big]\!\Big]^{s3} \vdots \overline{\boldsymbol{\Psi}}^3, \qquad (4.5\text{-}29)\end{aligned}$$

$$\mu\boldsymbol{\nabla}\cdot\tilde{\mathbf{v}}^0 = -\Big[\!\Big[\widetilde{\mathbf{V}}^0 \Big]\!\Big]^s : \overline{\boldsymbol{\Psi}}^2 - \Big[\!\Big[\widetilde{\mathbf{V}}^1 \Big]\!\Big]^s \vdots \overline{\boldsymbol{\Psi}}^3, \qquad (4.5\text{-}30)$$

$$\mu\mathbf{v}^0 = \mathbf{0} \qquad \forall\,(\mathbf{r}\in s_p)\,. \qquad (4.5\text{-}31)$$

Since this trio of equations is linear in the constants $\overline{\boldsymbol{\Psi}}^m(|\mathbf{R}')$, dependence upon these constants can be removed. In particular the constant $\overline{\boldsymbol{\Psi}}^1(|\mathbf{R}')$ can be removed via the $\mathcal{O}(0)$ *cell problem* while $\overline{\boldsymbol{\Psi}}^2(|\mathbf{R}')$ may be removed by using the $\mathcal{O}(1)$ *cell problem.* Previously, when a solution was sought for $\{\tilde{\mathbf{v}}^0, \tilde{p}^0\}$ and the $\mathcal{O}(1)$ *cell problem* derived in § 4.4.5, an adjustment had to be made to the continuity condition based on *auxiliary condition* #1 before removal of the constants could be effected. This is *not* the case here as the solution for $\tilde{\mathbf{v}}^0(\mathbf{r}|\mathbf{R}')$ will involve a term like $\widetilde{\mathbf{V}}^1 : \overline{\boldsymbol{\Psi}}^2$ and a term like $\widetilde{\mathbf{V}}^2 \vdots \overline{\boldsymbol{\Psi}}^3$ [cf. (4.5-32)]. The continuity condition (4.5-30) will then produce a term like $\big(\boldsymbol{\nabla}\cdot\widetilde{\mathbf{V}}^1\big) : \overline{\boldsymbol{\Psi}}^2$, which when converted via the $\mathcal{O}(1)$ *cell problem* continuity condition, will cancel the term double-dotting $\overline{\boldsymbol{\Psi}}^2$ in (4.5-30). This, in turn, will leave the residual term $\big\langle\widetilde{\mathbf{V}}^0\big\rangle : \overline{\boldsymbol{\Psi}}^2$. But upon replacing the latter with $-\big\langle\widetilde{\mathbf{V}}^1\big\rangle \vdots \overline{\boldsymbol{\Psi}}^3$ from *auxiliary condition* #1 for this truncated second-order flow (4.5-26), the result will be to effectively have an inhomogeneous term appearing in the continuity condition for $\widetilde{\mathbf{V}}^2(\mathbf{r})$, such a term possessing a zero mean [cf. (4.5-36)]. Indeed, this which was the reason for rewriting the continuity condition in § 4.4.5 in the first place.

To this end, define the tetradic field $\widetilde{\mathbf{V}}^2(\mathbf{r})$ and the triadic field $\widetilde{\boldsymbol{\Pi}}^2(\mathbf{r})$ as

$$\mu\tilde{\mathbf{v}}^0(\mathbf{r}|\mathbf{R}') \overset{\text{def}}{=} \widetilde{\mathbf{V}}^0(\mathbf{r})\cdot\overline{\boldsymbol{\Psi}}^1(|\mathbf{R}') + \widetilde{\mathbf{V}}^1(\mathbf{r}) : \overline{\boldsymbol{\Psi}}^2(|\mathbf{R}') + \widetilde{\mathbf{V}}^2(\mathbf{r}) \vdots \overline{\boldsymbol{\Psi}}^3(|\mathbf{R}'),$$

(4.5-32)

$$\tilde{p}^0(\mathbf{r}|\mathbf{R}') \stackrel{\text{def}}{=} \overline{\Psi}^0(|\mathbf{R}') + \widetilde{\Pi}^0(\mathbf{r}) \cdot \overline{\Psi}^1(|\mathbf{R}') + \widetilde{\Pi}^1(\mathbf{r}) : \overline{\Psi}^2(|\mathbf{R}') + \widetilde{\Pi}^2(\mathbf{r}) \vdots \overline{\Psi}^3(|\mathbf{R}'), \tag{4.5-33}$$

with

$$\overline{\Psi}^0(|\mathbf{R}') \stackrel{\text{def}}{=} \left\langle \tilde{p}^0(\mathbf{r}|\mathbf{R}') \right\rangle \tag{4.5-34}$$

included to remove the arbitrary constant in $\tilde{p}^0(\mathbf{r}|\mathbf{R}')$. Substitute (4.5-32) and (4.5-33) into (4.5-29) to (4.5-31) and simplify the resulting expressions by using the characteristic cell problems and the auxiliary conditions to determine the characteristic problem satisfied by $\widetilde{\mathbf{V}}^2(\mathbf{r})$ and $\widetilde{\mathbf{\Pi}}^2(\mathbf{r})$, namely,

$$\nabla^2 \widetilde{\mathbf{V}}^2 - \boldsymbol{\nabla} \widetilde{\mathbf{\Pi}}^2 = \left[\!\!\left[\mathbf{I}\widetilde{\mathbf{\Pi}}^1 - 2^{\dagger}\left(\boldsymbol{\nabla}\widetilde{\mathbf{V}}^1\right) - \widetilde{\mathbf{V}}^0\mathbf{I} \right]\!\!\right]^{s3}, \tag{4.5-35}$$

$$\boldsymbol{\nabla} \cdot \widetilde{\mathbf{V}}^2 = -\left[\!\!\left[\widetilde{\mathbf{V}}^1 - \left\langle \widetilde{\mathbf{V}}^1 \right\rangle \right]\!\!\right]^{s}, \tag{4.5-36}$$

$$\widetilde{\mathbf{V}}^2 = \mathbf{0} \qquad \forall (\mathbf{r} \in s_p), \tag{4.5-37}$$

together with the normalization condition

$$\left\langle \widetilde{\mathbf{\Pi}}^2 \right\rangle = \mathbf{0}. \tag{4.5-38}$$

Equations (4.5-35) to (4.5-38) constitute the $\mathcal{O}(2)$ *cell problem* to be solved for the fields $\left[\widetilde{\mathbf{V}}^2(\mathbf{r}), \widetilde{\mathbf{\Pi}}^2(\mathbf{r})\right]$. These fields are determined entirely from the unit cell geometry. Furthermore, because of the symmetry of the inhomogeneous terms in (4.5-35) and (4.5-36), $\widetilde{\mathbf{V}}^2(\mathbf{r})$ is symmetric with respect to its *last* three indices, while $\widetilde{\mathbf{\Pi}}^2(\mathbf{r})$ is symmetric with respect to *all* three of its indices.

4.5.8 Uniqueness of $\widetilde{\mathbf{V}}^2(\mathbf{r})$ and $\widetilde{\mathbf{\Pi}}^2(\mathbf{r})$

As in §§4.3.4 and 4.4.6, uniqueness of these fields may be proved by first assuming that there exist at least two different solutions $\left(\widetilde{\mathbf{V}}', \widetilde{\mathbf{\Pi}}'\right)$ and $\left(\widetilde{\mathbf{V}}'', \widetilde{\mathbf{\Pi}}''\right)$ of the system of equations (4.5-35) to (4.5-38). Uniqueness will be proved by showing that the quantities $\left(\widetilde{\mathbf{V}}, \widetilde{\mathbf{\Pi}}\right)$ defined as

$$\widetilde{\mathbf{V}} \stackrel{\text{def}}{=} \widetilde{\mathbf{V}}' - \widetilde{\mathbf{V}}'' \tag{4.5-39}$$

$$\widetilde{\mathbf{\Pi}} \stackrel{\text{def}}{=} \widetilde{\mathbf{\Pi}}' - \widetilde{\mathbf{\Pi}}'' \tag{4.5-40}$$

are identically

$$\widetilde{\mathbf{V}} = \mathbf{0} \tag{4.5-41}$$

$$\widetilde{\mathbf{\Pi}} = \mathbf{0}. \tag{4.5-42}$$

As the primed and double-primed fields each satisfy (4.5-35) to (4.5-38), and the uniqueness of both $\widetilde{\mathbf{V}}^0$, $\widetilde{\mathbf{\Pi}}^0$ and $\widetilde{\mathbf{V}}^1$, $\widetilde{\mathbf{\Pi}}^1$ were shown in §§4.3.4 and 4.4.6, it follows from the linearity of these equations that $\left(\widetilde{\mathbf{V}}, \widetilde{\mathbf{\Pi}}\right)$ satisfy

$$\nabla^2 \widetilde{\mathbf{V}} = \boldsymbol{\nabla} \widetilde{\mathbf{\Pi}} \tag{4.5-43}$$

$$\boldsymbol{\nabla} \cdot \widetilde{\mathbf{V}} = \mathbf{0} \tag{4.5-44}$$

$$\widetilde{\mathbf{V}} = \mathbf{0} \qquad \forall (\mathbf{r} \in s_p) \tag{4.5-45}$$

$$\left\langle \widetilde{\mathbf{\Pi}} \right\rangle = \mathbf{0}. \tag{4.5-46}$$

As in §§4.3.4 and 4.4.6, quadruple-dot multiply (4.5-43) by $\widetilde{\mathbf{V}}$ (contracting on equivalent indices), use differentiation by parts, apply (4.5-44), integrate the result over τ_f, use the divergence theorem, apply (4.5-45) to the integral over s_p, and finally note that the surface integrals of spatially periodic functions over $\partial\tau_0$ vanish. These eventually yield

$$\int_{\tau_f} \left(\nabla_l \widetilde{V}_{ijkm}\right) \left(\nabla_l \widetilde{V}_{ijkm}\right) \, \mathrm{d}^3\mathbf{r} = 0. \tag{4.5-47}$$

As a consequence of the nonnegative nature of this quadratic integrand at each point $\mathbf{r} \in \tau_f$, the tensor $\boldsymbol{\nabla}\widetilde{\mathbf{V}}$ itself must be identically zero, implying that $\widetilde{\mathbf{V}}$ is at most

a constant. But from (4.5-45) the value of this constant must be identically zero, thereby proving (4.5-41). It then follows from (4.5-41) and (4.5-43) that $\nabla\widetilde{\Pi} = \mathbf{0}$ at all points $\mathbf{r} \in \tau_f$, implying $\widetilde{\Pi}$ is at most a constant. But from (4.5-46) this constant is identically zero, whereupon (4.5-42) follows. (Q.E.D.)

4.5.9 Dependence of $\overline{\Psi}^m(|\mathbf{R}')$ upon the Choice of Reference Point

Combining the microscale velocity field representation (4.5-4) with the solutions (4.5-10) , (4.5-22) and (4.5-32) yields, upon suppressing the arguments ($\mathbf{r}$) of the fields and the reference point dependence ($|\mathbf{R}'$) of the constants, the truncated second-order velocity field

$$\begin{aligned}\mu\mathbf{v}(\mathbf{R_n},\mathbf{r}) &= \widetilde{\mathbf{V}}^0\cdot\left[\overline{\Psi}^1+\overline{\Psi}^2\cdot\{\mathbf{R}-\mathbf{R}'\}+\frac{1}{2}\overline{\Psi}^3:\{\mathbf{R}-\mathbf{R}'\}^2\right]\\ &\quad+\widetilde{\mathbf{V}}^1:\left[\overline{\Psi}^2+\overline{\Psi}^3\cdot\{\mathbf{R}-\mathbf{R}'\}\right]\\ &\quad+\widetilde{\mathbf{V}}^2{:}\overline{\Psi}^3. \end{aligned} \tag{4.5-48}$$

Likewise, the corresponding pressure field can be written upon combining (4.5-6) with the solutions (4.5-11), (4.5-23) and (4.5-33) as

$$\begin{aligned}p(\mathbf{R_n},\mathbf{r}) &= \overline{\Psi}^0+\overline{\Psi}^1\cdot\{\mathbf{R}-\mathbf{R}'\}+\frac{1}{2}\overline{\Psi}^2:\{\mathbf{R}-\mathbf{R}'\}^2+\frac{1}{6}\overline{\Psi}^3{:}\{\mathbf{R}-\mathbf{R}'\}^3\\ &\quad+\widetilde{\Pi}^0\cdot\left[\overline{\Psi}^1+\overline{\Psi}^2\cdot\{\mathbf{R}-\mathbf{R}'\}+\frac{1}{2}\overline{\Psi}^3:\{\mathbf{R}-\mathbf{R}'\}^2\right]\\ &\quad+\widetilde{\Pi}^1:\left[\overline{\Psi}^2+\overline{\Psi}^3\cdot\{\mathbf{R}-\mathbf{R}'\}\right]\\ &\quad+\widetilde{\Pi}^2{:}\overline{\Psi}^3. \end{aligned} \tag{4.5-49}$$

This truncated second-order flow field must be independent of the choice of reference point $\mathbf{R}'$. As such, choosing a different reference point, $\mathbf{R}''$, say, and equating the velocity and pressure fields when written for these two different reference points, results in equations relating the values of the two sets of constants $\overline{\Psi}^m(|\mathbf{R}')$ and

$\overline{\Psi}^m(|\mathbf{R}'')$:

$$\overline{\Psi}^m(|\mathbf{R}'') = \sum_{j=0}^{3-m} \frac{1}{j!} \overline{\Psi}^{m-j}(|\mathbf{R}') \{\cdot\}^j \{\mathbf{R}'' - \mathbf{R}'\}^j \qquad \forall (m = 0, 1, 2, 3). \tag{4.5-50}$$

4.5.10 Summary of Truncated Second-order Flow

In summary, the truncated second-order microscale velocity and pressure fields—defined by truncating the discrete form of the Taylor series (4.2-6) for the velocity at three terms—are given from (4.5-48) and (4.5-49) as

$$\begin{aligned} \mu \mathbf{v}(\mathbf{R_n}, \mathbf{r}) \;=\; & \widetilde{\mathbf{V}}^0 \cdot \left[\overline{\Psi}^1 + \overline{\Psi}^2 \cdot \{\mathbf{R} - \mathbf{R}'\} + \frac{1}{2} \overline{\Psi}^3 : \{\mathbf{R} - \mathbf{R}'\}^2 \right] \\ & + \widetilde{\mathbf{V}}^1 : \left[\overline{\Psi}^2 + \overline{\Psi}^3 \cdot \{\mathbf{R} - \mathbf{R}'\} \right] \\ & + \widetilde{\mathbf{V}}^2 : \overline{\Psi}^3 \end{aligned} \tag{4.5-51}$$

and

$$\begin{aligned} p(\mathbf{R_n}, \mathbf{r}) \;=\; & \overline{\Psi}^0 + \overline{\Psi}^1 \cdot \{\mathbf{R} - \mathbf{R}'\} + \frac{1}{2} \overline{\Psi}^2 : \{\mathbf{R} - \mathbf{R}'\}^2 + \frac{1}{6} \overline{\Psi}^3 \vdots \{\mathbf{R} - \mathbf{R}'\}^3 \\ & + \widetilde{\Pi}^0 \cdot \left[\overline{\Psi}^1 + \overline{\Psi}^2 \cdot \{\mathbf{R} - \mathbf{R}'\} + \frac{1}{2} \overline{\Psi}^3 : \{\mathbf{R} - \mathbf{R}'\}^2 \right] \\ & + \widetilde{\Pi}^1 : \left[\overline{\Psi}^2 + \overline{\Psi}^3 \cdot \{\mathbf{R} - \mathbf{R}'\} \right] \\ & + \widetilde{\Pi}^2 : \overline{\Psi}^3. \end{aligned} \tag{4.5-52}$$

All of the microscale flow characteristics are contained in the fully spatially periodic fields $\left\{ \widetilde{\mathbf{V}}^m(\mathbf{r}), \widetilde{\Pi}^m(\mathbf{r}) \right\}$ calculated from the $\mathcal{O}(0)$ *cell problem* (4.3-52), the $\mathcal{O}(1)$ *cell problem* (4.4-56) and the $\mathcal{O}(2)$ *cell problem* determined from (4.5-35) to (4.5-38):

$\mathcal{O}(2)$ *Cell Problem*: (4.5-53)

$$\begin{aligned} \nabla^2 \widetilde{\mathbf{V}}^2 - \boldsymbol{\nabla} \widetilde{\Pi}^2 \;&=\; \left[\!\!\left[\mathbf{I} \widetilde{\Pi}^1 - 2^{\dagger} \left(\boldsymbol{\nabla} \widetilde{\mathbf{V}}^1 \right) - \widetilde{\mathbf{V}}^0 \mathbf{I} \right]\!\!\right]^{s3}, \\ \boldsymbol{\nabla} \cdot \widetilde{\mathbf{V}}^2 \;&=\; -\left[\!\!\left[\widetilde{\mathbf{V}}^1 - \left\langle \widetilde{\mathbf{V}}^1 \right\rangle \right]\!\!\right]^{s}, \end{aligned}$$

$$\widetilde{\mathbf{V}}^2 = \mathbf{0} \qquad \forall\,(\mathbf{r} \in s_p)\,,$$

$$\left\langle \widetilde{\mathbf{\Pi}}^2 \right\rangle = \mathbf{0}.$$

This problem possesses a unique solution $\left[\widetilde{\mathbf{V}}^2(\mathbf{r}), \widetilde{\mathbf{\Pi}}^2(\mathbf{r})\right]$ determined entirely from the unit cell geometry. All the macroscale details of the flow are contained in the constants $\overline{\mathbf{\Psi}}^0(|\mathbf{R}')$, $\overline{\mathbf{\Psi}}^1(|\mathbf{R}')$, $\overline{\mathbf{\Psi}}^2(|\mathbf{R}')$ and $\overline{\mathbf{\Psi}}^3$. It is obvious that upon setting $\overline{\mathbf{\Psi}}^3 = \mathbf{0}$ in (4.5-51) and (4.5-52) that the truncated first-order flow field is recovered, while setting $\overline{\mathbf{\Psi}}^3 = \mathbf{0}$ and $\overline{\mathbf{\Psi}}^2 = \mathbf{0}$ recovers the truncated zeroth-order flow field. These constant tensors are fully symmetric, but not totally arbitrary in order that the resulting flow field satisfies continuity. The restrictions are determined from the first and second auxiliary conditions, (4.5-15) and (4.5-26) respectively, namely

$$\left\langle \widetilde{\mathbf{V}}^0 \right\rangle : \overline{\mathbf{\Psi}}^2 + \left\langle \widetilde{\mathbf{V}}^1 \right\rangle \dddot{:} \overline{\mathbf{\Psi}}^3 = 0, \tag{4.5-54}$$

$$\left\langle \widetilde{\mathbf{V}}^0 \right\rangle : \overline{\mathbf{\Psi}}^3 = \mathbf{0}. \tag{4.5-55}$$

The explicit dependence of $\overline{\mathbf{\Psi}}^m(|\mathbf{R}')$ upon the choice of reference point $\mathbf{R}'$ can be expressed as

$$\overline{\mathbf{\Psi}}^m(|\mathbf{R}'') = \sum_{j=0}^{3-m} \frac{1}{j!} \overline{\mathbf{\Psi}}^{m-j}(|\mathbf{R}')\,\{\cdot\}^j\,\{\mathbf{R}'' - \mathbf{R}'\}^j \qquad \forall\,(m = 0, 1, 2, 3)\,. \tag{4.5-56}$$

4.6 General Microscale Flow

The net results of the previous sections (§§ 4.3, 4.4 and 4.5) has been to determine a conveninent way to express the velocity and pressure fields existing in a spatially periodic model of a porous medium in circumstances where the mean flow is arbitrary (except for the requirement that it be incompressible). In the present section, those results for various degrees of truncation are cast into a more general framework, allowing one to inductively establish the expansion for an arbitrary degree of truncation of the series expansion.

4.6.1 Microscale Velocity $\mathbf{v}(\mathbf{R})$ and Pressure $p(\mathbf{R})$

The velocity and pressure fields for the zero-, first- and second-order flows show by induction that the discrete form of the Taylor series (4.2-6) and (4.2-7) for $\mathbf{v}(\mathbf{R})$ and $p(\mathbf{R})$, namely

$$\mathbf{v}(\mathbf{R}) = \sum_{m=0}^{\infty} \frac{1}{m!} \mathbf{v}^m(\mathbf{r}|\mathbf{R}') \{\cdot\}^m \{\mathbf{R_n} - \mathbf{R}'\}^m$$

and

$$p(\mathbf{R}) = \sum_{m=0}^{\infty} \frac{1}{m!} \mathbf{p}^m(\mathbf{r}|\mathbf{R}') \{\cdot\}^m \{\mathbf{R_n} - \mathbf{R}'\}^m$$

possess the equivalent representations

$$\mathbf{v}(\mathbf{R}) = \sum_{m=0}^{\infty} \frac{1}{m!} \tilde{\mathbf{v}}^m(\mathbf{r}|\mathbf{R}') \{\cdot\}^m \{\mathbf{R} - \mathbf{R}'\}^m, \tag{4.6-1}$$

$$p(\mathbf{R}) = \sum_{m=0}^{\infty} \frac{1}{m!} \tilde{\mathbf{p}}^m(\mathbf{r}|\mathbf{R}') \{\cdot\}^m \{\mathbf{R} - \mathbf{R}'\}^m. \tag{4.6-2}$$

The key difference between the two lies in the fact that the latter expressions involve *fully* spatially periodic functions and powers of a continuous position vector.

The relationship between the field $\mathbf{v}^m(\mathbf{r}|\mathbf{R}')$ and the fully spatially periodic field $\tilde{\mathbf{v}}^m(\mathbf{r}|\mathbf{R}')$ can be established by rewriting (4.6-1) while expanding the position vector $\mathbf{R}$ using the decomposition (3.3-9) in conjunction with the identity (3.3-12) (with the

choices $\mathbf{a} = \mathbf{r}$ and $\mathbf{b} = \mathbf{R_n} - \mathbf{R}'$). This yields

$$\mathbf{v} = \sum_{m=0}^{\infty} \frac{1}{m!} \tilde{\mathbf{v}}^m \{\cdot\}^m \sum_{j=0}^{m} \begin{pmatrix} m \\ j \end{pmatrix} \left[\!\left[\mathbf{r}^{m-j} \{\mathbf{R_n} - \mathbf{R}'\}^j \right]\!\right]^s .$$

Since $\tilde{\mathbf{v}}^m(\mathbf{r}|\mathbf{R}')$ is symmetric with respect to its last m indices [cf. (4.2-8)], the symmetry operator appearing in the last term may be deleted. Moreover, upon inverting the order of the summation (3.2-11), the previous equation may be rewritten as

$$\mathbf{v} = \sum_{j=0}^{\infty} \frac{1}{j!} \left[\sum_{m=0}^{\infty} \frac{1}{m!} \tilde{\mathbf{v}}^{m+j} \{\cdot\}^m \mathbf{r}^m \right] \{\cdot\}^j \{\mathbf{R_n} - \mathbf{R}'\}^j .$$

Comparison of this expression with the discrete Taylor series (4.2-6) furnishes the expression

$$\mathbf{v}^m(\mathbf{r}|\mathbf{R}') = \sum_{j=0}^{\infty} \frac{1}{j!} \tilde{\mathbf{v}}^{j+m}(\mathbf{r}|\mathbf{R}') \{\cdot\}^j \mathbf{r}^j \qquad \forall\, (m = 0, 1, 2, \ldots) \tag{4.6-3}$$

relating the fields $\mathbf{v}^m(\mathbf{r}|\mathbf{R}')$ to the fully spatially periodic fields $\tilde{\mathbf{v}}^m(\mathbf{r}|\mathbf{R}')$. In a similar manner, the relation between $\mathbf{p}^m(\mathbf{r}|\mathbf{R}')$ and $\tilde{\mathbf{p}}^m(\mathbf{r}|\mathbf{R}')$ is found to be

$$\mathbf{p}^m(\mathbf{r}|\mathbf{R}') = \sum_{j=0}^{\infty} \frac{1}{j!} \tilde{\mathbf{p}}^{j+m}(\mathbf{r}|\mathbf{R}') \{\cdot\}^j \mathbf{r}^j \qquad \forall\, (m = 0, 1, 2, \ldots) . \tag{4.6-4}$$

The inverse of (4.6-3), namely an explicit expression for $\tilde{\mathbf{v}}^m(\mathbf{r}|\mathbf{R}')$ in terms of $\mathbf{v}^m(\mathbf{r}|\mathbf{R}')$, may be derived by replacing $\mathbf{R_n}$ by $\mathbf{R} - \mathbf{r}$ in the discrete Taylor series (4.2-6), using the identity (3.3-12) (with the choices $\mathbf{a} = -\mathbf{r}$ and $\mathbf{b} = \mathbf{R} - \mathbf{R}'$), and switching the order of the summations to obtain

$$\mathbf{v} = \sum_{j=0}^{\infty} \frac{1}{j!} \left[\sum_{m=0}^{\infty} \frac{1}{m!} \mathbf{v}^{m+j} \{\cdot\}^m \{-\mathbf{r}\}^m \right] \{\cdot\}^j \{\mathbf{R} - \mathbf{R}'\}^j .$$

Comparison with (4.6-1) gives

$$\tilde{\mathbf{v}}^m(\mathbf{r}|\mathbf{R}') = \sum_{j=0}^{\infty} \frac{(-1)^j}{j!} \mathbf{v}^{j+m}(\mathbf{r}|\mathbf{R}') \{\cdot\}^j \mathbf{r}^j \qquad \forall\, (m = 0, 1, 2, \ldots) . \tag{4.6-5}$$

A similar procedure yields the inverse of (4.6-4), namely

$$\tilde{\mathbf{p}}^m(\mathbf{r}|\mathbf{R}') = \sum_{j=0}^{\infty} \frac{(-1)^j}{j!} \mathbf{p}^{j+m}(\mathbf{r}|\mathbf{R}') \{\cdot\}^j \mathbf{r}^j \qquad \forall (m = 0, 1, 2, \ldots) . \tag{4.6-6}$$

As in the preceding sections, the goal now is to separate out the dependence of $\tilde{\mathbf{v}}^m(\mathbf{r}|\mathbf{R}')$ and $\tilde{\mathbf{p}}^m(\mathbf{r}|\mathbf{R}')$ upon the choice of reference point $\mathbf{R}'$.

4.6.2 Equations Satisfied by $\tilde{\mathbf{v}}^m(\mathbf{r}|\mathbf{R}')$ and $\tilde{\mathbf{p}}^m(\mathbf{r}|\mathbf{R}')$

This subsection developes the differential equations and boundary conditions governing the fully spatially periodic fields $\tilde{\mathbf{v}}^m(\mathbf{r}|\mathbf{R}')$ and $\tilde{\mathbf{p}}^m(\mathbf{r}|\mathbf{R}')$.

Equation (4.6-5) combines with the no-slip condition (4.2-14) on the particle surfaces to show that $\tilde{\mathbf{v}}^m(\mathbf{r}|\mathbf{R}')$ also satisfies the no-slip condition:

$$\tilde{\mathbf{v}}^m = \mathbf{0} \qquad \forall (\mathbf{r} \in s_p) , \tag{4.6-7}$$

valid for $m = 0, 1, 2, \ldots$.

Form the divergence of (4.6-5) and differentiate the result by parts to obtain

$$\boldsymbol{\nabla} \cdot \tilde{\mathbf{v}}^m = \sum_{j=0}^{\infty} \frac{(-1)^j}{j!} \left[\boldsymbol{\nabla} \cdot \mathbf{v}^{j+m}\right] \{\cdot\}^j \mathbf{r}^j + \sum_{j=1}^{\infty} \frac{(-1)^j}{(j-1)!} \mathbf{I} : \mathbf{v}^{j+m} \{\cdot\}^{j-1} \mathbf{r}^{j-1},$$

whose derivation has utilized the identity

$$\boldsymbol{\nabla} \left(\mathbf{r}^j\right) = j \left[\!\!\left[\mathbf{I} \mathbf{r}^{j-1} \right]\!\!\right]^{sj} \qquad \forall (j = 1, 2, 3, \ldots) \tag{4.6-8}$$

as well as the symmetry of $\mathbf{v}^m(\mathbf{r}|\mathbf{R}')$. The first sum on the right-hand side of the equation preceding the above is identically zero by the continuity condition (4.2-13) while the second sum may be rewritten, obtaining

$$\boldsymbol{\nabla} \cdot \tilde{\mathbf{v}}^m = -\mathbf{I} : \sum_{j=0}^{\infty} \frac{(-1)^j}{j!} \mathbf{v}^{j+1+m} \{\cdot\}^j \mathbf{r}^j .$$

However, from (4.6-5) the previous summation is identically $\tilde{\mathbf{v}}^{m+1}(\mathbf{r}|\mathbf{R}')$, whence the

incompressibility requirement satisfied by $\tilde{\mathbf{v}}^m(\mathbf{r}|\mathbf{R}')$ requires that

$$\boldsymbol{\nabla} \cdot \tilde{\mathbf{v}}^m = -\mathbf{I} : \tilde{\mathbf{v}}^{m+1}, \tag{4.6-9}$$

valid for $m = 0, 1, 2, \ldots$.

The linear momentum equation satisfied by $\tilde{\mathbf{v}}^m(\mathbf{r}|\mathbf{R}')$ and $\tilde{\mathbf{p}}^m(\mathbf{r}|\mathbf{R}')$ can be derived by first forming the gradient of (4.6-5) and differentiating the resultant expression by parts to obtain

$$\boldsymbol{\nabla}\tilde{\mathbf{v}}^m = \sum_{j=0}^{\infty} \frac{(-1)^j}{j!} \left[\boldsymbol{\nabla}\mathbf{v}^{j+m}\right] \{\cdot\}^j \mathbf{r}^j + \sum_{j=1}^{\infty} \frac{(-1)^j}{(j-1)!} \dagger_{\mathbf{v}^{j+m}} \{\cdot\}^{j-1} \mathbf{r}^{j-1},$$

wherein the identity (4.6-8) together with the symmetry of $\mathbf{v}^m(\mathbf{r}|\mathbf{R}')$ have been used. Next, form the divergence of the previous equation and again differentiate by parts and use (4.6-8) and symmetry to obtain

$$\begin{aligned}
\nabla^2\tilde{\mathbf{v}}^m &= \sum_{j=0}^{\infty} \frac{(-1)^j}{j!} \left[\nabla^2\mathbf{v}^{j+m}\right] \{\cdot\}^j \mathbf{r}^j \\
&\quad + \sum_{j=1}^{\infty} \frac{(-1)^j}{(j-1)!} \left[\boldsymbol{\nabla} \cdot \dagger_{\mathbf{v}^{j+m}}\right] \{\cdot\}^{j-1} \mathbf{r}^{j-1} \\
&\quad + \boldsymbol{\nabla} \cdot \sum_{j=1}^{\infty} \frac{(-1)^j}{(j-1)!} \dagger_{\mathbf{v}^{j+m}} \{\cdot\}^{j-1} \mathbf{r}^{j-1}.
\end{aligned}$$

Convert the second summation using differentiation by parts and combine with the third summation, resulting in the expression

$$\begin{aligned}
\nabla^2\tilde{\mathbf{v}}^m &= \sum_{j=0}^{\infty} \frac{(-1)^j}{j!} \left[\nabla^2\mathbf{v}^{j+m}\right] \{\cdot\}^j \mathbf{r}^j \\
&\quad + 2\boldsymbol{\nabla} \cdot \sum_{j=1}^{\infty} \frac{(-1)^j}{(j-1)!} \dagger_{\mathbf{v}^{j+m}} \{\cdot\}^{j-1} \mathbf{r}^{j-1} \\
&\quad - \sum_{j=2}^{\infty} \frac{(-1)^j}{(j-2)!} \mathbf{v}^{j+m} \{\cdot\}^j \left[\mathbf{I}\mathbf{r}^{j-2}\right].
\end{aligned}$$

Rearrangement of the summations gives

$$\begin{aligned}\nabla^2\tilde{\mathbf{v}}^m &= \sum_{j=0}^{\infty}\frac{(-1)^j}{j!}\left[\nabla^2\mathbf{v}^{j+m}\right]\{\cdot\}^j\,\mathbf{r}^j \\ &\quad -2\boldsymbol{\nabla}\cdot\dagger\left[\sum_{j=0}^{\infty}\frac{(-1)^j}{j!}\mathbf{v}^{j+1+m}\{\cdot\}^j\,\mathbf{r}^j\right] \\ &\quad -\left[\sum_{j=0}^{\infty}\frac{(-1)^j}{j!}\mathbf{v}^{j+2+m}\{\cdot\}^j\,\mathbf{r}^j\right]:\mathbf{I}.\end{aligned}$$

Upon comparison of the last two terms with (4.6-5) the above ultimately becomes

$$\nabla^2\tilde{\mathbf{v}}^m=\sum_{j=0}^{\infty}\frac{(-1)^j}{j!}\left[\nabla^2\mathbf{v}^{j+m}\right]\{\cdot\}^j\,\mathbf{r}^j-2\boldsymbol{\nabla}\cdot\dagger\tilde{\mathbf{v}}^{m+1}-\tilde{\mathbf{v}}^{m+2}:\mathbf{I}. \tag{4.6-10}$$

In a similar manner, form the gradient of (4.6-6), use differentiation by parts together with the identity (4.6-8) and the symmetry conditions imposed upon $\mathbf{p}^m(\mathbf{r}|\mathbf{R}')$ to eventually obtain

$$\boldsymbol{\nabla}\tilde{\mathbf{p}}^m=\sum_{j=0}^{\infty}\frac{(-1)^j}{j!}\left[\boldsymbol{\nabla}\mathbf{p}^{j+m}\right]\{\cdot\}^j\,\mathbf{r}^j-\tilde{\mathbf{p}}^{m+1}. \tag{4.6-11}$$

Multiply (4.6-10) by μ, subtract from this (4.6-11) and use the linear momentum equation (4.2-12) to obtain

$$\mu\nabla^2\tilde{\mathbf{v}}^m-\boldsymbol{\nabla}\tilde{\mathbf{p}}^m=\tilde{\mathbf{p}}^{m+1}-2\mu\boldsymbol{\nabla}\cdot\dagger\tilde{\mathbf{v}}^{m+1}-\mu\tilde{\mathbf{v}}^{m+2}:\mathbf{I}, \tag{4.6-12}$$

valid for $m=0,1,2,\ldots$. In summary, whereas the aperiodic fields $\mathbf{v}^m(\mathbf{r}|\mathbf{R}')$ and $\mathbf{p}^m(\mathbf{r}|\mathbf{R}')$ satisfy equations (4.2-12) to (4.2-14) and jump conditions (4.2-18) to (4.2-21), the fully spatially periodic fields $\tilde{\mathbf{v}}^m(\mathbf{r}|\mathbf{R}')$ and $\tilde{\mathbf{p}}^m(\mathbf{r}|\mathbf{R}')$ satisfy (4.6-12), (4.6-9) and (4.6-7), namely

$$\mu\nabla^2\tilde{\mathbf{v}}^m-\boldsymbol{\nabla}\tilde{\mathbf{p}}^m=\tilde{\mathbf{p}}^{m+1}-2\mu\boldsymbol{\nabla}\cdot\dagger\tilde{\mathbf{v}}^{m+1}-\mu\tilde{\mathbf{v}}^{m+2}:\mathbf{I}, \tag{4.6-13}$$

$$\boldsymbol{\nabla}\cdot\tilde{\mathbf{v}}^m=-\mathbf{I}:\tilde{\mathbf{v}}^{m+1}, \tag{4.6-14}$$

$$\tilde{\mathbf{v}}^m=\mathbf{0}\qquad\forall\,(\mathbf{r}\in s_p), \tag{4.6-15}$$

with the jump condition (3.4-3) implicitly satisfied by their fully spatially periodic nature.

4.6.3 Characteristic Cell Problems and General Auxiliary Conditions

Similar to the definitions (4.3-20) for the zero-order flow, (4.4-23) and (4.4-35) for the first-order flow, and (4.5-12), (4.5-24) together with (4.5-34) for the second-order flow, define the constants $\overline{\mathbf{\Psi}}^m(|\mathbf{R}')$ as

$$\overline{\mathbf{\Psi}}^m(|\mathbf{R}') \stackrel{\text{def}}{=} \langle \tilde{\mathbf{p}}^m(\mathbf{r}|\mathbf{R}') \rangle \,. \tag{4.6-16}$$

Observing the patterns of equations (4.5-10), (4.5-11), (4.5-22), (4.5-23), (4.5-32) and (4.5-33) of the second-order flow problem, it seems resonable to assume (subject, of course, to *a posteriori* verification) that the dependence of $\tilde{\mathbf{v}}^m(\mathbf{r}|\mathbf{R}')$ and $\tilde{\mathbf{p}}^m(\mathbf{r}|\mathbf{R}')$ upon the constants $\overline{\mathbf{\Psi}}^m(|\mathbf{R}')$ (and hence upon $\mathbf{R}'$) is linear and can be removed by defining solutions of the respective forms

$$\mu\tilde{\mathbf{v}}^m(\mathbf{r}|\mathbf{R}') \stackrel{\text{def}}{=} \sum_{j=0}^{\infty} \widetilde{\mathbf{V}}^j(\mathbf{r}) \{\cdot\}^{j+1} \overline{\mathbf{\Psi}}^{j+1+m}(|\mathbf{R}'), \tag{4.6-17}$$

$$\tilde{\mathbf{p}}^m(\mathbf{r}|\mathbf{R}') \stackrel{\text{def}}{=} \overline{\mathbf{\Psi}}^m(|\mathbf{R}') + \sum_{j=0}^{\infty} \widetilde{\mathbf{\Pi}}^j(\mathbf{r}) \{\cdot\}^{j+1} \overline{\mathbf{\Psi}}^{j+1+m}(|\mathbf{R}'), \tag{4.6-18}$$

where the spatially periodic fields $\widetilde{\mathbf{V}}^m(\mathbf{r})$ and $\widetilde{\mathbf{\Pi}}^m(\mathbf{r})$ are to be determined. Upon forming the cellular average of (4.6-18) and using the normalization condition (4.6-16) we obtain

$$\sum_{j=0}^{\infty} \left\langle \widetilde{\mathbf{\Pi}}^j(\mathbf{r}) \right\rangle \{\cdot\}^{j+1} \overline{\mathbf{\Psi}}^{j+1+m}(|\mathbf{R}') = \mathbf{0}.$$

Since this must hold for all values of $m = 0, 1, 2, \ldots$, this shows that $\widetilde{\mathbf{\Pi}}^m(\mathbf{r})$ must be normalized as

$$\left\langle \widetilde{\mathbf{\Pi}}^m \right\rangle = \mathbf{0}. \tag{4.6-19}$$

The no-slip condition (4.6-7) written for the proposed solution (4.6-17) gives

$$\sum_{j=0}^{\infty} \widetilde{\mathbf{V}}^j \{\cdot\}^{j+1} \overline{\mathbf{\Psi}}^{j+1+m} = \mathbf{0} \qquad \forall (\mathbf{r} \in s_p) .$$

As this must apply for all m, equality is satisfied by the choice

$$\widetilde{\mathbf{V}}^m = \mathbf{0} \qquad \forall (\mathbf{r} \in s_p) , \tag{4.6-20}$$

valid for $m = 0, 1, 2, \ldots$.

Integrate the continuity condition (4.6-9) over the fluid domain τ_f, use the divergence theorem, the spatially periodic nature of these fields, and the fact (4.6-7) that they vanish on the particle surfaces to derive the restriction

$$\mathbf{I} : \left\langle \tilde{\mathbf{v}}^{m+1} \right\rangle = \mathbf{0} \qquad \forall (m = 0, 1, 2, \ldots) . \tag{4.6-21}$$

Substitution of the proposed solution (4.6-17) into the above equation thereby furnishes the generalized auxiliary conditions:

$$\sum_{j=0}^{\infty} \left\langle \widetilde{\mathbf{V}}^j \right\rangle \{\cdot\}^{j+2} \overline{\mathbf{\Psi}}^{j+2+m} = \mathbf{0} \qquad \forall (m = 0, 1, 2, \ldots) , \tag{4.6-22}$$

restricting the values of the constant tensors $\overline{\mathbf{\Psi}}^m(|\mathbf{R}')$. This equation is what was previously termed *auxiliary condition #m*, possessing the form (4.4-57) for the truncated first-order flow field and (4.5-54) and (4.5-55) for the truncated second-order field.

Rewrite the continuity condition (4.6-9) as

$$\boldsymbol{\nabla} \cdot \tilde{\mathbf{v}}^m + \mathbf{I} : \tilde{\mathbf{v}}^{m+1} = \mathbf{0},$$

and substitute into this the proposed solution (4.6-17) to obtain

$$\sum_{j=0}^{\infty} \left[\boldsymbol{\nabla} \cdot \widetilde{\mathbf{V}}^j \right] \{\cdot\}^{j+1} \overline{\mathbf{\Psi}}^{j+1+m} + \sum_{j=0}^{\infty} \widetilde{\mathbf{V}}^j \{\cdot\}^{j+2} \overline{\mathbf{\Psi}}^{j+2+m} = \mathbf{0}.$$

This may be rewritten equivalently as

$$\left[\boldsymbol{\nabla}\cdot\widetilde{\mathbf{V}}^0\right]\cdot\overline{\boldsymbol{\Psi}}^{1+m}+\sum_{j=1}^{\infty}\left[\boldsymbol{\nabla}\cdot\widetilde{\mathbf{V}}^j\right]\{\cdot\}^{j+1}\,\overline{\boldsymbol{\Psi}}^{j+1+m}+\sum_{j=0}^{\infty}\widetilde{\mathbf{V}}^j\,\{\cdot\}^{j+2}\,\overline{\boldsymbol{\Psi}}^{j+2+m}=\mathbf{0}.$$

The latter two summations may be combined by replacing the dummy index j by $j+1$ in the second term, yielding

$$\left[\boldsymbol{\nabla}\cdot\widetilde{\mathbf{V}}^0\right]\cdot\overline{\boldsymbol{\Psi}}^{1+m}+\sum_{j=0}^{\infty}\left[\boldsymbol{\nabla}\cdot\widetilde{\mathbf{V}}^{j+1}+\widetilde{\mathbf{V}}^j\right]\{\cdot\}^{j+2}\,\overline{\boldsymbol{\Psi}}^{j+2+m}=\mathbf{0}. \tag{4.6-23}$$

This must be satisfied for all $m=0,1,2,\ldots$. Set $m=0$ in the latter and note that the vector $\overline{\boldsymbol{\Psi}}^1(|\mathbf{R}')$ is arbitrary, and not otherwise restricted by the generalized auxiliary conditions (4.6-22). This reveals that the dyadic field $\widetilde{\mathbf{V}}^0(\mathbf{r})$ must satisfy the continuity condition

$$\boldsymbol{\nabla}\cdot\widetilde{\mathbf{V}}^0=\mathbf{0}. \tag{4.6-24}$$

The latter two displayed equations combine to give

$$\sum_{j=0}^{\infty}\left[\boldsymbol{\nabla}\cdot\widetilde{\mathbf{V}}^{j+1}+\widetilde{\mathbf{V}}^j\right]\{\cdot\}^{j+2}\,\overline{\boldsymbol{\Psi}}^{j+2+m}=\mathbf{0}.$$

This relation would appear to require that $\boldsymbol{\nabla}\cdot\widetilde{\mathbf{V}}^{j+1}=-\widetilde{\mathbf{V}}^j$. However, this would lead to the erroneous conclusion that $\left\langle\widetilde{\mathbf{V}}^j\right\rangle=\mathbf{0}$. The source of error resides in the fact that the tensors $\overline{\boldsymbol{\Psi}}^m(|\mathbf{R}')$ are not totally arbitrary, but rather must satisfy the general auxiliary conditions (4.6-22). It is because of this fact that the latter equation may be rewritten in the equivalent form

$$\sum_{j=0}^{\infty}\left[\boldsymbol{\nabla}\cdot\widetilde{\mathbf{V}}^{j+1}+\widetilde{\mathbf{V}}^j-\left\langle\widetilde{\mathbf{V}}^j\right\rangle\right]\{\cdot\}^{j+2}\,\overline{\boldsymbol{\Psi}}^{j+2+m}=\mathbf{0}.$$

Furthermore, since every $\overline{\boldsymbol{\Psi}}^m(|\mathbf{R}')$ is a fully symmetric tensor, this equation may be satisfied by the choice

$$\boldsymbol{\nabla}\cdot\widetilde{\mathbf{V}}^{m+1}=-\left[\!\left[\,\widetilde{\mathbf{V}}^m-\left\langle\widetilde{\mathbf{V}}^m\right\rangle\,\right]\!\right]^s. \tag{4.6-25}$$

Equations (4.6-24) and (4.6-25) combine to furnish the following 'continuity constraint' on $\widetilde{\mathbf{V}}^m(\mathbf{r})$:

$$\boldsymbol{\nabla}\cdot\widetilde{\mathbf{V}}^m = \begin{cases} \mathbf{0} & (m=0), \\ -\left[\!\left[\, \widetilde{\mathbf{V}}^{m-1} - \left\langle \widetilde{\mathbf{V}}^{m-1} \right\rangle \,\right]\!\right]^s & \forall (m=1,2,3,\ldots). \end{cases} \tag{4.6-26}$$

The linear momentum equation governing $\widetilde{\mathbf{V}}^m(\mathbf{r})$ and $\widetilde{\boldsymbol{\Pi}}^m(\mathbf{r})$ can be derived as follows. Rewrite (4.6-12) as

$$\mu\nabla^2\tilde{\mathbf{v}}^m - \boldsymbol{\nabla}\tilde{\mathbf{p}}^m - \tilde{\mathbf{p}}^{m+1} + 2\mu\boldsymbol{\nabla}\cdot{}^{\dagger}\tilde{\mathbf{v}}^{m+1} + \mu\tilde{\mathbf{v}}^{m+2} : \mathbf{I} = \mathbf{0},$$

and substitute into this the proposed solutions (4.6-17) and (4.6-18), thereby obtaining

$$\begin{aligned} &\sum_{j=0}^{\infty}\left[\nabla^2\widetilde{\mathbf{V}}^j - \boldsymbol{\nabla}\widetilde{\boldsymbol{\Pi}}^j\right]\{\cdot\}^{j+1}\,\overline{\boldsymbol{\Psi}}^{j+1+m} \\ &\quad -\overline{\boldsymbol{\Psi}}^{m+1} - \sum_{j=0}^{\infty}\widetilde{\boldsymbol{\Pi}}^j\,\{\cdot\}^{j+1}\,\overline{\boldsymbol{\Psi}}^{j+2+m} \\ &\quad +2\sum_{j=0}^{\infty}{}^{\dagger}\left[\boldsymbol{\nabla}\widetilde{\mathbf{V}}^j\right]\{\cdot\}^{j+2}\,\overline{\boldsymbol{\Psi}}^{j+2+m} \\ &\quad +\sum_{j=0}^{\infty}\widetilde{\mathbf{V}}^j\,\{\cdot\}^{j+1}\,\overline{\boldsymbol{\Psi}}^{j+3+m} : \mathbf{I} \;=\; \mathbf{0}. \end{aligned}$$

Next, separate out the $j=0$ and $j=1$ terms of the first summation, the first term of the second summation, the first term of the third summation, and collect terms to obtain

$$\begin{aligned} &\left[\nabla^2\widetilde{\mathbf{V}}^0 - \boldsymbol{\nabla}\widetilde{\boldsymbol{\Pi}}^0 - \mathbf{I}\right]\cdot\overline{\boldsymbol{\Psi}}^{m+1} \\ &+\left[\nabla^2\widetilde{\mathbf{V}}^1 - \boldsymbol{\nabla}\widetilde{\boldsymbol{\Pi}}^1 - \mathbf{I}\widetilde{\boldsymbol{\Pi}}^0 + 2^{\dagger}\left(\boldsymbol{\nabla}\widetilde{\mathbf{V}}^0\right)\right] : \overline{\boldsymbol{\Psi}}^{m+2} \\ &+\sum_{j=2}^{\infty}\left[\nabla^2\widetilde{\mathbf{V}}^j - \boldsymbol{\nabla}\widetilde{\boldsymbol{\Pi}}^j\right]\{\cdot\}^{j+1}\,\overline{\boldsymbol{\Psi}}^{j+1+m} \\ &+\sum_{j=1}^{\infty}\left[-\mathbf{I}\widetilde{\boldsymbol{\Pi}}^j + 2^{\dagger}\left(\boldsymbol{\nabla}\widetilde{\mathbf{V}}^j\right)\right]\{\cdot\}^{j+2}\,\overline{\boldsymbol{\Psi}}^{j+2+m} \end{aligned}$$

$$+\sum_{j=0}^{\infty}\left[\widetilde{\mathbf{V}}^{j}\mathbf{I}\right]\{\cdot\}^{j+3}\,\overline{\mathbf{\Psi}}^{j+3+m} \;=\; \mathbf{0}.$$

The three summations in the latter may be combined upon expressing the first two as sums from $j = 0$ to ∞, thus resulting in the expression

$$\begin{aligned}
&\left[\nabla^2\widetilde{\mathbf{V}}^0 - \boldsymbol{\nabla}\widetilde{\mathbf{\Pi}}^0 - \mathbf{I}\right]\cdot\overline{\mathbf{\Psi}}^{m+1} \\
&+\left[\nabla^2\widetilde{\mathbf{V}}^1 - \boldsymbol{\nabla}\widetilde{\mathbf{\Pi}}^1 - \mathbf{I}\widetilde{\mathbf{\Pi}}^0 + 2^{\dagger}\left(\boldsymbol{\nabla}\widetilde{\mathbf{V}}^0\right)\right] : \overline{\mathbf{\Psi}}^{m+2} \\
+\sum_{j=0}^{\infty}&\left[\nabla^2\widetilde{\mathbf{V}}^{j+2} - \boldsymbol{\nabla}\widetilde{\mathbf{\Pi}}^{j+2} - \mathbf{I}\widetilde{\mathbf{\Pi}}^{j+1} + 2^{\dagger}\left(\boldsymbol{\nabla}\widetilde{\mathbf{V}}^{j+1}\right) + \widetilde{\mathbf{V}}^{j}\mathbf{I}\right]\{\cdot\}^{j+3}\,\overline{\mathbf{\Psi}}^{j+3+m} \;=\; \mathbf{0}.
\end{aligned}$$

Since this expression must be satisfied for $m = 0, 1, 2\ldots$, and because $\overline{\mathbf{\Psi}}^{m}(|\mathbf{R}')$ is a fully symmetric tensor, the fields $\widetilde{\mathbf{V}}^{m}(\mathbf{r})$ and $\widetilde{\mathbf{\Pi}}^{m}(\mathbf{r})$ necessarily satisfy the relations

$$\nabla^2\widetilde{\mathbf{V}}^{m} - \boldsymbol{\nabla}\widetilde{\mathbf{\Pi}}^{m} = \begin{cases} \mathbf{I} & (m=0), \\ \left[\!\left[\, \mathbf{I}\widetilde{\mathbf{\Pi}}^{0} - 2^{\dagger}\left(\boldsymbol{\nabla}\widetilde{\mathbf{V}}^{0}\right) \right]\!\right]^{s2} & (m=1), \\ \left[\!\left[\, \mathbf{I}\widetilde{\mathbf{\Pi}}^{m-1} - 2^{\dagger}\left(\boldsymbol{\nabla}\widetilde{\mathbf{V}}^{m-1}\right) - \widetilde{\mathbf{V}}^{m-2}\mathbf{I} \right]\!\right]^{sm+1} & \forall(m\geq 2). \end{cases} \tag{4.6-27}$$

The latter equation along with (4.6-26), (4.6-20) and (4.6-19), namely

$$\boldsymbol{\nabla}\cdot\widetilde{\mathbf{V}}^{m} = \begin{cases} \mathbf{0} & (m=0), \\ -\left[\!\left[\, \widetilde{\mathbf{V}}^{m-1} - \left\langle\widetilde{\mathbf{V}}^{m-1}\right\rangle \right]\!\right]^{s} & \forall(m\geq 1), \end{cases} \tag{4.6-28}$$

$$\widetilde{\mathbf{V}}^{m} = \mathbf{0} \qquad \forall\left(\mathbf{r}\in s_p\right), \tag{4.6-29}$$

$$\left\langle\widetilde{\mathbf{\Pi}}^{m}\right\rangle = \mathbf{0}, \tag{4.6-30}$$

constitute the $\mathcal{O}(m)$ *cell problem* for $m = 0, 1, 2, \ldots$ as were derived in the previous sections (4.3-52), (4.4-56) and (4.5-53) for the special cases of $m = 0$, $m = 1$ and $m = 2$. Notice that although equations (4.6-12), (4.6-9) and (4.6-7) satisfied

by $(\tilde{\mathbf{v}}^m, \tilde{\mathbf{p}}^m)$ were expressed in terms of *higher* solutions (making a general solution somewhat unclear), the characteristic cell problems (4.6-27), (4.6-26), (4.6-20) and (4.6-19) for the fields $\left(\widetilde{\mathbf{V}}^m, \widetilde{\mathbf{\Pi}}^m\right)$ are expressed in terms of *lower* solutions. (This also furnishes one of the reasons that solutions derived in the previous sections had to begin with the highest-order terms, subsequently to be solved successively for each lower term.) The generation of the characteristic cell problems and their uniqueness at each order confirms the proposed solutions (4.6-17) and (4.6-18) of the fields $\tilde{\mathbf{v}}^m(\mathbf{r}|\mathbf{R}')$ and $\tilde{\mathbf{p}}^m(\mathbf{r}|\mathbf{R}')$.

4.6.4 Microscale Velocity and Pressure Fields

Substitute (4.6-17) into (4.6-1) to obtain

$$\mu\mathbf{v}(\mathbf{R}) = \sum_{m=0}^{\infty} \frac{1}{m!} \left[\sum_{j=0}^{\infty} \widetilde{\mathbf{V}}^j(\mathbf{r}) \{\cdot\}^{j+1} \overline{\mathbf{\Psi}}^{j+1+m}(|\mathbf{R}') \right] \{\cdot\}^m \{\mathbf{R} - \mathbf{R}'\}^m . \tag{4.6-31}$$

Several ways exist to express the latter in a more useful form. An obvious form would be to group together summations involving like powers of $\overline{\mathbf{\Psi}}^m(|\mathbf{R}')$. This can be done by replacing j by $j - m$, followed by interchanging the order of the summations to obtain

$$\begin{aligned} \mu\mathbf{v}(\mathbf{R}) &= \sum_{j=0}^{\infty} \left[\sum_{m=0}^{j} \frac{1}{m!} \widetilde{\mathbf{V}}^{j-m} \{\mathbf{R} - \mathbf{R}'\}^m \right] \{\cdot\}^{j+1} \overline{\mathbf{\Psi}}^{j+1} \\ &\equiv \widetilde{\mathbf{V}}^0 \cdot \overline{\mathbf{\Psi}}^1 + \left[\widetilde{\mathbf{V}}^1 + \widetilde{\mathbf{V}}^0 \{\mathbf{R} - \mathbf{R}'\} \right] : \overline{\mathbf{\Psi}}^2 \\ &\quad + \left[\widetilde{\mathbf{V}}^2 + \widetilde{\mathbf{V}}^1 \{\mathbf{R} - \mathbf{R}'\} + \frac{1}{2} \widetilde{\mathbf{V}}^0 \{\mathbf{R} - \mathbf{R}'\}^2 \right] \vdots \overline{\mathbf{\Psi}}^3 + \cdots . \end{aligned} \tag{4.6-32}$$

A similar procedure in which (4.6-2) is combined with (4.6-18) yields

$$p(\mathbf{R}) = \overline{\Psi}^0 + \sum_{j=0}^{\infty} \left[\frac{1}{(j+1)!} \{\mathbf{R} - \mathbf{R}'\}^{j+1} + \sum_{m=0}^{j} \frac{1}{m!} \widetilde{\mathbf{\Pi}}^{j-m} \{\mathbf{R} - \mathbf{R}'\}^m \right] \{\cdot\}^{j+1} \overline{\mathbf{\Psi}}^{j+1} . \tag{4.6-33}$$

Equations (4.6-32) and (4.6-33) represent the general forms of the microscale velocity and pressure fields. The choice of $\overline{\Psi}^m(|\mathbf{R}') = \mathbf{0}$ for $m \geq 2$, 3 or 4 yields the truncated zeroth- first- and second-order solutions respectively, as outlined in previous sections.

Alternatively, (4.6-31) may be regrouped in terms of tensor functions multiplying each cell solution $\tilde{\mathbf{v}}^m(\mathbf{r})$. Interchanging the summations in (4.6-31) yields

$$\mu\mathbf{v}(\mathbf{R}) = \sum_{j=0}^{\infty} \widetilde{\mathbf{V}}^j \{\cdot\}^{j+1} \left[\sum_{m=0}^{\infty} \frac{1}{m!} \overline{\Psi}^{j+1+m} \{\cdot\}^m \{\mathbf{R} - \mathbf{R}'\}^m \right]. \tag{4.6-34}$$

Notice that the term in brackets has the form of a Taylor series. This suggests defining the *scalar* field

$$\psi(\mathbf{R}) \stackrel{\text{def}}{=} \sum_{m=0}^{\infty} \frac{1}{m!} \overline{\Psi}^m(|\mathbf{R}') \{\cdot\}^m \{\mathbf{R} - \mathbf{R}'\}^m, \tag{4.6-35}$$

wherein any dependence of $\psi(\mathbf{R})$ upon choice of reference point does not appear for the same reasons it is absent from (4.6-34). This allows (4.6-34) to be rewritten as

$$\mu\mathbf{v}(\mathbf{R}) = \sum_{j=0}^{\infty} \widetilde{\mathbf{V}}^j(\mathbf{R}) \{\cdot\}^{j+1} \boldsymbol{\nabla}^{j+1} \psi(\mathbf{R}). \tag{4.6-36}$$

Likewise, the microscale pressure field may also be written in terms of the function $\psi(\mathbf{R})$ as

$$p(\mathbf{R}) = \psi(\mathbf{R}) + \sum_{j=0}^{\infty} \widetilde{\Pi}^j(\mathbf{R}) \{\cdot\}^{j+1} \boldsymbol{\nabla}^{j+1} \psi(\mathbf{R}). \tag{4.6-37}$$

To understand the significance of the function $\psi(\mathbf{R})$, it is useful to look at the microscale solutions generated by various forms of $\psi(\mathbf{R})$. The case $\psi = \overline{\Psi}^0$ results in $\mathbf{v}(\mathbf{R}) = \mathbf{0}$ and $p(\mathbf{R}) = \overline{\Psi}^0$ which corresponds to a quiescent fluid in a porous medium. The case $\psi = \overline{\Psi}^0 + \overline{\Psi}^1 \cdot \mathbf{R}$ corresponds to the zeroth-order flow field with the velocity being spatially periodic and the pressure being composed of a spatially periodic part (a homogeneous flow field on the macroscale) and a part varying linearly with $\mathbf{R}$. Including higher order powers of $\mathbf{R}$ in $\psi(\mathbf{R})$ results in higher order inhomogeneities in the corresponding flow fields.

4.6.5 General Auxiliary Condition Imposed Upon $\psi(\mathbf{R})$

Since the fluid is incompressible, a restriction upon the choice of the function $\psi(\mathbf{R})$ exists. Form the divergence of (4.6-36) to obtain

$$\mu \boldsymbol{\nabla} \cdot \mathbf{v} = 0 = \sum_{j=0}^{\infty} \left[\boldsymbol{\nabla} \cdot \widetilde{\mathbf{V}}^j \right] \{\cdot\}^{j+1} \boldsymbol{\nabla}^{j+1} \psi + \sum_{j=0}^{\infty} \widetilde{\mathbf{V}}^j \{\cdot\}^{j+2} \boldsymbol{\nabla}^{j+2} \psi,$$

which can be rewritten as

$$0 = \left[\boldsymbol{\nabla} \cdot \widetilde{\mathbf{V}}^0 \right] \psi + \sum_{j=0}^{\infty} \left[\boldsymbol{\nabla} \cdot \widetilde{\mathbf{V}}^{j+1} + \widetilde{\mathbf{V}}^j \right] \{\cdot\}^{j+2} \boldsymbol{\nabla}^{j+2} \psi.$$

Use of the cellular continuity condition (4.6-26) enables the latter to be expressed as

$$0 = \sum_{j=0}^{\infty} \left\langle \widetilde{\mathbf{V}}^j \right\rangle \{\cdot\}^{j+2} \boldsymbol{\nabla}^{j+2} \psi. \tag{4.6-38}$$

This represents an alternative form of the generalized auxiliary conditions, since if we substitute the definition (4.6-35) into (4.6-38), rearrange yields

$$\sum_{m=0}^{\infty} \frac{1}{m!} \left[\sum_{j=0}^{\infty} \left\langle \widetilde{\mathbf{V}}^j \right\rangle \{\cdot\}^{j+2} \overline{\boldsymbol{\Psi}}^{j+2+m} \right] \{\cdot\}^m \{\mathbf{R} - \mathbf{R}'\}^m = 0,$$

which must be valid for all powers of $\mathbf{R} - \mathbf{R}'$. As such, the inner summation must be identically zero for all m. This is precisely the generalized auxiliary condition (4.6-22) derived previously. The utility of the forms (4.6-36), (4.6-37) and (4.6-38) is that the solution $\mathbf{v}(\mathbf{R})$, $p(\mathbf{R})$ no longer needs to be described in terms of the set of reference cell dependent tensors $\overline{\boldsymbol{\Psi}}^m(|\mathbf{R}')$, but rather in terms of the scalar function $\psi(\mathbf{R})$.

4.6.6 Summary of Generalized Microscale Flow

The microscale velocity $\mathbf{v}(\mathbf{R})$ and pressure $p(\mathbf{R})$ fields satisfying the steady, incompressible, creeping flow equations (4.2-1) and (4.2-2) at all points $\mathbf{R}$ in the interstitial fluid domain together with the no-slip condition (4.2-3) on particle surfaces can be

written in the respective forms

$$\mu \mathbf{v}(\mathbf{R}) = \sum_{j=0}^{\infty} \widetilde{\mathbf{V}}^j(\mathbf{R}) \{\cdot\}^{j+1} \boldsymbol{\nabla}^{j+1} \psi(\mathbf{R}) \tag{4.6-39}$$

and

$$p(\mathbf{R}) = \psi(\mathbf{R}) + \sum_{j=0}^{\infty} \widetilde{\boldsymbol{\Pi}}^j(\mathbf{R}) \{\cdot\}^{j+1} \boldsymbol{\nabla}^{j+1} \psi(\mathbf{R}). \tag{4.6-40}$$

The microscale information pertaining to the flow fields is contained in the fully spatially periodic fields $\left[\widetilde{\mathbf{V}}^m(\mathbf{r}), \widetilde{\boldsymbol{\Pi}}^m(\mathbf{r})\right]$, which represent solutions of the $\mathcal{O}(m)$ *cell problem*:

$$\mathcal{O}(m) \text{ cell problem:} \tag{4.6-41}$$

$$\nabla^2 \widetilde{\mathbf{V}}^m - \boldsymbol{\nabla} \widetilde{\boldsymbol{\Pi}}^m = \begin{cases} \mathbf{I} & (m=0), \\ \left[\!\left[\mathbf{I} \widetilde{\boldsymbol{\Pi}}^0 - 2^{\dagger} \left(\boldsymbol{\nabla} \widetilde{\mathbf{V}}^0 \right) \right]\!\right]^{s2} & (m=1), \\ \left[\!\left[\mathbf{I} \widetilde{\boldsymbol{\Pi}}^{m-1} - 2^{\dagger} \left(\boldsymbol{\nabla} \widetilde{\mathbf{V}}^{m-1} \right) - \widetilde{\mathbf{V}}^{m-2} \mathbf{I} \right]\!\right]^{sm+1} & \forall (m \geq 2); \end{cases}$$

$$\boldsymbol{\nabla} \cdot \widetilde{\mathbf{V}}^m = \begin{cases} \mathbf{0} & (m=0), \\ -\left[\!\left[\widetilde{\mathbf{V}}^{m-1} - \left\langle \widetilde{\mathbf{V}}^{m-1} \right\rangle \right]\!\right]^{s} & \forall (m \geq 1); \end{cases}$$

$$\widetilde{\mathbf{V}}^m = \mathbf{0} \qquad \forall (\mathbf{r} \in s_p; m \geq 1);$$

$$\left\langle \widetilde{\boldsymbol{\Pi}}^m \right\rangle = \mathbf{0} \qquad \forall (m \geq 1).$$

Likewise, the macroscale information pertaining to the original flow fields is contained in the scalar function $\psi(\mathbf{R})$, which obeys the restriction

$$\sum_{j=0}^{\infty} \left\langle \widetilde{\mathbf{V}}^j \right\rangle \{\cdot\}^{j+2} \boldsymbol{\nabla}^{j+2} \psi = 0. \tag{4.6-42}$$

but is totally arbitrary apart from this. The function $\psi(\mathbf{R})$ may be chosen so as to describe externally imposed macroscale fields.

Chapter 5

Generalized Macroscale Flow through Porous Media

5.1 Introduction

The exact solution determined in Chapter 4 will be analysed in this chapter to determine the relevant macroscale fields, namely the macroscale velocity $\overline{\mathbf{v}}$ and stress $\overline{\mathbf{P}}$. These macroscale fields will be expressed in terms of the tensors $\overline{\mathbf{\Psi}}^m$ for each order of flow. The velocity relation ultimately obtained in this way can then be inverted so as to express the macroscale pressure gradient in terms of the macroscale velocity and its gradients. Ultimately, both Darcy's law and a Brinkman-like generalization thereof—together with the phenomenological coefficients appearing therein—can be determined from the unit cell geometry.

5.2 Basic Macroscopic Flow Theory

In general, any transport process occuring in a porous media is characterized by two different length scales on which the phenomena may be viewed. These are represented respectively by the characteristic length scale ℓ of the particles (or the unit cell) over which the relevant microscale fields vary due to boundary conditions satisfied on the particle surfaces s_p, and the length scale L over which the mean or average fields vary sensibly. In general L will refer to the linear dimensions of the boundaries of the porous medium. A detailed description of the procedure used to derive the macroscale equations from their microscale counterparts is given by Brenner and Edwards [28] and by Nitsche and Brenner [82]; hence, only a brief review is given here.

5.2.1 Macroscale Metrics

In formulating a macroscale description of an exact microscale field such as $\mathbf{v}(\mathbf{R})$, it is important to note that at the macroscale the distinct fluid and particle phases do not possess separate identities. Instead, any macroscale field [such as $\overline{\mathbf{v}}(\overline{\mathbf{R}})$] when evaluated at a macroscopic 'point' is a composite entity, deriving from the properties of both the fluid and particle phases. On this coarse scale, distances less that the characteristic length ℓ of a unit cell are irresolvable. As such, the macroscale position vector in this continuum limit is defined as

$$\overline{\mathbf{R}} \stackrel{\text{def}}{=} \mathbf{R_n}, \tag{5.2-1}$$

while the macroscopic 'differential' displacement vector $\mathrm{d}\overline{\mathbf{R}}$ between the neighboring cells $\overline{\mathbf{R}}$ and $\overline{\mathbf{R}} + \mathrm{d}\overline{\mathbf{R}}$ (i.e., between $\mathbf{R_n}$ and $\mathbf{R_n} + \mathbf{l}_k$), defined as the displacement vector connecting two adjacent lattice points, is by definition

$$\mathrm{d}\overline{\mathbf{R}} \stackrel{\text{def}}{=} \mathbf{l}_k, \tag{5.2-2}$$

with $\mathbf{l}_k$ any basic lattice vector.

Again, since distances less than $|\mathbf{l}_k|$ cannot be resolved at the macroscale, the

directed area of a curvilinear face of a unit cell can be interpreted from a macroscale viewpoint as being

$$\mathrm{d}\overline{\mathbf{S}} \stackrel{\text{def}}{=} \mathbf{s}_k, \tag{5.2-3}$$

in which $\mathrm{d}\overline{\mathbf{S}}$ is regarded as a 'differential' element of surface area of the macrocontinuum.

The volume τ_0 of a unit cell is infinitesimal when viewed at the macroscale; hence, one can define the macroscale differential volume element, denoted by $\mathrm{d}\overline{V}$ or $\mathrm{d}^3\overline{\mathbf{R}}$, as

$$\left\{\mathrm{d}\overline{V} \text{ or } \mathrm{d}^3\overline{\mathbf{R}}\right\} \stackrel{\text{def}}{=} \tau_0. \tag{5.2-4}$$

It then follows from (B.0-10) together with (5.2-2) to (5.2-4) that since $\tau_0 = \mathbf{s}_k \cdot \mathbf{l}_k$ (no sum on k) then

$$\mathrm{d}\overline{V} = \mathrm{d}\overline{\mathbf{S}} \cdot \mathrm{d}\overline{\mathbf{R}}, \tag{5.2-5}$$

which is consistent with the findamental definition of an elementary differential volume. The quantities $\mathrm{d}\overline{\mathbf{R}}$, $\mathrm{d}\overline{\mathbf{S}}$ and $\mathrm{d}\overline{V}$ serve to characterize the differential macroscale geometry.

5.2.2 Macroscale Velocity, $\overline{\mathbf{v}}$

Consider the net volumetric flow rate of fluid q_k through the cell face $\mathbf{s}_k$ of cell $\mathbf{n}$:

$$q_k \stackrel{\text{def}}{=} \int\limits_{\mathbf{s}_k\{\mathbf{n}\}} \mathrm{d}\mathbf{S} \cdot \mathbf{v}(\mathbf{R}_\mathbf{n}, \mathbf{r}). \tag{5.2-6}$$

We seek to express (5.2-6) in the form

$$q_k = \mathbf{s}_k \cdot \overline{\mathbf{v}}(\mathbf{R}_\mathbf{n}), \tag{5.2-7}$$

where $\overline{\mathbf{v}}$ is independent of the particular choice k ($k = \pm 1, \pm 2, \pm 3$) of cell face. Furthermore, from a macroscale viewpoint, q_k, defined by (5.2-6), possesses the in-

terpretation [28, 82]

$$d\overline{q} \stackrel{\text{def}}{=} q_k, \tag{5.2-8}$$

the quantity $d\overline{q}$ denoting a differential flow rate through the surface $d\overline{\mathbf{S}}(\equiv \mathbf{s}_k)$ on the macroscale. Hence, in combination with (5.2-1) and (5.2-3), the relation (5.2-7) may be expressed in the classical, Eulerian form

$$d\overline{q} = d\overline{\mathbf{S}} \cdot \overline{\mathbf{v}}(\overline{\mathbf{R}}). \tag{5.2-9}$$

The physical significance of (5.2-9) resides in the fact that it constitutes a purely macroscale definition of the macroscale velocity vector $\overline{\mathbf{v}}$, completely analagous to the comparable definition of the microscale velocity $\mathbf{v}$ appropriate to a true continuum, namely

$$dq = d\mathbf{S} \cdot \mathbf{v}. \tag{5.2-10}$$

In particular, $\overline{\mathbf{v}}$ is that vector *which is independent of the magnitude and the direction of the areal vector* $d\overline{\mathbf{S}}$, such that when dot multiplied by the differential macroscale area $d\overline{\mathbf{S}}$, gives the volumetric flow rate $d\overline{q}$ through $d\overline{\mathbf{S}}$. Definitions of $\overline{\mathbf{v}}$ based purely on volume averages [14, 102, 103, 121] of $\mathbf{v}$ are inappropriate since such definitions fail to provide a *physical* proof of (5.2-9).

5.2.3 Macroscale Stress, $\overline{\mathbf{P}}$

Just as the macroscale velocity $\overline{\mathbf{v}}$ possesses a purely macroscale interpretation (5.2-9), one similarily expects the macroscale stress $\overline{\mathbf{P}}$ to be defined as that dyadic (independent of $d\overline{\mathbf{S}}$) which when dotted with $d\overline{\mathbf{S}}$ gives the force $d\overline{\mathbf{f}}$ exerted by the material lying on the positive side of $d\overline{\mathbf{S}}$ (that side into which $d\overline{\mathbf{S}}$ points) upon the material on the negative side, i.e.,

$$d\overline{\mathbf{f}} = d\overline{\mathbf{S}} \cdot \overline{\mathbf{P}}(\overline{\mathbf{R}}). \tag{5.2-11}$$

To this end, consider the force $\mathbf{f}_k$ exerted by the fluid on the positive side of $\mathbf{s}_k$ upon the fluid on the negative side of $\mathbf{s}_k$ of cell $\mathbf{n}$,

$$\mathbf{f}_k \stackrel{\text{def}}{=} \int\limits_{\mathbf{s}_k\{\mathbf{n}\}} \mathrm{d}\mathbf{S} \cdot \mathbf{P}(\mathbf{R}_\mathbf{n}, \mathbf{r}), \tag{5.2-12}$$

where the microscale stress $\mathbf{P}$ is defined as

$$\mathbf{P} \stackrel{\text{def}}{=} -\mathbf{I}p + 2\mu\mathbf{S} \tag{5.2-13}$$

with

$$\mathbf{S} \stackrel{\text{def}}{=} \frac{1}{2}\left[(\boldsymbol{\nabla}\mathbf{v}) + {}^{\dagger}(\boldsymbol{\nabla}\mathbf{v})\right] \equiv {}^{s}(\boldsymbol{\nabla}\mathbf{v}) \tag{5.2-14}$$

the symmetric rate of strain tensor. Here, ${}^{s}\mathbf{A}$ represents the symmetric part of the tensor function $\mathbf{A}$ with respect to its first two indices.

The next step consists of expressing (5.2-12) as

$$\mathbf{f}_k = \mathbf{s}_k \cdot \overline{\mathbf{P}}(\mathbf{R}_\mathbf{n}), \tag{5.2-15}$$

where $\overline{\mathbf{P}}$ is independent of the particular choice k ($k = \pm 1, \pm 2, \pm 3$) of cell face. As in (5.2-8) and (5.2-3), the macroscale interpretation of $\mathbf{f}_k$ is [28, 82]

$$\mathrm{d}\overline{\mathbf{f}} \stackrel{\text{def}}{=} \mathbf{f}_k. \tag{5.2-16}$$

This macroscale stress can be decomposed into normal and deviatoric stresses as follows:

$$\overline{\mathbf{P}} \stackrel{\text{def}}{=} -\mathbf{I}\overline{p} + \overline{\mathbf{T}} \tag{5.2-17}$$

$$\equiv -\mathbf{I}\overline{p} + \overline{\mathbf{T}}^{s} + \overline{\mathbf{T}}^{a}. \tag{5.2-18}$$

In the latter,

$$\overline{p} \stackrel{\text{def}}{=} -\nu\mathbf{I} : \overline{\mathbf{P}} \tag{5.2-19}$$

and

$$\overline{\mathbf{T}}^{s} \stackrel{\text{def}}{=} \frac{1}{2}\left(\overline{\mathbf{P}} + \overline{\mathbf{P}}^{\dagger}\right) - \nu\mathbf{I}\left(\mathbf{I} : \overline{\mathbf{P}}\right), \tag{5.2-20}$$

$$\overline{\mathbf{T}}^{a} \stackrel{\text{def}}{=} \frac{1}{2}\left(\overline{\mathbf{P}} - \overline{\mathbf{P}}^{\dagger}\right). \tag{5.2-21}$$

Here,

$$\nu \stackrel{\text{def}}{=} (\mathbf{I} : \mathbf{I})^{-1} \tag{5.2-22}$$

denotes the inverse of the dimensionality N of space, namely $\nu = 1/N$. Explicitly, $\nu = 1/2$ or $\nu = 1/3$ for N a 2-dimensional or 3-dimensional problem respectively. Equation (5.2-19) defines the macroscale mean pressure $\overline{p}$. Similarily, $\overline{\mathbf{T}}$ is the macroscopic, traceless, deviatoric stress tensor—which is further broken down into its (traceless) symmetric and antisymmetric parts, $\overline{\mathbf{T}}^{s}$ and $\overline{\mathbf{T}}^{a}$, respectively. The antisymmetric dyadic $\overline{\mathbf{T}}^{a}$ can further be expressed in terms of the pseudovector $\overline{\mathbf{P}}_{\times}$ as

$$\overline{\mathbf{T}}^{a} = \frac{1}{2}\boldsymbol{\epsilon} \cdot \overline{\mathbf{P}}_{\times} \tag{5.2-23}$$

where $\overline{\mathbf{P}}_{\times}$ is defined as

$$\begin{aligned} \overline{\mathbf{P}}_{\times} &\stackrel{\text{def}}{=} -\boldsymbol{\epsilon} : \overline{\mathbf{P}} \\ &\equiv -\boldsymbol{\epsilon} : \overline{\mathbf{T}} \\ &\equiv -\boldsymbol{\epsilon} : \overline{\mathbf{T}}^{a}, \end{aligned} \tag{5.2-24}$$

with $\boldsymbol{\epsilon}$ the unit isotropic triadic (unit alternating tensor).

Note that no aphysical assumptions have to be made regarding the possible existence of a (microscale) pressure field or pressure gradient within the particle *interiors*, in contrast with the case of a volume average approach [6, 45, 73, 103, 120], where this ambiguous and physically undefined concept plays a key role.

5.2.4 External Body Force Density

Consider the force (per unit superficial volume) exerted by the fluid upon the particles in cell $\{\mathbf{n}\}$:

$$\overline{\mathbf{F}} = -\frac{1}{\tau_0} \oint_{s_p\{\mathbf{n}\}} \mathrm{d}\mathbf{S} \cdot \mathbf{P}, \tag{5.2-25}$$

where $\mathrm{d}\mathbf{S}$ points into the particles. Since the particles are fixed in space, Newton's law of conservation of momentum requires that the sum of the various forces exerted upon the particles is identically zero:

$$\overline{\mathbf{F}} + \overline{\mathbf{F}}^{(e)} = \mathbf{0}. \tag{5.2-26}$$

From the latter two equations, it follows that

$$\overline{\mathbf{F}}^{(e)} = \frac{1}{\tau_0} \oint_{s_p\{\mathbf{n}\}} \mathrm{d}\mathbf{S} \cdot \mathbf{P} \tag{5.2-27}$$

represents the external force (per unit superficial volume) exerted by an agency lying 'outside' the porous medium upon the particles. This can be converted into a surface integral by using the divergence theorem while noting that the microscale stress field is divergence free; hence the result

$$\overline{\mathbf{F}}^{(e)} = -\frac{1}{\tau_0} \oint_{\partial\tau_0} \mathrm{d}\mathbf{S} \cdot \mathbf{P}(\mathbf{R}_\mathbf{n}, \mathbf{r}). \tag{5.2-28}$$

5.2.5 External Body Couple Density

The torque (per unit superficial volume, and with respect to an origin at the point from which $\mathbf{R}$ originates) exerted by the fluid upon the particles in cell $\{\mathbf{n}\}$ is, by definition,

$$\overline{\mathbf{L}} = -\frac{1}{\tau_0} \oint_{s_p\{\mathbf{n}\}} \mathbf{R} \times (\mathrm{d}\mathbf{S} \cdot \mathbf{P}). \tag{5.2-29}$$

As the particles neither translate nor rotate, conservation of angular momentum requires

$$\overline{\mathbf{L}} + \overline{\mathbf{L}}^{(e)} = \mathbf{0} \tag{5.2-30}$$

which shows that the volumetric external torque density exerted by an agency lying 'outside' the porous medium upon the particles is given by

$$\overline{\mathbf{L}}^{(e)} = \frac{1}{\tau_0} \oint_{s_p\{\mathbf{n}\}} \mathbf{R} \times (\mathrm{d}\mathbf{S} \cdot \mathbf{P}) \,. \tag{5.2-31}$$

Upon use of the divergence theorem this gives the intermediate result:

$$\overline{\mathbf{L}}^{(e)} = -\frac{1}{\tau_0} \int_{\tau_f\{\mathbf{n}\}} \boldsymbol{\nabla} \cdot (\mathbf{P} \times \mathbf{R}) \, \mathrm{d}^3\mathbf{r} - \frac{1}{\tau_0} \oint_{\partial\tau_0\{\mathbf{n}\}} \mathbf{R} \times (\mathrm{d}\mathbf{S} \cdot \mathbf{P}) \,. \tag{5.2-32}$$

But, as a consequence of the identity

$$\boldsymbol{\nabla} \cdot (\mathbf{P} \times \mathbf{R}) = (\boldsymbol{\nabla} \cdot \mathbf{P}) \times \mathbf{R} - \mathbf{P}_{\times}, \tag{5.2-33}$$

jointly with the facts that $\mathbf{P}$ is divergence free and symmetric, this simplifies to

$$\overline{\mathbf{L}}^{(e)} = -\frac{1}{\tau_0} \oint_{\partial\tau_0\{\mathbf{n}\}} \mathbf{R} \times (\mathrm{d}\mathbf{S} \cdot \mathbf{P}) \,. \tag{5.2-34}$$

Decompose $\mathbf{R}$ into $\mathbf{R_n}$ and $\mathbf{r}$ (B.0-1), and write

$$\overline{\mathbf{L}}^{(e)} = \mathbf{R_n} \times \left(-\frac{1}{\tau_0} \oint_{\partial\tau_0} \mathrm{d}\mathbf{S} \cdot \mathbf{P} \right) - \frac{1}{\tau_0} \oint_{\partial\tau_0} \mathbf{r} \times (\mathrm{d}\mathbf{S} \cdot \mathbf{P}) \,, \tag{5.2-35}$$

which has the form

$$\overline{\mathbf{L}}^{(e)} = \overline{\mathbf{R}} \times \overline{\mathbf{F}}^{(e)} + \overline{\mathbf{N}}^{(e)} \tag{5.2-36}$$

with the external body force density $\overline{\mathbf{F}}^{(e)}$ given in (5.2-28) and the external body couple density $\overline{\mathbf{N}}^{(e)}$ given as

$$\overline{\mathbf{N}}^{(e)} = -\frac{1}{\tau_0} \oint_{\partial\tau_0} \mathbf{r} \times [\mathrm{d}\mathbf{S} \cdot \mathbf{P}(\mathbf{R_n}, \mathbf{r})] \,. \tag{5.2-37}$$

5.2.6 Macroscale Linear Momentum Equation

Since the macroscale definitions of $\overline{\mathbf{v}}$ and $\overline{\mathbf{P}}$ [see Eqs. (5.2-9) and (5.2-11)] are identical to their microscale counterparts, effective-medium equations follow naturally from Newton's laws of motion and continuum-mechanical theory. Cauchy's linear momentum equation written for this macroscale continuum is

$$\frac{\mathrm{D}\overline{\mathbf{M}}}{\mathrm{D}t} = \overline{\mathbf{F}}^{(e)} + \overline{\boldsymbol{\nabla}} \cdot \overline{\mathbf{P}} \tag{5.2-38}$$

where $\overline{\mathbf{M}}$ is the volumetric momentum density and $\mathrm{D}/\mathrm{D}t$ the material derivative. At each flow order (and hence for a general flow) it will be shown that the macroscale stress $\overline{\mathbf{P}}$ computed from (5.2-11) and the external body force density $\overline{\mathbf{F}}^{(e)}$ computed from (5.2-28) satisfy the relation

$$\overline{\mathbf{F}}^{(e)} + \overline{\boldsymbol{\nabla}} \cdot \overline{\mathbf{P}} = \mathbf{0} \tag{5.2-39}$$

The solution scheme involves computing $\overline{\mathbf{v}}$, $\overline{\mathbf{P}}$ (or $\overline{\mathbf{T}}$) and $\overline{\mathbf{F}}^{(e)}$ for each order of flow from the exact microscale results of Chapter 4. Subsequently, the dependence of $\overline{\mathbf{T}}$ and $\overline{\mathbf{F}}^{(e)}$ upon $\overline{\mathbf{v}}$ and its macroscale gradients is determined. The macroscale momentum equation can then be derived from (5.2-39) and (5.2-17) as

$$\overline{\boldsymbol{\nabla}}\overline{p} = \overline{\mathbf{F}}^{(e)} + \overline{\boldsymbol{\nabla}} \cdot \overline{\mathbf{T}}. \tag{5.2-40}$$

With $\overline{\mathbf{T}}$ and $\overline{\mathbf{F}}^{(e)}$ expressed as a function of $\overline{\mathbf{v}}$, Eq. (5.2-40) will ultimately produce the relation between the macroscale pressure gradient and the macroscale velocity field [cf. Eq. (5.3-39) for the zeroth-order flow]. Finally, the macroscale continuity

condition

$$\overline{\nabla} \cdot \overline{\mathbf{v}} = 0 \tag{5.2-41}$$

will be shown to arise from the auxiliary conditions (4.6-22) imposed upon the microscale velocity field.

5.2.7 Macroscale Angular Momentum Equation

Again, from the macroscale definitions of $\overline{\mathbf{v}}$ and $\overline{\mathbf{P}}$, Cauchy's angular momentum equation written for this continuum is

$$\frac{\mathrm{D}\overline{\mathbf{I}}}{\mathrm{D}t} = \overline{\mathbf{P}}_{\times} + \overline{\mathbf{N}}^{(e)} + \overline{\nabla} \cdot \overline{\mathbf{C}} \tag{5.2-42}$$

where $\overline{\mathbf{I}}$ is the volumetric intrinsic angular momentum density. At each flow order it will be shown that the macroscale antisymmetric stress (represented by its pseudovector, $\overline{\mathbf{P}}_{\times}$) calculated from (5.2-11) and the external body couple density $\overline{\mathbf{N}}^{(e)}$ computed from (5.2-37) satisfy the relation

$$\overline{\mathbf{P}}_{\times} + \overline{\mathbf{N}}^{(e)} = \mathbf{0}. \tag{5.2-43}$$

As such, the macroscale couple stress $\overline{\mathbf{C}}$ for this macroscopic description of flow in porous media is at most a constant (possibly zero).

5.3 Zeroth-order Macroscale Flow

For zeroth-order flow, the velocity and pressure are given by (4.3-50) and (4.3-51) as

$$\mu \mathbf{v}(\mathbf{R}) = \widetilde{\mathbf{V}}^0(\mathbf{R}) \cdot \overline{\mathbf{\Psi}}^1 \tag{5.3-1}$$

and

$$\begin{aligned} p(\mathbf{R}) &= \overline{\Psi}^0 + \overline{\mathbf{\Psi}}^1 \cdot \mathbf{R} \\ &\quad + \widetilde{\mathbf{\Pi}}^0(\mathbf{R}) \cdot \overline{\mathbf{\Psi}}^1. \end{aligned} \tag{5.3-2}$$

The dependence of these and subsequent microscale fields upon the arbitrary reference point $\mathbf{R}'$ has been suppressed in the interest of clarity, as well as the fact that its choice does not effect the final results.

5.3.1 Macroscale Velocity, $\overline{\mathbf{v}}$

Substitute (5.3-2) into (5.2-6) to obtain

$$q_k = \frac{1}{\mu} \left(\int_{\mathbf{s}_k} \mathrm{d}\mathbf{S} \cdot \widetilde{\mathbf{V}}^0 \right) \cdot \overline{\mathbf{\Psi}}^1, \tag{5.3-3}$$

where the explicit dependence of $\mathbf{s}_k$ upon $\mathbf{n}$ has been deleted since the integrand is independent of $\mathbf{n}$. This integral can be simplified by using the identity (Brenner and Edwards [28])

$$\int_{\mathbf{s}_k} \mathrm{d}\mathbf{S} \cdot \widetilde{\mathbf{A}} \equiv \mathbf{s}_k \cdot \frac{1}{\tau_0} \oint_{\partial \tau_0} \mathbf{r} \mathrm{d}\mathbf{S} \cdot \widetilde{\mathbf{A}}, \tag{5.3-4}$$

valid for any tensor function $\widetilde{\mathbf{A}}$ whose jump is zero (i.e., $\left\| \widetilde{\mathbf{A}} \right\| = \mathbf{0}$). Consequently, (5.3-3) becomes

$$q_k = \mathbf{s}_k \cdot \frac{1}{\mu} \left(\frac{1}{\tau_0} \oint_{\partial \tau_0} \mathbf{r} \mathrm{d}\mathbf{S} \cdot \widetilde{\mathbf{V}}^0 \right) \cdot \overline{\mathbf{\Psi}}^1. \tag{5.3-5}$$

This possesses the same form as (5.2-7). Hence, upon recognizing that the term in brackets is simply $\overline{\mathbf{V}}^0$, the zeroth-order macroscale velocity field is found to be

$$\mu\overline{\mathbf{v}}(\overline{\mathbf{R}}) = \overline{\mathbf{V}}^0 \cdot \overline{\mathbf{\Psi}}^1. \tag{5.3-6}$$

This shows the macroscale velocity field for the zeroth-order flow to be homogeneous, i.e., a constant independent of $\overline{\mathbf{R}}$. Since $\overline{\mathbf{V}}^0$ is both symmetric and negative definite, its inverse exists and is unique. As such, (5.3-6) can be inverted to express the vector $\overline{\mathbf{\Psi}}^1$ as a function of $\overline{\mathbf{v}}$:

$$\overline{\mathbf{\Psi}}^1 = \mu\overline{\mathbf{\Lambda}}^0 \cdot \overline{\mathbf{v}}, \tag{5.3-7}$$

where $\overline{\mathbf{\Lambda}}^0 = (\overline{\mathbf{V}}^0)^{-1}$.

5.3.2 Macroscale Stress, $\overline{\mathbf{P}}$

From (5.3-1), (5.3-2), (5.2-13) and (5.2-14) the microscale zeroth-order stress field is

$$\begin{aligned} \mathbf{P}(\mathbf{R}) &= -\mathbf{I}\left(\overline{\Psi}^0 + \overline{\mathbf{\Psi}}^1 \cdot \mathbf{R}\right) \\ &\quad + \widetilde{\mathbf{P}}^0(\mathbf{R}) \cdot \overline{\mathbf{\Psi}}^1, \end{aligned} \tag{5.3-8}$$

where the $(n+3)$rd rank tensor $\widetilde{\mathbf{P}}^n(\mathbf{R})$ is defined as

$$\widetilde{\mathbf{P}}^n \overset{\text{def}}{=} -\mathbf{I}\widetilde{\mathbf{\Pi}}^n + 2^s\left(\nabla\widetilde{\mathbf{V}}^n\right) \qquad \forall\,(n = 0, 1, 2, \ldots), \tag{5.3-9}$$

representing the geometric stress determined from the unit cell problems. It is obviously symmetric with respect to its first two indices.

Substitute (5.3-8) into (5.2-12) to obtain

$$\mathbf{f}_k = -\left(\int_{\mathbf{s}_k} \mathrm{d}\mathbf{S}\right)\overline{\Psi}^0 - \left(\int_{\mathbf{s}_k} \mathrm{d}\mathbf{S}\mathbf{r}\right) \cdot \overline{\mathbf{\Psi}}^1 - \left(\int_{\mathbf{s}_k} \mathrm{d}\mathbf{S}\right)\mathbf{R}_\mathbf{n} \cdot \overline{\mathbf{\Psi}}^1 + \left(\int_{\mathbf{s}_k} \mathrm{d}\mathbf{S} \cdot \widetilde{\mathbf{P}}^0\right) \cdot \overline{\mathbf{\Psi}}^1,$$

of which the first and third integrals are, by definition, $\mathbf{s}_k$. The second may be

rewritten by using (B.0-10) and the fourth by using (5.3-4), thereby obtaining

$$\mathbf{f}_k = \mathbf{s}_k \cdot \left[-\mathbf{I}\overline{\Psi}^0 - \left(\mathbf{l}_k \frac{1}{\tau_0} \int_{\mathbf{s}_k} \mathrm{d}\mathbf{S}\mathbf{r} + \mathbf{I}\mathbf{R}_\mathbf{n} \right) \cdot \overline{\mathbf{\Psi}}^1 + \left(\frac{1}{\tau_0} \oint_{\partial\tau_0} \mathbf{r}\mathrm{d}\mathbf{S} \cdot \tilde{\mathbf{P}}^0 \right) \cdot \overline{\mathbf{\Psi}}^1 \right]. \quad (5.3\text{-}10)$$

The $\mathbf{l}_k$ term appearing above is of $\mathcal{O}\left(|\mathrm{d}\overline{\mathbf{R}}|\right)$ while the next term is of $\mathcal{O}\left(|\overline{\mathbf{R}}|\right)$. Hence, since $|\overline{\mathbf{R}}| \gg |\mathrm{d}\overline{\mathbf{R}}|$, the former term may be neglected compared with the latter. Upon defining the mean geometric stress tensor $\overline{\mathbf{P}}^n$ of rank $(n+3)$ as

$$\overline{\mathbf{P}}^n \stackrel{\text{def}}{=} \frac{1}{\tau_0} \oint_{\partial\tau_0} \mathbf{r}\mathrm{d}\mathbf{S} \cdot \tilde{\mathbf{P}}^n(\mathbf{r}) \qquad \forall\, (n = 0, 1, 2, \ldots), \quad (5.3\text{-}11)$$

and comparing (5.3-10) with (5.2-15), it follows that the zeroth-order macroscale stress field is

$$\begin{aligned} \overline{\mathbf{P}}(\overline{\mathbf{R}}) \;=\; & -\mathbf{I}\left(\overline{\Psi}^0 + \overline{\mathbf{\Psi}}^1 \cdot \overline{\mathbf{R}}\right) \\ & + \overline{\mathbf{P}}^0 \cdot \overline{\mathbf{\Psi}}^1, \end{aligned} \quad (5.3\text{-}12)$$

which is accurate to $\mathcal{O}\left(|\mathrm{d}\overline{\mathbf{R}}|\right)$.

The macroscale pressure determined from (5.2-19) is then

$$\begin{aligned} \overline{p}(\overline{\mathbf{R}}) \;=\; & \overline{\Psi}^0 + \overline{\mathbf{\Psi}}^1 \cdot \overline{\mathbf{R}} \\ & - \nu\mathbf{I} : \overline{\mathbf{P}}^0 \cdot \overline{\mathbf{\Psi}}^1, \end{aligned} \quad (5.3\text{-}13)$$

consisting of a constant term and one that grows linearly with $\overline{\mathbf{R}}$.

The symmetric part of the traceless, deviatoric stress calculated from (5.2-20) and (5.3-12) is

$$\overline{\mathbf{T}}^s = \left[\frac{1}{2} \left(\overline{\mathbf{P}}^0 + {}^\dagger\overline{\mathbf{P}}^0 \right) - \nu\mathbf{I}\mathbf{I} : \overline{\mathbf{P}}^0 \right] \cdot \overline{\mathbf{\Psi}}^1, \quad (5.3\text{-}14)$$

while the antisymmetric part derived from (5.2-23), (5.2-24) and (5.3-12) is

$$\overline{\mathbf{P}}_\times = -\boldsymbol{\epsilon} : \overline{\mathbf{P}}^0 \cdot \overline{\mathbf{\Psi}}^1. \quad (5.3\text{-}15)$$

Whereas the mean macroscale pressure $\overline{p}$ depended linearly upon $\overline{\mathbf{R}}$, the symmetric portion of the macroscale deviatoric stress is a constant, independent of $\overline{\mathbf{R}}$. By using (5.3-7), the constant $\overline{\mathbf{\Psi}}^1$ can be replaced by the macroscale velocity $\overline{\mathbf{v}}$, enabling the two parts of the deviatoric stress to be respectively expressed as

$$\overline{\mathbf{T}}^s = \mu\, \overline{\mathbf{K}}^{(l)} \cdot \overline{\mathbf{v}} \tag{5.3-16}$$

and

$$\overline{\mathbf{P}}_\times = \mu\, \overline{\mathbf{c}}^{(l)} \cdot \overline{\mathbf{v}}. \tag{5.3-17}$$

The constant triadic $\overline{\mathbf{K}}^{(l)}$, linearly relating the macroscale velocity to the symmetric part of the deviatoric stress, is defined in cartesian tensor summation notation as

$$\overline{K}^{(l)}_{ijk} \stackrel{\text{def}}{=} \left[\frac{1}{2}\left(\overline{P}^0_{ijm} + \overline{P}^0_{jim}\right) - \nu\delta_{ij}\overline{P}^0_{llm}\right]\overline{\Lambda}^0_{mk}. \tag{5.3-18}$$

From the properties of $\overline{\mathbf{T}}^s$, this triadic is symmetric and traceless, each with respect to the first two indices of $\overline{K}^{(l)}_{ijk}$:

$$\overline{K}^{(l)}_{ijk} = \overline{K}^{(l)}_{jik} \tag{5.3-19}$$

and

$$\overline{K}^{(l)}_{iij} = 0 \qquad \forall\,(j = 1, 2, 3)\,. \tag{5.3-20}$$

Hence, of the 27 components (for three dimensions or 8 for two dimensions) of $\overline{\mathbf{K}}^{(l)}$, at most 15 (or 4) are independent. This number decreases as a result of any geometric symmetries possessed by the skeletal spatially periodic medium. The constant pseudodyadic $\overline{\mathbf{c}}^{(l)}$ relating the macroscale velocity to the macroscale stress pseudovector (or antisymmetric stress) is defied as

$$\overline{c}^{(l)}_{ij} \stackrel{\text{def}}{=} -\epsilon_{ikl}\overline{P}^0_{lkm}\overline{\Lambda}^0_{mj}. \tag{5.3-21}$$

Since $\overline{\mathbf{c}}^{(l)}$ transforms a true vector $\overline{\mathbf{v}}$ into a pseudovector $\overline{\mathbf{P}}_\times$, a porous medium (such as a square array of circular cylinders or spheres) possessing reflection symmetry will be characterized by $\overline{\mathbf{c}}^{(l)} = \mathbf{0}$.

5.3.3 External Body Force Density, $\overline{\mathbf{F}}^{(e)}$

From (5.2-28) and (5.3-8), the external force per unit of superficial volume exerted on the particles in order to prevent them from translating or rotating in the presence of this zeroth-order flow field is given by

$$\overline{\mathbf{F}}^{(e)} = -\frac{1}{\tau_0}\oint_{\partial\tau_0} \mathrm{d}\mathbf{S}\cdot\left[-\mathbf{I}\left(\overline{\Psi}^0 + \overline{\Psi}^1\cdot\mathbf{R}\right) + \tilde{\mathbf{P}}^0\cdot\overline{\Psi}^1\right]. \tag{5.3-22}$$

The latter may be simplified upon using the decomposition (B.0-1), and recognizing that surface integrals of spatially periodic functions (of which constants are special cases) are identically zero (4.3-39); hence,

$$\overline{\mathbf{F}}^{(e)} = \frac{1}{\tau_0}\oint_{\partial\tau_0} \mathrm{d}\mathbf{S}\mathbf{r}\cdot\overline{\Psi}^1. \tag{5.3-23}$$

Together with the identity

$$\begin{aligned}\frac{1}{\tau_0}\oint_{\partial\tau_0} \mathrm{d}\mathbf{S}\mathbf{r} &= \frac{1}{\tau_0}\int_{\tau_0} \boldsymbol{\nabla}\mathbf{r}\,\mathrm{d}^3\mathbf{r} \\ &\equiv \mathbf{I}\frac{1}{\tau_0}\int_{\tau_0} \mathrm{d}^3\mathbf{r} \\ &\equiv \mathbf{I}\end{aligned} \tag{5.3-24}$$

one thereby ultimately obtains

$$\overline{\mathbf{F}}^{(e)} = \overline{\Psi}^1. \tag{5.3-25}$$

Essentially, the external force required to keep the particles from translating or rotating is uniform throughout the porous medium for this zeroth-order flow field; that is, it is independent of $\{\mathbf{n}\}$ and hence of $\overline{\mathbf{R}}$. Combine the latter with (5.3-7) to obtain

$$\overline{\mathbf{F}}^{(e)} = \mu\overline{\boldsymbol{\Lambda}}^0\cdot\overline{\mathbf{v}}, \tag{5.3-26}$$

which shows the external force depends linearly upon $\overline{\mathbf{v}}$. Now, form the macroscale

divergence of $\overline{\mathbf{P}}$ from (5.3-12),

$$\overline{\boldsymbol{\nabla}} \cdot \overline{\mathbf{P}} = -\overline{\boldsymbol{\Psi}}^1, \tag{5.3-27}$$

and compare this to the expression for the external body force density (5.3-25), thereby obtaining the macroscale linear momentum equation

$$\overline{\mathbf{F}}^{(e)} + \overline{\boldsymbol{\nabla}} \cdot \overline{\mathbf{P}} = \mathbf{0} \tag{5.3-28}$$

satisfied by the zeroth-order flow field. Hence, the divergence of the macroscale stress (determined by considering the forces acting on the cell faces) is balanced by the external body force density (determined by considering the forces acting on the particles). Equation (5.3-28) provides confirmation that (*sans* inertia) Cauchy's linear momentum equation (5.2-38) is satisfied by the macroscale fields, at least for this zeroth-order flow field.

5.3.4 External Body Couple Density, $\overline{\mathbf{N}}^{(e)}$

From (5.2-37) and (5.3-8), the external couple volumetric density exerted on the particles, which prevents them from translating and rotating as a result of this zeroth-order flow field, is given by

$$\overline{\mathbf{N}}^{(e)} = \boldsymbol{\epsilon} : \frac{1}{\tau_0} \oint_{\partial\tau_0} \mathbf{r}\, \mathrm{d}\mathbf{S} \cdot \left[-\mathbf{I} \left(\overline{\Psi}^0 + \overline{\boldsymbol{\Psi}}^1 \cdot \mathbf{R} \right) + \tilde{\mathbf{P}}^0 \cdot \overline{\boldsymbol{\Psi}}^1 \right]. \tag{5.3-29}$$

In the preceding, the identity

$$\mathbf{a} \times \mathbf{b} = -\boldsymbol{\epsilon} : \mathbf{ab} \tag{5.3-30}$$

has been used to rewrite the cross product between any two vectors $\mathbf{a}$ and $\mathbf{b}$. Expanding $\mathbf{R}$ via (B.0-1) and using similar arguments to those invoked in simplifying (5.3-10) yields

$$\overline{\mathbf{N}}^{(e)} = \boldsymbol{\epsilon} : \left[-\mathbf{I} \left(\overline{\Psi}^0 + \overline{\boldsymbol{\Psi}}^1 \cdot \overline{\mathbf{R}} \right) + \overline{\mathbf{P}}^0 \cdot \overline{\boldsymbol{\Psi}}^1 \right]. \tag{5.3-31}$$

Since $\boldsymbol{\epsilon} : \mathbf{I} = \mathbf{0}$, this reduces to

$$\overline{\mathbf{N}}^{(e)} = \boldsymbol{\epsilon} : \overline{\mathbf{P}}^{0} \cdot \overline{\boldsymbol{\Psi}}^{1}, \tag{5.3-32}$$

which upon introduction of (5.3-7) gives

$$\overline{\mathbf{N}}^{(e)} = \boldsymbol{\epsilon} : \overline{\mathbf{P}}^{0} \cdot \overline{\boldsymbol{\Lambda}}^{0} \cdot \overline{\mathbf{v}}. \tag{5.3-33}$$

This shows that the external body couple is a constant, independent of $\overline{\mathbf{R}}$, and that it depends linearly upon the (constant) macroscale velocity. Comparison of (5.3-32) with (5.3-15) shows that

$$\overline{\mathbf{P}}_{\times} + \overline{\mathbf{N}}^{(e)} = \mathbf{0} \tag{5.3-34}$$

for this zeroth-order flow field. Basically, the pseudovector $\overline{\mathbf{P}}_{\times}$ characterizing the antisymmetric portion of the macroscale stress is shown here to be the negative of the external body couple density for this order of flow. As a result, the couple stress $\overline{\mathbf{C}}$ in Cauchy's angular momentum equation (5.2-42) does not contribute, and may be a constant, or at least of order $\mathrm{d}\overline{\mathbf{R}}$ smaller than the external body couple and antisymmetric macroscale stress.

5.3.5 Macroscale Equation: Darcy's Law

The macroscale relation between $\overline{\boldsymbol{\nabla}}\overline{p}$ and the velocity field may be derived from (5.2-40) along with the corresponding expressions for $\overline{\mathbf{T}}^{s}$ (5.3-16), $\overline{\mathbf{P}}_{\times}$ (5.3-17) and $\overline{\mathbf{F}}^{(e)}$ (5.3-26) as

$$\overline{\boldsymbol{\nabla}}\overline{p} = \overline{\mathbf{F}}^{(e)} + \overline{\boldsymbol{\nabla}} \cdot \left(\overline{\mathbf{T}}^{s} + \frac{1}{2}\boldsymbol{\epsilon} \cdot \overline{\mathbf{P}}_{\times} \right), \tag{5.3-35}$$

wherein

$$\overline{\mathbf{F}}^{(e)} = \mu \overline{\boldsymbol{\Lambda}}^{0} \cdot \overline{\mathbf{v}}, \tag{5.3-36}$$

$$\overline{\mathbf{T}}^{s} = \mu \overline{\mathbf{K}}^{(l)} \cdot \overline{\mathbf{v}}, \tag{5.3-37}$$

$$\overline{\mathbf{P}}_{\times} = \mu \overline{\mathbf{c}}^{(l)} \cdot \overline{\mathbf{v}}, \tag{5.3-38}$$

with $\overline{\mathbf{K}}^{(l)}$ and $\overline{\mathbf{c}}^{(l)}$ defined as in (5.3-18) and (5.3-21) respectively. [1]

As $\overline{\mathbf{v}}$ is *constant* for this zeroth-order flow field, the stress contributions in (5.3-35) disappear upon forming the divergence, so that the resulting macroscale linear momentum equation is simply

$$\overline{\boldsymbol{\nabla}}\,\overline{p} = -\mu\mathbf{k}^{-1}\cdot\overline{\mathbf{v}}, \tag{5.3-39}$$

where the permeability dyadic is defined as

$$\mathbf{k} \overset{\text{def}}{=} -\overline{\mathbf{V}}^{0}. \tag{5.3-40}$$

Accordingly, $\mathbf{k}$ is a symmetric, positive-definite dyadic. Equation (5.3-39) is, of course, Darcy's law. The continuity equation ($\overline{\boldsymbol{\nabla}}\cdot\overline{\mathbf{v}} = 0$) for this zeroth-order flow is automatically satisfied because $\overline{\mathbf{v}}$ is a constant for this flow. [However, a continuity condition will appear for higher-order flows as a consequence of the auxiliary conditions (4.6-22).]

[1] Caution should be taken when combining the generic linear momentum equation (5.3-35) with the zeroth-order constitutive relations (5.3-37) and (5.3-38) for the stresses because this could lead to the erroneous result

$$\frac{1}{\mu}\overline{\boldsymbol{\nabla}}\overline{p} = \overline{\boldsymbol{\Lambda}}^{0}\cdot\overline{\mathbf{v}} + \left[{}^{\dagger}\overline{\mathbf{K}}^{(l)} - \frac{1}{2}\boldsymbol{\epsilon}\cdot\overline{\mathbf{c}}^{(l)}\right] : (\overline{\boldsymbol{\nabla}}\overline{\mathbf{v}})^{\dagger}$$

where the term ${}^{\dagger}\overline{\mathbf{K}}^{(l)} - \frac{1}{2}\boldsymbol{\epsilon}\cdot\overline{\mathbf{c}}^{(l)}$ may be thought of as relating the macroscale velocity gradient to the macroscale pressure gradient. However, from the results of higher order flow fields, the external body force density $\overline{\mathbf{F}}^{(e)}$ will have contributions dependent upon higher order macroscale gradients of $\overline{\mathbf{v}}$, hence there will also be a contribution to $\overline{\boldsymbol{\nabla}}\overline{p}$ which is linear in $\overline{\boldsymbol{\nabla}}\overline{\mathbf{v}}$ but which comes from the external body force density.

5.4 First-order Macroscale Flow

For the first-order flow, the microscale velocity and pressure fields are respectively given by (4.4-54) and (4.4-55) as

$$\begin{aligned}\mu \mathbf{v}(\mathbf{R}) &= \widetilde{\mathbf{V}}^0(\mathbf{R}) \cdot \left[\overline{\mathbf{\Psi}}^1 + \overline{\mathbf{\Psi}}^2 \cdot \mathbf{R}\right] \\ &\quad + \widetilde{\mathbf{V}}^1(\mathbf{R}) : \overline{\mathbf{\Psi}}^2 \end{aligned} \tag{5.4-1}$$

and

$$\begin{aligned} p(\mathbf{R}) &= \overline{\Psi}^0 + \overline{\mathbf{\Psi}}^1 \cdot \mathbf{R} + \frac{1}{2}\overline{\mathbf{\Psi}}^2 : \mathbf{R}\mathbf{R} \\ &\quad + \widetilde{\mathbf{\Pi}}^0(\mathbf{R}) \cdot \left[\overline{\mathbf{\Psi}}^1 + \overline{\mathbf{\Psi}}^2 \cdot \mathbf{R}\right] \\ &\quad + \widetilde{\mathbf{\Pi}}^1(\mathbf{R}) : \overline{\mathbf{\Psi}}^2 . \end{aligned} \tag{5.4-2}$$

5.4.1 Macroscale Velocity, $\overline{\mathbf{v}}$

As in the definition (4.3-41) of $\overline{\mathbf{V}}^0$, define the $(n+2)$ rank tensor

$$\overline{\mathbf{V}}^n \stackrel{\text{def}}{=} \frac{1}{\tau_0} \oint_{\partial \tau_0} \mathbf{r} \mathrm{d}\mathbf{S} \cdot \widetilde{\mathbf{V}}^n(\mathbf{r}) \qquad \forall\, (n = 0, 1, 2, \ldots) . \tag{5.4-3}$$

This tensor is obviously symmetric with respect to its last $n+1$ indices. Substitute (5.4-1) into (5.2-6) and rearrange using (5.3-4) and (B.0-10) while utilizing the definitions of $\overline{\mathbf{V}}^0$ and $\overline{\mathbf{V}}^1$. This yields

$$q_k = \mathbf{s}_k \cdot \frac{1}{\mu} \left[\overline{\mathbf{V}}^0 \cdot \overline{\mathbf{\Psi}}^1 + \left(\mathbf{l}_k \frac{1}{\tau_0} \int_{\mathbf{s}_k} \mathrm{d}\mathbf{S} \cdot \widetilde{\mathbf{V}}^0 \mathbf{r} + \overline{\mathbf{V}}^0 \mathbf{R}_\mathbf{n} \right) : \overline{\mathbf{\Psi}}^2 + \overline{\mathbf{V}}^1 : \overline{\mathbf{\Psi}}^2 \right] . \tag{5.4-4}$$

As in the comparable stress calculation of §5.3.2 the second, $\mathbf{l}_k$, term may be neglected when compared with the third. Comparison of (5.4-4) with (5.2-7) then gives

$$\begin{aligned}\mu \overline{\mathbf{v}}(\overline{\mathbf{R}}) &= \overline{\mathbf{V}}^0 \cdot \left[\overline{\mathbf{\Psi}}^1 + \overline{\mathbf{\Psi}}^2 \cdot \overline{\mathbf{R}}\right] \\ &\quad + \overline{\mathbf{V}}^1 : \overline{\mathbf{\Psi}}^2 \end{aligned} \tag{5.4-5}$$

for the first-order macroscale velocity field $\overline{\mathbf{v}}(\overline{\mathbf{R}})$, accurate to within an error of $\mathcal{O}\left(|\mathrm{d}\overline{\mathbf{R}}|\right)$. The macroscale velocity field for this first-order flow is seen to be composed of a homogeneous part plus a part which varies linearly with $\overline{\mathbf{R}}$. Of course, setting $\overline{\mathbf{\Psi}}^2 = \mathbf{0}$ recovers the homogeneous zeroth-order flow field, discussed in § 5.3.1.

Form the macroscale gradient of (5.4-5) to obtain

$$\mu \overline{\boldsymbol{\nabla}}\, \overline{\mathbf{v}} = \overline{\mathbf{\Psi}}^2 \cdot \overline{\mathbf{V}}^0, \tag{5.4-6}$$

wherein the symmetries of $\overline{\mathbf{\Psi}}^2$ and $\overline{\mathbf{V}}^0$ have been used. Upon computing the trace of (5.4-6) and comparing the result with auxiliary condition #1 (4.4-25), it follows that the latter may be expressed in the alternate form

$$\overline{\boldsymbol{\nabla}} \cdot \overline{\mathbf{v}} = 0, \tag{5.4-7}$$

corresponding to the macroscale continuity equation.

Equation (5.4-6) can be inverted and expressed in Cartesian tensor notation as

$$\left[\overline{\mathbf{\Psi}}^2\right]_{ij} = \mu I^4_{iljm} \overline{\Lambda}^0_{mk}\, \overline{\nabla}_l\, \overline{v}_k, \tag{5.4-8}$$

with the fourth-rank isotropic tensor $\mathbf{I}^4$ defined as

$$I^4_{ijkl} \overset{\text{def}}{=} \left[\!\left[\delta_{ij}\delta_{kl} \right]\!\right]^{sik} \tag{5.4-9}$$

$$\equiv \frac{1}{2}\left(\delta_{ij}\delta_{kl} + \delta_{kj}\delta_{il}\right). \tag{5.4-10}$$

The velocity gradient in (5.4-8) may be further decomposed by rewriting $\overline{\boldsymbol{\nabla}}\overline{\mathbf{v}}$ as

$$\overline{\boldsymbol{\nabla}}\overline{\mathbf{v}} = \overline{\mathbf{S}} + \frac{1}{2}\boldsymbol{\epsilon} \cdot \overline{\boldsymbol{\omega}}, \tag{5.4-11}$$

where $\overline{\mathbf{S}}$ is the macroscale symmetric rate-of-strain dyadic, defined as

$$\overline{\mathbf{S}} \overset{\text{def}}{=} \frac{1}{2}\left[\left(\overline{\boldsymbol{\nabla}}\overline{\mathbf{v}}\right) + {}^{\dagger}\left(\overline{\boldsymbol{\nabla}}\overline{\mathbf{v}}\right)\right], \tag{5.4-12}$$

and $\overline{\boldsymbol{\omega}}$ is the macroscale pseudovector vorticity, defined as

$$\overline{\boldsymbol{\omega}} \stackrel{\text{def}}{=} \overline{\boldsymbol{\nabla}} \times \overline{\mathbf{v}}. \tag{5.4-13}$$

Equation (5.4-8) then adopts the equivalent form

$$\begin{aligned} \left[\overline{\boldsymbol{\Psi}}^2\right]_{ij} &= \mu\, I^4_{injm} \overline{\Lambda}^0_{mo} I^4_{lnko}\, \overline{S}_{lk} \\ &\quad + \mu\, I^4_{injm} \overline{\Lambda}^0_{mo} \frac{1}{2} \epsilon_{nok}\, \overline{\omega}_k. \end{aligned} \tag{5.4-14}$$

Substitution of (5.4-14) into (5.4-5) ultimately gives

$$\begin{aligned} \left[\overline{\boldsymbol{\Psi}}^1 + \overline{\boldsymbol{\Psi}}^2 \cdot \overline{\mathbf{R}}\right]_i &= \mu\, \overline{\Lambda}^0_{ij}\, \overline{v}_j \\ &\quad - \mu\, \overline{\Lambda}^0_{il} \overline{V}^1_{lmn} \overline{\Lambda}^0_{no} I^4_{kmjo}\, \overline{S}_{kj} \\ &\quad - \mu\, \overline{\Lambda}^0_{il} \overline{V}^1_{lmn} \overline{\Lambda}^0_{no} \frac{1}{2} \epsilon_{moj}\, \overline{\omega}_j, \end{aligned} \tag{5.4-15}$$

in which the symmetry of $\overline{\mathbf{V}}^1$ with respect to its last two indices has been used.

5.4.2 Macroscale Stress, $\overline{\mathbf{P}}$

The microscale stress tensor for this first-order flow, determined from (5.4-1), (5.4-2), (5.2-13), (5.2-14) and (5.3-9), is

$$\begin{aligned} \mathbf{P}(\mathbf{R}) &= -\mathbf{I}\left[\overline{\Psi}^0 + \overline{\boldsymbol{\Psi}}^1 \cdot \mathbf{R} + \frac{1}{2} \overline{\boldsymbol{\Psi}}^2 : \mathbf{R}\mathbf{R}\right] \\ &\quad + \tilde{\mathbf{P}}^0(\mathbf{R}) \cdot \left[\overline{\boldsymbol{\Psi}}^1 + \overline{\boldsymbol{\Psi}}^2 \cdot \mathbf{R}\right] \\ &\quad + \tilde{\mathbf{P}}^1(\mathbf{R}) : \overline{\boldsymbol{\Psi}}^2 + 2^{\,s}\left[\widetilde{\mathbf{V}}^0(\mathbf{R}) \cdot \overline{\boldsymbol{\Psi}}^2\right]. \end{aligned} \tag{5.4-16}$$

Introduce this into (5.2-12) and again compare the relative orders of the resulting terms, enabling one to replace $\mathbf{R}^n$ by $\mathbf{R}^n_{\mathbf{n}}$ and ultimately by $\overline{\mathbf{R}}^n$. Thereby, one obtains the first-order macroscale stress field,

$$\overline{\mathbf{P}}(\overline{\mathbf{R}}) = -\mathbf{I}\left[\overline{\Psi}^0 + \overline{\boldsymbol{\Psi}}^1 \cdot \overline{\mathbf{R}} + \frac{1}{2} \overline{\boldsymbol{\Psi}}^2 : \overline{\mathbf{R}}\,\overline{\mathbf{R}}\right]$$

$$+\overline{\mathbf{P}}^0 \cdot \left[\overline{\mathbf{\Psi}}^1 + \overline{\mathbf{\Psi}}^2 \cdot \overline{\mathbf{R}}\right]$$
$$+\left[\overline{\mathbf{P}}^1 + \overline{\overline{\mathbf{V}}}^0\right] : \overline{\mathbf{\Psi}}^2 + \overline{\mathbf{V}}^0 \cdot \overline{\mathbf{\Psi}}^2, \tag{5.4-17}$$

to within an error $\mathcal{O}\left(|\mathrm{d}\overline{\mathbf{R}}|\right)$, in which the $(n+4)$th rank tensor $\overline{\overline{\mathbf{V}}}^n$ is defined as

$$\overline{\overline{\mathbf{V}}}^n \stackrel{\text{def}}{=} \frac{1}{\tau_0} \oint_{\partial\tau_0} \mathbf{r}\widetilde{\mathbf{V}}^n(\mathbf{r})\mathrm{d}\mathbf{S}. \tag{5.4-18}$$

The latter yields $\overline{\mathbf{V}}^n$ upon forming its trace with respect to its second and last indices.

From (5.2-19) the macroscale pressure field is

$$\begin{aligned}\overline{p}(\overline{\mathbf{R}}) \;=\; & \overline{\Psi}^0 + \overline{\mathbf{\Psi}}^1 \cdot \overline{\mathbf{R}} + \frac{1}{2}\overline{\mathbf{\Psi}}^2 : \overline{\mathbf{R}}\,\overline{\mathbf{R}} \\ & -\nu\mathbf{I} : \overline{\mathbf{P}}^0 \cdot \left[\overline{\mathbf{\Psi}}^1 + \overline{\mathbf{\Psi}}^2 \cdot \overline{\mathbf{R}}\right] \\ & -\nu\left[\mathbf{I} : \left(\overline{\mathbf{P}}^1 + \overline{\overline{\mathbf{V}}}^0\right) + \overline{\mathbf{V}}^0\right] : \overline{\mathbf{\Psi}}^2,\end{aligned} \tag{5.4-19}$$

in which the last term in the latter will ultimately vanish as a consequence of auxiliary condition #1 (4.4-25). The macroscale pressure field for this first-order flow thus possesses constant, linear, and quadratic contributions from the macroscale position vector $\overline{\mathbf{R}}$.

The symmetric deviatoric stress, computed by combining (5.4-17) and (5.2-20) with the inversion relations (5.4-14) and (5.4-15), can be expressed as

$$\overline{\mathbf{T}}^s = \mu\left[\overline{\mathbf{K}}^{(l)} \cdot \overline{\mathbf{v}} + \overline{\mathbf{K}}^{(r)} \cdot \overline{\boldsymbol{\omega}} + \overline{\mathbf{K}}^{(s)} : \overline{\mathbf{S}}\right], \tag{5.4-20}$$

where the constant triadic $\overline{\mathbf{K}}^{(l)}$ is as defined previously in (5.3-18). In the above, the constant triadic $\overline{\mathbf{K}}^{(r)}$ and constant tetradic $\overline{\mathbf{K}}^{(s)}$ are respectively defined as

$$\overline{K}^{(r)}_{ijk} \stackrel{\text{def}}{=} \left[-\overline{K}^{(l)}_{ijm}\overline{V}^1_{mop} + \overline{K}^1_{ijmn}I^4_{nomp}\right]\overline{\Lambda}^0_{pq}\frac{1}{2}\epsilon_{oqk} \tag{5.4-21}$$

and

$$\overline{K}^{(s)}_{ijkl} \stackrel{\text{def}}{=} \left[-\overline{K}^{(l)}_{ijm}\overline{V}^1_{mop} + \overline{K}^1_{ijmn}I^4_{nomp}\right]\overline{\Lambda}^0_{pq}I^4_{lokq}, \tag{5.4-22}$$

where the constant tetradic $\overline{\mathbf{K}}^1$ is defined as

$$\begin{aligned}\overline{K}^1_{ijkl} \overset{\text{def}}{=}\ & I^4_{imjn}\left[\overline{P}^1_{mnkl} + \overline{\overline{V}}^0_{mnkl} + \overline{V}^0_{ml}\delta_{nk}\right] \\ & -\nu\delta_{ij}\left[\overline{P}^1_{mmkl} + \overline{\overline{V}}^0_{mmkl} + \overline{V}^0_{kl}\right].\end{aligned} \tag{5.4-23}$$

The triadic $\overline{\mathbf{K}}^{(r)}$ couples the macroscale vorticity with the symmetric part of the macroscale stress. It is both symmetric and traceless with respect to its first two indices:

$$\overline{K}^{(r)}_{ijk} = \overline{K}^{(r)}_{jik}, \tag{5.4-24}$$

$$\overline{K}^{(r)}_{iij} = 0 \qquad \forall\,(j = 1,2,3)\,. \tag{5.4-25}$$

As well, as a result of the symmetry properties of $\overline{\mathbf{V}}^1$ and $\mathbf{I}^4$, $\overline{\mathbf{K}}^{(r)}$ vanishes when the permeability (or equivalently $\overline{\mathbf{\Lambda}}^0$) is isotropic, showing that a macroscale rotational flow field in this type of medium does not make a (linear) contribution to $\overline{\mathbf{T}}^s$.

The tetradic $\overline{\mathbf{K}}^{(s)}$ couples the macroscale symmetric rate-of-strain dyadic to the symmetric part of the macroscale stress. It is symmetric and traceless with respect to its first two indices, as well as symmetric with respect to its last two indices:

$$\overline{K}^{(s)}_{ijkl} = \overline{K}^{(s)}_{jikl} = \overline{K}^{(s)}_{ijlk} = \overline{K}^{(s)}_{jilk}, \tag{5.4-26}$$

$$\overline{K}^{(s)}_{iijk} = 0 \qquad \forall\,(\{j,k\} = 1,2,3)\,. \tag{5.4-27}$$

The pseudovector corresponding to the antisymmetric part of the macroscale stress may be derived by combining (5.4-17), (5.2-24), (5.4-14) and (5.4-15), ultimately yielding

$$\overline{\mathbf{P}}_\times = \mu\left[\overline{\mathbf{c}}^{(l)}\cdot\overline{\mathbf{v}} + \overline{\mathbf{c}}^{(r)}\cdot\overline{\boldsymbol{\omega}} + \overline{\mathbf{c}}^{(s)} : \overline{\mathbf{S}}\right], \tag{5.4-28}$$

where the constant dyadic $\overline{\mathbf{c}}^{(l)}$ is defined in (5.3-21). The constant dyadic $\overline{\mathbf{c}}^{(r)}$ and constant pseudotriadic $\overline{\mathbf{c}}^{(s)}$ are defined as

$$\overline{c}^{(r)}_{ij} \overset{\text{def}}{=} \left[-\overline{c}^{(l)}_{il}\overline{V}^1_{lno} + \overline{c}^1_{ilm}I^4_{mnlo}\right]\overline{\Lambda}^0_{op}\frac{1}{2}\epsilon_{npj}, \tag{5.4-29}$$

$$\overline{c}^{(s)}_{ijk} \overset{\text{def}}{=} \left[-\overline{c}^{(l)}_{il}\overline{V}^{1}_{lno} + \overline{c}^{1}_{ilm}I^{4}_{mnlo}\right]\overline{\Lambda}^{0}_{op}I^{4}_{knjp}, \tag{5.4-30}$$

where the constant triadic $\overline{\mathbf{c}}^{1}$ is defined as

$$\overline{c}^{1}_{ijk} \overset{\text{def}}{=} -\epsilon_{ilm}\left[\overline{P}^{1}_{mljk} + \overline{\overline{V}}^{0}_{mljk} + \delta_{lj}\overline{V}^{0}_{mk}\right]. \tag{5.4-31}$$

A porous medium possessing an isotropic permeability (or equivalently an isotropic tensor $\overline{\mathbf{\Lambda}}^{0}$) also has the property that $\overline{\mathbf{c}}^{(r)} = \mathbf{0}$; hence, a macroscale rotational flow field in this type of medium does not contribute (linearly) to $\overline{\mathbf{P}}_{\times}$.

The triadic $\overline{\mathbf{c}}^{(s)}$ is symmetric with respect to its last two indices:

$$\overline{c}^{(s)}_{ijk} = \overline{c}^{(s)}_{ikj}. \tag{5.4-32}$$

5.4.3 External Body Force Density, $\overline{\mathbf{F}}^{(e)}$

The external body force density, computed by substituting the expression for the microscale stress (5.4-16) into the defining relation (5.2-28), is

$$\overline{\mathbf{F}}^{(e)} = \overline{\mathbf{\Psi}}^{1} + \overline{\mathbf{\Psi}}^{2}\cdot\overline{\mathbf{R}} - \left(\overline{\overline{\mathbf{P}}}^{0}\right) : \overline{\mathbf{\Psi}}^{2} \tag{5.4-33}$$

for this first-order flow field. In the latter, order-of-magnitude considerations similar to those used in simplifying (5.3-10) were used. Unlike the zeroth-order external force (5.3-25), this first-order external force has a component that scales linearly with $\overline{\mathbf{R}}$. Putting $\overline{\mathbf{\Psi}}^{2} = \mathbf{0}$ in (5.4-33) recovers the lower-order result.

Form the macroscale divergence of $\overline{\mathbf{P}}$ from (5.4-17) and simplify the resulting expression to obtain

$$\overline{\boldsymbol{\nabla}}\cdot\overline{\mathbf{P}} = -\overline{\mathbf{\Psi}}^{1} - \overline{\mathbf{\Psi}}^{2}\cdot\overline{\mathbf{R}} + \left(\overline{\overline{\mathbf{P}}}^{0}\right) : \overline{\mathbf{\Psi}}^{2}. \tag{5.4-34}$$

Upon comparison with (5.4-33), the macroscale linear momentum equation satisfied

by this first-order flow is simply

$$\overline{\mathbf{F}}^{(e)} + \overline{\boldsymbol{\nabla}} \cdot \overline{\mathbf{P}} = \mathbf{0}, \tag{5.4-35}$$

as was the case too for the zeroth-order flow. The preceding equation confirms that the (inertia-free) macroscale form of Cauchy's linear momentum equation (5.2-38) is satisfied by this flow field.

To express the force density in terms of the macroscale velocity field, rewrite (5.4-33) using the inversion formulas (5.4-8) and (5.4-15) to obtain

$$\overline{\mathbf{F}}^{(e)} = \mu \overline{\boldsymbol{\Lambda}}^{0} \cdot \overline{\mathbf{v}} + \mu \overline{\boldsymbol{\nabla}} \cdot \left[\overline{\mathbf{f}}^{(l)} \cdot \overline{\mathbf{v}} \right], \tag{5.4-36}$$

where the constant triadic $\overline{\mathbf{f}}^{(l)}$ is defined as

$$\overline{f}^{(l)}_{ijk} \stackrel{\text{def}}{=} -\overline{\Lambda}^{0}_{jl} \overline{V}^{1}_{lim} \overline{\Lambda}^{0}_{mk} - \overline{P}^{0}_{ljn} I^{4}_{nilm} \overline{\Lambda}^{0}_{mk}. \tag{5.4-37}$$

In the latter two equations, a distinction between contributions to the external force arising from the symmetric $\overline{\mathbf{S}}$ and antisymmetric $\overline{\boldsymbol{\omega}}$ components of the macroscale velocity has not yet been made. Equation (5.4-36) will prove useful when determining the contributions from both the stress and the external force to the mean pressure gradient.

A similar analysis of the external body couple density $\overline{\mathbf{N}}^{(e)}$ computed from the definition (5.2-37) and the microscale (first-order) stress field (5.4-16), followed by comparison with the macroscale stress pseudovector $\overline{\mathbf{P}}_{\times}$ determined from (5.4-33), simply confirms the (inertia-free) angular momentum equation (5.2-43).

5.4.4 Macroscale Equation: Darcy's Law and Couple

As in (5.3-35), the general relation between $\overline{\boldsymbol{\nabla}}\overline{p}$ and $\overline{\mathbf{v}}$ is

$$\overline{\boldsymbol{\nabla}}\overline{p} = \overline{\mathbf{F}}^{(e)} + \overline{\boldsymbol{\nabla}} \cdot \left(\overline{\mathbf{T}}^{s} + \frac{1}{2} \boldsymbol{\epsilon} \cdot \overline{\mathbf{P}}_{\times} \right), \tag{5.4-38}$$

where the expressions for $\overline{\mathbf{F}}^{(e)}$, $\overline{\mathbf{T}}^{s}$ and $\overline{\mathbf{P}}_{\times}$ are given in (5.4-36), (5.4-20) and (5.4-28), namely

$$\overline{\mathbf{F}}^{(e)} = \mu\overline{\mathbf{\Lambda}}^{0}\cdot\overline{\mathbf{v}} + \mu\overline{\boldsymbol{\nabla}}\cdot\left[\overline{\mathbf{f}}^{(l)}\cdot\overline{\mathbf{v}}\right], \tag{5.4-39}$$

$$\overline{\mathbf{T}}^{s} = \mu\left[\overline{\mathbf{K}}^{(l)}\cdot\overline{\mathbf{v}} + \overline{\mathbf{K}}^{(r)}\cdot\overline{\boldsymbol{\omega}} + \overline{\mathbf{K}}^{(s)} : \overline{\mathbf{S}}\right], \tag{5.4-40}$$

$$\overline{\mathbf{P}}_{\times} = \mu\left[\overline{\mathbf{c}}^{(l)}\cdot\overline{\mathbf{v}} + \overline{\mathbf{c}}^{(r)}\cdot\overline{\boldsymbol{\omega}} + \overline{\mathbf{c}}^{(s)} : \overline{\mathbf{S}}\right]. \tag{5.4-41}$$

The definitions of the constants $\overline{\mathbf{f}}^{(l)}$, $\overline{\mathbf{K}}^{(l)}$, $\overline{\mathbf{K}}^{(r)}$, $\overline{\mathbf{K}}^{(s)}$, $\overline{\mathbf{c}}^{(l)}$, $\overline{\mathbf{c}}^{(r)}$ and $\overline{\mathbf{c}}^{(s)}$ may be found in (5.4-37), (5.3-18), (5.4-21), (5.4-22), (5.3-21), (5.4-29) and (5.4-30) respectively. Direct substitution of these expressions into the previous equation yields

$$\frac{1}{\mu}\overline{\boldsymbol{\nabla}}\,\overline{p} = -\mathbf{k}^{-1}\cdot\overline{\mathbf{v}} + \left[\overline{\mathbf{f}}^{(l)\dagger} + \overline{\mathbf{K}}^{(l)\dagger} - \frac{1}{2}\boldsymbol{\epsilon}\cdot\overline{\mathbf{c}}^{(l)}\right] : \left(\overline{\boldsymbol{\nabla}}\overline{\mathbf{v}}\right)^{\dagger}. \tag{5.4-42}$$

In writing (5.4-42), no contributions arise from the velocity gradients in the stress, because the gradient of the velocity field is a constant for this first-order flow. As such, any higher-order gradients are all identically zero. Comparison of (5.4-42) with the footnote on page 140 reveals that a contribution from the external force $\overline{\mathbf{f}}^{(l)}$ must be included when retaining higher-order velocity gradients in the momentum equation. Equation (5.4-42) may be expressed more succinctly as

$$\frac{1}{\mu}\overline{\boldsymbol{\nabla}}\,\overline{p} = -\mathbf{k}^{-1}\cdot\overline{\mathbf{v}} + \overline{\boldsymbol{\chi}}^{*} : \overline{\boldsymbol{\nabla}}\overline{\mathbf{v}}, \tag{5.4-43}$$

where the constant triadic $\overline{\boldsymbol{\chi}}^{*}$ is defined as

$$\overline{\chi}^{*}_{ijk} \stackrel{\text{def}}{=} \overline{f}^{(l)}_{kij} + \overline{K}^{(l)}_{kij} - \frac{1}{2}\epsilon_{ikl}\overline{c}^{(l)}_{lj}. \tag{5.4-44}$$

This can, in turn, be rewritten explicitly in terms of $\overline{\mathbf{S}}$ and $\overline{\boldsymbol{\omega}}$ as

$$\frac{1}{\mu}\overline{\boldsymbol{\nabla}}\,\overline{p} = -\mathbf{k}^{-1}\cdot\overline{\mathbf{v}} + \overline{\boldsymbol{\chi}}^{(r)}\cdot\overline{\boldsymbol{\omega}} + \overline{\boldsymbol{\chi}}^{(s)} : \overline{\mathbf{S}}, \tag{5.4-45}$$

where the constant dyadic $\overline{\boldsymbol{\chi}}^{(r)}$ is defined as

$$\overline{\chi}_{ij}^{(r)} \stackrel{\text{def}}{=} \overline{\chi}_{ikl}^{*} \frac{1}{2} \epsilon_{lkj}, \tag{5.4-46}$$

and the constant triadic $\overline{\boldsymbol{\chi}}^{(s)}$ as

$$\overline{\chi}_{ijk}^{(s)} \stackrel{\text{def}}{=} \frac{1}{2} \left(\overline{\chi}_{ijk}^{*} + \overline{\chi}_{ikj}^{*} \right). \tag{5.4-47}$$

Equation (5.4-43) [or (5.4-45)] constitutes the macroscale momentum equation for this first-order flow. It contains both a permeability term, as in (5.3-39), and a higher-order term, the latter correcting (5.3-39) for the presence of a macroscale velocity gradient. Equation (5.4-45) must be solved in conjunction with the continuity condition (5.4-7), namely

$$\overline{\boldsymbol{\nabla}} \cdot \overline{\mathbf{v}} = 0. \tag{5.4-48}$$

5.5 Second-order Macroscale Flow

In this section, the goal is to determine the contribution to the external body force density $\overline{\mathbf{f}}^{(e)}$ arising from second-order macroscale gradients of $\overline{\mathbf{v}}$, namely terms involving $\overline{\boldsymbol{\nabla}}\,\overline{\boldsymbol{\nabla}}\,\overline{\mathbf{v}}$. One may compute the contributions to the stress $\overline{\mathbf{P}}$ arising from these gradients, but when the momentum equation is formed, only those contributions to the stress up to and including terms involving $\overline{\boldsymbol{\nabla}}\,\overline{\mathbf{v}}$ [determined in the previous section and given in (5.4-20) and (5.4-28)] will contribute to second-order gradients in $\overline{\mathbf{v}}$. As such, the subsequent focus will be primarily on determining $\overline{\mathbf{f}}^{(r)}$ [cf. (5.5-21)] and $\overline{\mathbf{f}}^{(s)}$ [cf. (5.5-22)].

For second-order flow, the microscale velocity and pressure fields are given by (4.5-51) and (4.5-52) as

$$\begin{aligned}\mu\mathbf{v}(\mathbf{R}) &= \widetilde{\mathbf{V}}^0(\mathbf{R})\cdot\left[\overline{\boldsymbol{\Psi}}^1+\overline{\boldsymbol{\Psi}}^2\cdot\mathbf{R}+\frac{1}{2}\overline{\boldsymbol{\Psi}}^3:\mathbf{R}\mathbf{R}\right]\\ &\quad+\widetilde{\mathbf{V}}^1(\mathbf{R}):\left[\overline{\boldsymbol{\Psi}}^2+\overline{\boldsymbol{\Psi}}^3\cdot\mathbf{R}\right]\\ &\quad+\widetilde{\mathbf{V}}^2(\mathbf{R}):\overline{\boldsymbol{\Psi}}^3\end{aligned}\tag{5.5-1}$$

and

$$\begin{aligned}p(\mathbf{R}) &= \overline{\Psi}^0+\overline{\boldsymbol{\Psi}}^1\cdot\mathbf{R}+\frac{1}{2}\overline{\boldsymbol{\Psi}}^2:\mathbf{R}\mathbf{R}+\frac{1}{6}\overline{\boldsymbol{\Psi}}^3\mathbf{R}\mathbf{R}\mathbf{R}\\ &\quad+\widetilde{\Pi}^0(\mathbf{R})\cdot\left[\overline{\boldsymbol{\Psi}}^1+\overline{\boldsymbol{\Psi}}^2\cdot\mathbf{R}+\frac{1}{2}\overline{\boldsymbol{\Psi}}^3:\mathbf{R}\mathbf{R}\right]\\ &\quad+\widetilde{\boldsymbol{\Pi}}^1(\mathbf{R}):\left[\overline{\boldsymbol{\Psi}}^2+\overline{\boldsymbol{\Psi}}^3\cdot\mathbf{R}\right]\\ &\quad+\widetilde{\boldsymbol{\Pi}}^2(\mathbf{R}):\overline{\boldsymbol{\Psi}}^3.\end{aligned}\tag{5.5-2}$$

5.5.1 Macroscale Velocity, $\overline{\mathbf{v}}$

As in preceding sections, the microscale velocity field (5.5-1) is substituted into (5.2-6), and the corresponding macroscale velocity field calculated to be

$$\mu\overline{\mathbf{v}}(\overline{\mathbf{R}}) = \overline{\mathbf{V}}^0\cdot\left[\overline{\boldsymbol{\Psi}}^1+\overline{\boldsymbol{\Psi}}^2\cdot\overline{\mathbf{R}}+\frac{1}{2}\overline{\boldsymbol{\Psi}}^3:\overline{\mathbf{R}}\,\overline{\mathbf{R}}\right]$$

$$+\overline{\mathbf{V}}^1 : \left[\overline{\mathbf{\Psi}}^2 + \overline{\mathbf{\Psi}}^3 \cdot \overline{\mathbf{R}}\right]$$
$$+\overline{\mathbf{V}}^2 \vdots \overline{\mathbf{\Psi}}^3 \tag{5.5-3}$$

with an error of $\mathcal{O}\left(|\mathrm{d}\overline{\mathbf{R}}|\right)$. This second-order macroscale velocity field retains all the prior elements of the first-order macroscale velocity of § 5.4.1 plus an additional term quadratic in $\overline{\mathbf{R}}$. The choice $\overline{\mathbf{\Psi}}^3 = \mathbf{0}$ confirms the previous first-order result. Form the macroscale second derivative of (5.5-3) so as to obtain

$$\mu \overline{\boldsymbol{\nabla}}\, \overline{\boldsymbol{\nabla}}\, \overline{\mathbf{v}} = \overline{\mathbf{\Psi}}^3 \cdot \overline{\mathbf{V}}^0. \tag{5.5-4}$$

As will now be shown,

$$\overline{\boldsymbol{\nabla}} \cdot \overline{\mathbf{v}} = 0, \tag{5.5-5}$$

as with the first-order flow. To prove the above, form the gradient of (5.5-3),

$$\mu \overline{\boldsymbol{\nabla}}\, \overline{\mathbf{v}} = \left[\overline{\mathbf{\Psi}}^2 + \overline{\mathbf{\Psi}}^3 \cdot \overline{\mathbf{R}}\right] \cdot \overline{\mathbf{V}}^0 + \left(\overline{\mathbf{V}}^1 : \overline{\mathbf{\Psi}}^3\right)^\dagger, \tag{5.5-6}$$

whose trace yields

$$\mu \overline{\boldsymbol{\nabla}} \cdot \overline{\mathbf{v}} = \overline{\mathbf{V}}^0 : \overline{\mathbf{\Psi}}^2 + \left[\overline{\mathbf{R}}\, \overline{\mathbf{V}}^0 + \overline{\mathbf{V}}^1\right] \vdots \overline{\mathbf{\Psi}}^3. \tag{5.5-7}$$

Use of the definitions of $\overline{\mathbf{V}}^0$ and $\overline{\mathbf{V}}^1$, together with the divergence theorem and the equations satisfied by $\widetilde{\mathbf{V}}^0(\mathbf{r})$ and $\widetilde{\mathbf{V}}^1(\mathbf{r})$ gives

$$\mu \overline{\boldsymbol{\nabla}} \cdot \overline{\mathbf{v}} = \frac{\tau_f}{\tau_0}\left(\left\langle \widetilde{\mathbf{V}}^0 \right\rangle : \overline{\mathbf{\Psi}}^2 + \left\langle \widetilde{\mathbf{V}}^1 \right\rangle \vdots \overline{\mathbf{\Psi}}^3\right) + \frac{1}{\tau_0}\int_{\tau_f} \left(\overline{\mathbf{R}} - \mathbf{r} + \langle \mathbf{r} \rangle\right) \widetilde{\mathbf{V}}^0\, \mathrm{d}^3\mathbf{r} \vdots \overline{\mathbf{\Psi}}^3. \tag{5.5-8}$$

In the macroscale limit, $\mathbf{r}$ is of order $\mathrm{d}\overline{\mathbf{R}}$, whereupon the latter equation reduces to

$$\mu \overline{\boldsymbol{\nabla}} \cdot \overline{\mathbf{v}} = \frac{\tau_f}{\tau_0}\left(\left\langle \widetilde{\mathbf{V}}^0 \right\rangle : \overline{\mathbf{\Psi}}^2 + \left\langle \widetilde{\mathbf{V}}^1 \right\rangle \vdots \overline{\mathbf{\Psi}}^3\right) + \overline{\mathbf{V}}^0 : \overline{\mathbf{\Psi}}^3 \cdot \overline{\mathbf{R}}, \tag{5.5-9}$$

of which the first two terms are zero as a result of auxiliary condition #1, while the last term is identically zero as a result of auxiliary condition #2. Q. E. D.

Equations (5.5-4), (5.5-6) and (5.5-3) may be successively inverted to obtain the

respective partial sums

$$\left[\overline{\Psi}^3\right]_{ijk} = \mu I^6_{injmko}\,\overline{\Lambda}^0_{ol}\,\overline{\nabla}_n\overline{\nabla}_m\overline{v}_l, \tag{5.5-10}$$

$$\begin{aligned}\left[\overline{\Psi}^2 + \overline{\Psi}^3\cdot\overline{\mathbf{R}}\right]_{ij} &= \mu I^4_{iljm}\,\overline{\Lambda}^0_{mk}\,\overline{\nabla}_l\overline{v}_k \\ &\quad -\mu I^4_{jnio}\,\overline{\Lambda}^0_{np}\,\overline{V}^1_{pqr}\,I^6_{rmqlos}\,\overline{\Lambda}^0_{sk}\,\overline{\nabla}_m\overline{\nabla}_l\overline{v}_k\end{aligned} \tag{5.5-11}$$

and

$$\begin{aligned}\left[\overline{\Psi}^1 + \overline{\Psi}^2\cdot\overline{\mathbf{R}} + \frac{1}{2}\overline{\Psi}^3 : \overline{\mathbf{R}}\,\overline{\mathbf{R}}\right]_i &= \mu\overline{\Lambda}^0_{ij}\,\overline{v}_j \\ &\quad -\mu\overline{\Lambda}^0_{il}\,\overline{V}^1_{lkm}\,\overline{\Lambda}^0_{mj}\,\overline{\nabla}_k\overline{v}_j \\ &\quad +\mu\overline{\Lambda}^0_{im}\left(\overline{V}^1_{mno}\,\overline{\Lambda}^0_{op}\,\overline{V}^1_{pqr}\,I^6_{rlqkns} - \overline{V}^2_{mkls}\right)\overline{\Lambda}^0_{sj}\,\overline{\nabla}_l\overline{\nabla}_k\overline{v}_j,\end{aligned} \tag{5.5-12}$$

where the sixth rank isotropic tensor $\mathbf{I}^6$ is defined as

$$\begin{aligned}I^6_{ijklmn} &\overset{\text{def}}{=} \left[\!\left[\,\delta_{ij}\delta_{kl}\delta_{mn}\,\right]\!\right]^{sikm} \\ &\equiv \frac{1}{6}\left(\delta_{ij}\delta_{kl}\delta_{mn} + \delta_{ij}\delta_{ml}\delta_{kn} + \delta_{kj}\delta_{il}\delta_{mn} + \delta_{kj}\delta_{ml}\delta_{in} + \delta_{mj}\delta_{il}\delta_{kn} + \delta_{mj}\delta_{kl}\delta_{in}\right).\end{aligned} \tag{5.5-13}$$

5.5.2 Macroscale Stress, $\overline{\mathbf{P}}$

The microscale stress for this second-order flow, determined from (4.5-51), (4.5-52), (5.2-13), (5.2-14) and (5.3-9), is

$$\begin{aligned}\mathbf{P}(\mathbf{R}) &= -\mathbf{I}\left[\overline{\Psi}^0 + \overline{\Psi}^1\cdot\mathbf{R} + \frac{1}{2}\overline{\Psi}^2 : \mathbf{R}\,\mathbf{R} + \frac{1}{6}\overline{\Psi}^3 \vdots \mathbf{R}\,\mathbf{R}\,\mathbf{R}\right] \\ &\quad +\tilde{\mathbf{P}}^0(\mathbf{R})\cdot\left[\overline{\Psi}^1 + \overline{\Psi}^2\cdot\mathbf{R} + \frac{1}{2}\overline{\Psi}^3 : \mathbf{R}\,\mathbf{R}\right] \\ &\quad +\tilde{\mathbf{P}}^1(\mathbf{R}) : \left[\overline{\Psi}^2 + \overline{\Psi}^3\cdot\mathbf{R}\right] + 2^s\left(\widetilde{\mathbf{V}}^0(\mathbf{R})\cdot\left[\overline{\Psi}^2 + \overline{\Psi}^3\cdot\mathbf{R}\right]\right) \\ &\quad +\tilde{\mathbf{P}}^2(\mathbf{R}) \vdots \overline{\Psi}^3 + 2^s\left(\widetilde{\mathbf{V}}^1(\mathbf{R}) : \overline{\Psi}^3\right).\end{aligned} \tag{5.5-14}$$

Substitute (5.5-14) into (5.2-12), and compare terms so as to successively convert from $\mathbf{R}^n$ to $\mathbf{R}_\mathbf{n}^n$ to $\overline{\mathbf{R}}^n$, thereby obtaining the second-order macroscale stress field:

$$\begin{aligned}\overline{\mathbf{P}}(\overline{\mathbf{R}}) &= -\mathbf{I}\left[\overline{\Psi}^0+\overline{\Psi}^1\cdot\overline{\mathbf{R}}+\frac{1}{2}\overline{\Psi}^2:\overline{\mathbf{R}}\,\overline{\mathbf{R}}+\frac{1}{6}\overline{\Psi}^3\vdots\overline{\mathbf{R}}\,\overline{\mathbf{R}}\,\overline{\mathbf{R}}\right]\\ &\quad+\overline{\mathbf{P}}^0\cdot\left[\overline{\Psi}^1+\overline{\Psi}^2\cdot\overline{\mathbf{R}}+\frac{1}{2}\overline{\Psi}^3:\overline{\mathbf{R}}\,\overline{\mathbf{R}}\right]\\ &\quad+\left[\overline{\mathbf{P}}^1+\overline{\overline{\mathbf{V}}}^0\right]:\left[\overline{\Psi}^2+\overline{\Psi}^3\cdot\overline{\mathbf{R}}\right]+\overline{\mathbf{V}}^0\cdot\left[\overline{\Psi}^2+\overline{\Psi}^3\cdot\overline{\mathbf{R}}\right]\\ &\quad+\left[\overline{\mathbf{P}}^2+\overline{\overline{\mathbf{V}}}^1\right]\vdots\overline{\Psi}^3+\overline{\mathbf{V}}^1:\overline{\Psi}^3.\end{aligned}\tag{5.5-15}$$

Use of (5.2-19) shows that the macroscale pressure field for this second-order flow is given by

$$\begin{aligned}p(\overline{\mathbf{R}}) &= \overline{\Psi}^0+\overline{\Psi}^1\cdot\overline{\mathbf{R}}+\frac{1}{2}\overline{\Psi}^2:\overline{\mathbf{R}}\,\overline{\mathbf{R}}+\frac{1}{6}\overline{\Psi}^3\vdots\overline{\mathbf{R}}\,\overline{\mathbf{R}}\,\overline{\mathbf{R}}\\ &\quad-\nu\mathbf{I}:\overline{\mathbf{P}}^0\cdot\left[\overline{\Psi}^1+\overline{\Psi}^2\cdot\overline{\mathbf{R}}+\frac{1}{2}\overline{\Psi}^3:\overline{\mathbf{R}}\,\overline{\mathbf{R}}\right]\\ &\quad-\nu\left[\mathbf{I}:\left(\overline{\mathbf{P}}^1+\overline{\overline{\mathbf{V}}}^0\right)+\overline{\mathbf{V}}^0\right]:\left[\overline{\Psi}^2+\overline{\Psi}^3\cdot\overline{\mathbf{R}}\right]\\ &\quad-\nu\left[\mathbf{I}:\left(\overline{\mathbf{P}}^2+\overline{\overline{\mathbf{V}}}^1\right)+\overline{\mathbf{V}}^1\right]\vdots\overline{\Psi}^3.\end{aligned}\tag{5.5-16}$$

This second-order pressure field retains all the previous characteristics of the zeroth- and first-order fields plus terms multiplied by $\overline{\Psi}^3$, most notably a term cubic in $\overline{\mathbf{R}}$.

As mentioned in the beginning of this section, interest lies in determining the second-order contribution to the external force $\overline{\mathbf{F}}^{(e)}$ rather than the comparable contributions to $\overline{\mathbf{T}}^s$ and $\overline{\mathbf{P}}_\times$.

5.5.3 External Body Force Density, $\overline{\mathbf{F}}^{(e)}$

The external body force density computed from (5.2-28) and (5.5-14) is

$$\begin{aligned}\overline{\mathbf{F}}^{(e)} &= \overline{\Psi}^1+\overline{\Psi}^2\cdot\overline{\mathbf{R}}+\frac{1}{2}\overline{\Psi}^3:\overline{\mathbf{R}}\,\overline{\mathbf{R}}\\ &\quad-\left(\overline{\nabla\mathbf{P}}^0\right):\left[\overline{\Psi}^2+\overline{\Psi}^3\cdot\overline{\mathbf{R}}\right]\\ &\quad-\left[\overline{\nabla\mathbf{P}}^1+\overline{\overline{\nabla\mathbf{V}}}^0\right]\vdots\overline{\Psi}^3-\overline{\mathbf{V}}^0:\overline{\Psi}^3.\end{aligned}\tag{5.5-17}$$

The latter may be compared with that obtained by forming $\overline{\boldsymbol{\nabla}} \cdot \overline{\mathbf{P}}$ from (5.5-15), thereby showing that the divergence of the stress and the external body force density properly sum to zero for this second-order flow field. The inversion formulas (5.5-10)–(5.5-12) can be used to express the external force in terms of $\overline{\mathbf{v}}$ and its gradients, thereby converting (5.5-17) into the form

$$\overline{\mathbf{F}}^{(e)} = \mu \overline{\boldsymbol{\Lambda}}^0 \cdot \overline{\mathbf{v}} + \mu \overline{\boldsymbol{\nabla}} \cdot \left[\overline{\mathbf{f}}^{(l)} \cdot \overline{\mathbf{v}} + \overline{\mathbf{f}}^1 : \overline{\boldsymbol{\nabla}} \overline{\mathbf{v}} \right]. \tag{5.5-18}$$

The latter is similar to (5.4-36), but now with an additional contribution arising from the second-order gradient of $\overline{\mathbf{v}}$. The constant triadic $\overline{\mathbf{f}}^{(l)}$ was defined in (5.4-37); the constant tetradic $\overline{\mathbf{f}}^1$ is defined as

$$\overline{f}^1_{ijkl} \stackrel{\text{def}}{=} -\left[I^6_{minlop} \left(\overline{f}^{(l)}_{ojq} \overline{V}^1_{qnm} + \overline{P}^1_{ojnm} + \overline{\overline{V}}^0_{ojnm} + \delta_{oj} \overline{V}^0_{nm} \right) + \overline{\Lambda}^0_{jm} \overline{V}^2_{mlip} \right] \overline{\Lambda}^0_{pk}. \tag{5.5-19}$$

The macroscale velocity gradient appearing in (5.5-18) may be rewritten in terms of $\overline{\mathbf{S}}$ and $\overline{\boldsymbol{\omega}}$, ultimately enabling the external body force density to be expressed as

$$\overline{\mathbf{F}}^{(e)} = \mu \overline{\boldsymbol{\Lambda}}^0 \cdot \overline{\mathbf{v}} + \mu \overline{\boldsymbol{\nabla}} \cdot \left[\overline{\mathbf{f}}^{(l)} \cdot \overline{\mathbf{v}} + \overline{\mathbf{f}}^{(r)} \cdot \overline{\boldsymbol{\omega}} + \overline{\mathbf{f}}^{(s)} : \overline{\mathbf{S}} \right], \tag{5.5-20}$$

where the constant triadic $\overline{\mathbf{f}}^{(r)}$ is defined as

$$\overline{f}^{(r)}_{ijk} \stackrel{\text{def}}{=} \overline{f}^1_{ijlm} \frac{1}{2} \epsilon_{mlk} \tag{5.5-21}$$

and the constant tetradic $\overline{\mathbf{f}}^{(s)}$ as

$$\overline{f}^{(s)}_{ijkl} \stackrel{\text{def}}{=} \frac{1}{2} \left(\overline{f}^1_{ijkl} + \overline{f}^1_{ijlk} \right). \tag{5.5-22}$$

The form of (5.5-20) will be useful when comparing contributions in the momentum equation arising from either the macroscale stress or external body force density.

As in previous sections, one may also compute the external body couple density $\overline{\mathbf{N}}^{(e)}$ from (5.2-37) and (5.5-14), as well as the macroscale stress pseudovector $\overline{\mathbf{P}}_\times$

directly from (5.5-15). The sum of these terms is found to be zero [to within errors of $\mathcal{O}\left(|\mathrm{d}\overline{\mathbf{R}}|\right)$], confirming the angular momentum equation (5.2-43).

5.5.4 Macroscale Equation: Brinkman's Equation and Couple

The relation between $\overline{\boldsymbol{\nabla}}\overline{p}$ and $\overline{\mathbf{v}}$ for this second-order flow is similar to that computed for the first-order flow [equations (5.3-35), (5.4-20) and (5.4-28)], but now with the external body force density, $\overline{\mathbf{F}}^{(e)}$ given by (5.5-20), namely

$$\overline{\mathbf{F}}^{(e)} = \mu\overline{\boldsymbol{\Lambda}}^{0} \cdot \overline{\mathbf{v}} + \mu\overline{\boldsymbol{\nabla}} \cdot \left[\overline{\mathbf{f}}^{(l)} \cdot \overline{\mathbf{v}} + \overline{\mathbf{f}}^{(r)} \cdot \overline{\boldsymbol{\omega}} + \overline{\mathbf{f}}^{(s)} : \overline{\mathbf{S}}\right], \tag{5.5-23}$$

wherein the additional constant tensors $\overline{\mathbf{f}}^{(r)}$ and $\overline{\mathbf{f}}^{(s)}$ are defined in (5.5-21) and (5.5-22) respectively. Upon combining these relations, the momentum equation may be written in a similar form to (5.4-45) as

$$\frac{1}{\mu}\overline{\boldsymbol{\nabla}}\,\overline{p} = -\mathbf{k}^{-1} \cdot \overline{\mathbf{v}} + \overline{\boldsymbol{\chi}}^{(r)} \cdot \overline{\boldsymbol{\omega}} + \overline{\boldsymbol{\chi}}^{(s)} : \overline{\mathbf{S}} + \overline{\boldsymbol{\nabla}} \cdot \left(\frac{1}{\mu}\overline{\boldsymbol{\mu}}^{(r)} \cdot \overline{\boldsymbol{\omega}} + \frac{1}{\mu}\overline{\boldsymbol{\mu}}^{(s)} : \overline{\mathbf{S}}\right), \tag{5.5-24}$$

where the triadic $\overline{\boldsymbol{\mu}}^{(r)}$ is defined as

$$\frac{1}{\mu}\overline{\boldsymbol{\mu}}^{(r)} \stackrel{\text{def}}{=} \overline{\mathbf{f}}^{(r)} + \overline{\mathbf{K}}^{(r)} + \frac{1}{2}\boldsymbol{\epsilon} \cdot \overline{\mathbf{c}}^{(r)}, \tag{5.5-25}$$

and the tetradic $\overline{\boldsymbol{\mu}}^{(s)}$ as

$$\frac{1}{\mu}\overline{\boldsymbol{\mu}}^{(s)} \stackrel{\text{def}}{=} \overline{\mathbf{f}}^{(s)} + \overline{\mathbf{K}}^{(s)} + \frac{1}{2}\boldsymbol{\epsilon} \cdot \overline{\mathbf{c}}^{(s)}. \tag{5.5-26}$$

The momentum equation (5.5-24) could similarily be expressed in a form analagous to (5.4-43) as

$$\frac{1}{\mu}\overline{\boldsymbol{\nabla}}\,\overline{p} = -\mathbf{k}^{-1} \cdot \overline{\mathbf{v}} + \overline{\boldsymbol{\chi}}^{*} : \overline{\boldsymbol{\nabla}}\overline{\mathbf{v}} + \frac{1}{\mu}\overline{\boldsymbol{\mu}}^{*} \vdots \overline{\boldsymbol{\nabla}}\,\overline{\boldsymbol{\nabla}}\,\overline{\mathbf{v}}, \tag{5.5-27}$$

where the 'effective' viscosity tetradic $\overline{\boldsymbol{\mu}}^*$ appearing therein is defined as

$$\overline{\boldsymbol{\mu}}^* \stackrel{\text{def}}{=} \overline{\overset{\dagger}{\boldsymbol{\mu}}}^{(s)} - \overline{\overset{\dagger}{\boldsymbol{\mu}}}^{(r)} \cdot \boldsymbol{\epsilon}. \tag{5.5-28}$$

Equations (5.5-24) or (5.5-27) must be solved simultaneously with the continuity condition (5.5-5), namely

$$\overline{\boldsymbol{\nabla}} \cdot \overline{\mathbf{v}} = 0. \tag{5.5-29}$$

5.6 General Macroscale Flow

It is clear from the preceding lower-order cases that the macroscale velocity vector $\overline{\mathbf{v}}$, the stress tensor $\overline{\mathbf{P}}$ and, of course, the macroscale momentum equation, can all be expressed in terms of known geometric constants characterizing the skeletal porous medium, and partial sums of the $\overline{\Psi}^n$'s. Furthermore, upon inverting these partial sums in terms of the gradients of $\overline{\mathbf{v}}$ [see Eq. (5.3-7) for the zeroth-order, Eqs. (5.4-8) and (5.4-15) for the first-order, and Eqs. (5.5-10), (5.5-11) and (5.5-12) for the second-order], it is now apparent that any terms including $\overline{\Psi}^4$, $\overline{\Psi}^5$, etc., for higher-order flows will ultimately contribute terms of order $\overline{\nabla}^3\overline{\mathbf{v}}$ and higher. Hence, the applicability of the system of equations

$$\frac{1}{\mu}\overline{\nabla}\,\overline{p} = -\mathbf{k}^{-1}\cdot\overline{\mathbf{v}} + \overline{\boldsymbol{\chi}}^{*} : \overline{\nabla}\,\overline{\mathbf{v}} + \frac{1}{\mu}\overline{\boldsymbol{\mu}}^{*} \vdots \overline{\nabla}\,\overline{\nabla}\,\overline{\mathbf{v}} \tag{5.6-1}$$

$$\overline{\nabla}\cdot\overline{\mathbf{v}} = 0 \tag{5.6-2}$$

in describing an *arbitrary* inhomogeneous flow in a porous medium is correct to order $\overline{\nabla}\,\overline{\nabla}\,\overline{\mathbf{v}}$, as can be shown explicitly from the general microscale flow field developed previously.

A more insightful way to express the momentum equation is as shown in (5.3-35), namely

$$\overline{\nabla}\,\overline{p} = \overline{\mathbf{F}}^{(e)} + \overline{\nabla}\cdot\left(\overline{\mathbf{T}}^{s} + \frac{1}{2}\boldsymbol{\epsilon}\cdot\overline{\mathbf{P}}_{\times}\right), \tag{5.6-3}$$

explicitly showing the contributions to the macroscale pressure drop from the external voumetric body force density $\overline{\mathbf{F}}^{(e)}$, symmetric deviatoric stress $\overline{\mathbf{T}}^{s}$ and stress pseudovector $\overline{\mathbf{P}}_{\times}$ (being the negative of the external volumetric body couple density, $\overline{\mathbf{N}}^{(e)}$). In turn, the dependencies of these quantities upon the macroscale velocity $\overline{\mathbf{v}}$, vorticity $\overline{\boldsymbol{\omega}}$ and symmetric rate-of-strain dyadic $\overline{\mathbf{S}}$ are given as

$$\overline{\mathbf{F}}^{(e)} = -\mu\mathbf{k}^{-1}\cdot\overline{\mathbf{v}} + \mu\overline{\nabla}\cdot\left[\overline{\mathbf{f}}^{(l)}\cdot\overline{\mathbf{v}} + \overline{\mathbf{f}}^{(r)}\cdot\overline{\boldsymbol{\omega}} + \overline{\mathbf{f}}^{(s)} : \overline{\mathbf{S}}\right], \tag{5.6-4}$$

$$\overline{\mathbf{T}}^{s} = \mu\left[\overline{\mathbf{K}}^{(l)}\cdot\overline{\mathbf{v}} + \overline{\mathbf{K}}^{(r)}\cdot\overline{\boldsymbol{\omega}} + \overline{\mathbf{K}}^{(s)} : \overline{\mathbf{S}}\right], \tag{5.6-5}$$

$$\overline{\mathbf{P}}_{\times} \;=\; \mu\left[\overline{\mathbf{c}}^{(l)}\cdot\overline{\mathbf{v}}+\overline{\mathbf{c}}^{(r)}\cdot\overline{\boldsymbol{\omega}}+\overline{\mathbf{c}}^{(s)}:\overline{\mathbf{S}}\right] \tag{5.6-6}$$

with the phenomenological coefficients appearing therein uniquely determined from the first three lattice fields $\left(\widetilde{\mathbf{V}}^0,\widetilde{\mathbf{\Pi}}^0\right)$, $\left(\widetilde{\mathbf{V}}^1,\widetilde{\mathbf{\Pi}}^1\right)$ and $\left(\widetilde{\mathbf{V}}^2,\widetilde{\mathbf{\Pi}}^2\right)$.

Chapter 6

Flow through Two-dimensional Arrays

6.1 Introduction

Here, the first three microscale lattice fields $\widetilde{\mathbf{V}}^n$ and $\widetilde{\mathbf{\Pi}}^n$, whose equations were determined in Chapter 4, are computed numerically for two-dimensional square arrays of cylinders and ellipses. These fields are then manipulated as outlined in Chapter 5 in order to derive the relevant phenomenological coefficients describing the dependence of the macroscale symmetric deviatoric stress $\overline{\mathbf{T}}^s$, stress pseudovector $\overline{\mathbf{P}}_\times$ and external body force density $\overline{\mathbf{F}}^{(e)}$ upon the macroscale flow field and porous medium geometry. As well, the macroscale momentum equation—relating the pressure drop $\overline{\nabla}\,\overline{p}$ to the velocity field $\overline{\mathbf{v}}$ and its gradients—is derived for these two types of arrays.

6.2 Microscale Fields

The exact microscale solutions (4.6-39) and (4.6-40) for arbitrary velocity $\mathbf{v}(\mathbf{R})$ and pressure $p(\mathbf{R})$ fields requires solutions of the cellular lattice fields $\widetilde{\mathbf{V}}^m(\mathbf{r})$ and $\widetilde{\mathbf{\Pi}}^m(\mathbf{r})$. The differential equations characterizing each $\mathcal{O}(m)$ *cell problem* are set forth in the system of equations (4.6-41).

The number of unknowns to be solved for (or equations to be solved) increases with m, since the rank of the lattice field increases correspondingly. In general, the fields $\widetilde{\mathbf{V}}^m$ and $\widetilde{\mathbf{\Pi}}^m$ possess 2^{m+2} and 2^{m+1} components (in two dimensions or 3^{m+2} and 3^{m+1} components in three dimensions) respectively, revealing that each cell problem (4.6-41) consists of $3 \times 2^{m+1}$ (or $4 \times 3^{m+1}$) unknowns and equations. However, the linear operator in (4.6-41) only affects the first index of $\widetilde{\mathbf{V}}^m$ and $\widetilde{\mathbf{\Pi}}^m$. As such, the equations decouple into linearly independent sets of equations of the Stokes-like form

$$\nabla^2 \tilde{\mathbf{v}} - \boldsymbol{\nabla} \tilde{p} = \tilde{\mathbf{f}}, \tag{6.2-1}$$

$$\boldsymbol{\nabla} \cdot \tilde{\mathbf{v}} = \tilde{g}, \tag{6.2-2}$$

$$\tilde{\mathbf{v}} = \mathbf{0} \qquad \forall (\mathbf{r} \in s_p), \tag{6.2-3}$$

$$\langle \tilde{p} \rangle = 0, \tag{6.2-4}$$

along with the requirement on the cell faces $\partial\tau_0$ that $\tilde{\mathbf{v}}$ and $\tilde{p}$ are fully spatially periodic functions. In this Stokes-like problem, $\tilde{\mathbf{v}}(\mathbf{r})$ is a *vector* 'velocity' field and $\tilde{p}(\mathbf{r})$ a *scalar* pressure field. These equations are forced by the fully spatially periodic vector and scalar fields $\tilde{\mathbf{f}}(\mathbf{r})$ and $\tilde{g}(\mathbf{r})$. As a consequence of the continuity condition (6.2-2), the no-slip condition (6.2-3), and the spatially periodic nature of $\tilde{\mathbf{v}}$, it is apparent that the function $\tilde{g}(\mathbf{r})$ is restricted by the requirement that

$$\langle \tilde{g} \rangle = 0. \tag{6.2-5}$$

This condition is automatically satisfied since $\tilde{g}$ derives from the inhomogeneous term in the continuity condition in (4.6-41).

Since the number of unknowns in (6.2-1)–(6.2-4) is 3 (or 4), it would appear that one needs to solve (6.2-1)–(6.2-4) 2^{m+1} (or 3^{m+1}) separate times in order to construct $\widetilde{\mathbf{V}}^m$ and $\widetilde{\mathbf{\Pi}}^m$. The actual number is less as a consequence of the symmetric nature of $\widetilde{\mathbf{V}}^m$ (which is symmetric with respect to its last $m+1$ indices) and $\widetilde{\mathbf{\Pi}}^m$ (which is symmetric with respect to all its m indicies). As such, the number of independent unknowns in $\widetilde{\mathbf{V}}^m$ and $\widetilde{\mathbf{\Pi}}^m$ is reduced. This fact ultimately shows that the number of separate times that (6.2-1)–(6.2-4) must be solved to construct $\widetilde{\mathbf{V}}^m$ and $\widetilde{\mathbf{\Pi}}^m$ is reduced to $m+2$.

For a two-dimensional array (with perpendicular unit vectors $\mathbf{i}_1 \equiv \mathbf{i}_x$ and $\mathbf{i}_2 \equiv \mathbf{i}_y$), Table 6.1 summarizes the choices of $\tilde{\mathbf{f}}$ and $\tilde{g}$ for each of the two times that (6.2-1)–(6.2-4) must be solved in order to construct the lattice fields $\widetilde{\mathbf{V}}^0$ and $\widetilde{\mathbf{\Pi}}^0$. Similarily, the construction of $\left(\widetilde{\mathbf{V}}^1, \widetilde{\mathbf{\Pi}}^1\right)$ and $\left(\widetilde{\mathbf{V}}^2, \widetilde{\mathbf{\Pi}}^2\right)$ is summarized in Tables 6.2 and 6.3 respectively. The explicit dependence of these fields upon previously calculated ones is apparent in the choices of $\tilde{\mathbf{f}}$ and $\tilde{g}$. The symmetric properties of $\widetilde{\mathbf{V}}^m$ and $\widetilde{\mathbf{\Pi}}^m$ are also obvious from their relations to $\tilde{\mathbf{v}}$ and $\tilde{p}$.

6.2.1 Numerical Solutions of the Lattice Fields

The inhomogeneous Stokes-like problems posed by Eqs. (6.2-1)–(6.2-4) to be solved in the construction of the lattice fields $\widetilde{\mathbf{V}}^m$ and $\widetilde{\mathbf{\Pi}}^m$ are *linear* in $\tilde{\mathbf{v}}$ and $\tilde{p}$; as such, solutions exist and are unique. The solutions for $\tilde{\mathbf{v}}$ and $\tilde{p}$ were obtained for various cell geometries by use of the Galerkin finite element technique (Strang & Fix [106]).

A mesh of the cell geometry was first constructed using an inhouse mesh generator.[1] A sample mesh for a square array of circular cylinders is given in Figure C-1 (on page 206) of Appendix C.

Within each element, $\tilde{v}_1$ and $\tilde{v}_2$ were approximated using continuous biquadratic basis functions $\phi^i(x,y)$, whereas $\tilde{p}$ was approximated with continuous bilinear basis

[1] All codes used here were adapted from pre-existing codes developed by David Bornside and Prof. Brown's research group.

Solution to $\widetilde{\mathbf{V}}^0$, $\widetilde{\mathbf{\Pi}}^0$			
Problem # 1	Input	$\widetilde{f}_1$	1
		$\widetilde{f}_2$	0
		$\widetilde{g}$	0
	Solution	$\widetilde{v}_1$	$\widetilde{V}^0_{11}$
		$\widetilde{v}_2$	$\widetilde{V}^0_{21}$
		$\widetilde{p}$	$\widetilde{\Pi}^0_1$
Problem # 2	Input	$\widetilde{f}_1$	0
		$\widetilde{f}_2$	1
		$\widetilde{g}$	0
	Solution	$\widetilde{v}_1$	$\widetilde{V}^0_{12}$
		$\widetilde{v}_2$	$\widetilde{V}^0_{22}$
		$\widetilde{p}$	$\widetilde{\Pi}^0_2$

Table 6.1: The dyadic field $\widetilde{\mathbf{V}}^0$ and vector field $\widetilde{\mathbf{\Pi}}^0$ for a two-dimensional geometry can be determined from *two* linearly independent solutions of the inhomogeneous Stokes equations.

Solution to $\widetilde{\mathbf{V}}^1$, $\widetilde{\mathbf{\Pi}}^1$			
Problem # 1	Input	$\tilde{f}_1$	$\tilde{\Pi}^0_1 - 2\nabla_1 \tilde{V}^0_{11}$
		$\tilde{f}_2$	$-2\nabla_1 \tilde{V}^0_{21}$
		$\tilde{g}$	$\left\langle \tilde{V}^0_{11} \right\rangle - \tilde{V}^0_{11}$
	Solution	$\tilde{v}_1$	$\tilde{V}^1_{111}$
		$\tilde{v}_2$	$\tilde{V}^1_{211}$
		$\tilde{p}$	$\tilde{\Pi}^1_{11}$
Problem # 2	Input	$\tilde{f}_1$	$\frac{1}{2}\tilde{\Pi}^0_2 - \nabla_1 \tilde{V}^0_{12} - \nabla_2 \tilde{V}^0_{11}$
		$\tilde{f}_2$	$\frac{1}{2}\tilde{\Pi}^0_1 - \nabla_1 \tilde{V}^0_{22} - \nabla_2 \tilde{V}^0_{21}$
		$\tilde{g}$	$\frac{1}{2}\left(\left\langle \tilde{V}^0_{12} \right\rangle - \tilde{V}^0_{12} + \left\langle \tilde{V}^0_{21} \right\rangle - \tilde{V}^0_{21}\right)$
	Solution	$\tilde{v}_1$	$\tilde{V}^1_{112}$ or $\tilde{V}^1_{121}$
		$\tilde{v}_2$	$\tilde{V}^1_{212}$ or $\tilde{V}^0_{221}$
		$\tilde{p}$	$\tilde{\Pi}^1_{12}$ or $\tilde{\Pi}^1_{21}$
Problem # 3	Input	$\tilde{f}_1$	$-2\nabla_2 \tilde{V}^0_{12}$
		$\tilde{f}_2$	$\tilde{\Pi}^0_2 - 2\nabla_2 \tilde{V}^0_{22}$
		$\tilde{g}$	$\left\langle \tilde{V}^0_{22} \right\rangle - \tilde{V}^0_{22}$
	Solution	$\tilde{v}_1$	$\tilde{V}^1_{122}$
		$\tilde{v}_2$	$\tilde{V}^1_{222}$
		$\tilde{p}$	$\tilde{\Pi}^1_{22}$

Table 6.2: The triadic field $\widetilde{\mathbf{V}}^1$ and dyadic field $\widetilde{\mathbf{\Pi}}^1$ for a two-dimensional geometry can be determined from *three* linearly independent solutions of the inhomogeneous Stokes equations. The symmetries of $\widetilde{\mathbf{V}}^1$ and $\widetilde{\mathbf{\Pi}}^1$ are apparent in problem # 2.

Solution to $\widetilde{\mathbf{V}}^2$, $\widetilde{\mathbf{\Pi}}^2$			
Problem # 1	Input	$\tilde{f}_1$	$\tilde{\Pi}^1_{11} - 2\nabla_1 \tilde{V}^1_{111} - \tilde{V}^0_{11}$
		$\tilde{f}_2$	$-2\nabla_1 \tilde{V}^1_{211} - \tilde{V}^0_{21}$
		$\tilde{g}$	$\left\langle \tilde{V}^1_{111} \right\rangle - \tilde{V}^1_{111}$
	Solution	$\tilde{v}_1$	$\tilde{V}^2_{1111}$
		$\tilde{v}_2$	$\tilde{V}^2_{2111}$
		$\tilde{p}$	$\tilde{\Pi}^2_{111}$
Problem # 2	Input	$\tilde{f}_1$	$\frac{2}{3}\tilde{\Pi}^1_{12} - \frac{4}{3}\nabla_1 \tilde{V}^1_{112} - \frac{2}{3}\nabla_2 \tilde{V}^1_{111} - \frac{1}{3}\tilde{V}^0_{12}$
		$\tilde{f}_2$	$\frac{1}{3}\tilde{\Pi}^1_{11} - \frac{4}{3}\nabla_1 \tilde{V}^1_{212} - \frac{2}{3}\nabla_2 \tilde{V}^1_{211} - \frac{1}{3}\tilde{V}^0_{22}$
		$\tilde{g}$	$\frac{2}{3}\left(\left\langle \tilde{V}^1_{112} \right\rangle - \tilde{V}^1_{112}\right) + \frac{1}{3}\left(\left\langle \tilde{V}^1_{211} \right\rangle - \tilde{V}^1_{211}\right)$
	Solution	$\tilde{v}_1$	$\tilde{V}^2_{1112}$ or $\tilde{V}^2_{1121}$ or $\tilde{V}^2_{1211}$
		$\tilde{v}_2$	$\tilde{V}^2_{2112}$ or $\tilde{V}^2_{2121}$ or $\tilde{V}^2_{2211}$
		$\tilde{p}$	$\tilde{\Pi}^2_{112}$ or $\tilde{\Pi}^2_{121}$ or $\tilde{\Pi}^2_{211}$
Problem # 3	Input	$\tilde{f}_1$	$\frac{1}{3}\tilde{\Pi}^1_{22} - \frac{4}{3}\nabla_2 \tilde{V}^1_{112} - \frac{2}{3}\nabla_1 \tilde{V}^1_{122} - \frac{1}{3}\tilde{V}^0_{11}$
		$\tilde{f}_2$	$\frac{2}{3}\tilde{\Pi}^1_{12} - \frac{4}{3}\nabla_2 \tilde{V}^1_{212} - \frac{2}{3}\nabla_1 \tilde{V}^1_{222} - \frac{1}{3}\tilde{V}^0_{21}$
		$\tilde{g}$	$\frac{2}{3}\left(\left\langle \tilde{V}^1_{212} \right\rangle - \tilde{V}^1_{212}\right) + \frac{1}{3}\left(\left\langle \tilde{V}^1_{122} \right\rangle - \tilde{V}^1_{122}\right)$
	Solution	$\tilde{v}_1$	$\tilde{V}^2_{1122}$ or $\tilde{V}^2_{1212}$ or $\tilde{V}^2_{1221}$
		$\tilde{v}_2$	$\tilde{V}^2_{2122}$ or $\tilde{V}^2_{2212}$ or $\tilde{V}^2_{2221}$
		$\tilde{p}$	$\tilde{\Pi}^2_{122}$ or $\tilde{\Pi}^2_{212}$ or $\tilde{\Pi}^2_{221}$
Problem # 4	Input	$\tilde{f}_1$	$-2\nabla_2 \tilde{V}^1_{122} - \tilde{V}^0_{12}$
		$\tilde{f}_2$	$\tilde{\Pi}^1_{22} - 2\nabla_2 \tilde{V}^1_{222} - \tilde{V}^0_{22}$
		$\tilde{g}$	$\left\langle \tilde{V}^1_{222} \right\rangle - \tilde{V}^1_{222}$
	Solution	$\tilde{v}_1$	$\tilde{V}^2_{1222}$
		$\tilde{v}_2$	$\tilde{V}^2_{2222}$
		$\tilde{p}$	$\tilde{\Pi}^2_{222}$

Table 6.3: The tetradic field $\widetilde{\mathbf{V}}^2$ and triadic field $\widetilde{\mathbf{\Pi}}^2$ for a two-dimensional geometry can be determined from *four* linearly independent solutions of the inhomogeneous Stokes equations. The symmetries of $\widetilde{\mathbf{V}}^2$ and $\widetilde{\mathbf{\Pi}}^2$ are apparent in problems # 2 and 3. The symmetries of $\widetilde{\mathbf{V}}^1$ and $\widetilde{\mathbf{\Pi}}^1$ have been considered in determining $\tilde{\mathbf{f}}$ and $\tilde{\mathbf{g}}$ for problems # 2 and 3.

functions $\psi^i(x,y)$. Within an element, the solution was approximated as

$$\begin{aligned}\widetilde{v}_1 &= \sum_{i=1}^{9} v_1^{(i)}\phi^i(x,y),\\ \widetilde{v}_2 &= \sum_{i=1}^{9} v_2^{(i)}\phi^i(x,y),\\ \widetilde{p} &= \sum_{i=1}^{3} p^{(i)}\psi^i(x,y),\end{aligned}$$

where $\mathbf{v}^{(i)}$ is the value of the approximation to $\widetilde{\mathbf{v}}$ at the ith biquadrtic node, while $p^{(i)}$ is the approximation to $\widetilde{p}$ at the ith bilinear node of a given element.

The code was adjusted to account for multiple pairs of spatially periodic boundaries. The code used to compute the resuduals at each node was adjusted to include the inhomogeneous forcing functions $\widetilde{\mathbf{f}}$ and $\widetilde{g}$. These additional contributions appear in the weak forms of (6.2-1) and (6.2-2). To generate the weak form of (6.2-1), dot multiply this equation with the vector $\mathbf{\Phi} = \mathbf{i}_j\phi^i$ $(j = 1,2)$, integrate over the fluid domain, and use the divergence theorem to obtain

$$\int_{\tau_f} -\mu\left(\boldsymbol{\nabla}\mathbf{\Phi}\right)^{\dagger} : \boldsymbol{\nabla}\widetilde{\mathbf{v}} + \widetilde{p}\boldsymbol{\nabla}\cdot\mathbf{\Phi} - \mathbf{\Phi}\cdot\widetilde{\mathbf{f}}\,\mathrm{d}^3\mathbf{r} + \oint_{\partial\tau_0+s_p} \mathrm{d}\mathbf{S}\cdot\left[\mu\left(\boldsymbol{\nabla}\widetilde{\mathbf{v}}\right)\cdot\mathbf{\Phi} - \mathbf{\Phi}\widetilde{p}\right] = 0.$$

In the preceding equation, the integral over s_p vanishes as a result of the essential condition (6.2-3), while the integral over $\partial\tau_0$ vanishes as a result of the spatially periodic nature of $\widetilde{\mathbf{v}}$ and $\mathbf{\Phi}$; hence, the weak form of (6.2-1) is[2]

$$\int_{\tau_f} \left(\boldsymbol{\nabla}\mathbf{\Phi}\right)^{\dagger} : \boldsymbol{\nabla}\widetilde{\mathbf{v}} - \widetilde{p}\boldsymbol{\nabla}\cdot\mathbf{\Phi} + \mathbf{\Phi}\cdot\widetilde{\mathbf{f}}\,\mathrm{d}^3\mathbf{r} = 0.$$

[2]Care should be taken when rewriting this relation in terms of the stress,

$$\widetilde{\mathbf{P}} = -\mathbf{I}\widetilde{p} + \mu\left[\boldsymbol{\nabla}\widetilde{\mathbf{v}} + {}^{\dagger}(\boldsymbol{\nabla}\widetilde{\mathbf{v}})\right]$$

because $\widetilde{\mathbf{v}}$ is not divergence free. As a result, the weak form of (6.2-1) possesses the equivalent form

$$\int_{\tau_f} \left(\boldsymbol{\nabla}\mathbf{\Phi}\right) : \widetilde{\mathbf{P}} + \mathbf{\Phi}\cdot\left(\widetilde{\mathbf{f}} + \boldsymbol{\nabla}\widetilde{g}\right)\,\mathrm{d}^3\mathbf{r} = 0.$$

n	Elements	$\overline{\overline{V}}^0_{1111}/\tau_0$	$\overline{P}^1_{1111}/\tau_0$	$\overline{V}^2_{1111}/\tau_0^2$
2	32	$-1.92922486 \times 10^{-2}$	$2.68448625 \times 10^{-2}$	$-1.20911403 \times 10^{-3}$
4	128	$-1.93871719 \times 10^{-2}$	$2.51720185 \times 10^{-2}$	$-1.21950257 \times 10^{-3}$
6	288	$-1.94014973 \times 10^{-2}$	$2.50671065 \times 10^{-2}$	$-1.22044396 \times 10^{-3}$
8	512	$-1.94049012 \times 10^{-2}$	$2.50602513 \times 10^{-2}$	$-1.22066585 \times 10^{-3}$
10	800	$-1.94060679 \times 10^{-2}$	$2.50646935 \times 10^{-2}$	$-1.22074187 \times 10^{-3}$
12	1152	$-1.94065713 \times 10^{-2}$	$2.50697386 \times 10^{-2}$	$-1.22077461 \times 10^{-3}$
14	1568	$-1.94068242 \times 10^{-2}$	$2.50738757 \times 10^{-2}$	$-1.22079102 \times 10^{-3}$
16	2048	$-1.94069663 \times 10^{-2}$	$2.50770839 \times 10^{-2}$	$-1.22080022 \times 10^{-3}$

Table 6.4: Dependence of some lattice constants upon mesh size. These are for circular cylinders in a square array of concentration $\phi = 0.2$. The meshes were constructed of 8 similar regions consisting of $n \times n$ elements within each region. All subsequent results were obtained with $n = 10$.

Similarily, multiply the continuity condition by ψ^i and integrate over τ_f to obtain the weak form of (6.2-2):

$$\int_{\tau_f} (\boldsymbol{\nabla} \cdot \tilde{\mathbf{v}} - \tilde{g})\, \psi^i \, \mathrm{d}^3\mathbf{r} = 0.$$

The solution of Eqs. (6.2-1)–(6.2-4), for the mesh shown in Figure C-1, takes roughly 4.5 minutes to compute on an HP735 Apollo. Since the analytic problem is linear, well-posed, and possesses a unique solution for given functions $\tilde{\mathbf{f}}$ and $\tilde{g}$, Newton's method converges in a single step. To check the numerical solution, various analytical functions for $\tilde{\mathbf{v}}$ and $\tilde{p}$ were chosen which satisfied condition (6.2-3). The corresponding analytical forms of $\tilde{\mathbf{f}}$ and $\tilde{g}$ were then obtained directly from (6.2-1) and (6.2-2). These same inhomogeneities were then used as data, from which numerical fields ere calculated. These numerical solutions were then compared compared with their original analytical counterparts.

Simulations were done with various mesh sizes in order to determine the accuracy of the solutions. The effect of mesh size upon typical constants appearing in the circular cylinder solution (see § 6.3.1) is shown in Table 6.4. All subsequent computations were performed using a mesh consisting of 800 elements.

6.2.2 Square Array of Circular Cylinders

The lattice fields within a porous medium composed of circular cylinders arranged on a square lattice were determined by the procedure outlined in Tables 6.1–6.3. Solutions of the first three cell problems (for a volume fraction of $\phi = 0.2$) are presented in Figures C-2–C-28 in Appendix C. Because of the symmetric nature of the array, these fields are invariant to interchanging the x- and y-directions. This is apparent, for example, upon comparing the results for $\widetilde{V}^2_{1222}$ (Figure C-20, page 225) and $\widetilde{V}^2_{2111}$ (Figure C-21, page 226). The relationship between these lattice fields and the physical microscale velocity $\mathbf{v}(\mathbf{R})$ and pressure $p(\mathbf{R})$ fields can be obtained directly from the microscale solutions (4.6-39) and (4.6-40), along with appropriate choices for the constant tensors $\overline{\mathbf{\Psi}}^n$.

6.2.3 Square Array of Elliptical Cylinders

Similar lattice fields were also calculated for a porous medium composed of elliptical cylinders arranged in a square array. A typical mesh corresponding to a volume fraction of $\phi = 0.2$ and eccentricity $e = 2$ (where e is the ratio of major to minor axis lengths) can be found in Figure D-1 on page 236 of Appendix D. Lattice fields corresponding to this mesh are shown in Figures D-2–D-28. Unlike the array of circular cylinders, this array is not invariant upon interchanging x and y. As such, the lattice fields for elliptical arrays do not have the symmetries mentioned previously for cylindrical arrays. Compare, for instance, the results for $\widetilde{V}^2_{1222}$ (Figure D-20, page 255) and $\widetilde{V}^2_{2111}$ (Figure D-21, page 256). Among other things, whereas the permeability is isotropic for the circular cylinders, it is anisotropic for the elliptical cylinders.

6.3 Macroscale Results for Two-dimensional Arrays

With the microscale lattice fields computed, the phenomenological coefficients appearing in the various expressions for the macroscale deviatoric stress, stress pseudovector, and external force may now be computed. These expressions related $\overline{\mathbf{T}}^s$, $\overline{\mathbf{P}}_\times$ and $\overline{\mathbf{F}}^{(e)}$ to the macroscale velocity and its gradients as follows:

$$\overline{\mathbf{T}}^s = \mu\left[\overline{\mathbf{K}}^{(l)}\cdot\overline{\mathbf{v}}+\overline{\mathbf{K}}^{(r)}\cdot\overline{\boldsymbol{\omega}}+\overline{\mathbf{K}}^{(s)}:\overline{\mathbf{S}}\right], \tag{6.3-1}$$

$$\overline{\mathbf{P}}_\times = \mu\left[\overline{\mathbf{c}}^{(l)}\cdot\overline{\mathbf{v}}+\overline{\mathbf{c}}^{(r)}\cdot\overline{\boldsymbol{\omega}}+\overline{\mathbf{c}}^{(s)}:\overline{\mathbf{S}}\right], \tag{6.3-2}$$

$$\overline{\mathbf{F}}^{(e)} = -\mu\mathbf{k}^{-1}\cdot\overline{\mathbf{v}}+\mu\overline{\boldsymbol{\nabla}}\cdot\left[\overline{\mathbf{f}}^{(l)}\cdot\overline{\mathbf{v}}+\overline{\mathbf{f}}^{(r)}\cdot\overline{\boldsymbol{\omega}}+\overline{\mathbf{f}}^{(s)}:\overline{\mathbf{S}}\right], \tag{6.3-3}$$

these being obtained from (5.4-20), (5.4-28) and (5.5-20) respectively. The various coefficients appearing in the previous equations are derived from the constant geometric tensors $\left(\overline{\mathbf{V}}^0,\overline{\mathbf{P}}^0,\overline{\overline{\mathbf{V}}}^0\right)$, $\left(\overline{\mathbf{V}}^1,\overline{\mathbf{P}}^1\right)$ and $\overline{\mathbf{V}}^2$, determined from the zeroth-, first- and second-order cell problems.

In two-dimensional arrays, the stress pseudovector $\overline{\mathbf{P}}_\times$ and macroscale vorticity vector $\overline{\boldsymbol{\omega}}$ are oriented in a direction perpendicular to $\mathbf{i}_1$ and $\mathbf{i}_2$, i.e. in the $\mathbf{i}_3 \equiv \mathbf{i}_z$ direction. As such, the constants coupling them are at most of the form

$$\begin{aligned}
\overline{K}^{(r)}_{ijk} &\equiv \overline{K}^{(r)}_{ij3},\\
\overline{c}^{(l)}_{ij} &\equiv \overline{c}^{(l)}_{3j},\\
\overline{c}^{(r)}_{ij} &\equiv \overline{c}^{(r)}_{33},\\
\overline{c}^{(s)}_{ijk} &\equiv \overline{c}^{(s)}_{3jk},\\
\overline{f}^{(r)}_{ijk} &\equiv \overline{f}^{(r)}_{ij3}
\end{aligned}$$

if they are nonzero at all.

6.3.1 Square Array of Circular Cylinders

A porous medium composed of circular cylinders arranged on a square lattice is invariant to either reflection about $\mathbf{i}_1$ or $\mathbf{i}_2$, or rotation through 90 degrees; hence, most of the phenomenological coefficients appearing in Eqs. (6.3-1) to (6.3-3) are identically zero. Various volume fractions ϕ were studied, with a typical unit cell for $\phi = 0.2$ shown in Figure C-1 (on page 206) of Appendix C. The geometric constant tensors for this type of array were found to be of the form

$$
\begin{aligned}
\overline{\mathbf{V}}^0 &= (\mathbf{i}_1\mathbf{i}_1 + \mathbf{i}_2\mathbf{i}_2)\,\overline{V}^0_{11}, \\
\overline{\mathbf{P}}^0 &= \mathbf{0}, \\
\overline{\overline{\mathbf{V}}}^0 &= (\mathbf{i}_1\mathbf{i}_1\mathbf{i}_1\mathbf{i}_1 + \mathbf{i}_2\mathbf{i}_2\mathbf{i}_2\mathbf{i}_2)\,\overline{\overline{V}}^0_{1111} + (\mathbf{i}_1\mathbf{i}_2\mathbf{i}_2\mathbf{i}_1 + \mathbf{i}_2\mathbf{i}_1\mathbf{i}_1\mathbf{i}_2)\,\overline{\overline{V}}^0_{1221}, \\
\overline{\mathbf{V}}^1 &= \mathbf{0}, \\
\overline{\mathbf{P}}^1 &= (\mathbf{i}_1\mathbf{i}_1\mathbf{i}_1\mathbf{i}_1 + \mathbf{i}_2\mathbf{i}_2\mathbf{i}_2\mathbf{i}_2)\,\overline{P}^1_{1111} + (\mathbf{i}_1\mathbf{i}_1\mathbf{i}_2\mathbf{i}_2 + \mathbf{i}_2\mathbf{i}_2\mathbf{i}_1\mathbf{i}_1)\,\overline{P}^1_{1122} \\
&\quad + (\mathbf{i}_1\mathbf{i}_2\mathbf{i}_1\mathbf{i}_2 + \mathbf{i}_1\mathbf{i}_2\mathbf{i}_2\mathbf{i}_1 + \mathbf{i}_2\mathbf{i}_1\mathbf{i}_1\mathbf{i}_2 + \mathbf{i}_2\mathbf{i}_1\mathbf{i}_2\mathbf{i}_1)\,\overline{P}^1_{1212}, \\
\overline{\mathbf{V}}^2 &= (\mathbf{i}_1\mathbf{i}_1\mathbf{i}_1\mathbf{i}_1 + \mathbf{i}_2\mathbf{i}_2\mathbf{i}_2\mathbf{i}_2)\,\overline{V}^2_{1111} \\
&\quad + (\mathbf{i}_1\mathbf{i}_1\mathbf{i}_2\mathbf{i}_2 + \mathbf{i}_1\mathbf{i}_2\mathbf{i}_1\mathbf{i}_2 + \mathbf{i}_1\mathbf{i}_2\mathbf{i}_2\mathbf{i}_1 + \mathbf{i}_2\mathbf{i}_1\mathbf{i}_1\mathbf{i}_2 + \mathbf{i}_2\mathbf{i}_1\mathbf{i}_2\mathbf{i}_1 + \mathbf{i}_2\mathbf{i}_2\mathbf{i}_1\mathbf{i}_1)\,\overline{V}^2_{1122}.
\end{aligned}
$$

Since $\overline{\mathbf{V}}^0$ can be formed from $\overline{\overline{\mathbf{V}}}^0$ (basically $\overline{V}^0_{ij} = \overline{\overline{V}}^0_{ikjk}$, such that for this array, $\overline{V}^0_{11} = \overline{\overline{V}}^0_{1111}$) the macroscale phenomenological coefficients depend at most upon seven constants. The values of these constants for various volume fractions are shown in Table 6.5. As a result of the forms of these tensors, the constants appearing in the relationship for the macroscale symmetric deviatoric stress (6.3-1) and computed from (5.3-18), (5.4-21), (5.4-22) and (5.4-23), have the forms[3]

$$
\overline{\mathbf{K}}^{(l)} = \mathbf{0},
$$

[3]Note that since the macroscale rate-of-strain $\overline{\mathbf{S}}$ is traceless (as a result of continuity, i.e. $\overline{\boldsymbol{\nabla}}\cdot\overline{\mathbf{v}} = 0$) $\overline{\mathbf{K}}^{(s)}$ has the equivalent representation

$$
\overline{\mathbf{K}}^{(s)} = 2\,(\mathbf{i}_1\mathbf{i}_1\mathbf{i}_1\mathbf{i}_1 + \mathbf{i}_2\mathbf{i}_2\mathbf{i}_2\mathbf{i}_2)\,K^s_1 + (\mathbf{i}_1\mathbf{i}_2\mathbf{i}_1\mathbf{i}_2 + \mathbf{i}_1\mathbf{i}_2\mathbf{i}_2\mathbf{i}_1 + \mathbf{i}_2\mathbf{i}_1\mathbf{i}_1\mathbf{i}_2 + \mathbf{i}_2\mathbf{i}_1\mathbf{i}_2\mathbf{i}_1)\,K^s_3.
$$

ϕ	0.05	0.2	0.4	0.6
$\overline{\overline{V}}^0_{1111}/\tau_0$	-6.426×10^{-2}	-1.941×10^{-2}	-4.589×10^{-3}	-5.670×10^{-4}
$\overline{\overline{V}}^0_{1221}/\tau_0$	-1.019×10^{-1}	-4.503×10^{-2}	-1.667×10^{-2}	-3.764×10^{-3}
$\overline{P}^1_{1111}/\tau_0$	2.978×10^{-2}	2.506×10^{-2}	2.620×10^{-2}	2.326×10^{-2}
$\overline{P}^1_{1122}/\tau_0$	3.243×10^{-2}	9.378×10^{-3}	-1.062×10^{-2}	-2.222×10^{-2}
$\overline{P}^1_{1212}/\tau_0$	4.541×10^{-2}	2.136×10^{-2}	7.847×10^{-3}	1.819×10^{-3}
$\overline{V}^2_{1111}/\tau_0^2$	-5.681×10^{-3}	-1.221×10^{-3}	-2.777×10^{-4}	-4.007×10^{-5}
$\overline{V}^2_{1122}/\tau_0^2$	1.424×10^{-3}	6.650×10^{-4}	1.546×10^{-4}	1.711×10^{-5}

Table 6.5: Non-zero components of the geometric constant tensors determined for a square array of circular cylinders at different volume fractions.

$$\begin{aligned}
\overline{\mathbf{K}}^{(r)} &= \mathbf{0}, \\
\overline{\mathbf{K}}^{(s)} &= (\mathbf{i}_1\mathbf{i}_1\mathbf{i}_1\mathbf{i}_1 + \mathbf{i}_2\mathbf{i}_2\mathbf{i}_2\mathbf{i}_2 - \mathbf{i}_1\mathbf{i}_1\mathbf{i}_2\mathbf{i}_2 - \mathbf{i}_2\mathbf{i}_2\mathbf{i}_1\mathbf{i}_1)\, K_1^s \\
&\quad + (\mathbf{i}_1\mathbf{i}_2\mathbf{i}_1\mathbf{i}_2 + \mathbf{i}_1\mathbf{i}_2\mathbf{i}_2\mathbf{i}_1 + \mathbf{i}_2\mathbf{i}_1\mathbf{i}_1\mathbf{i}_2 + \mathbf{i}_2\mathbf{i}_1\mathbf{i}_2\mathbf{i}_1)\, K_3^s. \qquad (6.3\text{-}4)
\end{aligned}$$

The constants appearing in the expression for the macroscale stress pseudovector (6.3-2), which computed from (5.3-21), (5.4-29), (5.4-30) and (5.4-31), are all identically zero for this type of geometry:

$$\begin{aligned}
\overline{\mathbf{c}}^{(l)} &= \mathbf{0}, \\
\overline{\mathbf{c}}^{(r)} &= \mathbf{0}, \\
\overline{\mathbf{c}}^{(s)} &= \mathbf{0}.
\end{aligned}$$

Finally, the constants appearing in the expression for the macroscale external volumetric body force density (6.3-3) and computed from (5.3-40), (5.4-37), (5.5-19), (5.5-21) and (5.5-22) are of the forms

$$\mathbf{k} = (\mathbf{i}_1\mathbf{i}_1 + \mathbf{i}_2\mathbf{i}_2)\, k \qquad (6.3\text{-}5)$$

and

$$\begin{aligned}
\overline{\mathbf{f}}^{(l)} &= \mathbf{0}, \\
\overline{\mathbf{f}}^{(r)} &= \mathbf{0}, \\
\overline{\mathbf{f}}^{(s)} &= (\mathbf{i}_1\mathbf{i}_1\mathbf{i}_1\mathbf{i}_1 + \mathbf{i}_2\mathbf{i}_2\mathbf{i}_2\mathbf{i}_2)\, f_1^s \\
&\quad + (\mathbf{i}_1\mathbf{i}_1\mathbf{i}_2\mathbf{i}_2 + \mathbf{i}_1\mathbf{i}_2\mathbf{i}_1\mathbf{i}_2 + \mathbf{i}_1\mathbf{i}_2\mathbf{i}_2\mathbf{i}_1 + \mathbf{i}_2\mathbf{i}_1\mathbf{i}_1\mathbf{i}_2 + \mathbf{i}_2\mathbf{i}_1\mathbf{i}_2\mathbf{i}_1 + \mathbf{i}_2\mathbf{i}_2\mathbf{i}_1\mathbf{i}_1)\, f_3^s.
\end{aligned} \tag{6.3-6}$$

Of the original seven parameters ($\overline{\overline{V}}^0_{1111}$, $\overline{\overline{V}}^0_{1221}$, $\overline{P}^1_{1111}$, $\overline{P}^1_{1122}$, $\overline{P}^1_{1212}$, $\overline{V}^2_{1111}$ and $\overline{V}^2_{1122}$) characterizing the geometric constant tensors, they appear in only 5 different groupings (k, K_1^s, K_3^s, f_1^s and f_3^s) in order to characterize the macroscale relationships (6.3-1)–(6.3-2) for this square array of circular cylinders.

The permeability for this square array of circular cylinders is isotropic, and a plot of k as a function of volume concentration is shown in Figure 6-1. Deviations between the permeability calculated here and that calculated by others (Sangani & Acrivos [95], Edwards *et al.* [47]) is less than 3%. As expected, the permeability decreases with increasing volume fraction.

For a square array of circular cylinders, the form of the constants appearing in (6.3-1)–(6.3-3), along with the definitions (5.2-18) and (5.2-23), show that the macroscale stress tensor (up to and including gradients of $\overline{\mathbf{v}}$) takes the form

$$\overline{\mathbf{P}} = -\mathbf{I}\overline{p} + \mu\overline{\mathbf{K}}^{(s)} : \overline{\mathbf{S}}. \tag{6.3-7}$$

This is similar to (5.2-13) for an incompressible newtonian fluid; however, the viscous-type tetradic $\overline{\mathbf{K}}^{(s)}$—coupling the macroscale stress to the macroscale symmetric rate-of-strain—is now characterized by two (dimensionless) geometric constants K_1^s and K_3^s. The presence of two constants characterizing $\overline{\mathbf{K}}^{(s)}$ also arises in the *suspension* case [125], where the no-slip condition is replaced by a stress-free condition. Note that the macroscale stress is symmetric. There is no external body couple acting on the cyllinders in the array. Furthermore, contributions to this symmetric stress

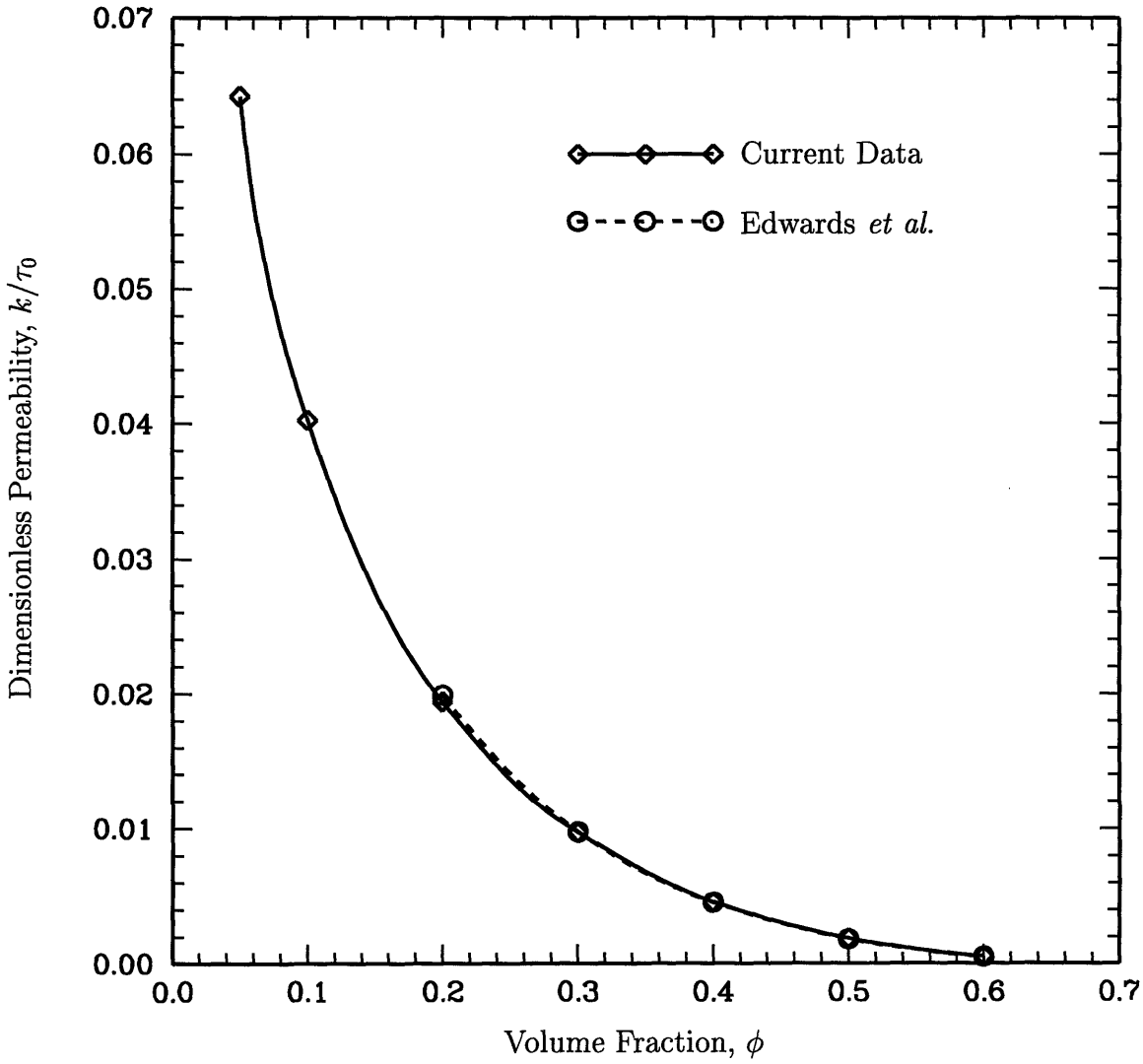

Figure 6-1: Permeability as a function of volume fraction for a square array of circular cylinders.

tensor and scaling with either $\overline{\mathbf{v}}$ or $\overline{\boldsymbol{\omega}}$ are absent. The values of K_1^s and K_3^s as a function of volume concentration are shown in Figure 6-2. The value of K_1^s decrease from $K_1^s \simeq 1.0$ at $\phi = 0.05$ to $K_1^s \simeq -40$ at $\phi = 0.6$. On the other hand, K_3^s remains roughly constant at a value of $K_3^s \simeq 0.6$, independent of ϕ.

The two coefficients f_1^s and f_3^s, characterizing the other non-zero constant $\overline{\mathbf{f}}^{(s)}$ in the external body force density (6.3-3), are shown in Figure 6-3. The coefficient f_1^s increases from 0.5 to 160 while f_3^s decreases from -0.5 to -67 as the volume fraction of particles is increased from 0.1 to 0.6. The general form of the momentum equation (5.5-26), accurate to order $\overline{\nabla}\,\overline{\nabla}\,\overline{\mathbf{v}}$ and written for this porous medium geometry, becomes

$$\frac{1}{\mu}\overline{\nabla}\,\overline{p} = -\mathbf{k}^{-1}\cdot\overline{\mathbf{v}} + \frac{1}{\mu}\overline{\boldsymbol{\mu}}^{*}\!:\!\overline{\nabla}\,\overline{\nabla}\,\overline{\mathbf{v}}. \tag{6.3-8}$$

As a result of the forms of $\overline{\mathbf{K}}^{(s)}$ and $\overline{\mathbf{f}}^{(s)}$, the effective 'viscosity' has the form

$$\begin{aligned}\frac{1}{\mu}\overline{\boldsymbol{\mu}}^{*} &= (\mathbf{i}_1\mathbf{i}_1\mathbf{i}_1\mathbf{i}_1 + \mathbf{i}_2\mathbf{i}_2\mathbf{i}_2\mathbf{i}_2)\,\alpha' + (\mathbf{i}_1\mathbf{i}_1\mathbf{i}_2\mathbf{i}_2 + \mathbf{i}_2\mathbf{i}_2\mathbf{i}_1\mathbf{i}_1)\,\beta \\ &\quad + (\mathbf{i}_1\mathbf{i}_2\mathbf{i}_1\mathbf{i}_2 + \mathbf{i}_1\mathbf{i}_2\mathbf{i}_2\mathbf{i}_1 + \mathbf{i}_2\mathbf{i}_1\mathbf{i}_1\mathbf{i}_2 + \mathbf{i}_2\mathbf{i}_1\mathbf{i}_2\mathbf{i}_1)\,\gamma.\end{aligned}$$

As this tetradic is to be contracted with the triadic $\overline{\nabla}\,\overline{\nabla}\,\overline{\mathbf{v}}$, which is traceless with respect to its last two and first and last indices, $\overline{\boldsymbol{\mu}}^{*}$ can be expressed in the more compact form

$$\frac{1}{\mu}\overline{\boldsymbol{\mu}}^{*} = (\mathbf{i}_1\mathbf{i}_1\mathbf{i}_1\mathbf{i}_1 + \mathbf{i}_2\mathbf{i}_2\mathbf{i}_2\mathbf{i}_2)\,\alpha + \mathbf{II}\beta, \tag{6.3-9}$$

where

$$\alpha \overset{\text{def}}{=} \alpha' - \beta - 2\gamma. \tag{6.3-10}$$

The constants α and β are plotted in Figure 6-4. Note that the momentum equation does not require a contribution from $\overline{\nabla}\,\overline{\mathbf{v}}$, since the constants $\overline{\mathbf{K}}^{(l)}$, $\overline{\mathbf{c}}^{(l)}$ and $\overline{\mathbf{f}}^{(l)}$ are all identically zero for this geometry.

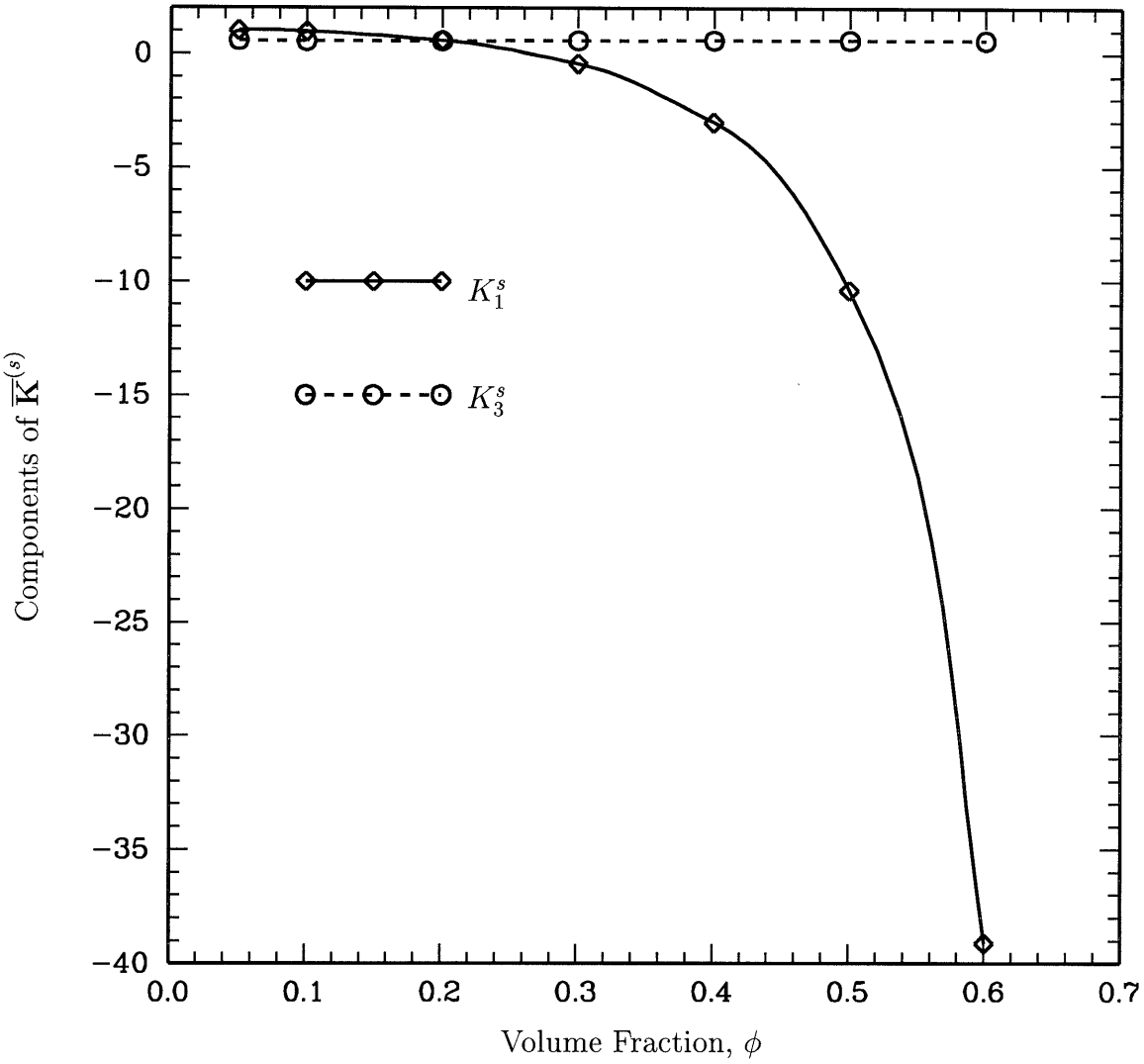

Figure 6-2: The components K_1^s and K_3^s as a function of particle volume fraction, ϕ for a square array of circular cylinders. These components characterize the constant tensor $\overline{\mathbf{K}}^{(s)}$ which couples the macroscale symmetric rate-of-strain $\overline{\mathbf{S}}$ to the macroscale stress $\overline{\mathbf{P}}$.

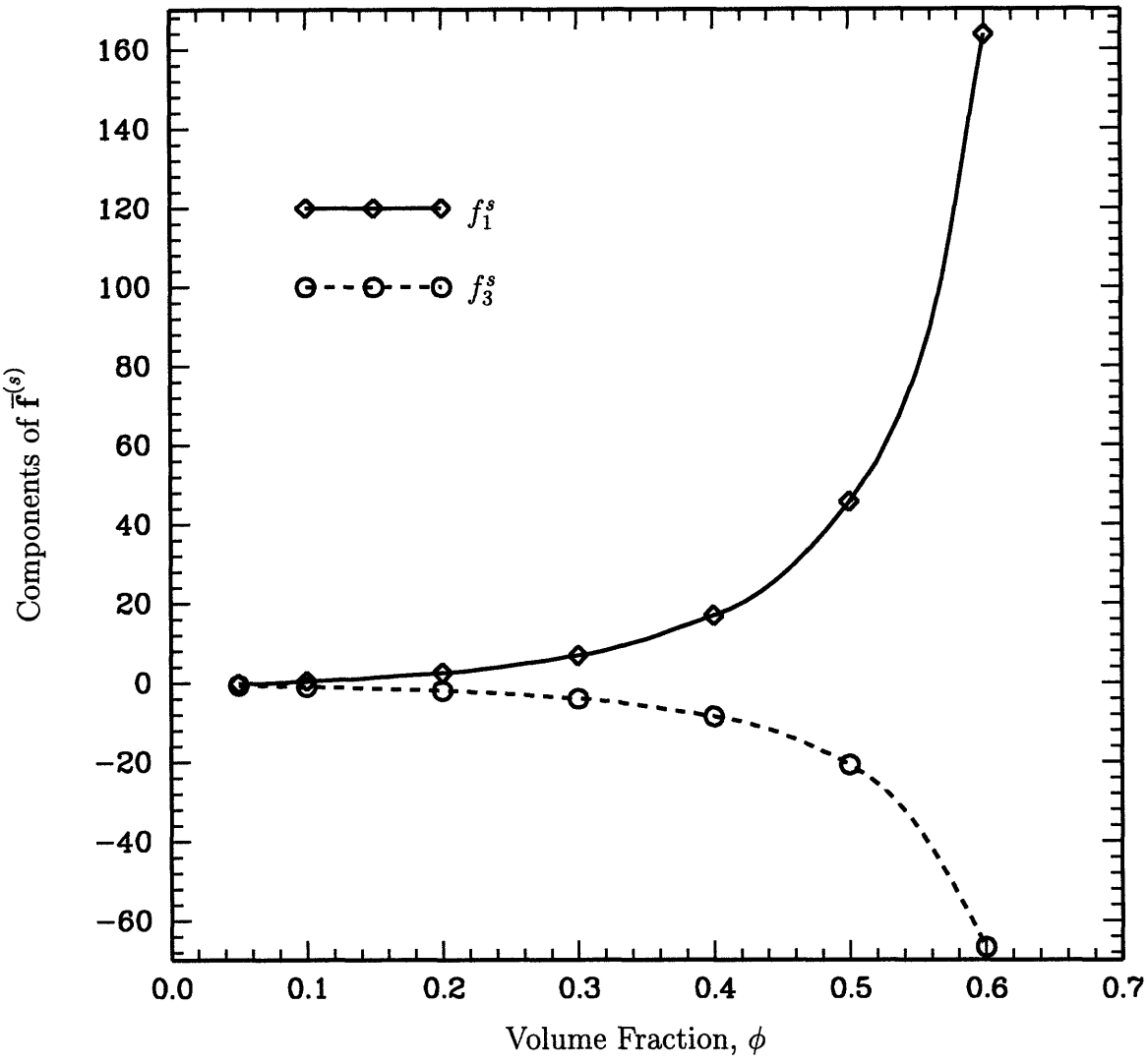

Figure 6-3: The components f_1^s and f_3^s as a function of particle volume fraction, ϕ for a square array of circular cylinders. These components characterize the constant tensor $\overline{\mathbf{f}}^{(s)}$, which couples gradients in the macroscale symmetric rate-of-strain $\overline{\mathbf{S}}$ to the external body force density $\overline{\mathbf{F}}^{(e)}$.

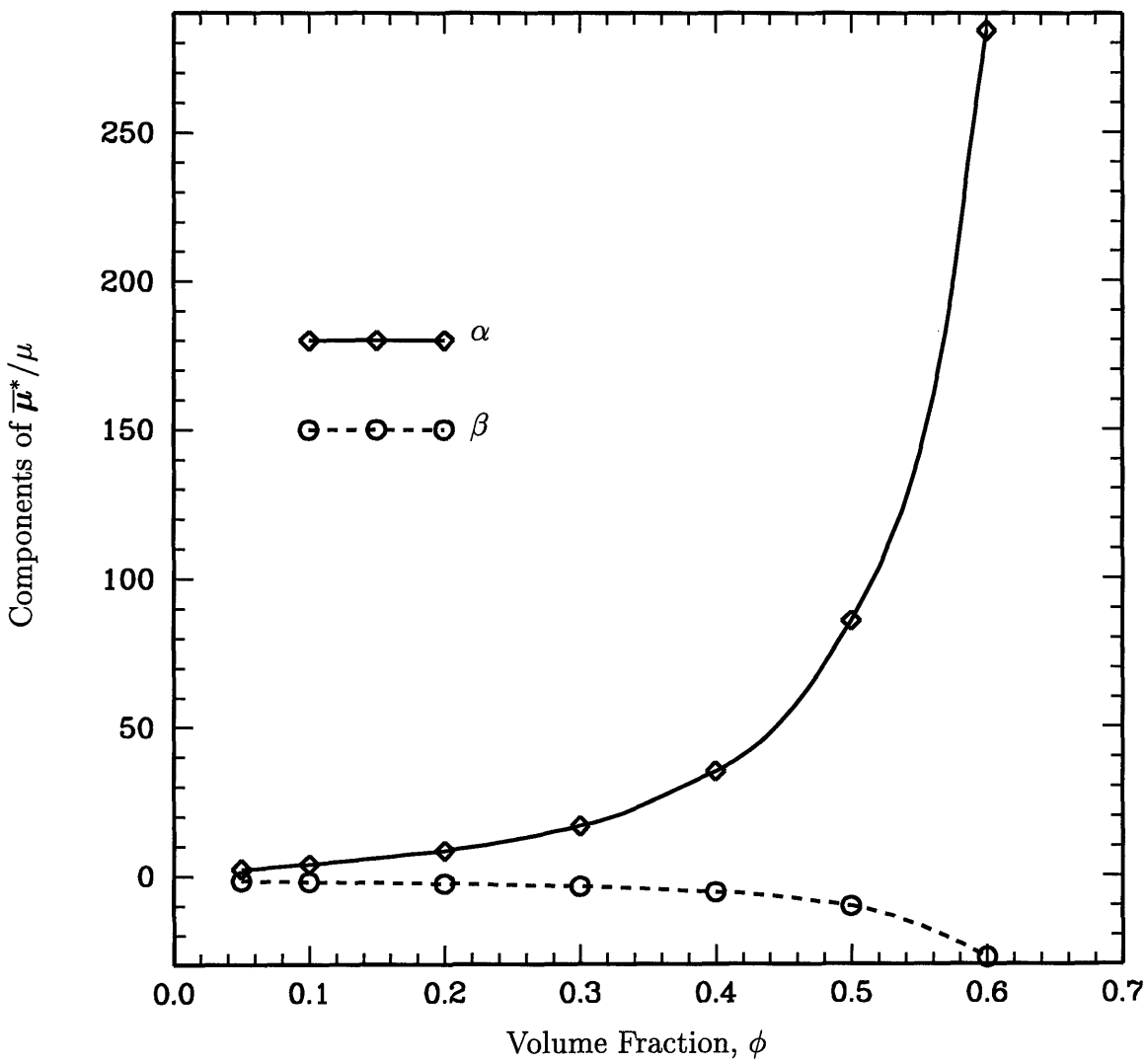

Figure 6-4: The components α and β as a function of particle volume fraction ϕ for a square array of circular cylinders. These components characterize the effective viscosity tetradic, which couples second-order gradients of the macroscale velocity to the macroscale pressure drop.

6.3.2 Square Array of Elliptical Cylinder

Results are presented in this section for a porous medium composed of elliptical cylinders and arranged on a square lattice. Because of the shapes of the elliptical particles, the macroscale material tensors cannot be isotropic. Consequently, the phenomenological coefficients appearing in Eqs. (6.3-1) to (6.3-3) will possess a more complex structure than their circular counterparts. In the subsequent computations, the volume fraction was kept constant at $\phi = 0.2$ and the eccentricity e of the ellipse allowed to vary up to a maximum of 2.0. A typical unit cell with $e = 2.0$ is shown in Figure D-1 on page 236 of Appendix D. The major axis is parallel to $\mathbf{i}_1$ and the minor axis parallel to $\mathbf{i}_2$. As a result of the loss of a symmetry axes, the geometric constant tensors were found to be of the forms

$$
\begin{aligned}
\overline{\mathbf{V}}^0 &= \mathbf{i}_1\mathbf{i}_1\overline{V}^0_{11} + \mathbf{i}_2\mathbf{i}_2\overline{V}^0_{22}, \\
\overline{\mathbf{P}}^0 &= \mathbf{0}, \\
\overline{\overline{\mathbf{V}}}^0 &= \mathbf{i}_1\mathbf{i}_1\mathbf{i}_1\mathbf{i}_1\overline{\overline{V}}^0_{1111} + \mathbf{i}_2\mathbf{i}_2\mathbf{i}_2\mathbf{i}_2\overline{\overline{V}}^0_{2222} + \mathbf{i}_1\mathbf{i}_2\mathbf{i}_2\mathbf{i}_1\overline{\overline{V}}^0_{1221} + \mathbf{i}_2\mathbf{i}_1\mathbf{i}_1\mathbf{i}_2\overline{V}^0_{2112}, \\
\overline{\mathbf{V}}^1 &= \mathbf{0}, \\
\overline{\mathbf{P}}^1 &= \mathbf{i}_1\mathbf{i}_1\mathbf{i}_1\mathbf{i}_1\overline{P}^1_{1111} + \mathbf{i}_2\mathbf{i}_2\mathbf{i}_2\mathbf{i}_2\overline{P}^1_{2222} + \mathbf{i}_1\mathbf{i}_1\mathbf{i}_2\mathbf{i}_2\overline{P}^1_{1122} + \mathbf{i}_2\mathbf{i}_2\mathbf{i}_1\mathbf{i}_1\overline{P}^1_{2211} \\
&\quad + (\mathbf{i}_1\mathbf{i}_2\mathbf{i}_1\mathbf{i}_2 + \mathbf{i}_1\mathbf{i}_2\mathbf{i}_2\mathbf{i}_1)\,\overline{P}^1_{1212} + (\mathbf{i}_2\mathbf{i}_1\mathbf{i}_1\mathbf{i}_2 + \mathbf{i}_2\mathbf{i}_1\mathbf{i}_2\mathbf{i}_1)\,\overline{P}^1_{2112}, \\
\overline{\mathbf{V}}^2 &= \mathbf{i}_1\mathbf{i}_1\mathbf{i}_1\mathbf{i}_1\overline{V}^2_{1111} + \mathbf{i}_2\mathbf{i}_2\mathbf{i}_2\mathbf{i}_2\overline{V}^2_{2222} \\
&\quad + (\mathbf{i}_1\mathbf{i}_1\mathbf{i}_2\mathbf{i}_2 + \mathbf{i}_1\mathbf{i}_2\mathbf{i}_1\mathbf{i}_2 + \mathbf{i}_1\mathbf{i}_2\mathbf{i}_2\mathbf{i}_1)\,\overline{V}^2_{1122} + (\mathbf{i}_2\mathbf{i}_1\mathbf{i}_1\mathbf{i}_2 + \mathbf{i}_2\mathbf{i}_1\mathbf{i}_2\mathbf{i}_1 + \mathbf{i}_2\mathbf{i}_2\mathbf{i}_1\mathbf{i}_1)\,\overline{V}^2_{1221},
\end{aligned}
$$

ultimately doubling the number of geometric variables (from 7 to 14) upon which the macrscale phenomenological coefficients depend. The values of these constants for various eccentricities are shown in Table 6.6. Included in the table are the values of the constants for the previous circular case ($e = 1$). Notice the deviation in these constants as the eccentricity is increased. From these constants, the forms of the phenomenological coefficients appearing in (6.3-1) to (6.3-3) can be derived. The coefficients describing the macroscale symmetric deviatoric stress (6.3-1) have the

e	1.0	1.2	1.6	2.0
$\overline{\overline{V}}^0_{1111}/\tau_0$	-1.941×10^{-2}	-2.282×10^{-2}	-2.784×10^{-2}	-3.133×10^{-2}
$\overline{\overline{V}}^0_{2222}/\tau_0$	-1.941×10^{-2}	-1.588×10^{-2}	-1.035×10^{-2}	-6.402×10^{-3}
$\overline{\overline{V}}^0_{1221}/\tau_0$	-4.503×10^{-2}	-3.878×10^{-2}	-2.812×10^{-2}	-1.950×10^{-2}
$\overline{\overline{V}}^0_{2112}/\tau_0$	-4.503×10^{-2}	-5.079×10^{-2}	-5.881×10^{-2}	-6.414×10^{-2}
$\overline{P}^1_{1111}/\tau_0$	2.506×10^{-2}	2.420×10^{-2}	2.287×10^{-2}	2.210×10^{-2}
$\overline{P}^1_{2222}/\tau_0$	2.506×10^{-2}	2.583×10^{-2}	2.682×10^{-2}	2.737×10^{-2}
$\overline{P}^1_{1122}/\tau_0$	9.378×10^{-3}	6.514×10^{-3}	1.465×10^{-3}	-2.854×10^{-3}
$\overline{P}^1_{2211}/\tau_0$	9.378×10^{-3}	1.202×10^{-2}	1.568×10^{-2}	1.813×10^{-2}
$\overline{P}^1_{1212}/\tau_0$	2.136×10^{-2}	1.793×10^{-2}	1.204×10^{-2}	7.220×10^{-3}
$\overline{P}^1_{2112}/\tau_0$	2.136×10^{-2}	2.454×10^{-2}	2.897×10^{-2}	3.194×10^{-2}
$\overline{V}^2_{1111}/\tau_0^2$	-1.221×10^{-3}	-1.518×10^{-3}	-1.985×10^{-3}	-2.322×10^{-3}
$\overline{V}^2_{2222}/\tau_0^2$	-1.221×10^{-3}	-9.353×10^{-4}	-5.394×10^{-4}	-2.999×10^{-4}
$\overline{V}^2_{1122}/\tau_0^2$	6.650×10^{-4}	5.570×10^{-4}	3.965×10^{-4}	2.882×10^{-4}
$\overline{V}^2_{2112}/\tau_0^2$	6.650×10^{-4}	7.738×10^{-4}	9.402×10^{-4}	1.060×10^{-3}

Table 6.6: Non-zero components of the geometric tensors determined for a square array of elliptical cylinders at different eccentricities. The volume fraction is $\phi = 0.2$.

following forms:

$$\begin{aligned}
\overline{\mathbf{K}}^{(l)} &= \mathbf{0}, \\
\overline{\mathbf{K}}^{(r)} &= (\mathbf{i}_1\mathbf{i}_2 + \mathbf{i}_2\mathbf{i}_1)\,\mathbf{i}_3 K^r, \qquad (6.3\text{-}11) \\
\overline{\mathbf{K}}^{(s)} &= (\mathbf{i}_1\mathbf{i}_1\mathbf{i}_1\mathbf{i}_1 - \mathbf{i}_2\mathbf{i}_2\mathbf{i}_1\mathbf{i}_1)\,K_1^s + (\mathbf{i}_2\mathbf{i}_2\mathbf{i}_2\mathbf{i}_2 - \mathbf{i}_1\mathbf{i}_1\mathbf{i}_2\mathbf{i}_2)\,K_2^s \\
&\quad + (\mathbf{i}_1\mathbf{i}_2\mathbf{i}_1\mathbf{i}_2 + \mathbf{i}_1\mathbf{i}_2\mathbf{i}_2\mathbf{i}_1 + \mathbf{i}_2\mathbf{i}_1\mathbf{i}_1\mathbf{i}_2 + \mathbf{i}_2\mathbf{i}_1\mathbf{i}_2\mathbf{i}_1)\,K_3^s. \qquad (6.3\text{-}12)
\end{aligned}$$

The constants pertaining to the macroscale stress pseudovector (6.3-2) now have the forms

$$\begin{aligned}
\overline{\mathbf{c}}^{(l)} &= \mathbf{0}, \\
\overline{\mathbf{c}}^{(r)} &= \mathbf{i}_3\mathbf{i}_3 c^r, \qquad (6.3\text{-}13) \\
\overline{\mathbf{c}}^{(s)} &= \mathbf{i}_3\,(\mathbf{i}_1\mathbf{i}_2 + \mathbf{i}_2\mathbf{i}_1)\,c^s, \qquad (6.3\text{-}14)
\end{aligned}$$

and, in general, are nonzero, unlike their circular counterparts. Finally, the constants describing the macroscale external body force density (6.3-3) now have the form

$$\mathbf{k} = \mathbf{i}_1\mathbf{i}_1 k_{11} + \mathbf{i}_2\mathbf{i}_2 k_{22} \qquad (6.3\text{-}15)$$

and

$$\begin{aligned}
\overline{\mathbf{f}}^{(l)} &= \mathbf{0}, \\
\overline{\mathbf{f}}^{(r)} &= \mathbf{i}_1\mathbf{i}_2\mathbf{i}_3 f_1^r + \mathbf{i}_2\mathbf{i}_1\mathbf{i}_3 f_2^r, \qquad (6.3\text{-}16) \\
\overline{\mathbf{f}}^{(s)} &= \mathbf{i}_1\mathbf{i}_1\mathbf{i}_1\mathbf{i}_1 f_1^s + \mathbf{i}_2\mathbf{i}_2\mathbf{i}_2\mathbf{i}_2 f_2^s \\
&\quad + \mathbf{i}_1\mathbf{i}_1\mathbf{i}_2\mathbf{i}_2 f_3^s + \mathbf{i}_2\mathbf{i}_2\mathbf{i}_1\mathbf{i}_1 f_4^s \\
&\quad + (\mathbf{i}_1\mathbf{i}_2\mathbf{i}_1\mathbf{i}_2 + \mathbf{i}_1\mathbf{i}_2\mathbf{i}_2\mathbf{i}_1)\,f_5^s + (\mathbf{i}_2\mathbf{i}_1\mathbf{i}_1\mathbf{i}_2 + \mathbf{i}_2\mathbf{i}_1\mathbf{i}_2\mathbf{i}_1)\,f_6^s. \qquad (6.3\text{-}17)
\end{aligned}$$

The permeability dyadic for this square array of elliptical cylinders is anisotropic and characterized by two constants, k_{11} and k_{22}. A plot of the directional perme-

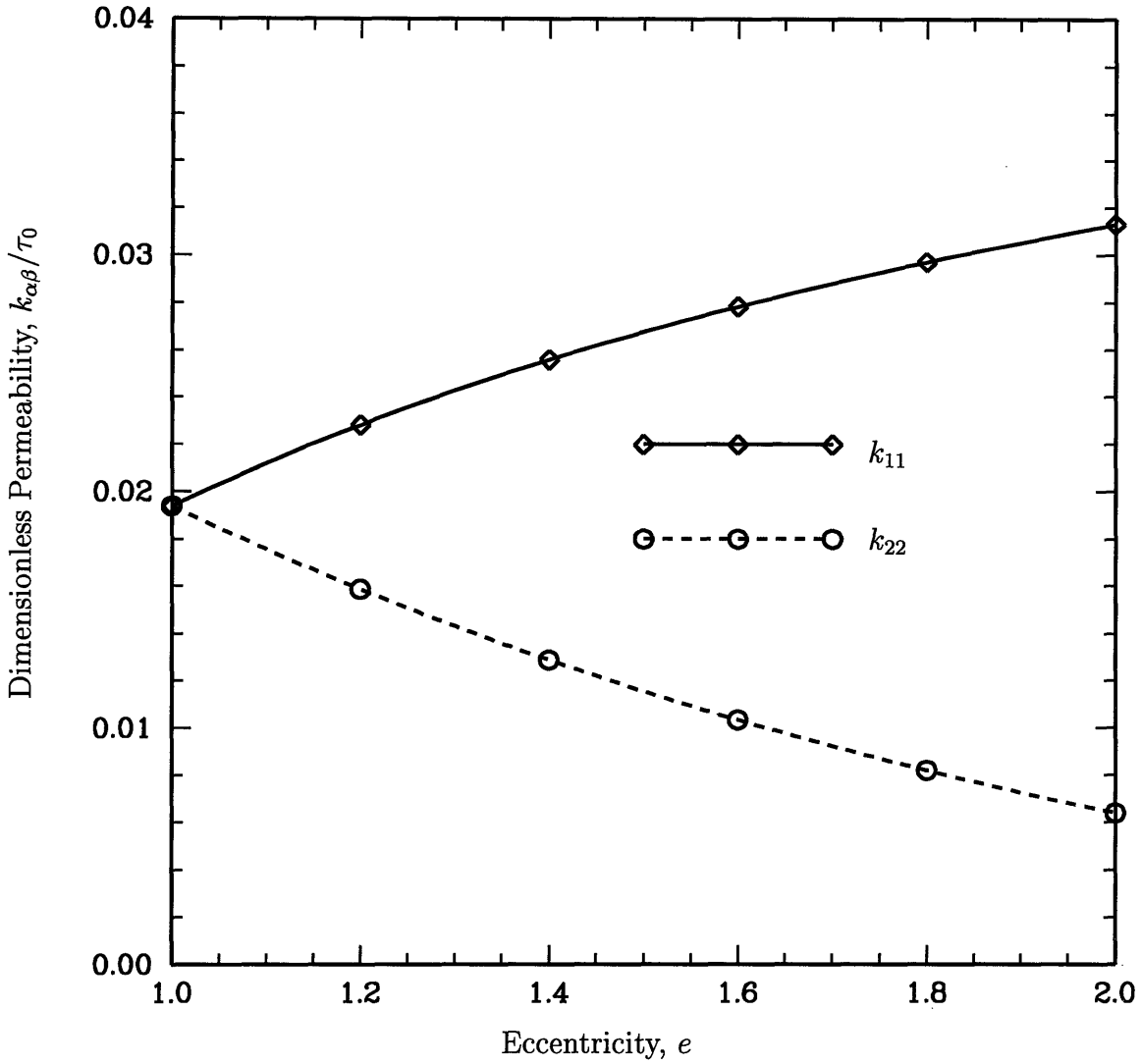

Figure 6-5: Permeability in each of the principal directions as a function of eccentricity for a square array of elliptical cylinders. The volume fraction of particles is $\phi = 0.2$.

abilities for various values of e is shown in Figure 6-5. As the eccentricity increases (with ϕ constant), flow in the x direction becomes less obstructed, while flow in the y direction becomes more so. This can be seen from the fact that k_{11} is increasing while k_{22} is decreasing relative to the circular cylinder case. Ultimately, in the limit $e \to \infty$, one would expect to recover the 'flat-plates' case with $k_{11}/\tau_0 = 1/12$ and $k_{22} = 0$.[4]

Unlike the case of circular cylinders, the macroscale stress may no longer be sym-

[4]Of course, if the impenetrability of each ellipse is taken into account, then the maximum eccentricity for this square array is $e \to \pi/(4\phi)$, at which point $k_{22} = 0$.

metric, as evidenced by the non-zero nature of $\overline{\mathbf{c}}^{(r)}$ and $\overline{\mathbf{c}}^{(s)}$. In the presence of a homogeneous macroscale flow ($\overline{\mathbf{v}}$ = const.) the stress is symmetric since $\overline{\mathbf{c}}^{(l)}$ is identically zero. On the other hand, a macroscale inhomogeneous flow field in this type of geometry now requires the presence of an external body couple density to keep the particles fixed. The constants c^r and c^s, which couple $\overline{\mathbf{P}}_\times$ with $\overline{\boldsymbol{\omega}}$ and $\overline{\mathbf{S}}$ respectively, are shown in Figure 6-6. Both these coefficients increase as the eccentricity is increased, attaining values of $c^r = 0.92$ and $c^s = 1.4$ at $e = 2$ for a particle volume fraction of 20%.

As in the case of an array of circular cylinders, the symmetric part of the sress does not depend linearly upon $\overline{\mathbf{v}}$ since $\overline{\mathbf{K}}^{(l)} = \mathbf{0}$. However, in contrast with this case, an array of elliptical cylinders manifests a symmetric deviatoric stress, dependent upon both $\overline{\boldsymbol{\omega}}$ and $\overline{\mathbf{S}}$. In all, four constants characterize this coupling. These constants (K^r, K_1^s, K_2^s and K_3^s) are shown in Figure 6-7.

Although the external body force density does not depend linearly upon $\overline{\mathbf{v}}$ as $\overline{\mathbf{f}}^{(l)} = \mathbf{0}$, a contribution to this force arising from gradients in both the macroscale vorticity and rate-of-strain arises for this array geometry. The contributions from the former (characterized by the two constants, f_1^r and f_2^r) are displayed in Figure 6-8, while contributions from the latter (namely f_1^s, f_2^s, f_3^s, f_4^s, f_5^s and f_6^s) are displayed in Figure 6-9.

Ultimately, the phenomenological coefficients characterizing these macroscale quantities can be combined to create the general linear momentum equation [accurate to $\mathcal{O}\left(\overline{\boldsymbol{\nabla}}\,\overline{\boldsymbol{\nabla}}\,\overline{\mathbf{v}}\right)$], similar to (5.5-24), namely

$$\frac{1}{\mu}\overline{\boldsymbol{\nabla}}\,\overline{p} = -\mathbf{k}^{-1}\cdot\overline{\mathbf{v}} + \overline{\boldsymbol{\nabla}}\cdot\left(\frac{1}{\mu}\overline{\boldsymbol{\mu}}^{(r)}\cdot\overline{\boldsymbol{\omega}} + \frac{1}{\mu}\overline{\boldsymbol{\mu}}^{(s)} : \overline{\mathbf{S}}\right). \tag{6.3-18}$$

In the above, $\overline{\boldsymbol{\mu}}^{(r)}$ is of the form

$$\frac{1}{\mu}\overline{\boldsymbol{\mu}}^{(r)} = \mathbf{i}_1\mathbf{i}_2\mathbf{i}_3\delta_1 + \mathbf{i}_2\mathbf{i}_1\mathbf{i}_3\delta_2, \tag{6.3-19}$$

whereas $\overline{\boldsymbol{\mu}}^{(s)}$ is

$$\begin{aligned}\frac{1}{\mu}\overline{\boldsymbol{\mu}}^{(s)} &= \mathbf{i}_1\mathbf{i}_1\mathbf{i}_1\mathbf{i}_1\alpha_1 + \mathbf{i}_2\mathbf{i}_2\mathbf{i}_2\mathbf{i}_2\alpha_2 \\ &\quad +\mathbf{i}_1\mathbf{i}_1\mathbf{i}_2\mathbf{i}_2\beta_1 + \mathbf{i}_2\mathbf{i}_2\mathbf{i}_1\mathbf{i}_1\beta_2 \\ &\quad + \left(\mathbf{i}_1\mathbf{i}_2\mathbf{i}_1\mathbf{i}_2 + \mathbf{i}_1\mathbf{i}_2\mathbf{i}_2\mathbf{i}_1\right)\gamma_1 + \left(\mathbf{i}_2\mathbf{i}_1\mathbf{i}_1\mathbf{i}_2 + \mathbf{i}_2\mathbf{i}_1\mathbf{i}_2\mathbf{i}_1\right)\gamma_2. \qquad (6.3\text{-}20)\end{aligned}$$

The constants characterizing these effective viscosities are shown in Figures 6-10 and 6-11 as functions of the eccentricity of the ellipses in the array. As in the circular case, the momentum equation does not contain a contribution arising from $\overline{\boldsymbol{\nabla}}\,\overline{\mathbf{v}}$ since the constants $\overline{\mathbf{K}}^{(l)}$, $\overline{\mathbf{c}}^{(l)}$ and $\overline{\mathbf{f}}^{(l)}$ are all identically zero.

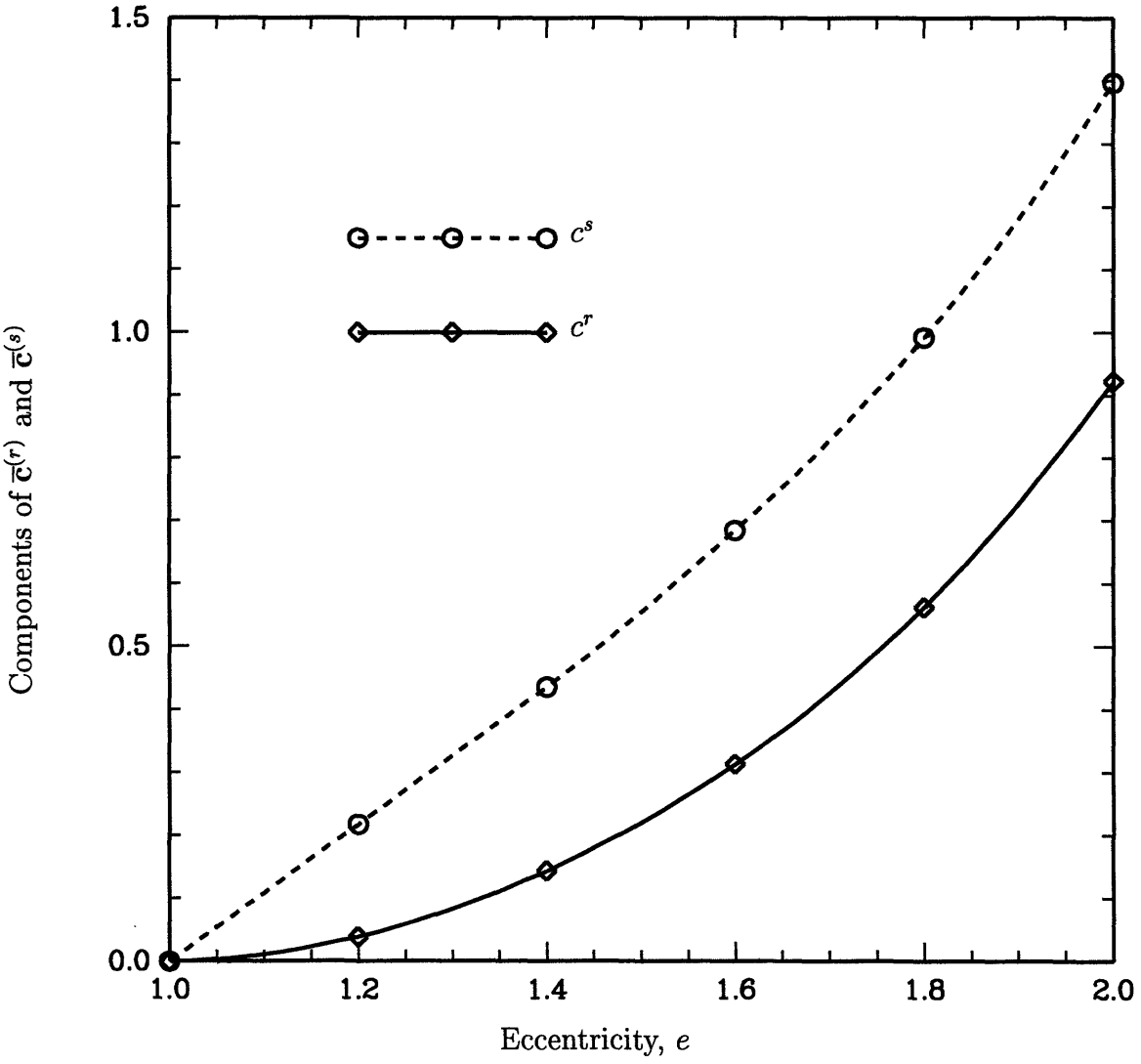

Figure 6-6: The components c^r and c^s as a function of eccentricity for a square array of elliptical cylinders with volume fraction $\phi = 0.2$. These components define $\overline{\mathbf{c}}^{(r)}$ and $\overline{\mathbf{c}}^{(s)}$, which relate the macroscale stress pseudovector to the macroscale vorticity and macroscale symmetric rate-of strain respectively.

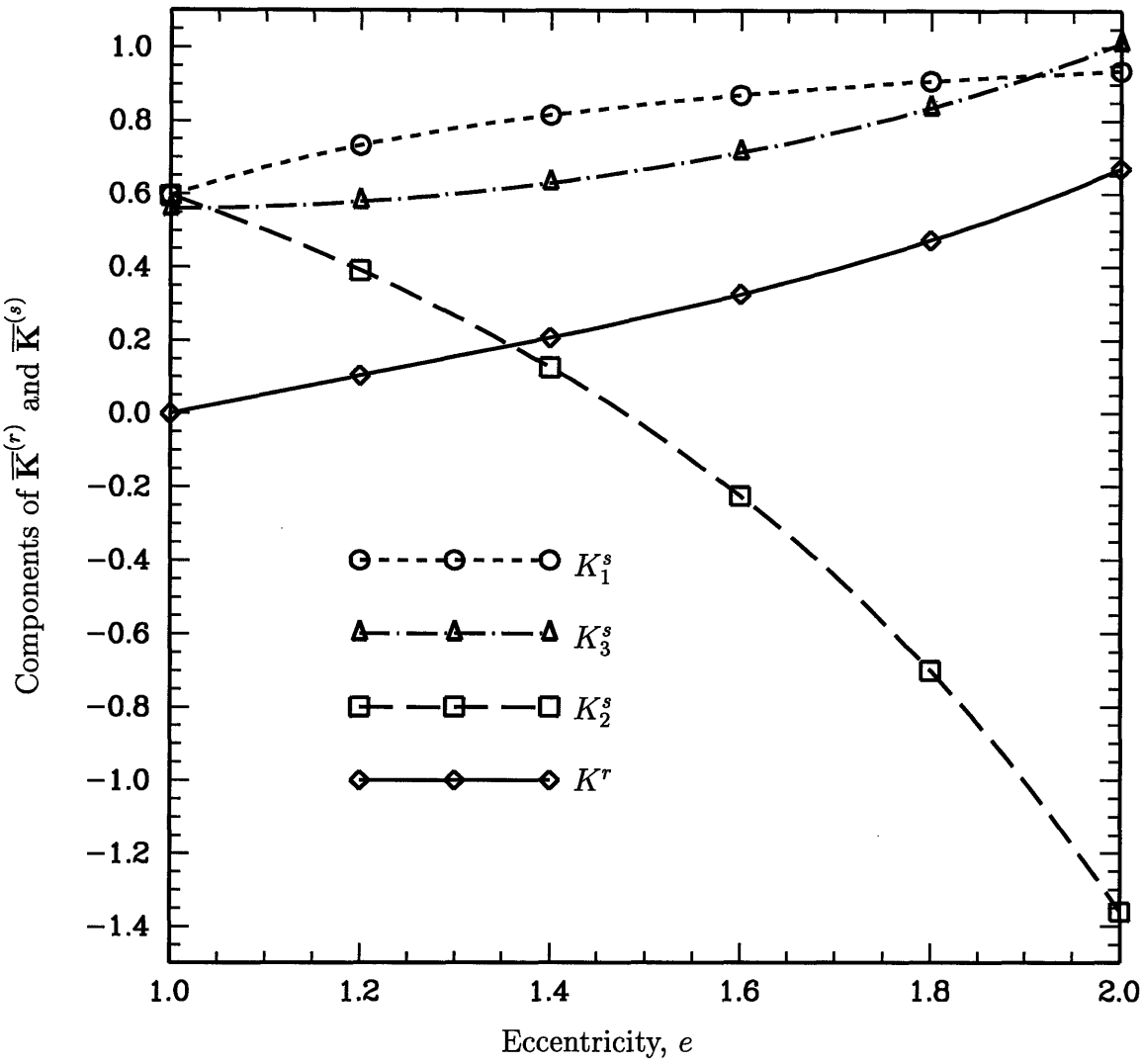

Figure 6-7: The components K^r, K_1^s, K_2^s and K_3^s as a function of eccentricity for a square array of elliptical cylinders with volume fraction $\phi = 0.2$. These components define $\overline{\mathbf{K}}^{(r)}$ and $\overline{\mathbf{K}}^{(s)}$, which relate the macroscale symmetric deviatoric stress to the macroscale vorticity and macroscale symmetric rate-of strain.

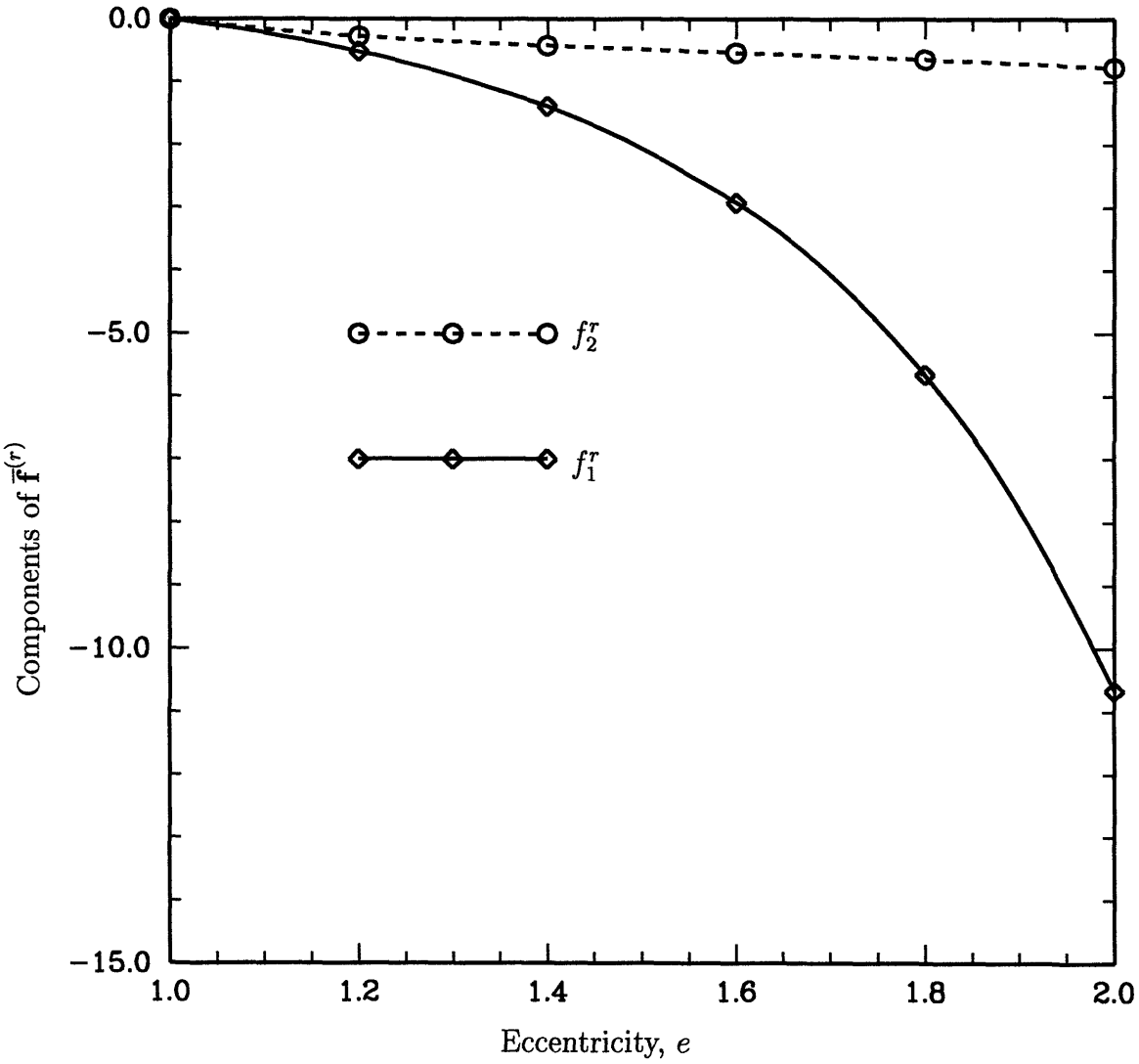

Figure 6-8: The components f_1^r and f_2^r as a function of eccentricity for a square array of elliptical cylinders with volume fraction $\phi = 0.2$. These components define $\overline{\mathbf{f}}^{(r)}$, which relates gradients in the macroscale vorticity to the external body force density.

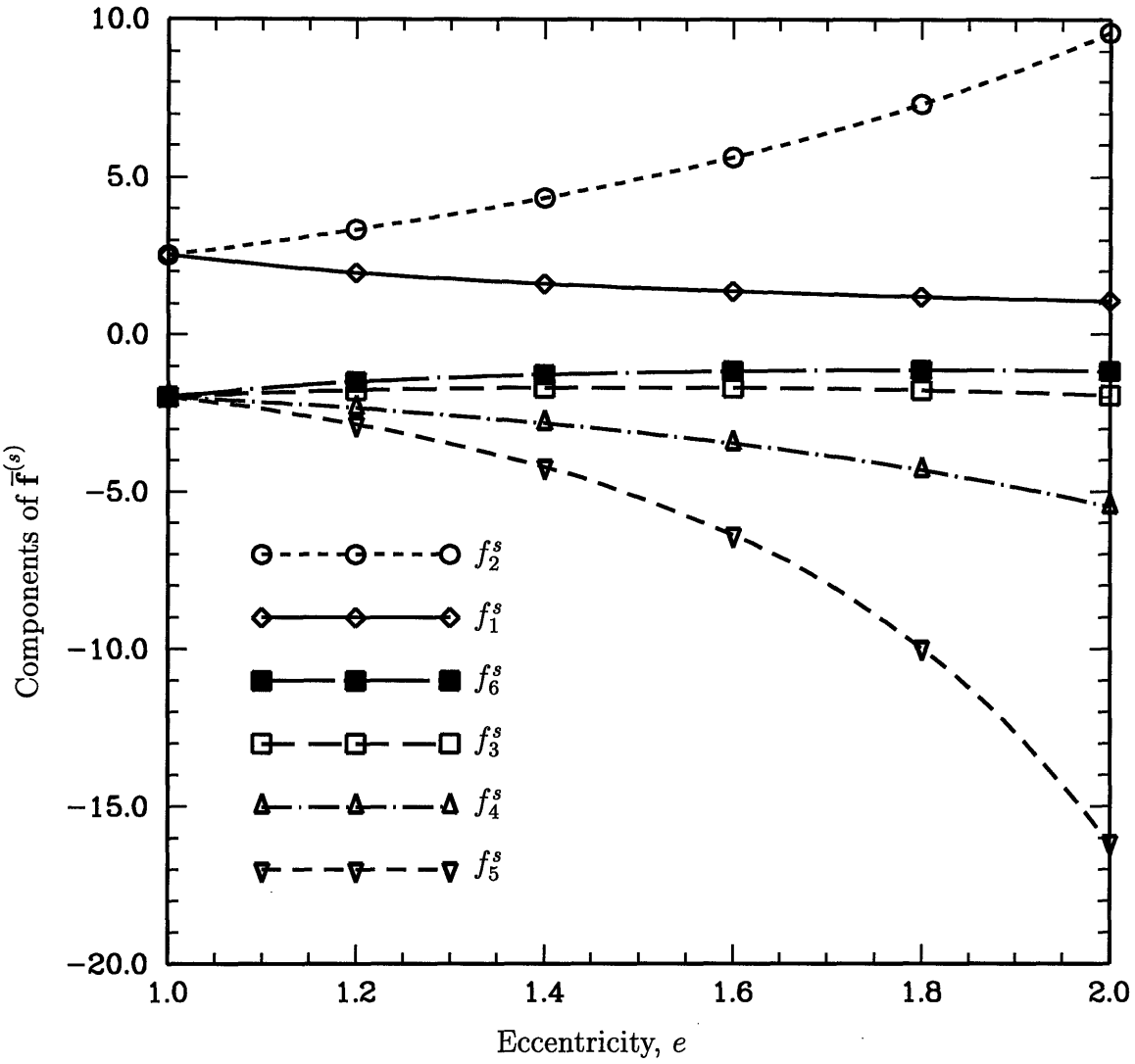

Figure 6-9: The components f_1^s, f_2^s, f_3^s, f_4^s, f_5^s and f_6^s as a function of eccentricity for a square array of elliptical cylinders with volume fraction $\phi = 0.2$. These components define $\bar{\mathbf{f}}^{(s)}$, which relates the macroscale symmetric rate-of-strain to the external body force density.

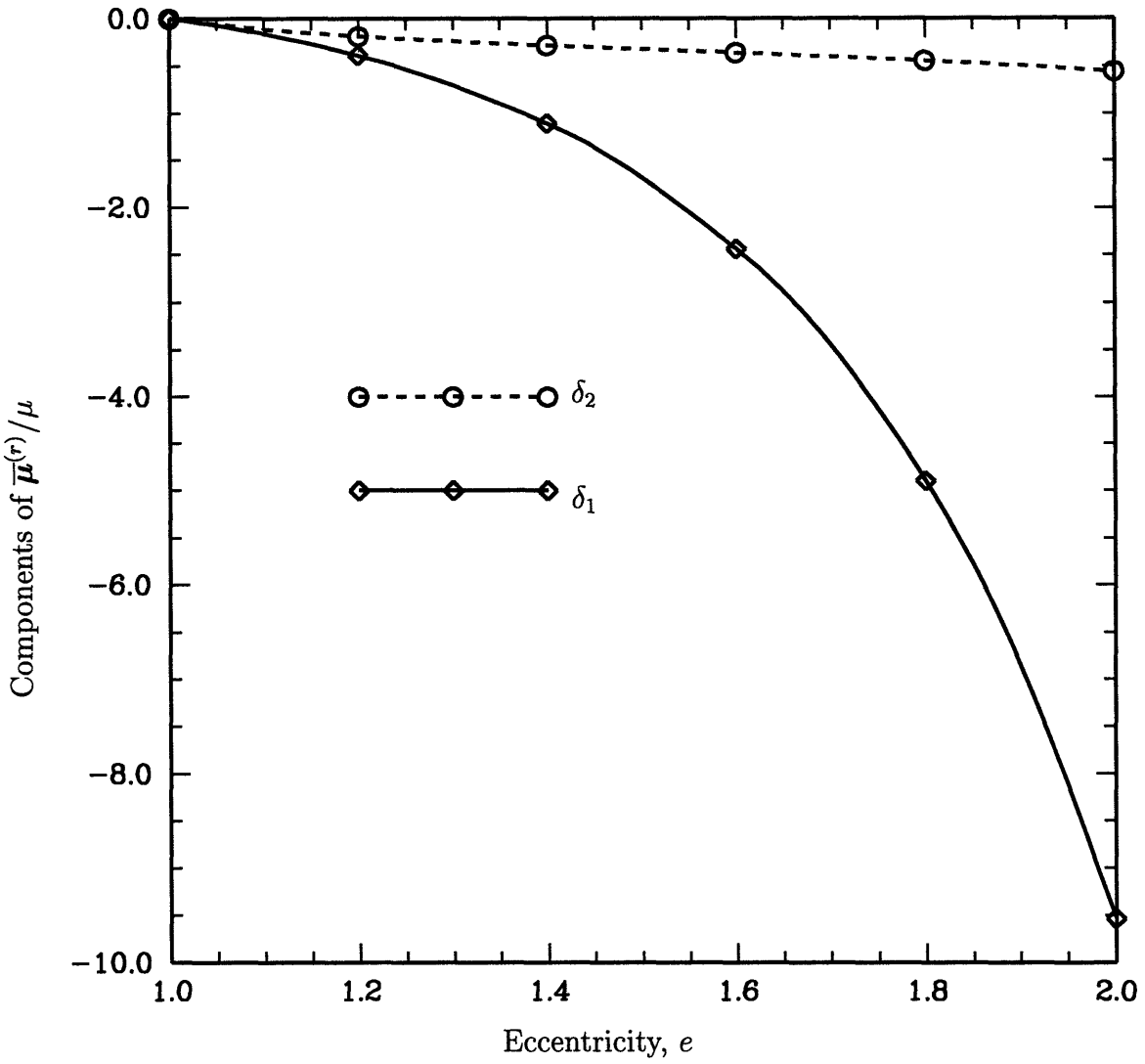

Figure 6-10: The components δ_1 and δ_2 as a function of eccentricity for a square array of elliptical cylinders with volume fraction $\phi = 0.2$. These components characterize that part of the effective viscosity which couples gradients in the macroscale vorticity to the macroscale pressure drop.

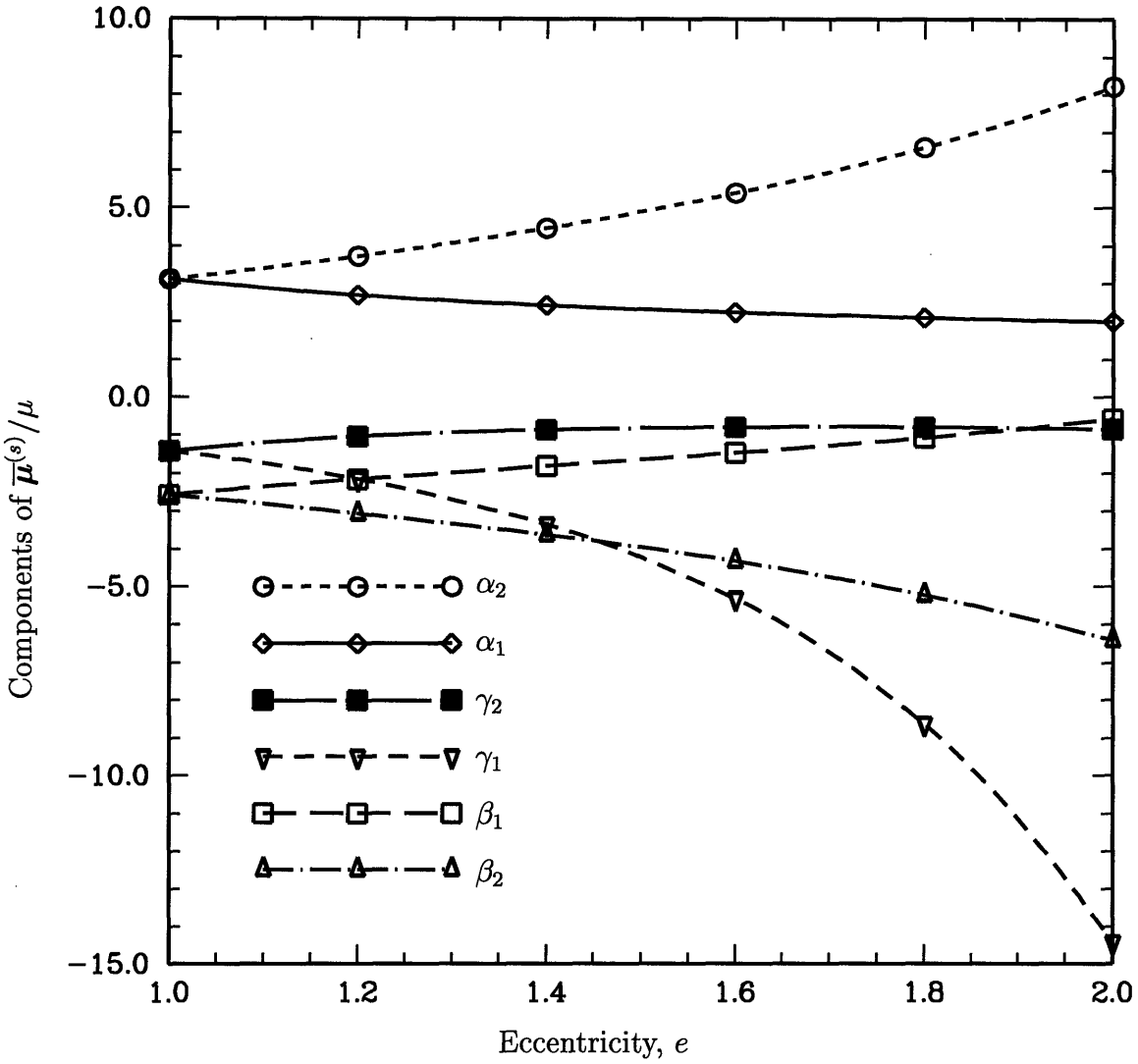

Figure 6-11: The components α_1, α_2, γ_1, γ_2, β_1 and β_2 as a function of eccentricity for a square array of elliptical cylinders with volume fraction $\phi = 0.2$. These components characterize that part of the effective viscosity which couples gradients in the macroscale symmetric rate-of-strain to the macroscale pressure drop.

Appendix A

Nomenclature

Selected Notation List

a	sphere radius
c^r	non-zero component of $\overline{\mathbf{c}}^{(r)}$
c^s	non-zero component of $\overline{\mathbf{c}}^{(s)}$
$\overline{\mathbf{c}}^{(l)}$	dyadic phenomenological coefficient coupling the dependence of $\overline{\mathbf{P}}_{\times}$ upon $\overline{\mathbf{v}}$
$\overline{\mathbf{c}}^{(r)}$	dyadic phenomenological coefficient coupling the dependence of $\overline{\mathbf{P}}_{\times}$ upon $\overline{\boldsymbol{\omega}}$
$\overline{\mathbf{c}}^{(s)}$	triadic phenomenological coefficient coupling the dependence of $\overline{\mathbf{P}}_{\times}$ upon $\overline{\mathbf{S}}$
$\overline{\mathbf{C}}$	macroscale couple stress dyadic

$d\overline{\mathbf{f}}$	macroscale differential force vector
$d\overline{q}$	macroscale differential volumetric flow rate
$d^3\mathbf{r}$	differential volume element
$d\overline{\mathbf{R}}$	macroscale differential displacement vector
$d\mathbf{S}$	directed differential element of surface area
$d\overline{\mathbf{S}}$	macroscale directed differential element of surface area
$d\overline{V}$	macroscale differential volume element
e	elliptical cylinder eccentricity
f_i^r	non-zero components of $\overline{\mathbf{f}}^{(r)}$
f_i^s	non-zero components of $\overline{\mathbf{f}}^{(s)}$
$\mathbf{f}_k$	force exerted by fluid on positive side of $\mathbf{s}_k$ upon fluid on negative side of $\mathbf{s}_k$
$\widetilde{\mathbf{f}}$	vector inhomogeneous forcing function in momentum equation
$\overline{\mathbf{f}}^{(l)}$	triadic phenomenological coefficient coupling the dependence of $\overline{\mathbf{F}}^{(e)}$ upon $\overline{\boldsymbol{\nabla}}\,\overline{\mathbf{v}}$
$\overline{\mathbf{f}}^{(r)}$	triadic phenomenological coefficient coupling the dependence of $\overline{\mathbf{F}}^{(e)}$ upon $\overline{\boldsymbol{\nabla}}\,\overline{\boldsymbol{\omega}}$

$\overline{\mathbf{f}}^{(s)}$	tetradic phenomenological coefficient coupling the dependence of $\overline{\mathbf{F}}^{(e)}$ upon $\overline{\boldsymbol{\nabla}}\,\overline{\mathbf{S}}$
$\overline{\mathbf{f}}^{m}(\|X')$	mth derivative of $\mathbf{f}(X)$ evaluated at $X = X'$
$\overline{\mathbf{F}}$	force (per unit superficial volume) exerted by the fluid upon the particles in cell $\{\mathbf{n}\}$
$\overline{\mathbf{F}}^{(e)}$	net external volumetric body force density
$\tilde{g}$	scalar inhomogeneous forcing function in continuity equation
$\mathbf{i}_j$	unit vector in jth direction
$\mathbf{I}$	dyadic idemfactor
$\mathbf{I}^4$	fourth-rank isotropic tensor
$\mathbf{I}^6$	sixth-rank isotropic tensor
$\overline{\mathbf{I}}$	macroscale volumetric intrinsic angular momentum density
k	scalar permeability
k_{ii}	non-zero components of permeability dyadic $\mathbf{k}$
$\mathbf{k}$	dyadic permeability
$\mathbf{k}^{-1}$	inverse of dyadic permeability

K	dimensionless scalar permeability
K_i^r	non-zero components of $\overline{\mathbf{K}}^{(r)}$
K_i^s	non-zero components of $\overline{\mathbf{K}}^{(s)}$
$\overline{\mathbf{K}}^{(l)}$	triadic phenomenological coefficient coupling the dependence of $\overline{\mathbf{T}}^s$ upon $\overline{\mathbf{v}}$
$\overline{\mathbf{K}}^{(r)}$	triadic phenomenological coefficient coupling the dependence of $\overline{\mathbf{T}}^s$ upon $\overline{\boldsymbol{\omega}}$
$\overline{\mathbf{K}}^{(s)}$	tetradic phenomenological coefficient coupling the dependence of $\overline{\mathbf{T}}^s$ upon $\overline{\mathbf{S}}$
ℓ	characteristic microscale or unit cell lenght scale
ℓ_k	lattice vector
$\mathcal{L}$	characteristic mesoscale lenght scale
L	characteristic macroscale lenght scale
$\overline{\mathbf{L}}$	torque (per unit superficial volume) exerted by the fluid upon the particles in cell $\{\mathbf{n}\}$
M	space dimensionality
$\overline{\mathbf{M}}$	macroscale volumetric momentum density

n	one-dimensional unit cell position
$\mathbf{n}$	unit cell position
$\overline{\mathbf{N}}^{(e)}$	net external volumetric body couple density
p	hydordynamic pressure
$\widetilde{p}$	fully spatially periodic pressure field satisfying inhomogeneous Stokes-like problem
$p^{(i)}$	approximation to $\widetilde{p}$ at ith bilinear node
$\overline{p}$	macroscale pressure
$\mathbf{p}^m$	mth rank tensor Taylor coefficient containing the $\mathbf{r}$ dependence of the expansion of p
$\overline{\mathbf{p}}^m$	mth gradient of p evaluated at $\mathbf{R}'$
$\widetilde{\mathbf{p}}^m$	mth rank fully spatially periodic tensor Taylor coefficient
$\mathbf{P}$	microscale stress tensor (dyadic)
$\widetilde{\mathbf{P}}^m$	$m+3$ rank geometric 'stress' field formed from $\widetilde{\mathbf{V}}^m$ and $\widetilde{\mathbf{\Pi}}^m$ as defined in (5.3-9)
$\overline{\mathbf{P}}$	macroscale stress tensor (dyadic)

$\overline{\mathbf{P}}^m$	$m+3$ rank mean of $\tilde{\mathbf{P}}^m$ as defined in (5.3-11)
$\overline{\mathbf{P}}_\times$	macroscale stress pseudovector
q_k	net volumetric flow rate of fluid through $\mathbf{s}_k$
$\mathbf{r}$	continuous local or cellular position vector
$\mathbf{R}$	position vector
$\mathbf{R}'$	reference position
$\overline{\mathbf{R}}$	macroscale position vector
$\mathbf{R_n}$	discrete global position vector
$\mathbf{s}_k$	directed area of a curvilinear face of a unit cell
s_p	particle surfaces
$\mathbf{S}$	symmetric rate-of-strain dyadic
$\overline{\mathbf{S}}$	macroscale symmetric rate-of-strain dyadic
$\overline{\mathbf{T}}$	macroscale deviatoric stress tensor (dyadic)
$\overline{\mathbf{T}}^a$	macroscale antisymmetric deviatoric stress tensor (dyadic)
$\overline{\mathbf{T}}^s$	macroscale symmetric deviatoric stress tensor (dyadic)

U	mean velocity
$\mathbf{v}$	microscale vector fluid velocity
$\tilde{\mathbf{v}}$	fully spatially periodic velocity field satisfying inhomogeneous Stokes-like problem
$\mathbf{v}^{(i)}$	approximation to $\tilde{\mathbf{v}}$ at ith biquadratic node
$\overline{\mathbf{v}}$	macroscale vector superficial velocity
$\mathbf{v}^m$	$m+1$ rank tensor Taylor coefficient containing the $\mathbf{r}$ dependence of the expansion of $\mathbf{v}$
$\overline{\mathbf{v}}^m$	mth gradient of $\mathbf{v}$ evaluated at $\mathbf{R}'$
$\tilde{\mathbf{v}}^m$	$m+1$ rank fully spatially periodic tensor Taylor coefficient
$\widetilde{\mathbf{V}}^m$	fully spatially periodic lattice field of rank $m+2$ and solution to mth order characteristic cell problem
$\overline{\widetilde{\mathbf{V}}}^m$	$m+2$ rank mean of $\widetilde{\mathbf{V}}^m$ as defined in (5.4-3)
$\overline{\overline{\widetilde{\mathbf{V}}}}^m$	$m+4$ rank mean of $\widetilde{\mathbf{V}}^m$ as defined in (5.4-18)
$\left\langle \widetilde{\mathbf{V}}^m \right\rangle$	$m+2$ rank interstitial average of $\widetilde{\mathbf{V}}^m$
x	one-dimensional continuous local position
X	one-dimensional position variable

X' one-dimensional reference point

X_n one-dimensional discrete global position

Greek Symbols

α non-zero component of $\overline{\boldsymbol{\mu}}^*$ or nondimensional slip coefficient

α' non-zero component of $\overline{\boldsymbol{\mu}}^*$

α_i non-zero components of $\overline{\boldsymbol{\mu}}^{(s)}$

β non-zero component of $\overline{\boldsymbol{\mu}}^*$

β_i non-zero components of $\overline{\boldsymbol{\mu}}^{(s)}$

γ non-zero component of $\overline{\boldsymbol{\mu}}^*$

γ_i non-zero components of $\overline{\boldsymbol{\mu}}^{(s)}$

δ_i non-zero components of $\overline{\boldsymbol{\mu}}^{(r)}$

δ_{ij} Cartesian tensor notation of $\mathbf{I}$

$\boldsymbol{\epsilon}$ unit isotropic triadic or unit alternating tensor

$\overline{\boldsymbol{\Lambda}}^0$ inverse of the dyadic $\overline{\mathbf{V}}^0$

μ	isotropic and uniform fluid viscosity
$\overline{\mu}^*$	scalar Brinkman viscosity
$\overline{\mu}_r^*$	scalar nonuniform Brinkman viscosity
$\overline{\boldsymbol{\mu}}^*$	tetradic phenomenological coefficient coupling the dependence of $\overline{\boldsymbol{\nabla}}\,\overline{p}$ upon $\overline{\boldsymbol{\nabla}}\,\overline{\boldsymbol{\nabla}}\,\overline{\mathbf{v}}$
$\overline{\boldsymbol{\mu}}^{(r)}$	triadic phenomenological coefficient coupling the dependence of $\overline{\boldsymbol{\nabla}}\,\overline{p}$ upon $\overline{\boldsymbol{\nabla}}\,\overline{\boldsymbol{\omega}}$
$\overline{\boldsymbol{\mu}}^{(s)}$	tetradic phenomenological coefficient coupling the dependence of $\overline{\boldsymbol{\nabla}}\,\overline{p}$ upon $\overline{\boldsymbol{\nabla}}\,\overline{\mathbf{S}}$
ν	inverse of the dimensionality of space
$\widetilde{\boldsymbol{\Pi}}^m$	fully spatially periodic lattice field of rank $m+1$ and solution to mth order characteristic cell problem
τ_f	cellular fluid domain
τ_0	cellular domain, fluid plus particles
$\partial\tau_0$	the closed surface bounding the unit cell externally
ϕ	particle volume fraction
ϕ^i	continuous biquadratic basis function

$\boldsymbol{\Phi}$ biquadratic vector used to generate weak form

$\overline{\boldsymbol{\chi}}^{*}$ triadic phenomenological coefficient coupling the dependence of $\overline{\boldsymbol{\nabla}}\,\overline{p}$ upon $\overline{\boldsymbol{\nabla}}\,\overline{\mathbf{v}}$

$\overline{\boldsymbol{\chi}}^{(r)}$ dyadic phenomenological coefficient coupling the dependence of $\overline{\boldsymbol{\nabla}}\,\overline{p}$ upon $\overline{\boldsymbol{\omega}}$

$\overline{\boldsymbol{\chi}}^{(s)}$ triadic phenomenological coefficient coupling the dependence of $\overline{\boldsymbol{\nabla}}\,\overline{p}$ upon $\overline{\mathbf{S}}$

ψ arbitrary scalar field

ψ^{i} continuous bilinear basis function

Ψ areal fraction of solids near a macroscale boundary

$\overline{\boldsymbol{\Psi}}^{m}$ arbitrary constant tensors (functions of $\mathbf{R}'$)

$\overline{\boldsymbol{\omega}}$ macroscale vorticity vector

Operators

$\cdot$ dot product, contraction between innermost indices

$:$ double-dot product, contraction between innermost two indicies

$\vdots$	tripple-dot product, contraction between innermost three indicies
$\{\cdot\}^m$	multiple-dot product, contraction between innermost m indices
$\boldsymbol{\nabla}$	vector gradient operator with respect to either $\mathbf{R}$ (3.3-3) or $\mathbf{r}$ (4.2-15)
$\overline{\boldsymbol{\nabla}}$	macroscale vector gradient operator with respect to $\overline{\mathbf{R}}$
$\boldsymbol{\nabla}^m$	mth rank gradient operator (3.3-2)
∇^2	Laplacian operator, $\boldsymbol{\nabla} \cdot \boldsymbol{\nabla}$
$\overline{\nabla}^2$	macroscale Laplacian operator, $\overline{\boldsymbol{\nabla}} \cdot \overline{\boldsymbol{\nabla}}$
$\boldsymbol{\nabla}\cdot$	divergence operator
$\overline{\boldsymbol{\nabla}}\cdot$	macroscale divergence operator
$\begin{pmatrix} i \\ j \end{pmatrix}$	binomial coefficient
$\|\mathbf{f}\|$	jump in the function $\mathbf{f}$
$[\![\,\mathbf{f}\,]\!]^s$	normalized permutation symmetrization operator
$[\![\,\mathbf{f}\,]\!]^{si}$	symmetrization operator with respect to the last i indices of $\mathbf{f}$
$\tilde{\mathbf{f}}$	denotes the field $\mathbf{f}$ as being fully spatially periodic

$\langle \mathbf{f} \rangle$	interstitial average
$\times$	cross product
$\dfrac{\mathrm{D}}{\mathrm{D}t}$	material derivative
$\mathcal{O}\,()$	order-of-magnitude

Appendix B

Geometry of Spatially Periodic Systems

Consider a spatially periodic porous medium composed of generally curvilinear unit cells (refer to Figures B-1 and B-2 on pages 203 and 204 for visual representations of the notation presented here). The position vector $\mathbf{R}$ of any point in the system can be represented by the decomposition

$$\mathbf{R} = \mathbf{R_n} + \mathbf{r}, \tag{B.0-1}$$

where $\mathbf{r}$ is a local position vector within a unit cell and $\mathbf{R_n}$ is a discrete lattice vector defining the location of the lattice point identifying the $\mathbf{n}$th cell in the array:

$$\mathbf{R_n} = n_1\mathbf{l}_1 + n_2\mathbf{l}_2 + n_3\mathbf{l}_3, \tag{B.0-2}$$

$$(n_i = 0, \pm 1, \pm 2, \pm 3, \ldots), \qquad (i = 1, 2, 3), \tag{B.0-3}$$

with $\{\mathbf{l}_1, \mathbf{l}_2, \mathbf{l}_3\}$ denoting a trio of basic lattice vectors.

The superficial volume of the cell is,

$$\tau_0 = \mathbf{l}_1 \cdot \mathbf{l}_2 \times \mathbf{l}_3. \tag{B.0-4}$$

The unit cell is bounded externally by the closed surface $\partial\tau_0$ and consists of the six faces, $s_{\pm j}$ $(j = 1, 2, 3)$; hence,

$$\partial\tau_0 \equiv \sum_{j=1}^{3} s_{-j} \oplus s_{+j}. \tag{B.0-5}$$

The location of the $\mathbf{n}$th cell in space can be specified either by the position vector $\mathbf{R_n}$ or, equivalently, by the triplet of integers,

$$\{n_1, n_2, n_3\} \equiv \{\mathbf{n}\}. \tag{B.0-6}$$

With $\tau_0\{\mathbf{n}\}$ the domain contained within the nth unit cell, the entire spatial domain V_0 encompassed by the periodic medium may be represented as

$$V_0 \equiv \sum_{\mathbf{n}} \tau_0\{\mathbf{n}\}, \tag{B.0-7}$$

where

$$\sum_{\mathbf{n}} \equiv \sum_{n_1=-\infty}^{\infty} \sum_{n_2=-\infty}^{\infty} \sum_{n_3=-\infty}^{\infty}. \tag{B.0-8}$$

The directed area of each of the six faces of the unit cell is defined as

$$\mathbf{s}_1 = \mathbf{l}_2 \times \mathbf{l}_3, \qquad \mathbf{s}_2 = \mathbf{l}_3 \times \mathbf{l}_1, \qquad \mathbf{s}_3 = \mathbf{l}_1 \times \mathbf{l}_2, \tag{B.0-9}$$

along with $\mathbf{s}_{-j} = -\mathbf{s}_{+j}$. It follows from these together with (B.0-4) that $\mathbf{l}_i$ and $\mathbf{s}_j$ are reciprocal to one another in the sense that,

$$\mathbf{l}_i \cdot \mathbf{s}_j = \delta_{ij}\tau_0 \qquad (i; j = 1, 2, 3), \tag{B.0-10}$$

with δ_{ij} the Kronecker delta.

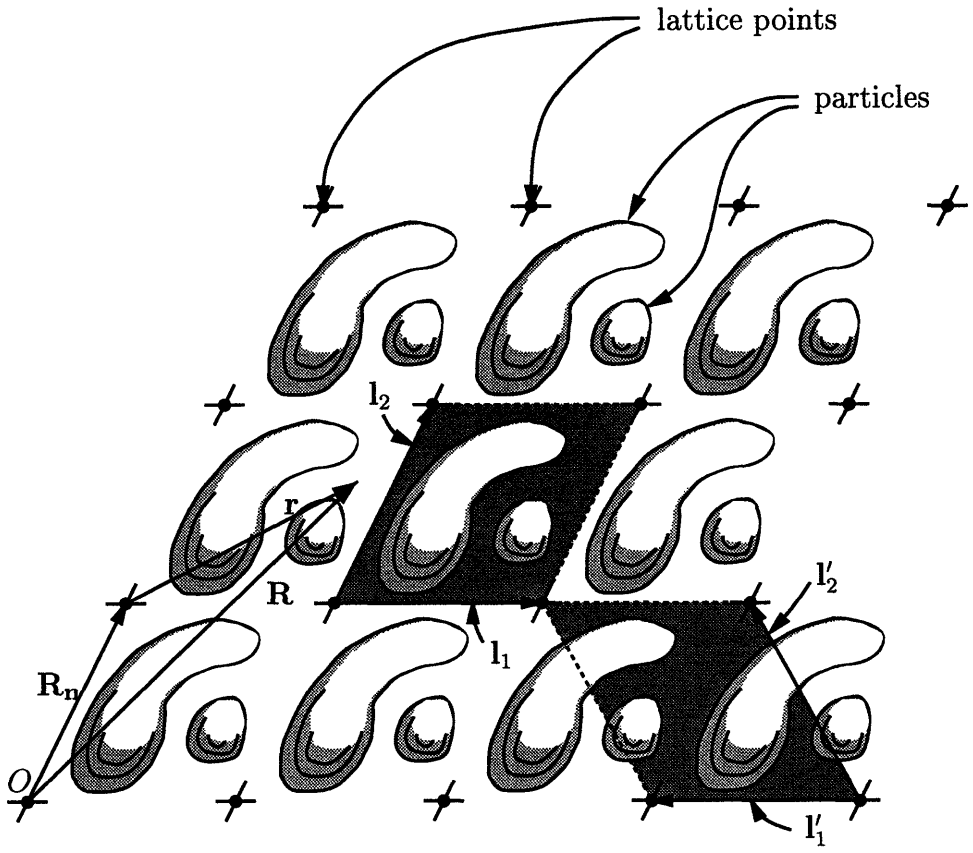

Figure B-1: A two-dimensional spatially periodic array. The spatially periodic character of the array is represented by the translational symmetry of the lattice points. The pair of planar basic vectors $(\mathbf{l}_1, \mathbf{l}_2)$ drawn between 'adjacent' lattice points forms a 'unit cell' in the shape of a parallelogram. Other choices, such as $(\mathbf{l}'_1, \mathbf{l}'_2)$ also qualify as a set of basic lattice vectors. These form a differently shaped unit cell, as shown. However, the magnitudes, $|\mathbf{l}_1 \times \mathbf{l}_2|$ and $|\mathbf{l}'_1 \times \mathbf{l}'_2|$, of the superficial unit cell areas are identical, as too are the respective particle and interstitial areas. Furthermore, any point in the infinite array specified by a vector $\mathbf{R}$ drawn from some origin O, may be represented by a discrete lattice vector $\mathbf{R_n}$ and continuous cellular vector $\mathbf{r}$.

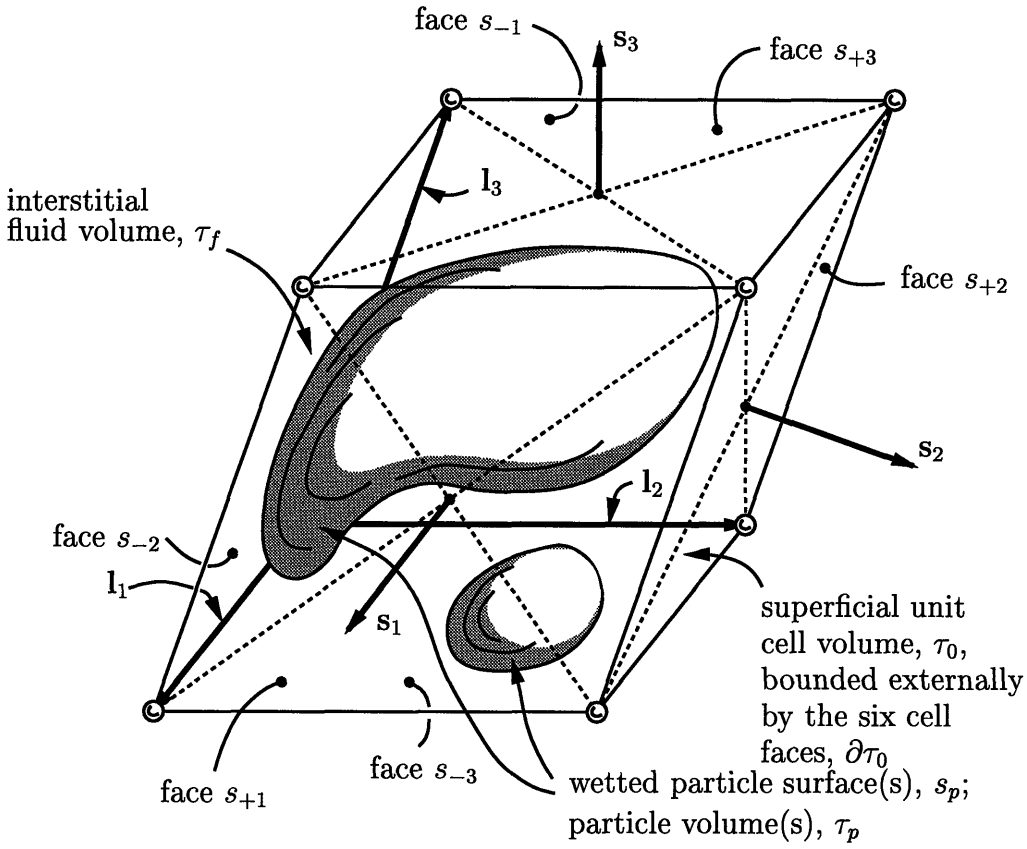

Figure B-2: Unit cell of a spatially periodic array. The unit cell is a parallelepiped formed from the set of basic lattice vectors $(\mathbf{l}_1, \mathbf{l}_2, \mathbf{l}_3)$. The directed areal vectors $(\mathbf{s}_1, \mathbf{s}_2, \mathbf{s}_3)$ are normal to the respective faces, pointing out of the cell, and are equal in magnitude to the areas of the respective faces.

Appendix C

Circular Cylinder Lattice Fields

The first three microscale lattice fields for a square array of circular cylinders of volume fraction $\phi = 0.2$ is shown here. Figure C-1 is the mesh of the unit cell. The various independent components of the fields $\left(\widetilde{\mathbf{V}}^0, \widetilde{\mathbf{\Pi}}^0\right)$, $\left(\widetilde{\mathbf{V}}^1, \widetilde{\mathbf{\Pi}}^1\right)$ and $\left(\widetilde{\mathbf{V}}^2, \widetilde{\mathbf{\Pi}}^2\right)$ are shown in Figures C-2–C-7, Figures C-8–C-16 and Figures C-17–C-28 respectively. For the given mesh, there corresponded 800 elements, 3360 nodes and 7600 equations (or unknowns).

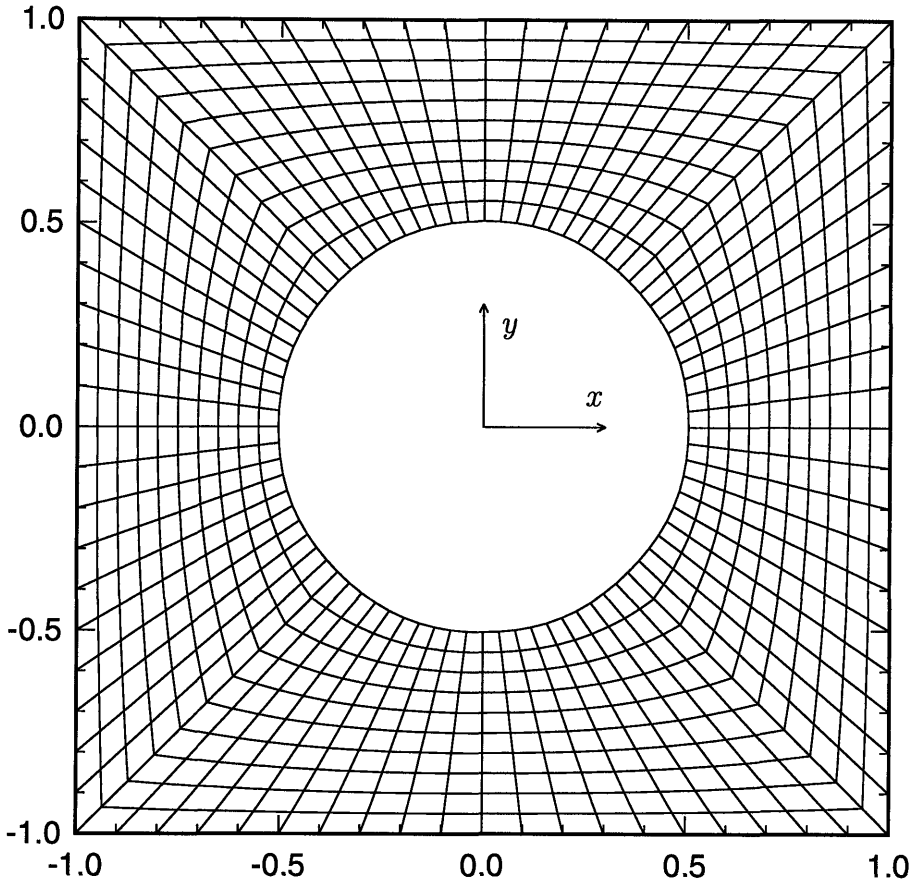

Figure C-1: Sample mesh of a square array of circular cylinders ($\phi = 0.2$). There are 800 elements, 3360 nodes and 7600 eqations. This unit cell has a 'volume' $\tau_0 = 4$.

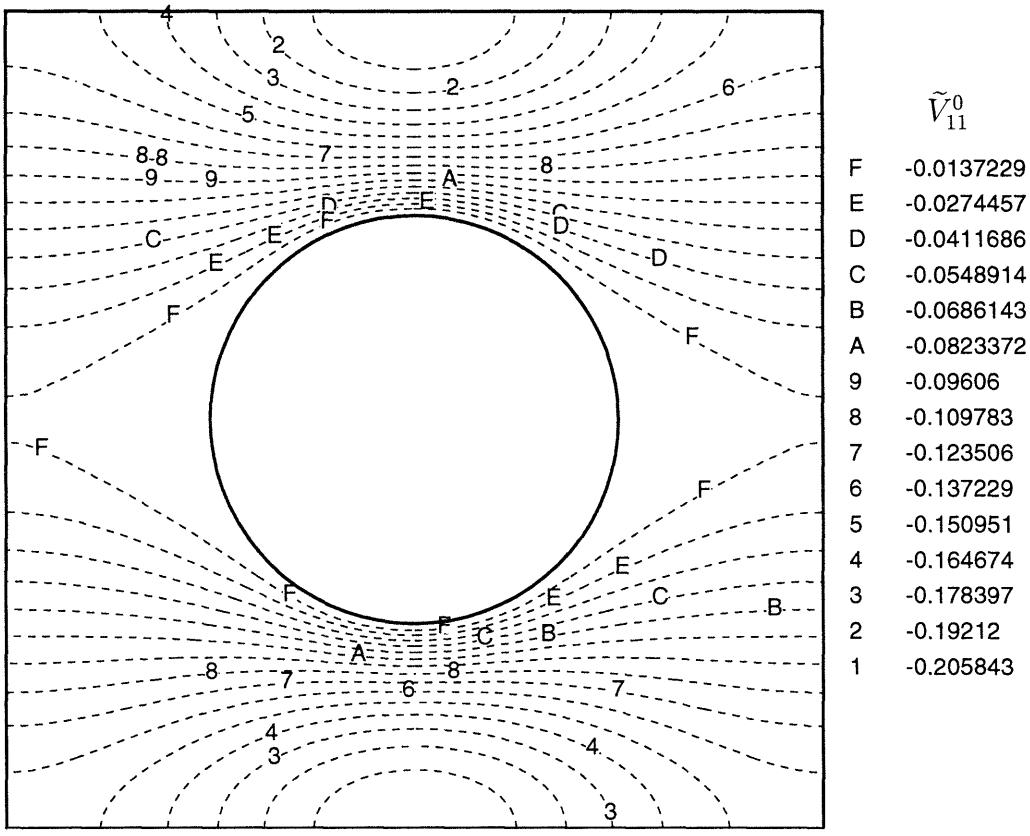

Figure C-2: Contours of $\widetilde{V}_{11}^{0}$ from the $\mathcal{O}(0)$ cell problem for a square array of circular cylinders of volume fraction $\phi = 0.2$.

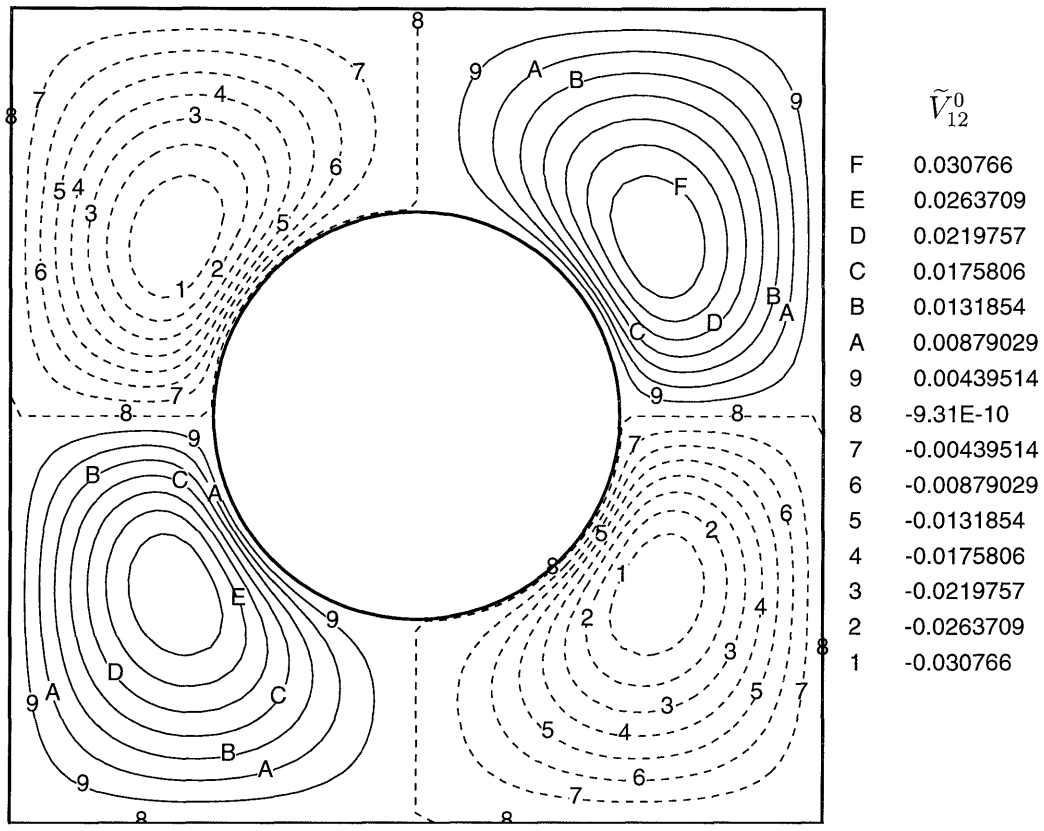

Figure C-3: Contours of $\widetilde{V}_{12}^{0}$ from the $\mathcal{O}(0)$ cell problem for a square array of circular cylinders of volume fraction $\phi = 0.2$.

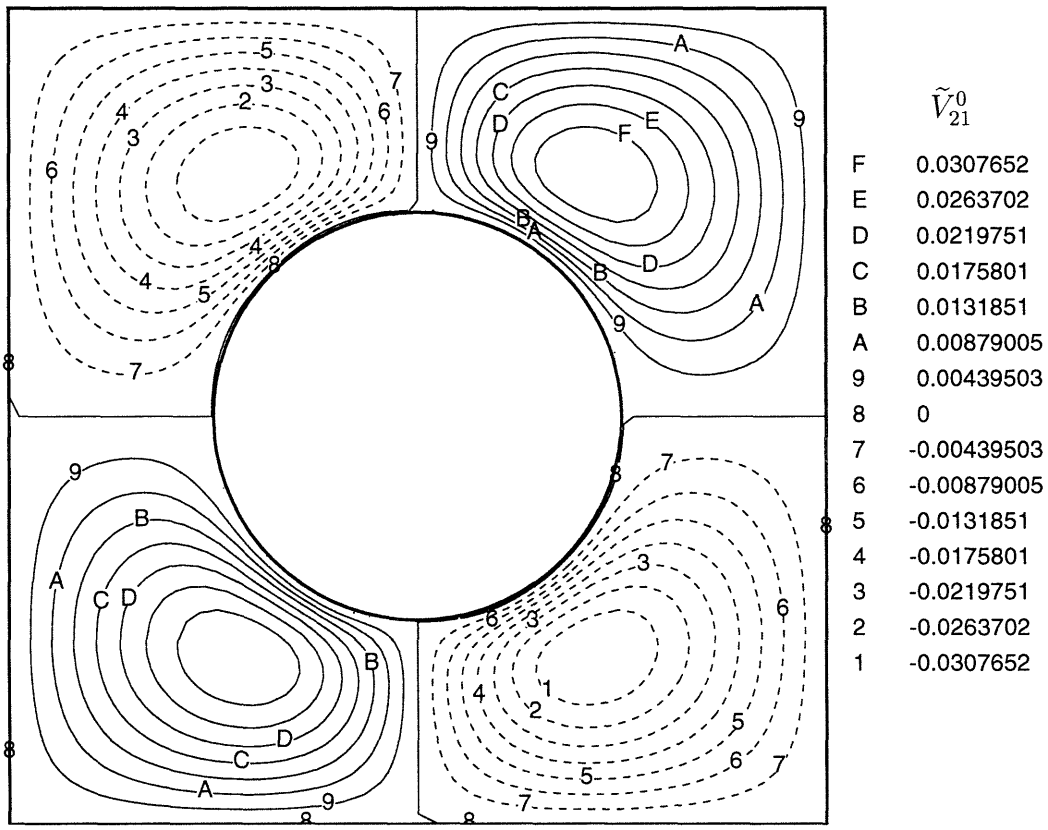

Figure C-4: Contours of $\tilde{V}_{21}^{0}$ from the $\mathcal{O}(0)$ cell problem for a square array of circular cylinders of volume fraction $\phi = 0.2$.

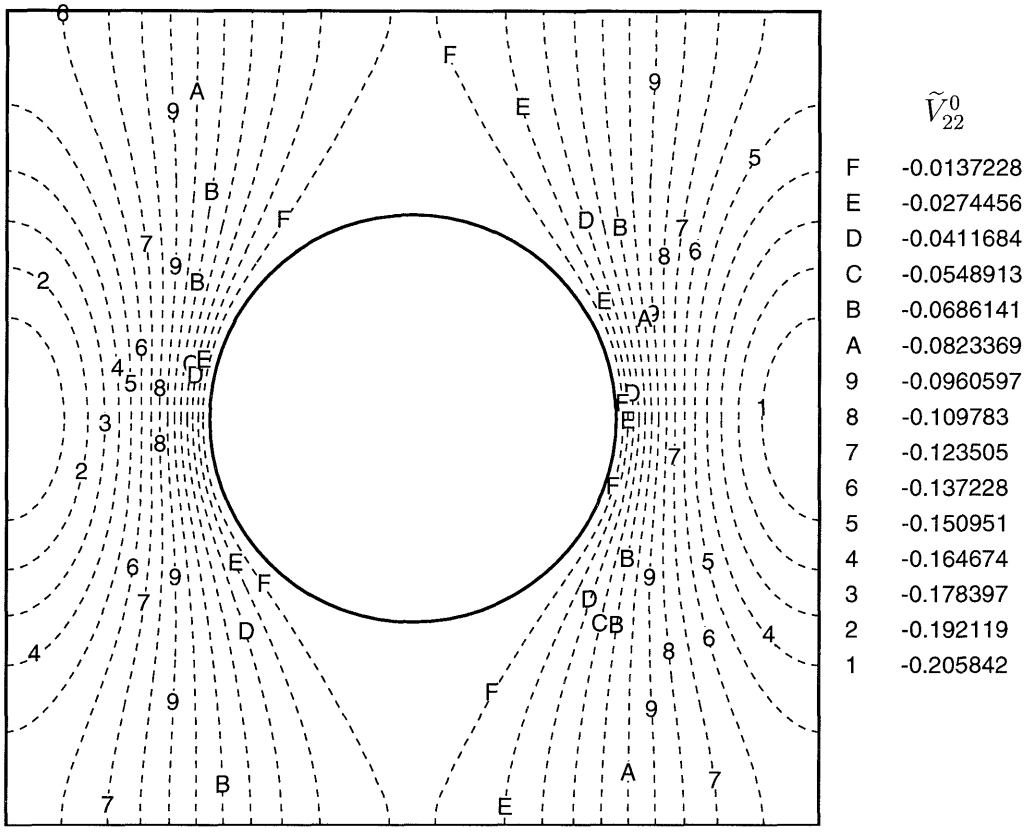

Figure C-5: Contours of $\widetilde{V}_{22}^{0}$ from the $\mathcal{O}(0)$ cell problem for a square array of circular cylinders of volume fraction $\phi = 0.2$.

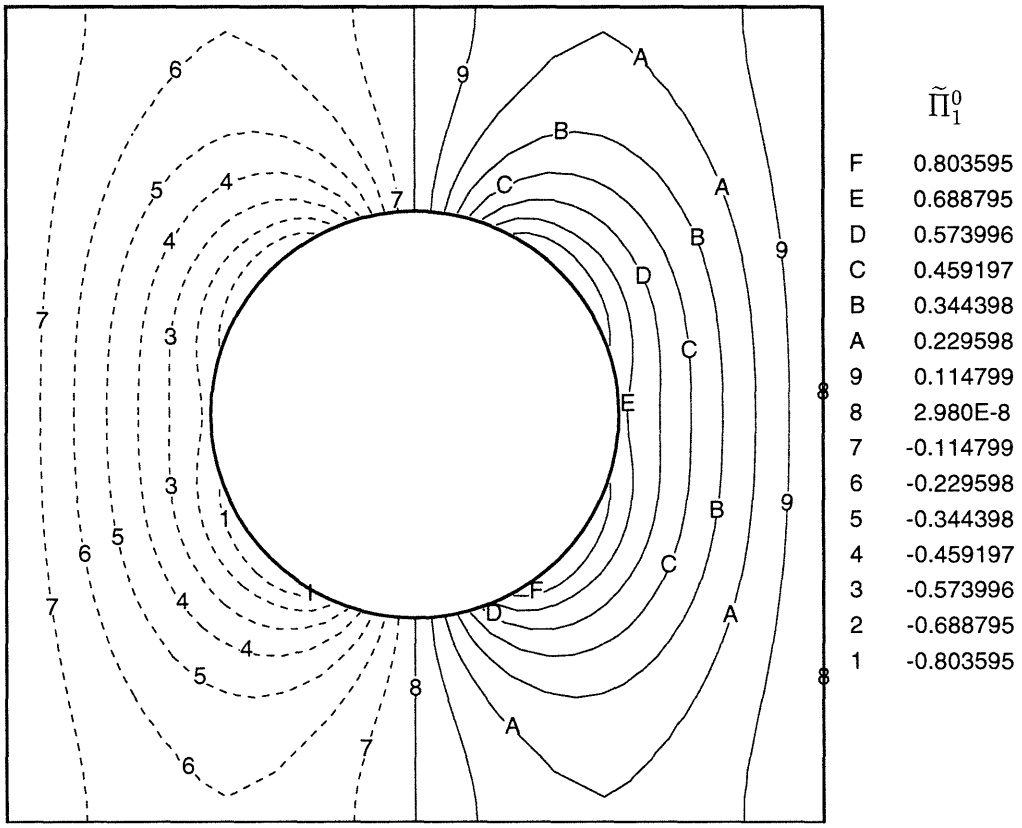

Figure C-6: Contours of $\widetilde{\Pi}_1^0$ from the $\mathcal{O}(0)$ cell problem for a square array of circular cylinders of volume fraction $\phi = 0.2$.

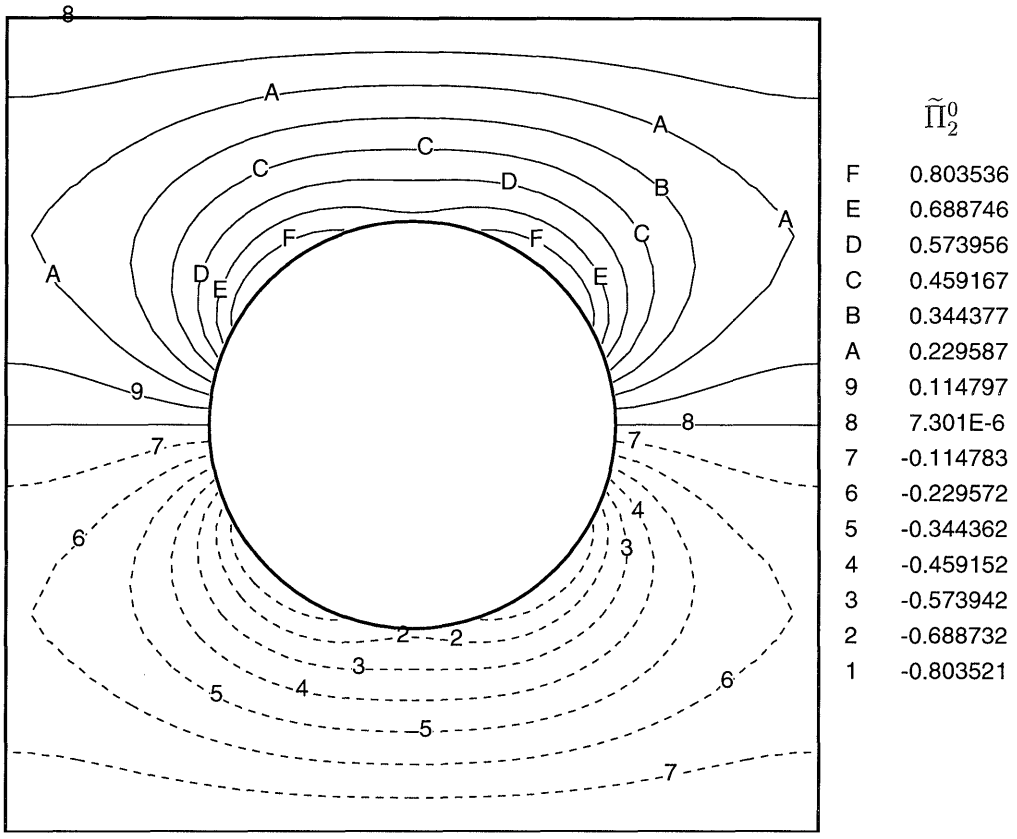

Figure C-7: Contours of $\widetilde{\Pi}_2^0$ from the $\mathcal{O}(0)$ cell problem for a square array of circular cylinders of volume fraction $\phi = 0.2$.

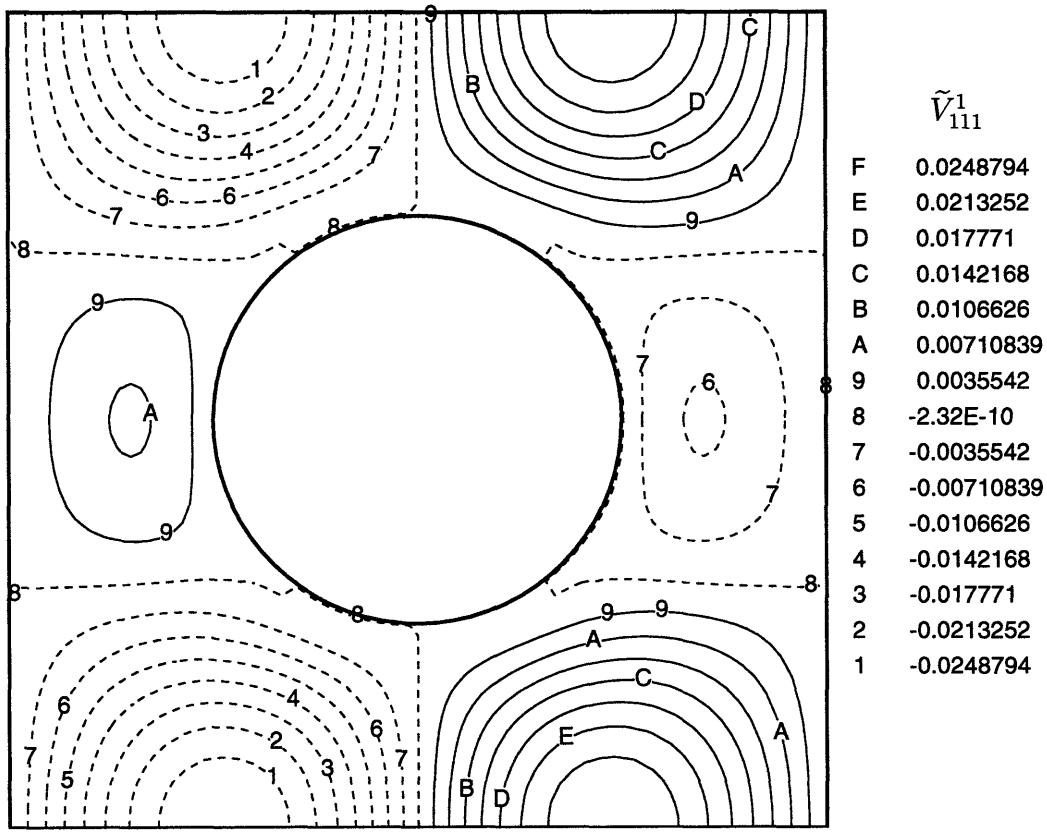

Figure C-8: Contours of $\tilde{V}^1_{111}$ from the $\mathcal{O}(1)$ cell problem for a square array of circular cylinders of volume fraction $\phi = 0.2$.

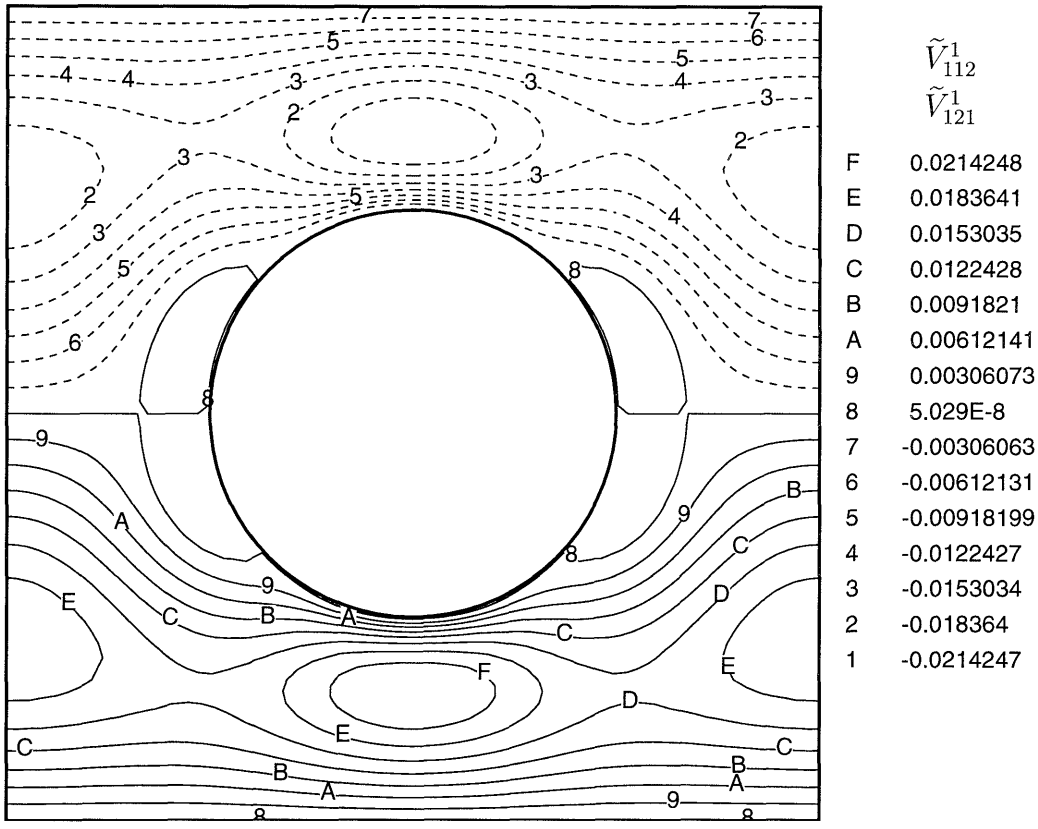

Figure C-9: Contours of $\widetilde{V}^1_{112}$ (or $\widetilde{V}^1_{121}$) from the $\mathcal{O}(1)$ cell problem for a square array of circular cylinders of volume fraction $\phi = 0.2$.

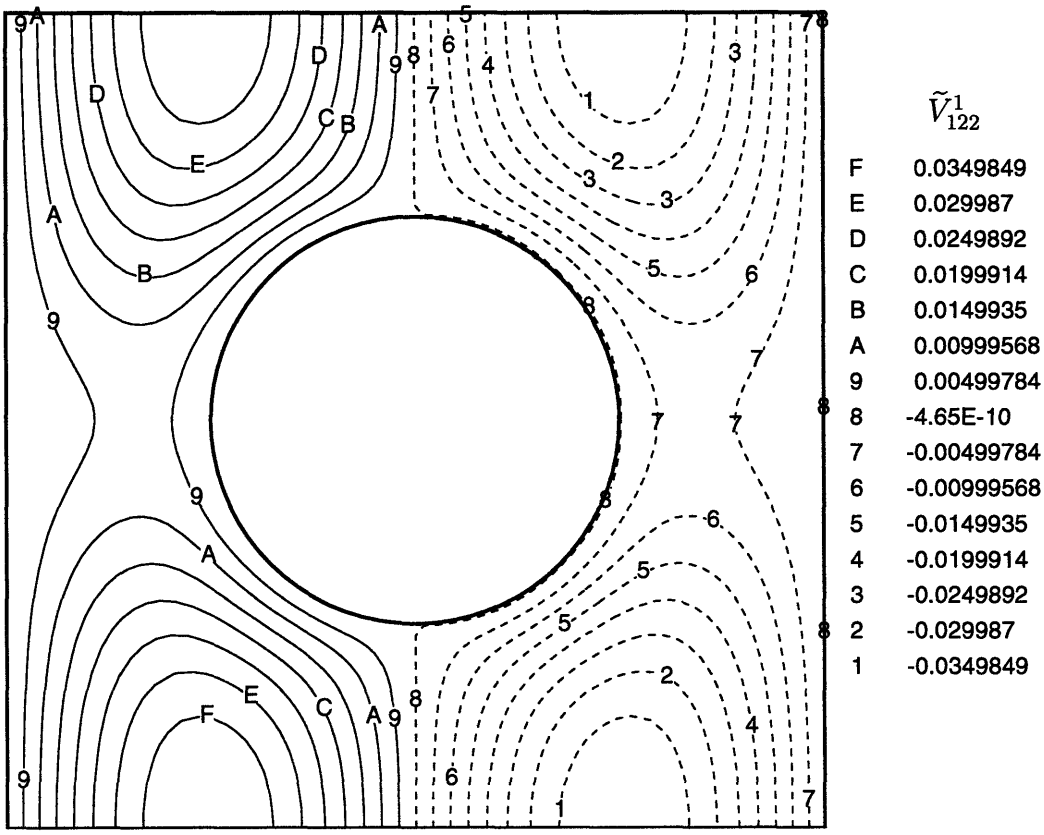

Figure C-10: Contours of $\tilde{V}^1_{122}$ from the $\mathcal{O}(1)$ cell problem for a square array of circular cylinders of volume fraction $\phi = 0.2$.

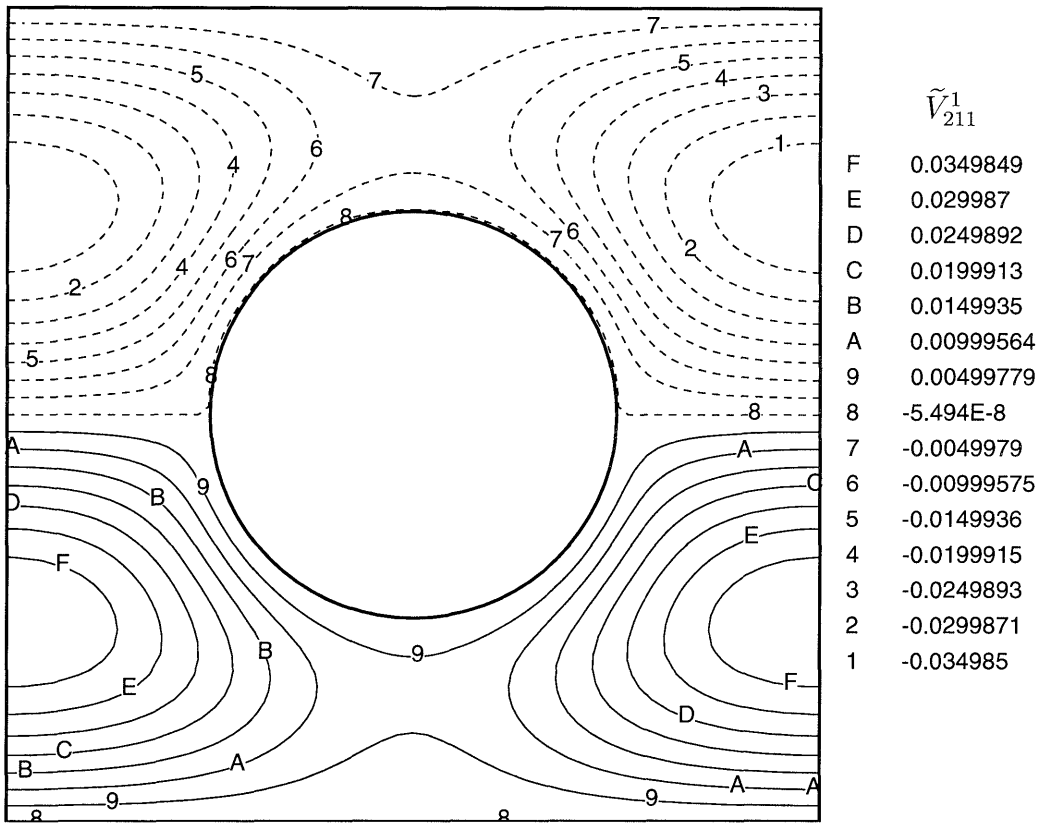

Figure C-11: Contours of $\widetilde{V}^1_{211}$ from the $\mathcal{O}(1)$ cell problem for a square array of circular cylinders of volume fraction $\phi = 0.2$.

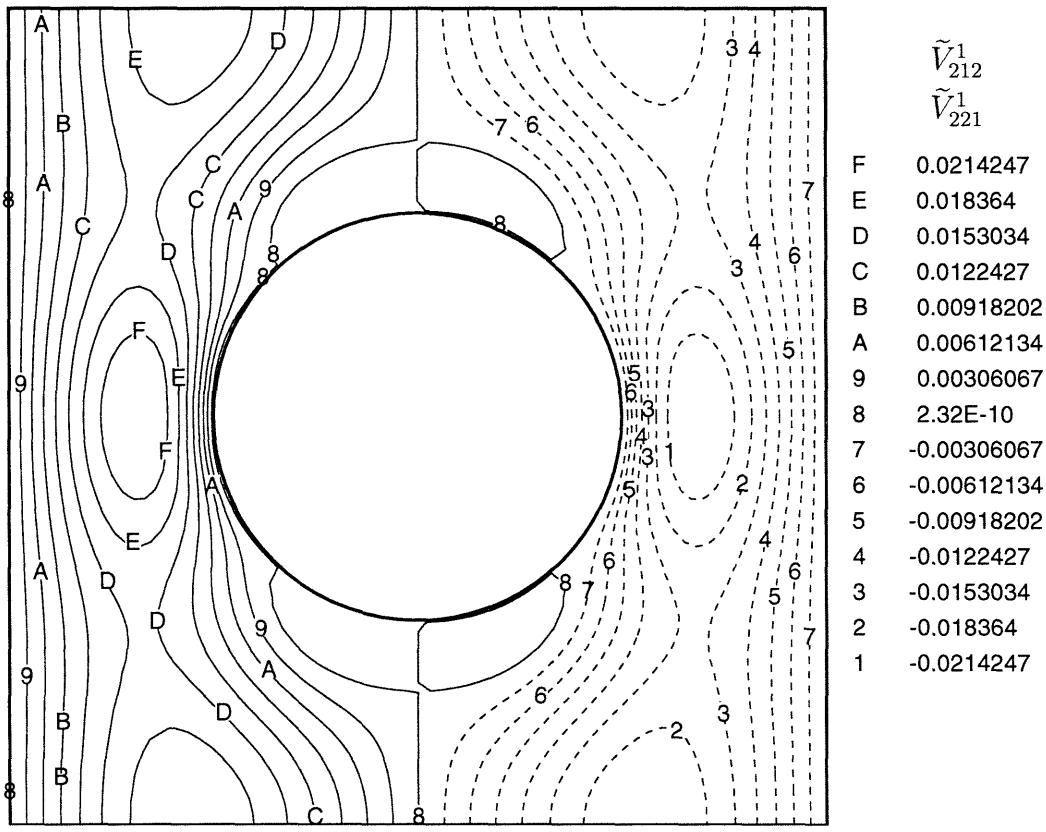

Figure C-12: Contours of $\widetilde{V}^1_{212}$ (or $\widetilde{V}^1_{221}$) from the $\mathcal{O}(1)$ cell problem for a square array of circular cylinders of volume fraction $\phi = 0.2$.

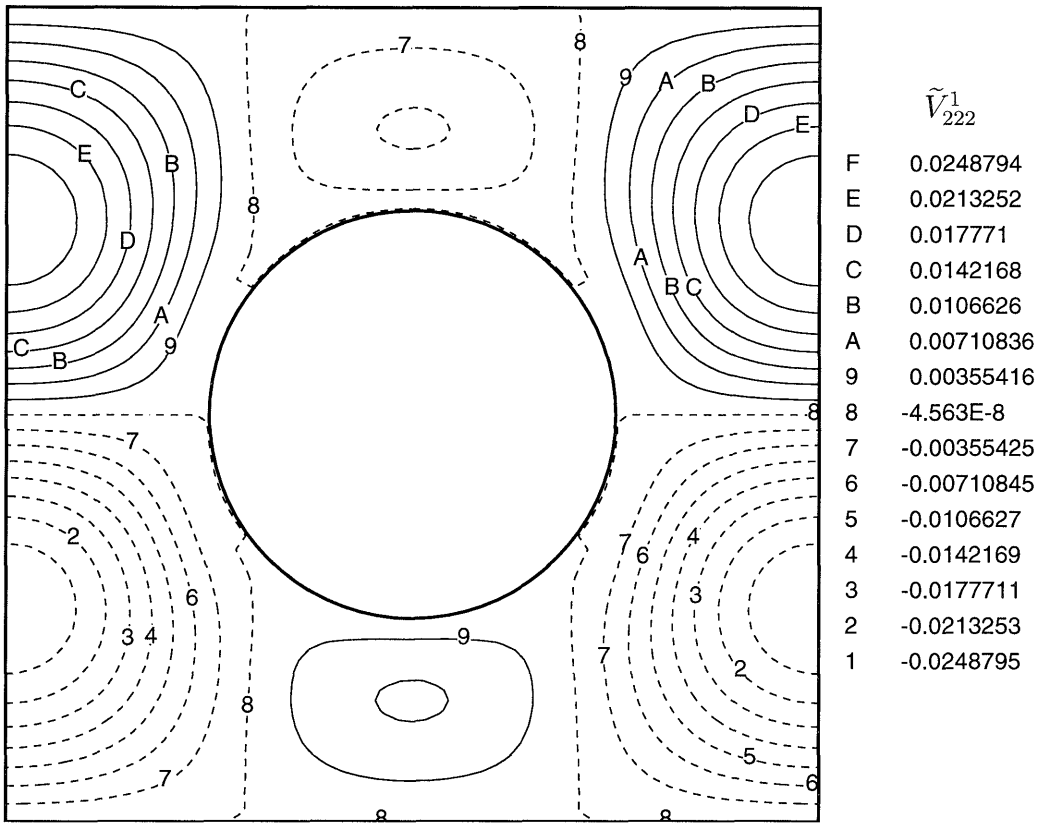

Figure C-13: Contours of $\widetilde{V}^1_{222}$ from the $\mathcal{O}(1)$ cell problem for a square array of circular cylinders of volume fraction $\phi = 0.2$.

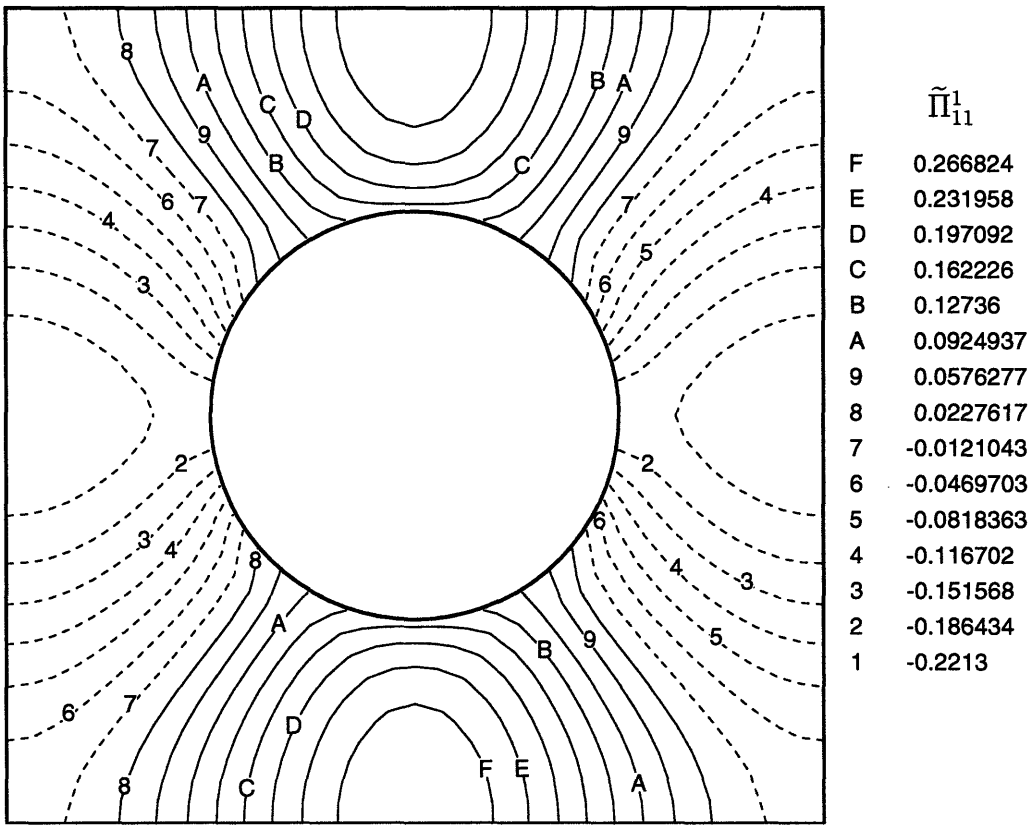

Figure C-14: Contours of $\widetilde{\Pi}^1_{11}$ from the $\mathcal{O}(1)$ cell problem for a square array of circular cylinders of volume fraction $\phi = 0.2$.

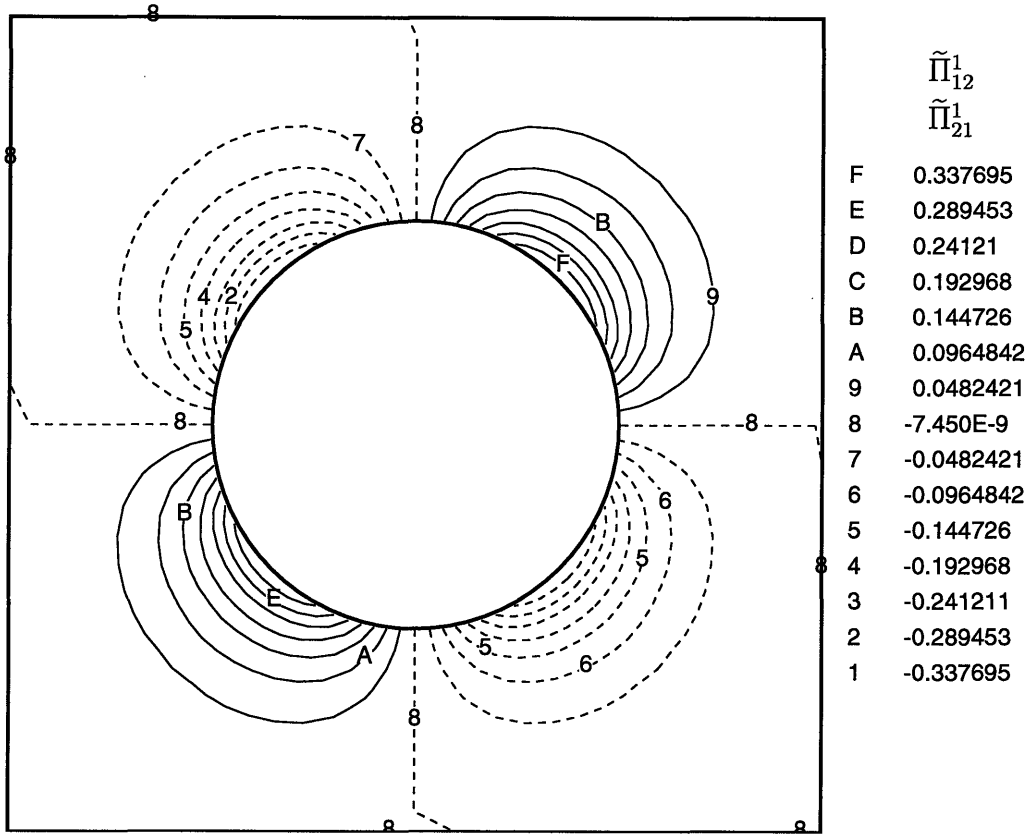

Figure C-15: Contours of $\tilde{\Pi}^1_{12}$ (or $\tilde{\Pi}^1_{21}$) from the $\mathcal{O}(1)$ cell problem for a square array of circular cylinders of volume fraction $\phi = 0.2$.

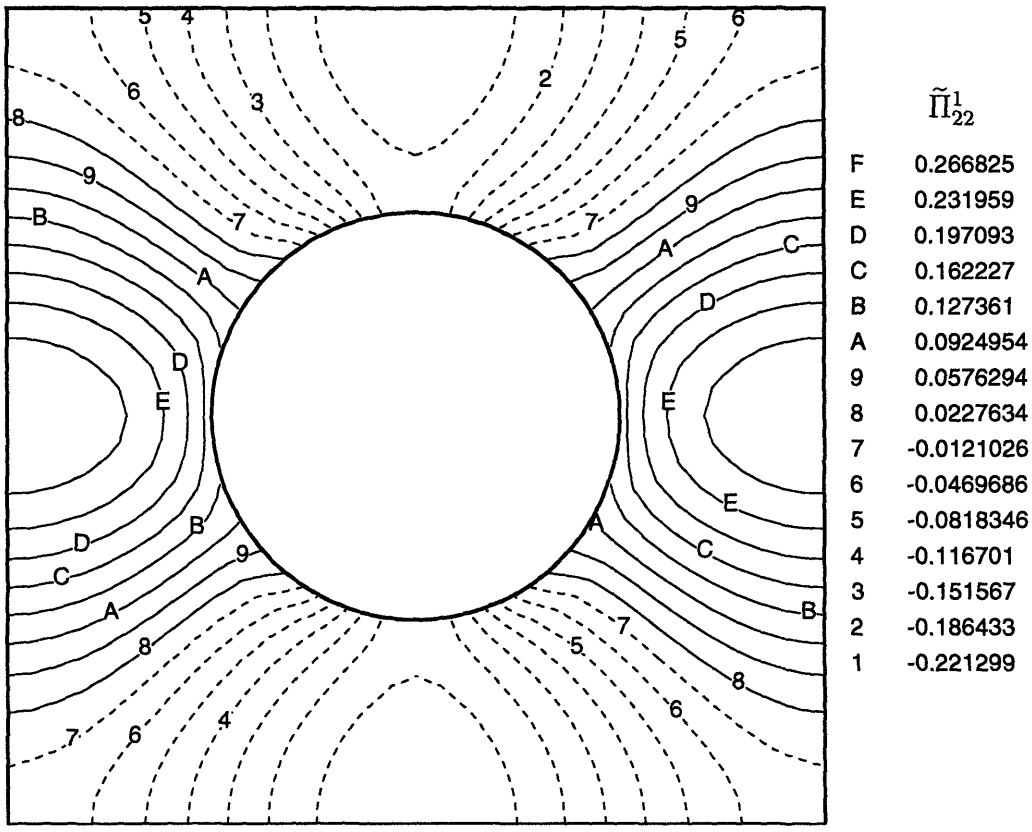

Figure C-16: Contours of $\widetilde{\Pi}^1_{22}$ from the $\mathcal{O}(1)$ cell problem for a square array of circular cylinders of volume fraction $\phi = 0.2$.

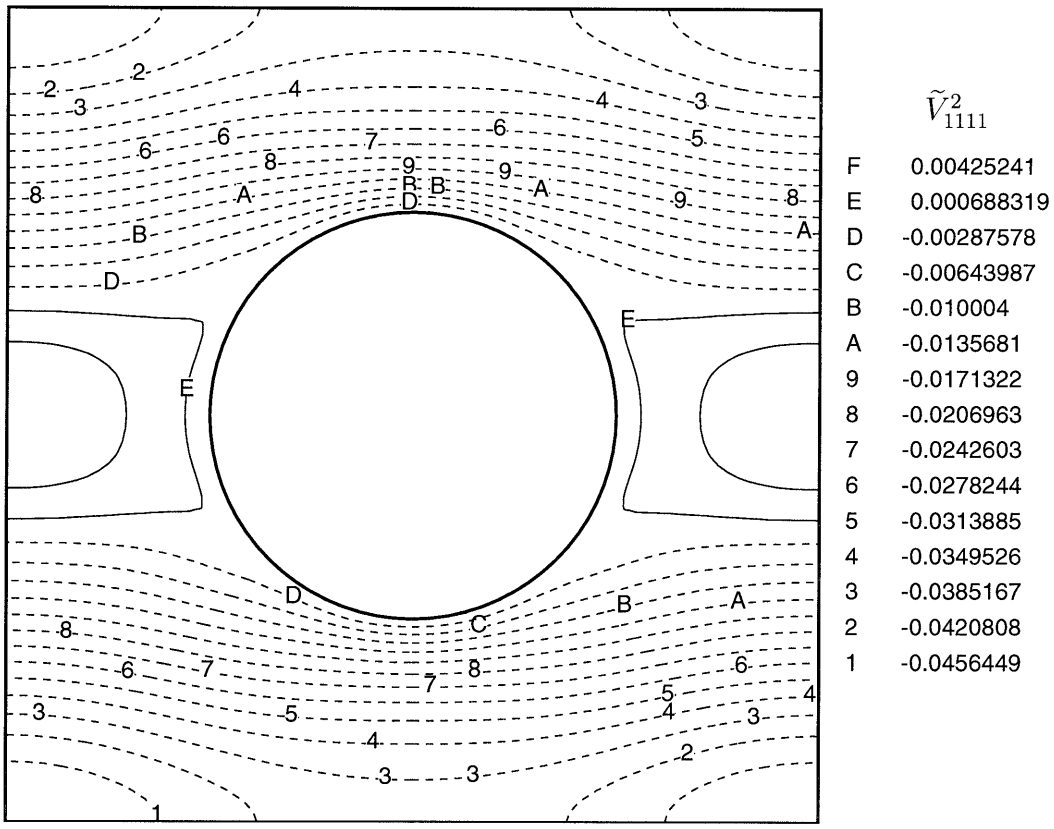

Figure C-17: Contours of $\widetilde{V}^2_{1111}$ from the $\mathcal{O}(2)$ cell problem for a square array of circular cylinders of volume fraction $\phi = 0.2$.

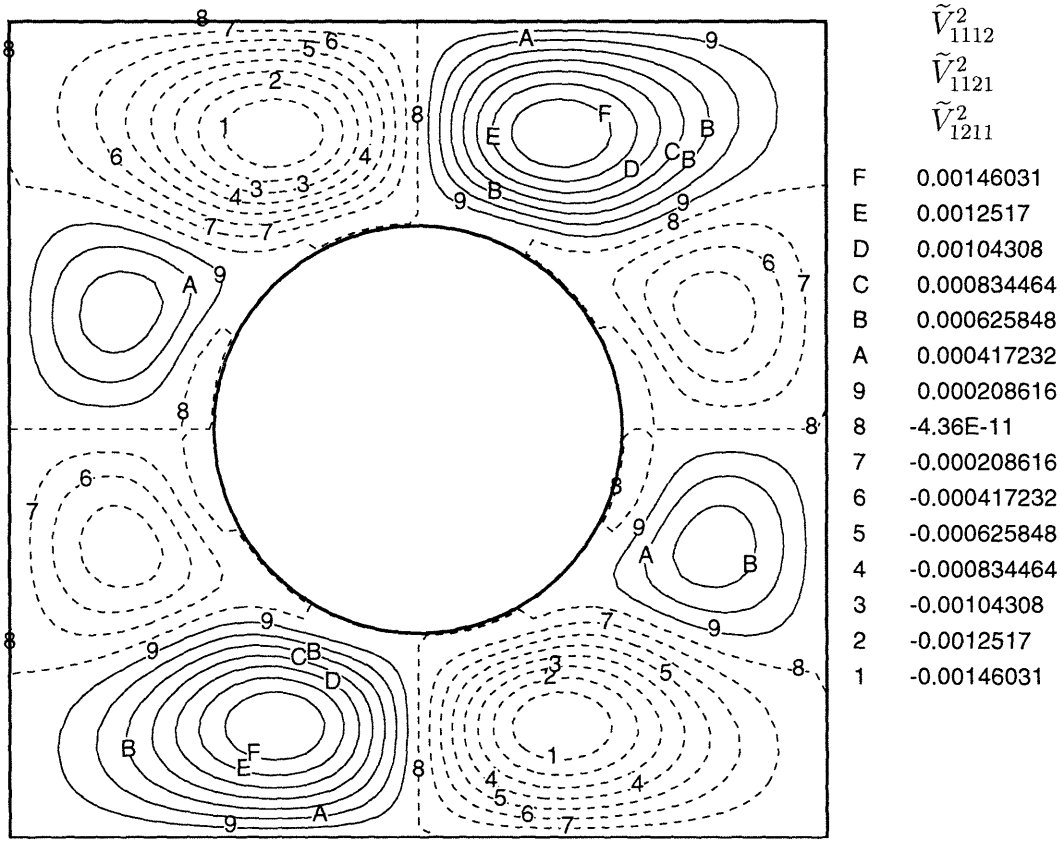

Figure C-18: Contours of $\widetilde{V}^2_{1112}$ (or $\widetilde{V}^2_{1121}$ or $\widetilde{V}^2_{1211}$) from the $\mathcal{O}(2)$ cell problem for a square array of circular cylinders of volume fraction $\phi = 0.2$.

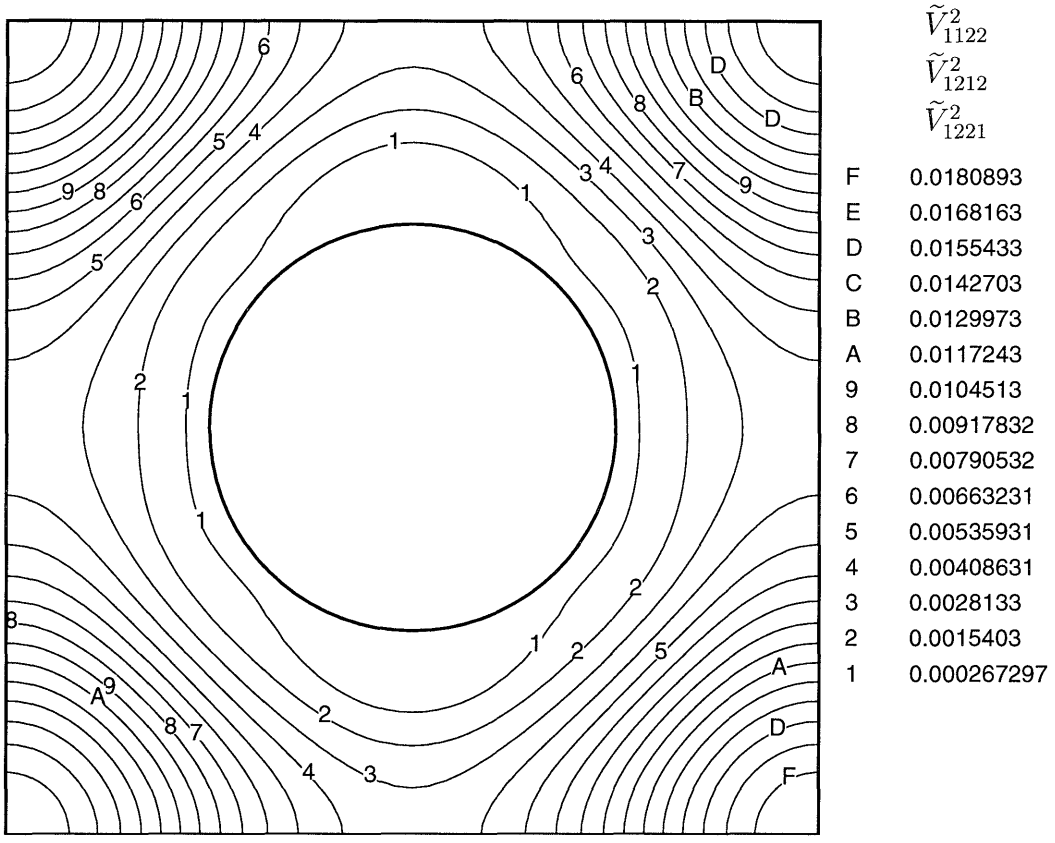

Figure C-19: Contours of $\widetilde{V}^2_{1122}$ (or $\widetilde{V}^2_{1212}$ or $\widetilde{V}^2_{1221}$) from the $\mathcal{O}(2)$ cell problem for a square array of circular cylinders of volume fraction $\phi = 0.2$.

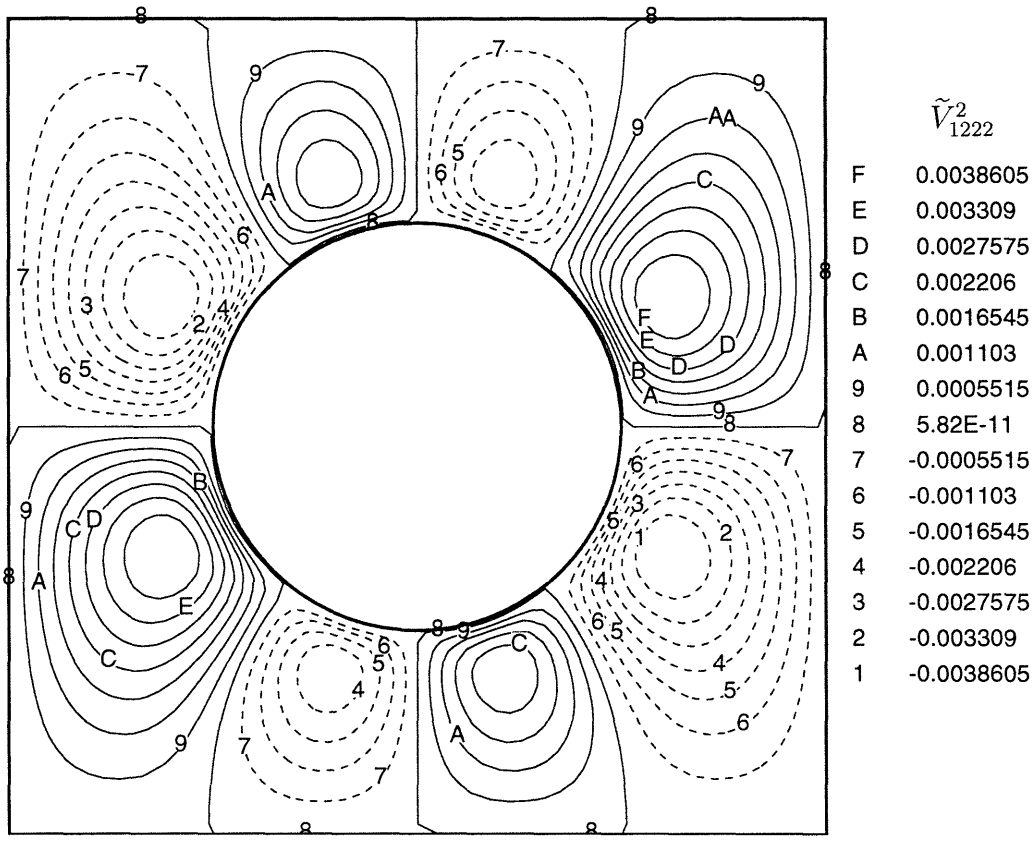

Figure C-20: Contours of $\tilde{V}^2_{1222}$ from the $\mathcal{O}(2)$ cell problem for a square array of circular cylinders of volume fraction $\phi = 0.2$.

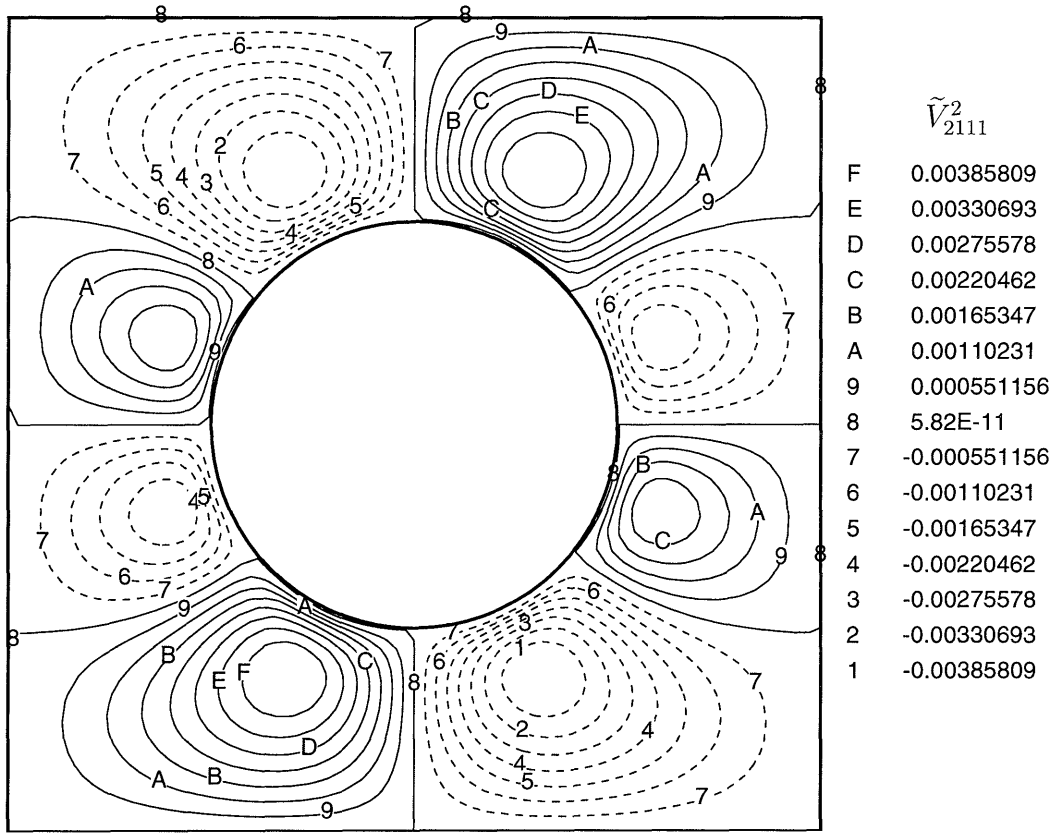

Figure C-21: Contours of $\tilde{V}^2_{2111}$ from the $\mathcal{O}(2)$ cell problem for a square array of circular cylinders of volume fraction $\phi = 0.2$.

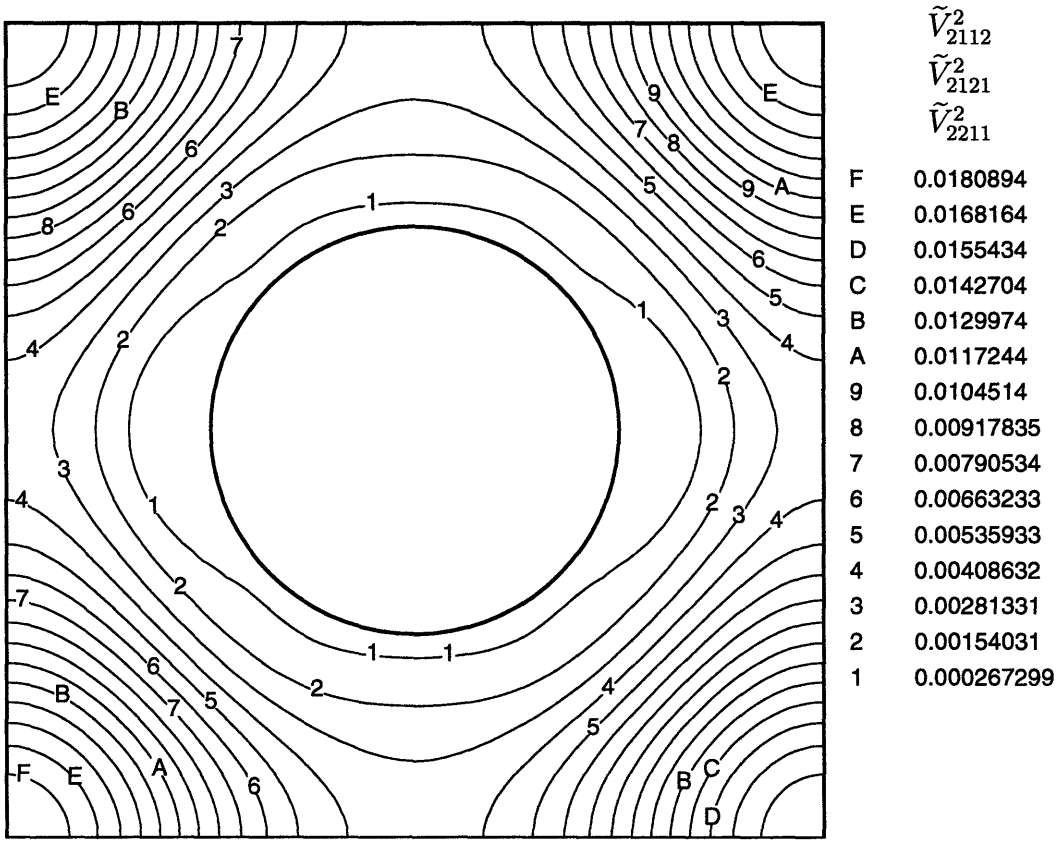

Figure C-22: Contours of $\tilde{V}^2_{2112}$ (or $\tilde{V}^2_{2121}$ or $\tilde{V}^2_{2211}$) from the $\mathcal{O}(2)$ cell problem for a square array of circular cylinders of volume fraction $\phi = 0.2$.

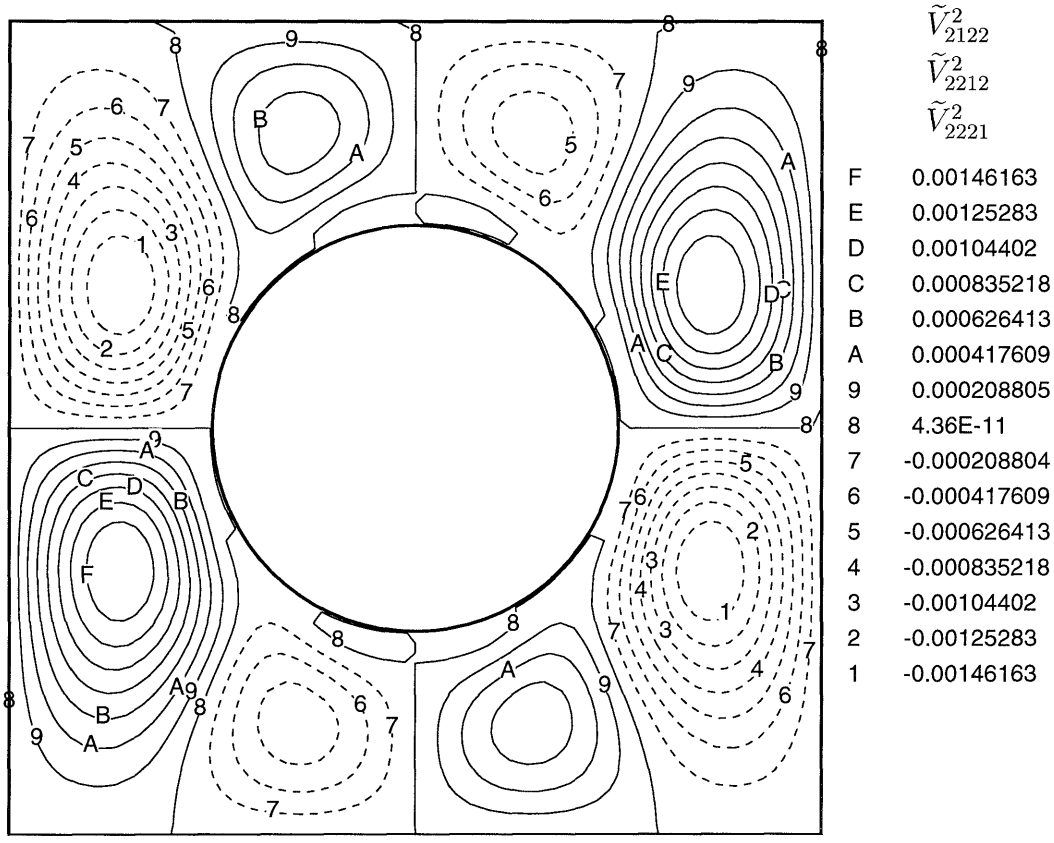

Figure C-23: Contours of $\tilde{V}^2_{2122}$ (or $\tilde{V}^2_{2212}$ or $\tilde{V}^2_{2221}$) from the $\mathcal{O}(2)$ cell problem for a square array of circular cylinders of volume fraction $\phi = 0.2$.

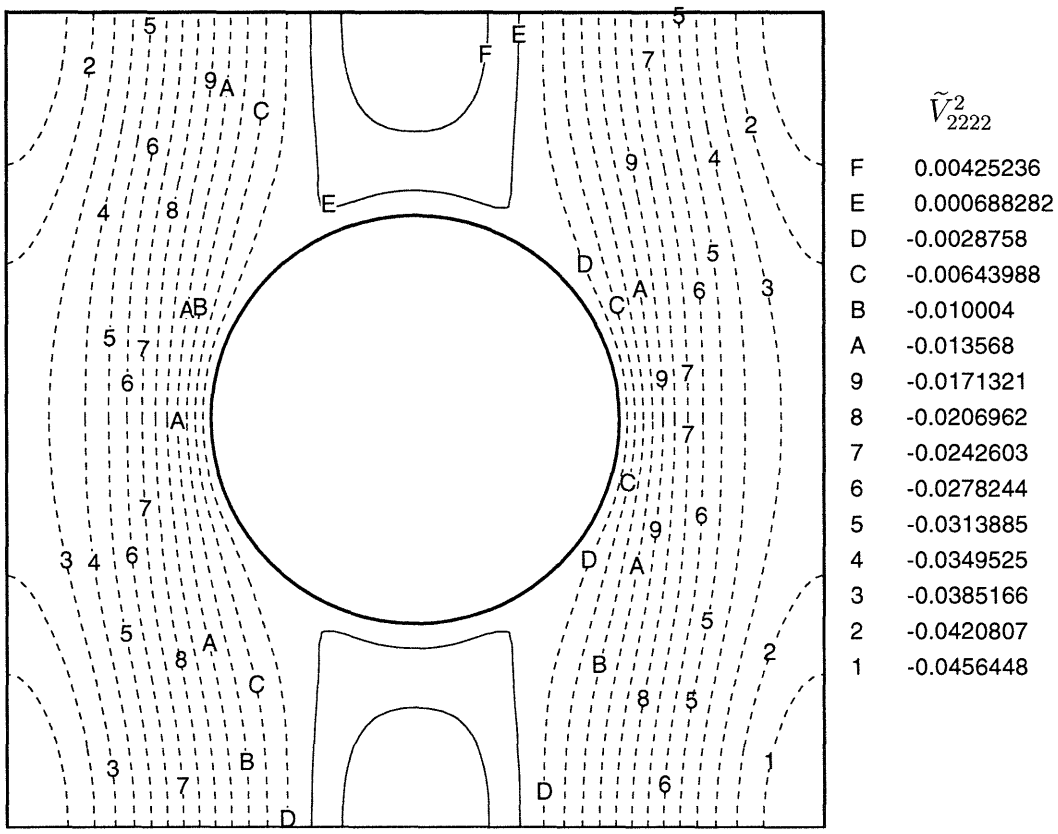

Figure C-24: Contours of $\tilde{V}^2_{2222}$ from the $\mathcal{O}(2)$ cell problem for a square array of circular cylinders of volume fraction $\phi = 0.2$.

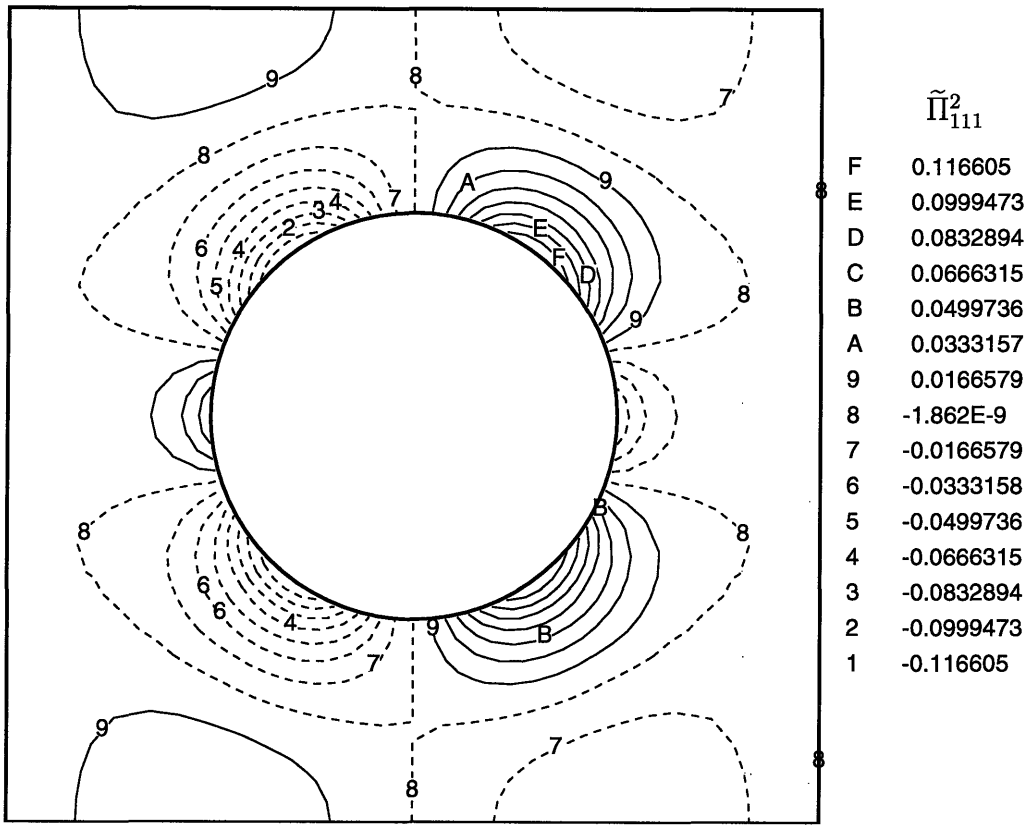

Figure C-25: Contours of $\tilde{\Pi}^2_{111}$ from the $\mathcal{O}(2)$ cell problem for a square array of circular cylinders of volume fraction $\phi = 0.2$.

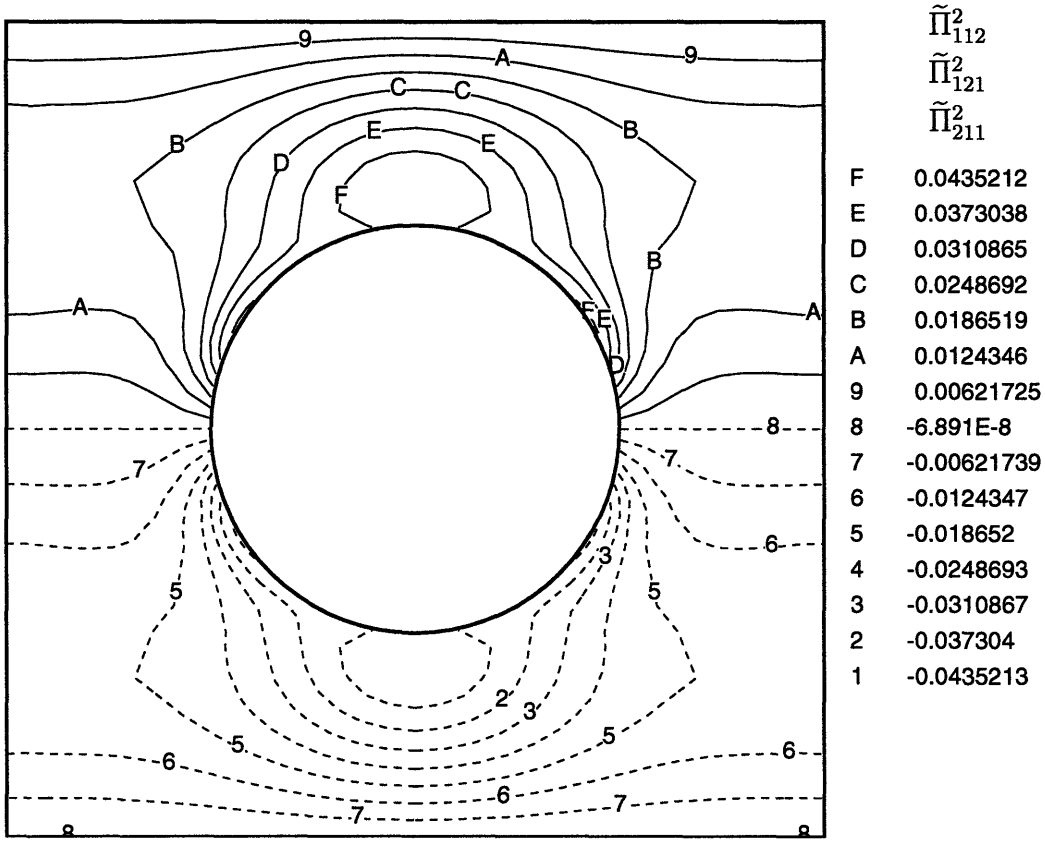

Figure C-26: Contours of $\tilde{\Pi}^2_{112}$ (or $\tilde{\Pi}^2_{121}$ or $\tilde{\Pi}^2_{211}$) from the $\mathcal{O}(2)$ cell problem for a square array of circular cylinders of volume fraction $\phi = 0.2$.

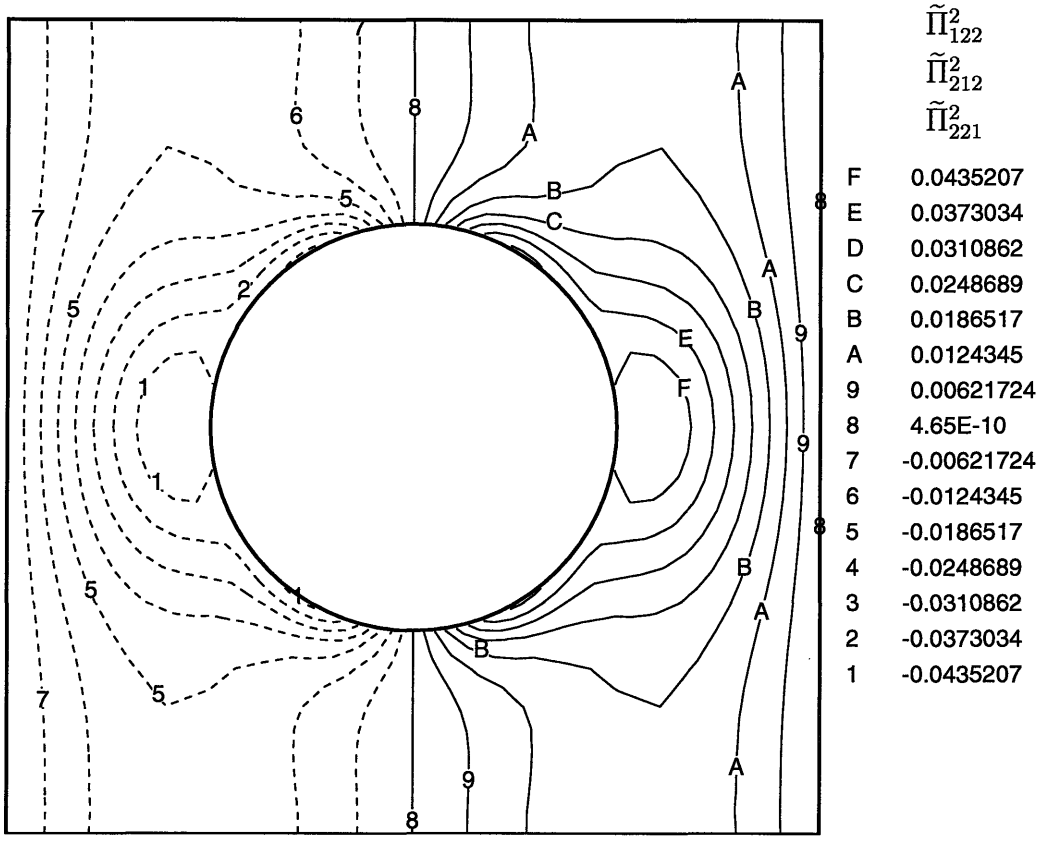

Figure C-27: Contours of $\tilde{\Pi}^2_{122}$ (or $\tilde{\Pi}^2_{212}$ or $\tilde{\Pi}^2_{221}$) from the $\mathcal{O}(2)$ cell problem for a square array of circular cylinders of volume fraction $\phi = 0.2$.

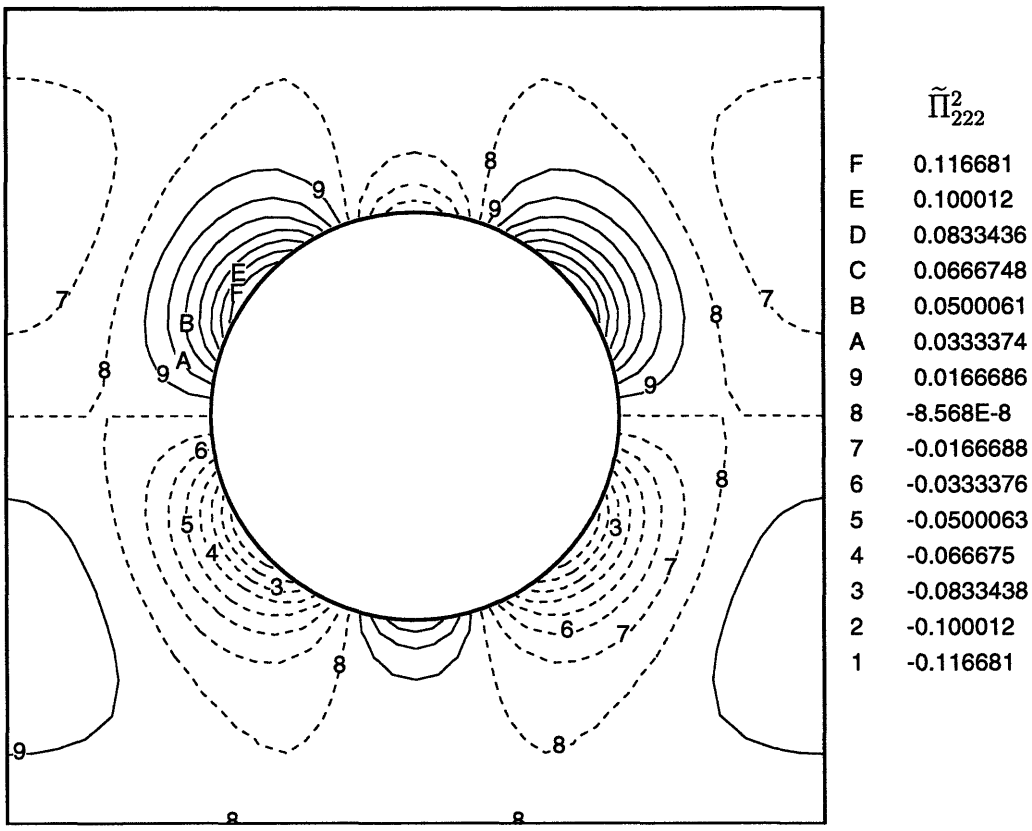

Figure C-28: Contours of $\widetilde{\Pi}^2_{222}$ from the $\mathcal{O}(2)$ cell problem for a square array of circular cylinders of volume fraction $\phi = 0.2$.

Appendix D

Elliptical Cylinder Lattice Fields

The first three microscale lattice fields for a square array of elliptical cylinders of volume fraction $\phi = 0.2$ and eccentricity $e = 2$ is shown here. Figure D-1 is the mesh of the unit cell. The various independent components of the fields $\left(\widetilde{\mathbf{V}}^0, \widetilde{\mathbf{\Pi}}^0\right)$, $\left(\widetilde{\mathbf{V}}^1, \widetilde{\mathbf{\Pi}}^1\right)$ and $\left(\widetilde{\mathbf{V}}^2, \widetilde{\mathbf{\Pi}}^2\right)$ are shown in Figures D-2–D-7, Figures D-8–D-16 and Figures D-17–D-28 respectively. For the given mesh, there corresponded 800 elements, 3360 nodes and 7600 equations (or unknowns).

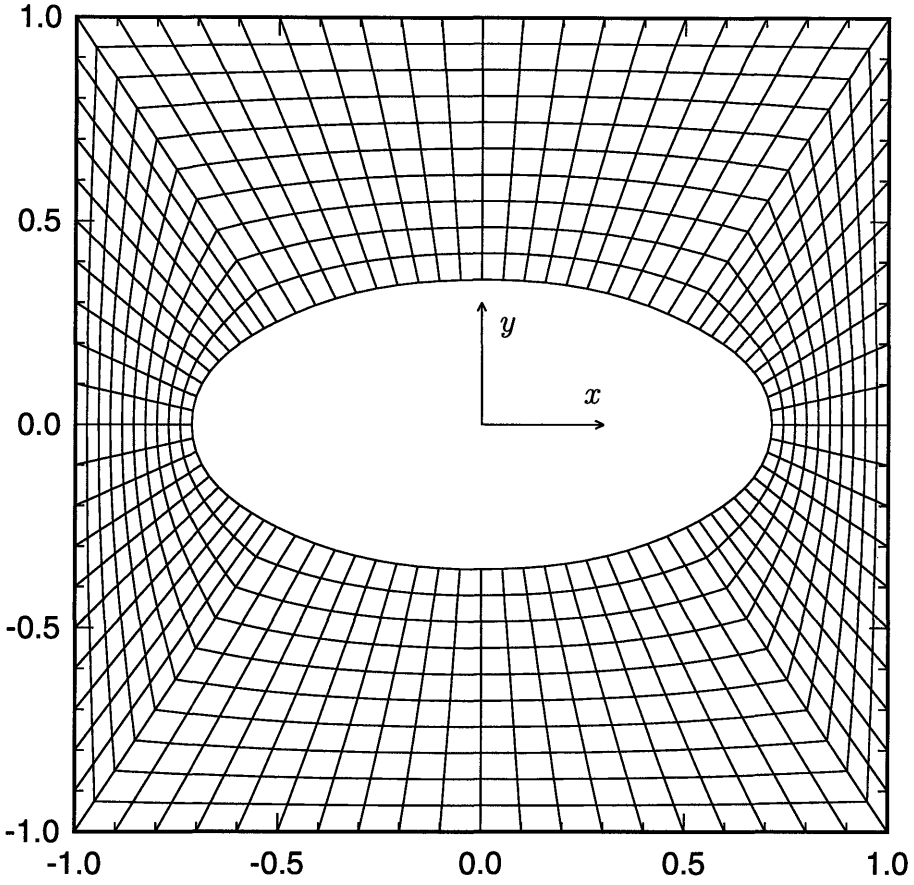

Figure D-1: Sample mesh of a square array of elliptical cylinders ($\phi = 0.2$, $e = 2$). There are 800 elements, 3360 nodes and 7600 eqations. This unit cell has a 'volume' $\tau_0 = 4$.

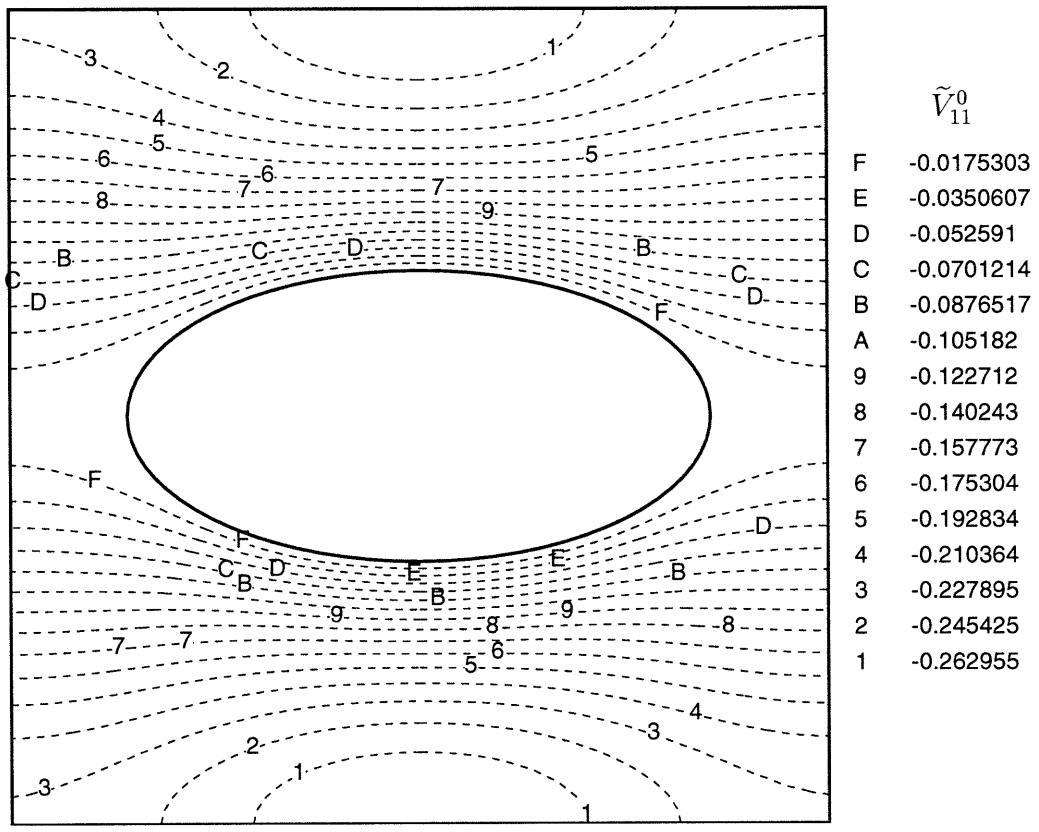

Figure D-2: Contours of $\widetilde{V}_{11}^{0}$ from the $\mathcal{O}(0)$ cell problem for a square array of elliptical cylinders of volume fraction $\phi = 0.2$ and eccentricity $e = 2$.

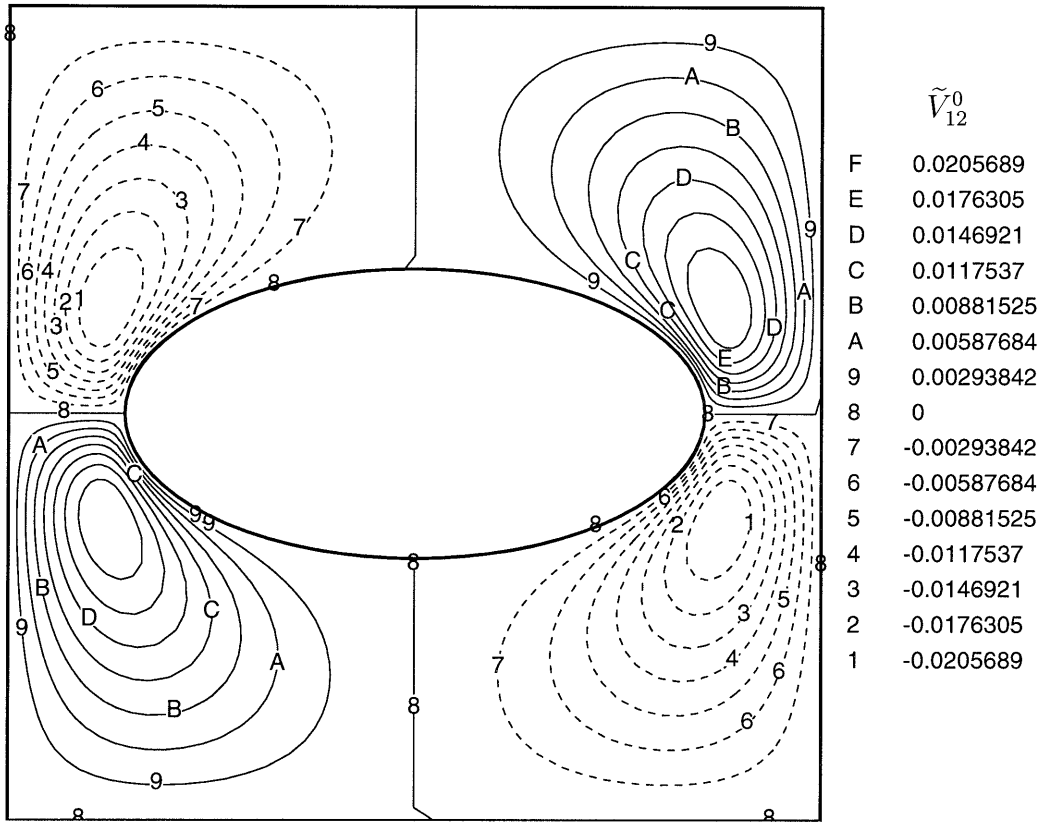

Figure D-3: Contours of $\widetilde{V}_{12}^{0}$ from the $\mathcal{O}(0)$ cell problem for a square array of elliptical cylinders of volume fraction $\phi = 0.2$ and eccentricity $e = 2$.

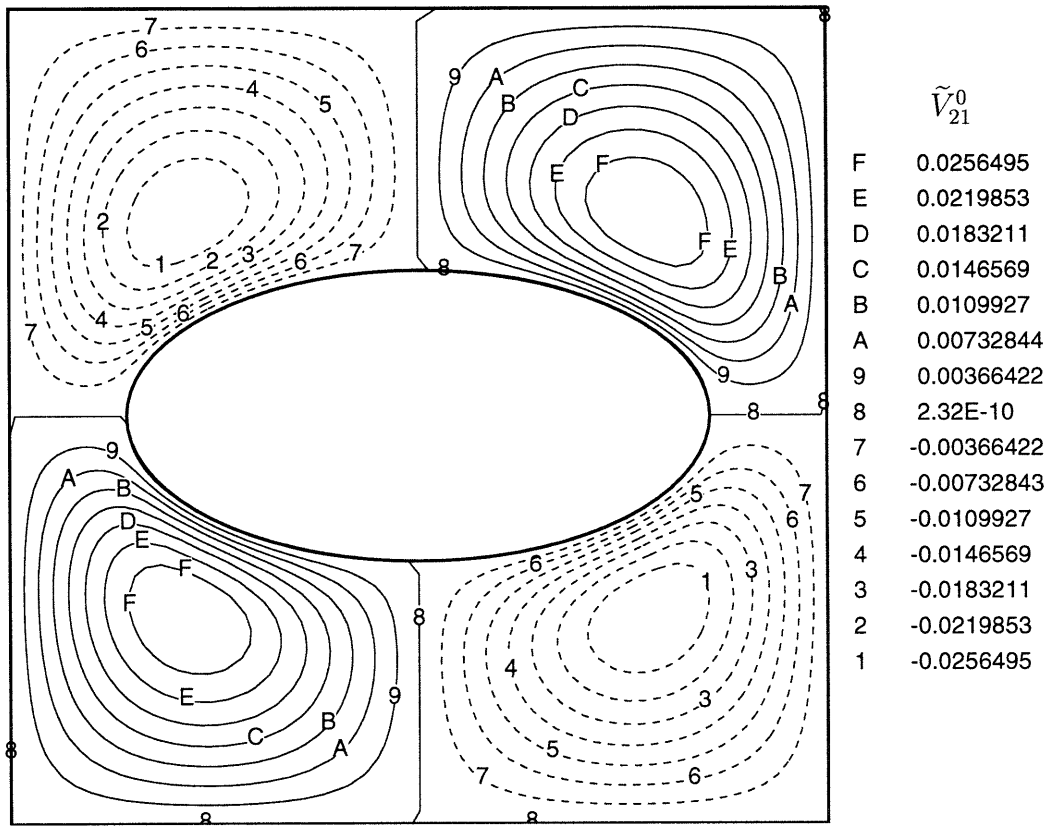

Figure D-4: Contours of $\widetilde{V}_{21}^{0}$ from the $\mathcal{O}(0)$ cell problem for a square array of elliptical cylinders of volume fraction $\phi = 0.2$ and eccentricity $e = 2$.

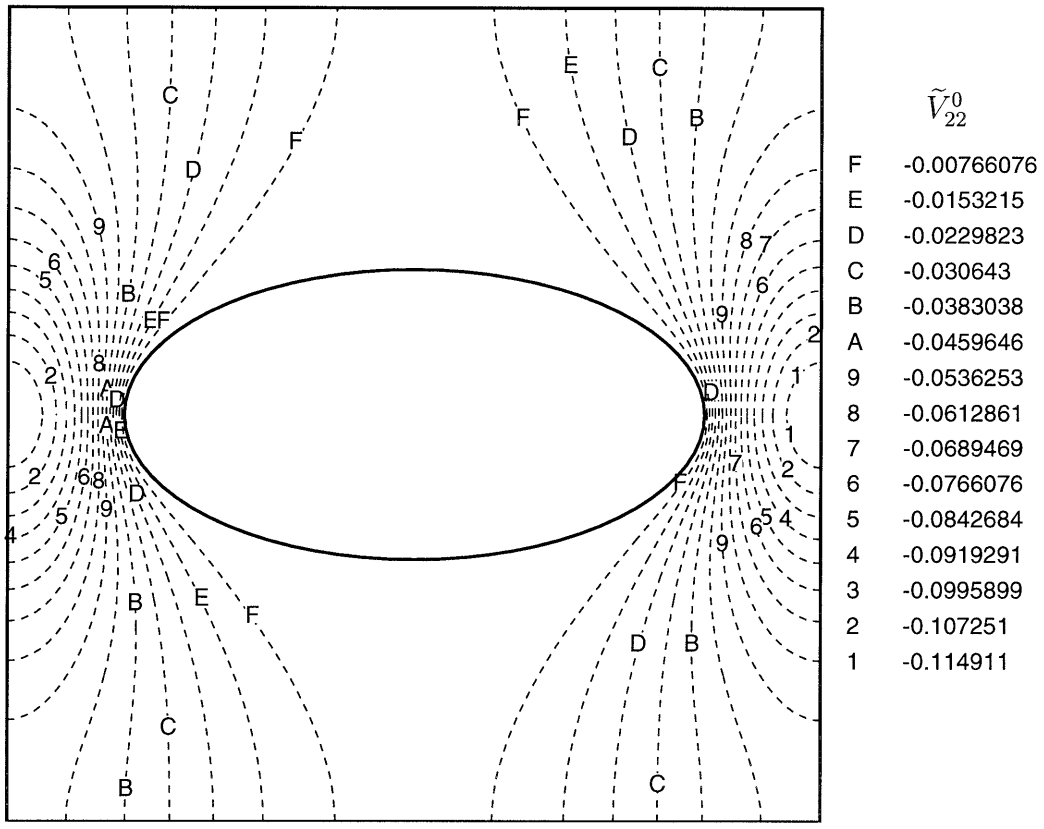

Figure D-5: Contours of $\widetilde{V}_{22}^{0}$ from the $\mathcal{O}(0)$ cell problem for a square array of elliptical cylinders of volume fraction $\phi = 0.2$ and eccentricity $e = 2$.

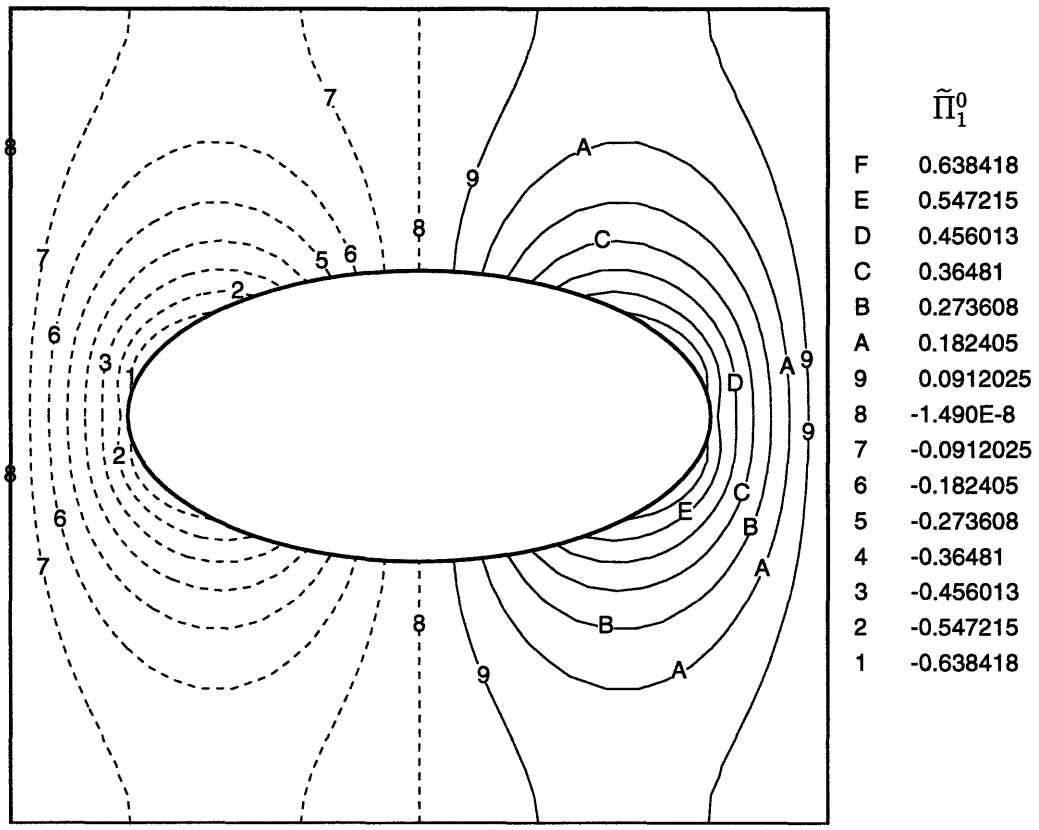

Figure D-6: Contours of $\widetilde{\Pi}_1^0$ from the $\mathcal{O}(0)$ cell problem for a square array of elliptical cylinders of volume fraction $\phi = 0.2$ and eccentricity $e = 2$.

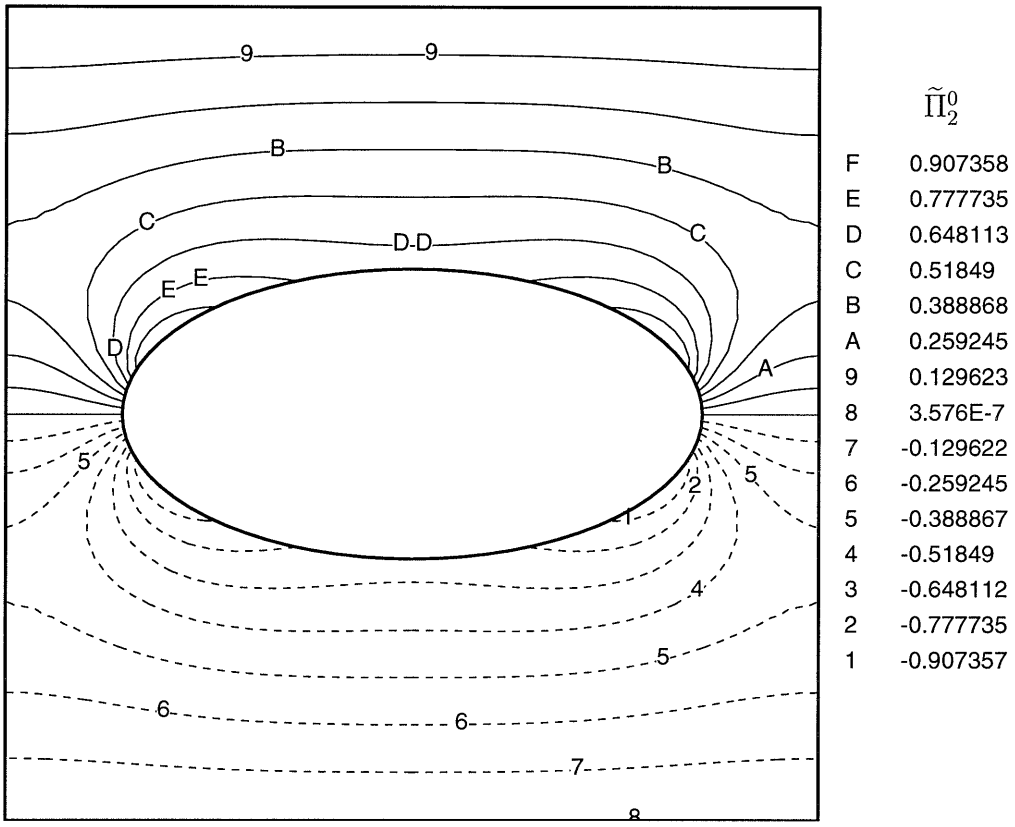

Figure D-7: Contours of $\widetilde{\Pi}_2^0$ from the $\mathcal{O}(0)$ cell problem for a square array of elliptical cylinders of volume fraction $\phi = 0.2$ and eccentricity $e = 2$.

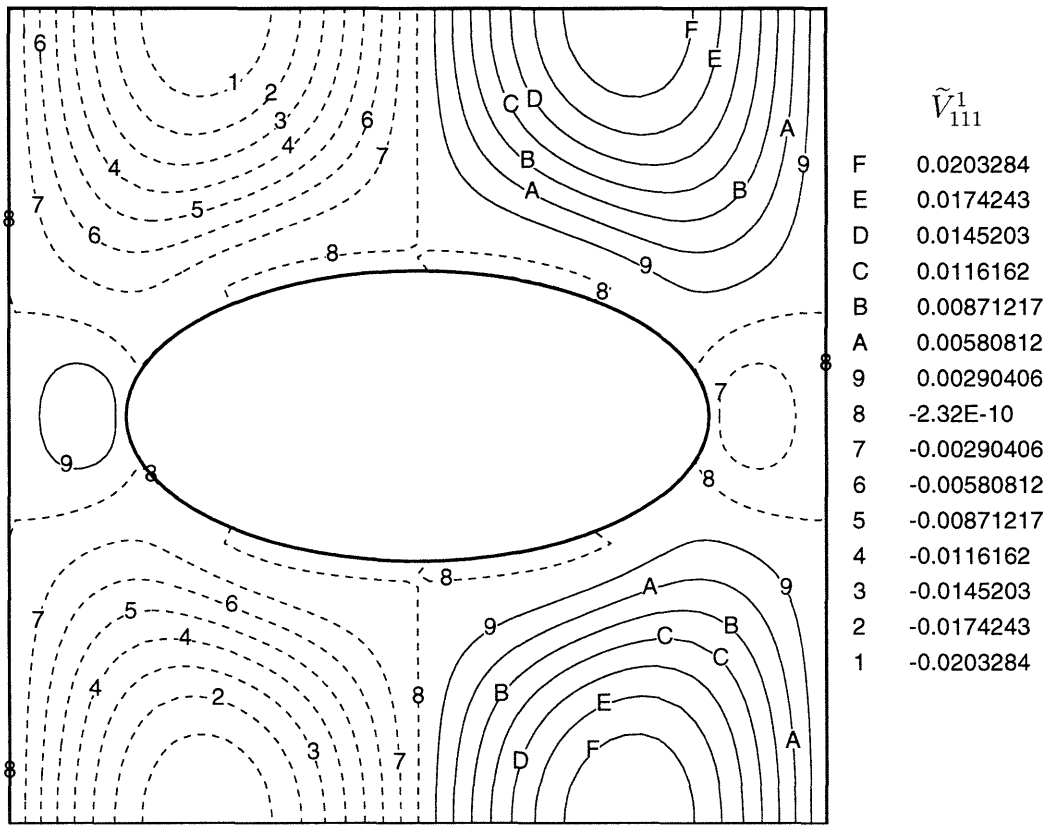

Figure D-8: Contours of $\widetilde{V}^1_{111}$ from the $\mathcal{O}(1)$ cell problem for a square array of elliptical cylinders of volume fraction $\phi = 0.2$ and eccentricity $e = 2$.

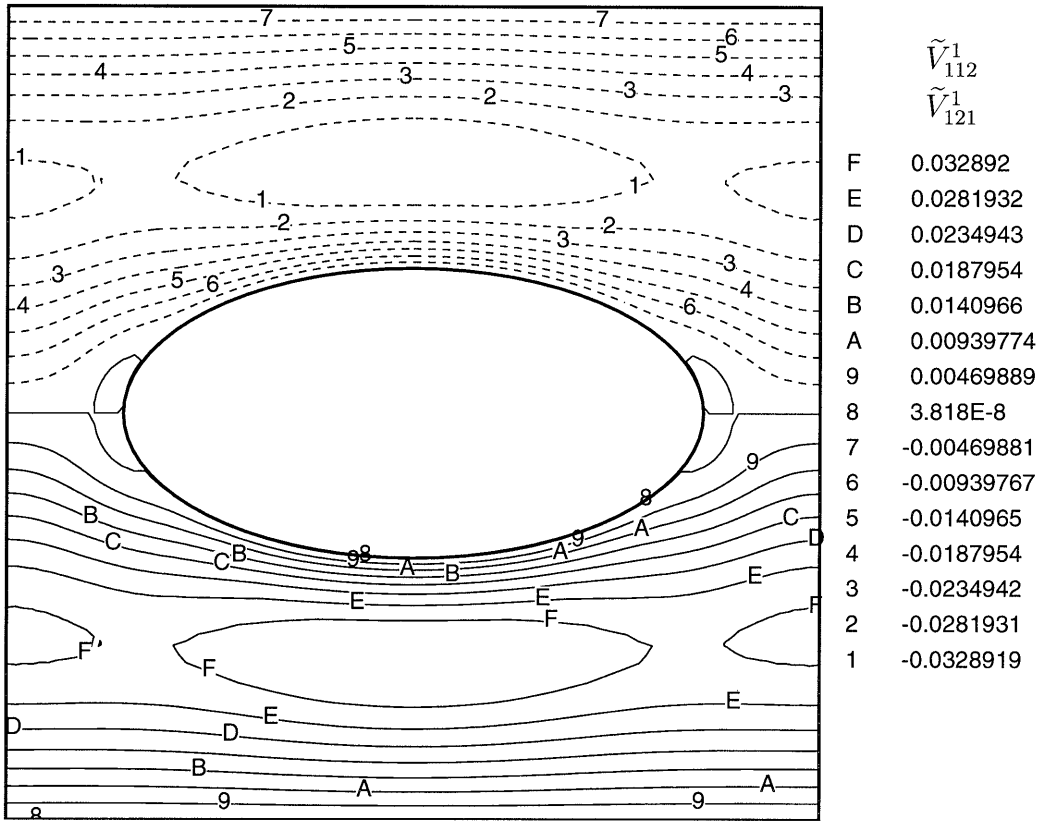

Figure D-9: Contours of $\widetilde{V}^1_{112}$ (or $\widetilde{V}^1_{121}$) from the $\mathcal{O}(1)$ cell problem for a square array of elliptical cylinders of volume fraction $\phi = 0.2$ and eccentricity $e = 2$.

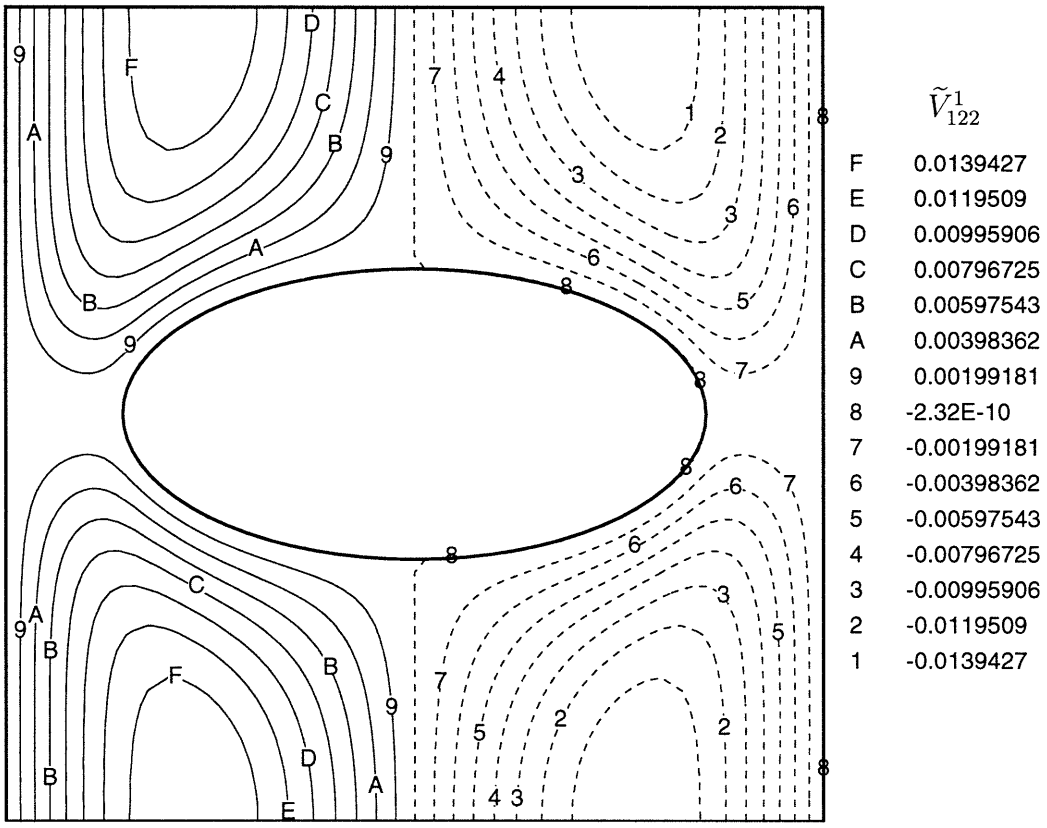

Figure D-10: Contours of $\tilde{V}^1_{122}$ from the $\mathcal{O}(1)$ cell problem for a square array of elliptical cylinders of volume fraction $\phi = 0.2$ and eccentricity $e = 2$.

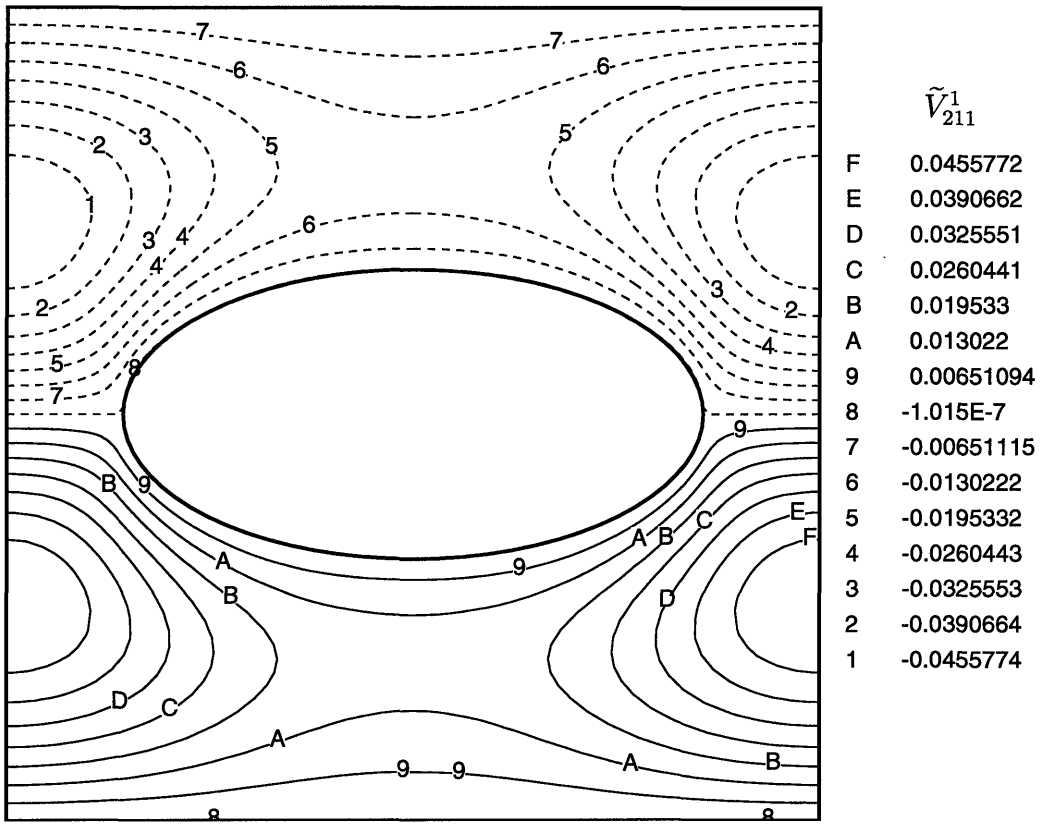

Figure D-11: Contours of $\tilde{V}^1_{211}$ from the $\mathcal{O}(1)$ cell problem for a square array of elliptical cylinders of volume fraction $\phi = 0.2$ and eccentricity $e = 2$.

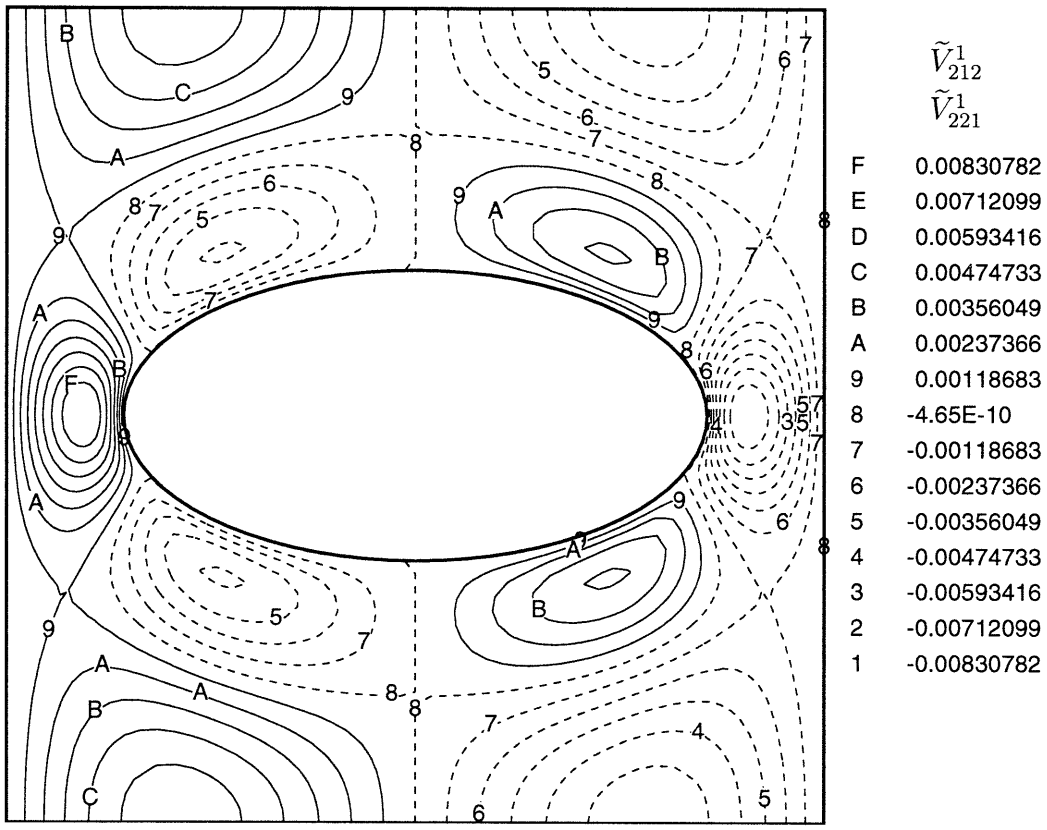

Figure D-12: Contours of $\tilde{V}^1_{212}$ (or $\tilde{V}^1_{221}$) from the $\mathcal{O}(1)$ cell problem for a square array of elliptical cylinders of volume fraction $\phi = 0.2$ and eccentricity $e = 2$.

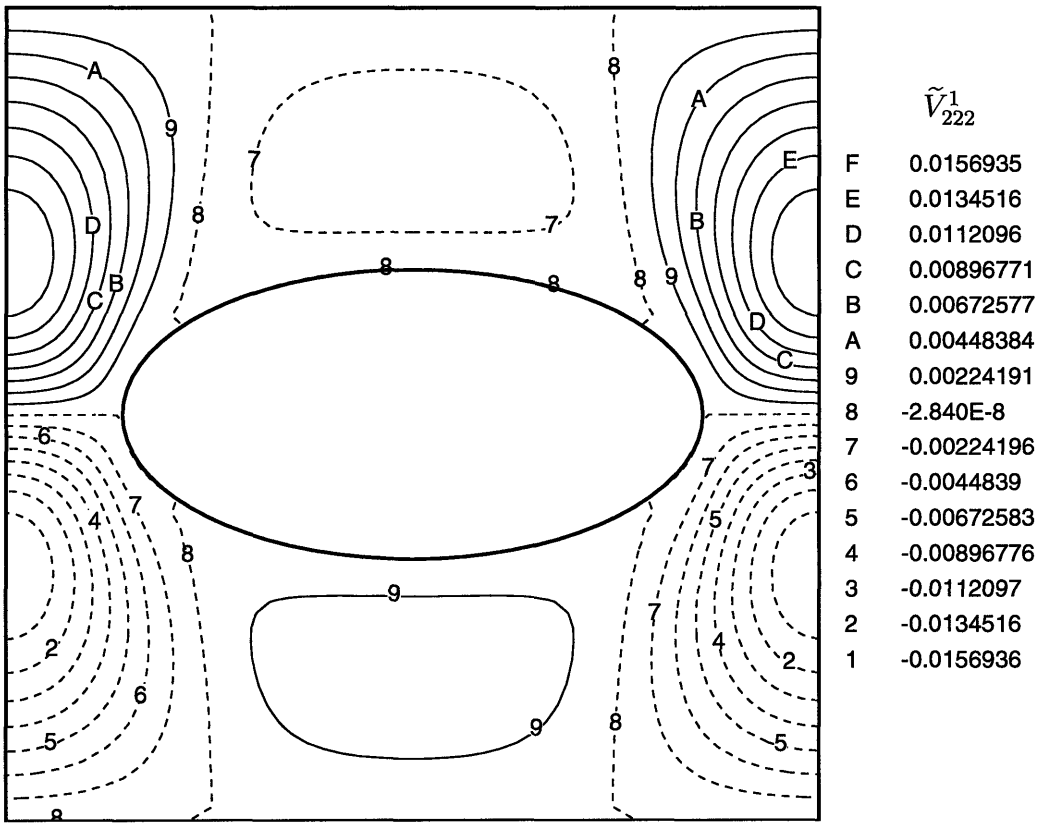

Figure D-13: Contours of $\tilde{V}^1_{222}$ from the $\mathcal{O}(1)$ cell problem for a square array of elliptical cylinders of volume fraction $\phi = 0.2$ and eccentricity $e = 2$.

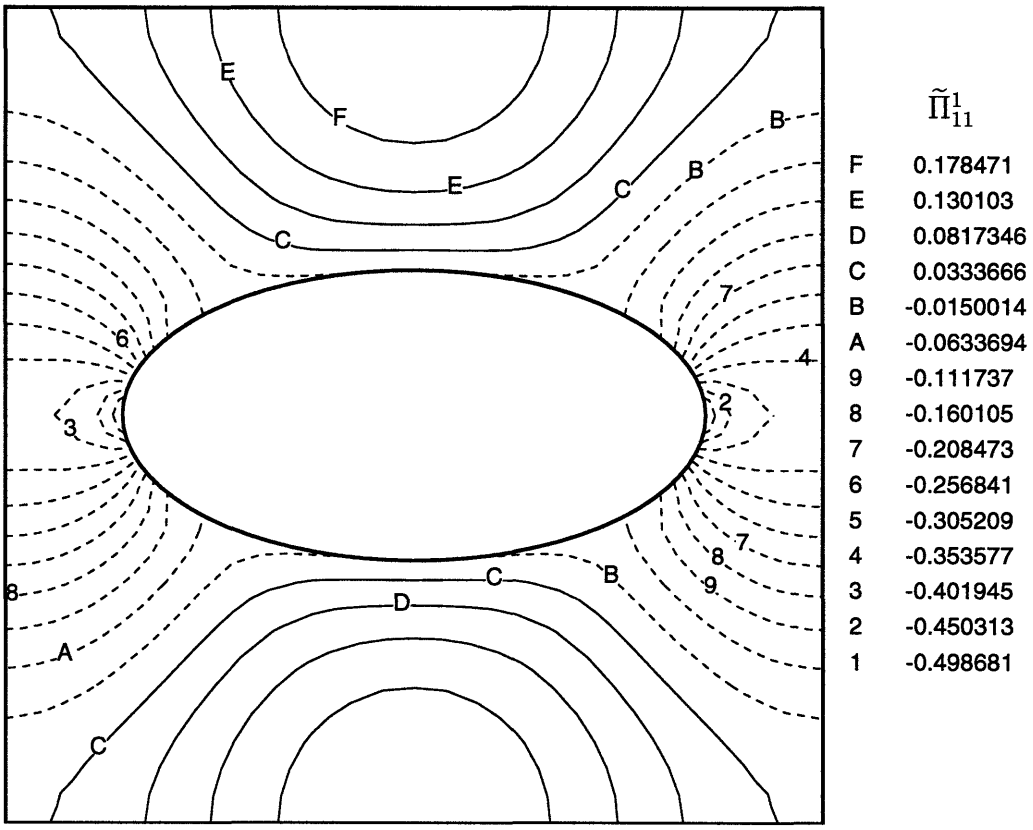

Figure D-14: Contours of $\widetilde{\Pi}^1_{11}$ from the $\mathcal{O}(1)$ cell problem for a square array of elliptical cylinders of volume fraction $\phi = 0.2$ and eccentricity $e = 2$.

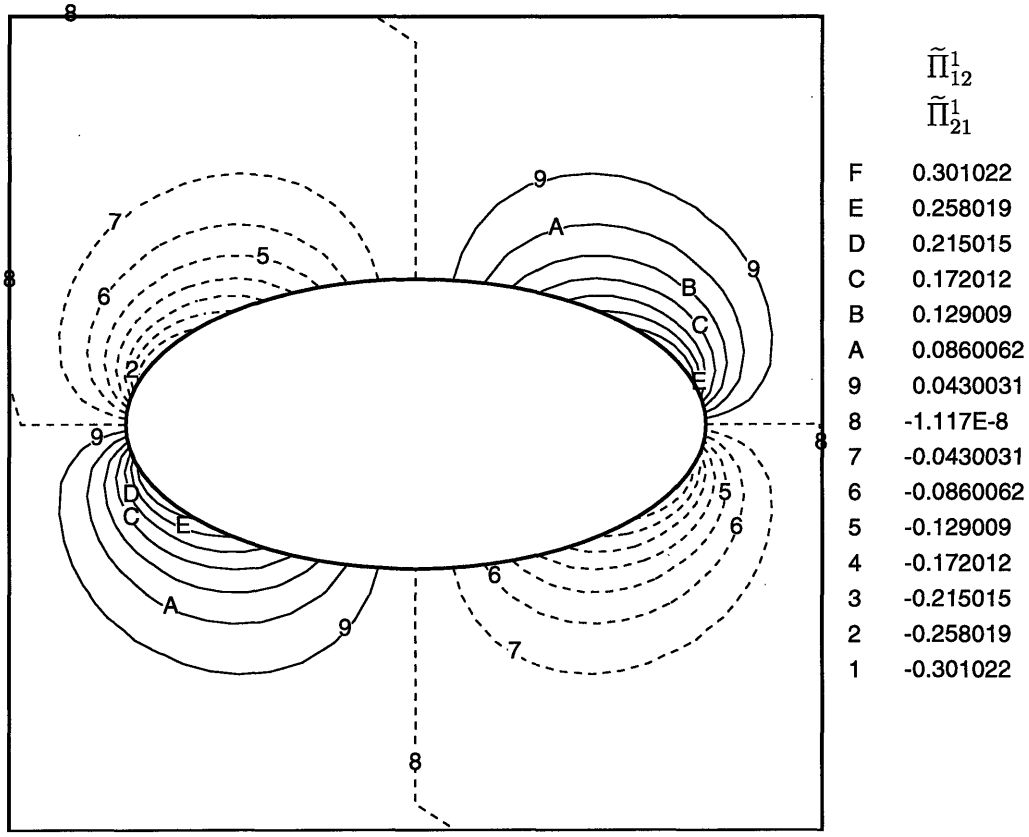

Figure D-15: Contours of $\tilde{\Pi}^1_{12}$ (or $\tilde{\Pi}^1_{21}$) from the $\mathcal{O}(1)$ cell problem for a square array of elliptical cylinders of volume fraction $\phi = 0.2$ and eccentricity $e = 2$.

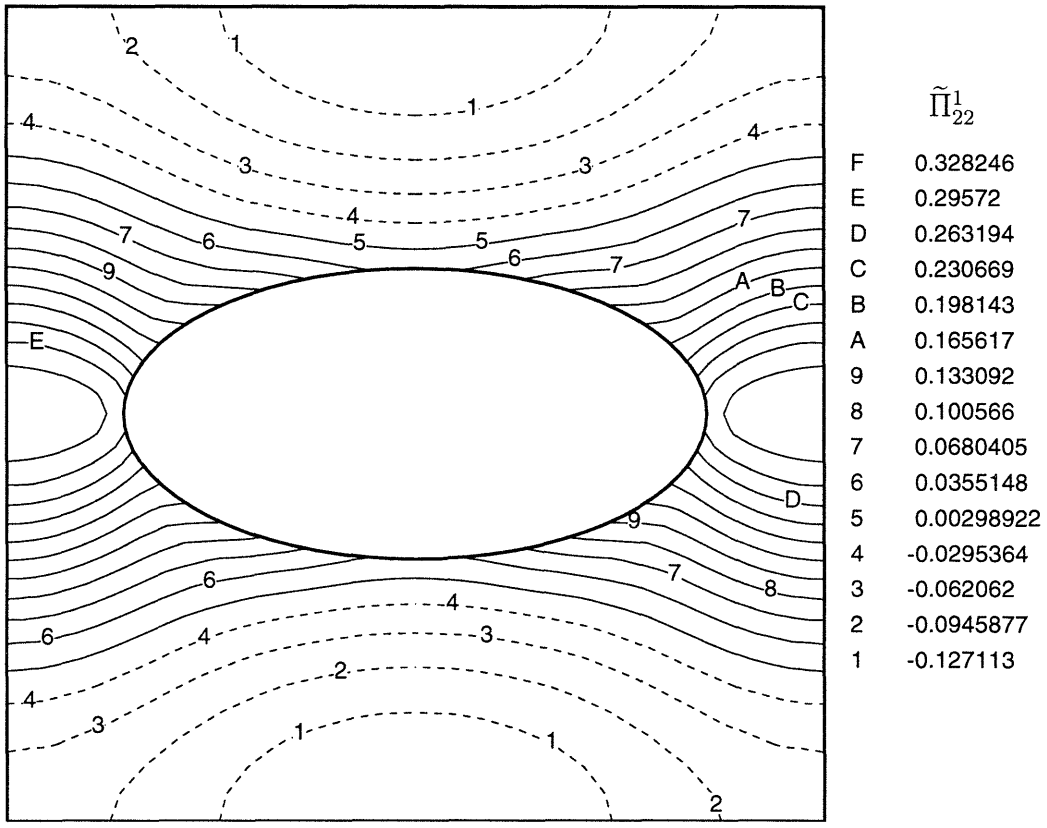

Figure D-16: Contours of $\widetilde{\Pi}^1_{22}$ from the $\mathcal{O}(1)$ cell problem for a square array of elliptical cylinders of volume fraction $\phi = 0.2$ and eccentricity $e = 2$.

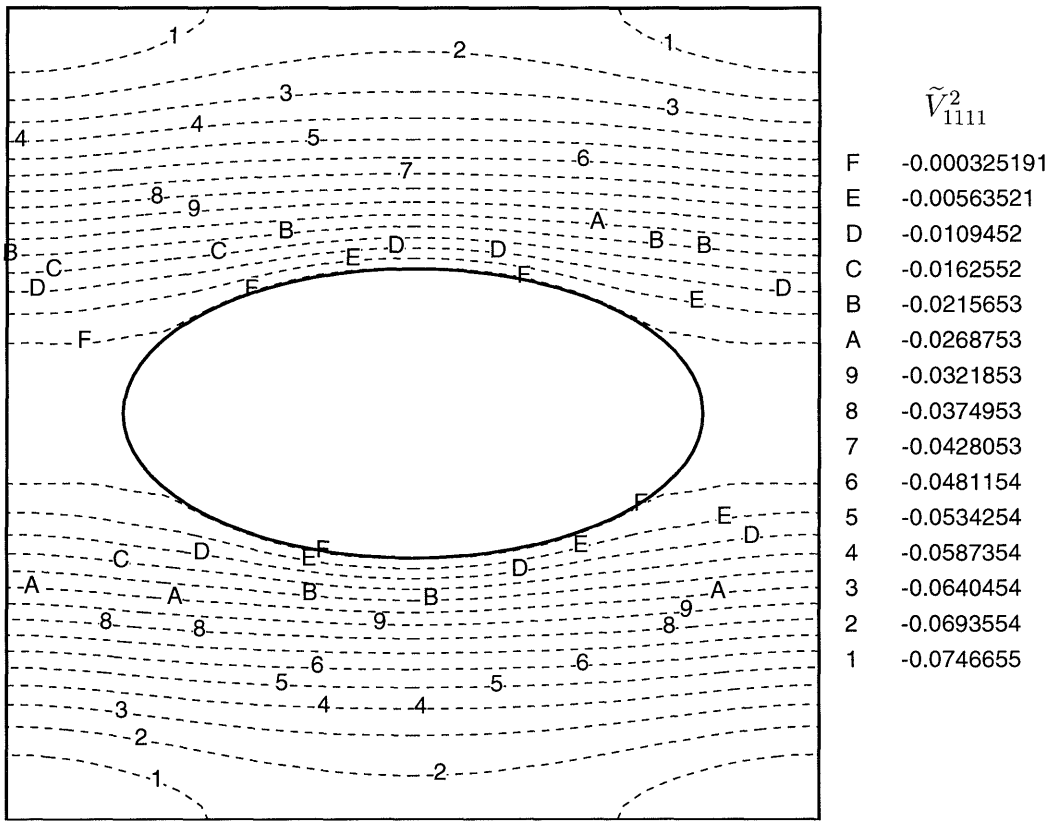

Figure D-17: Contours of $\widetilde{V}^2_{1111}$ from the $\mathcal{O}(2)$ cell problem for a square array of elliptical cylinders of volume fraction $\phi = 0.2$ and eccentricity $e = 2$.

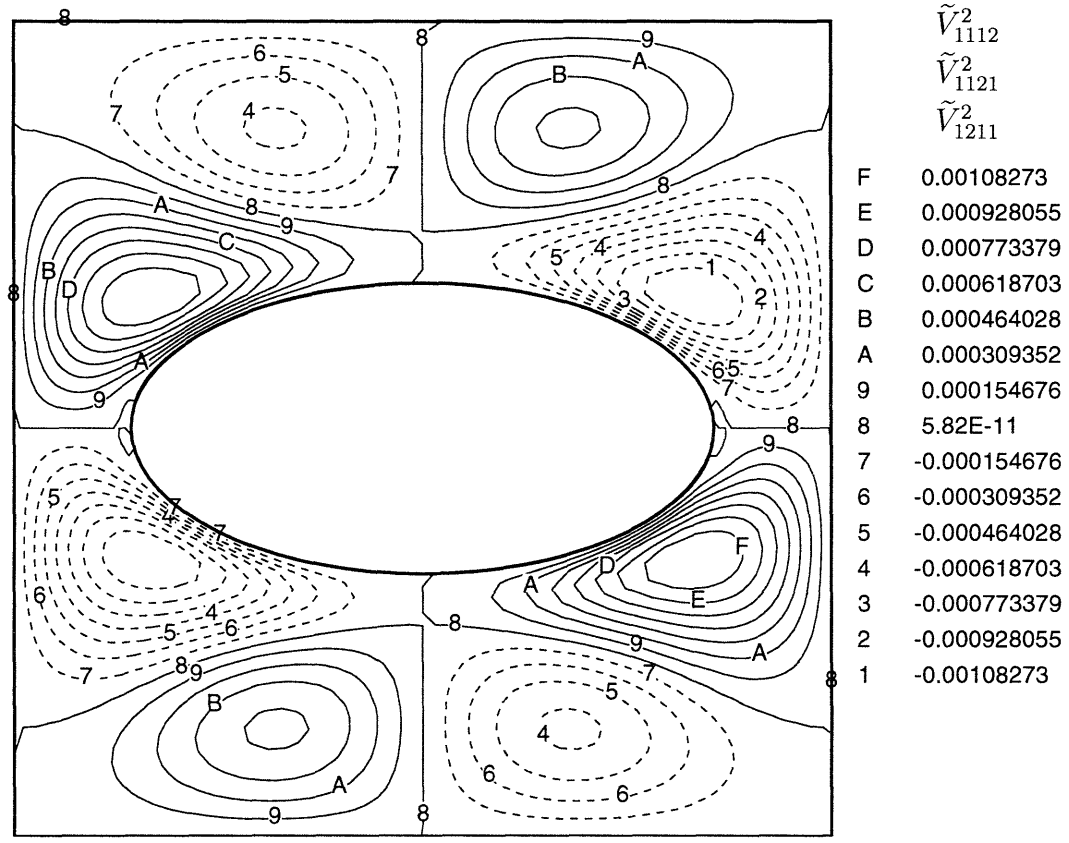

Figure D-18: Contours of $\tilde{V}^2_{1112}$ (or $\tilde{V}^2_{1121}$ or $\tilde{V}^2_{1211}$) from the $\mathcal{O}(2)$ cell problem for a square array of elliptical cylinders of volume fraction $\phi = 0.2$ and eccentricity $e = 2$.

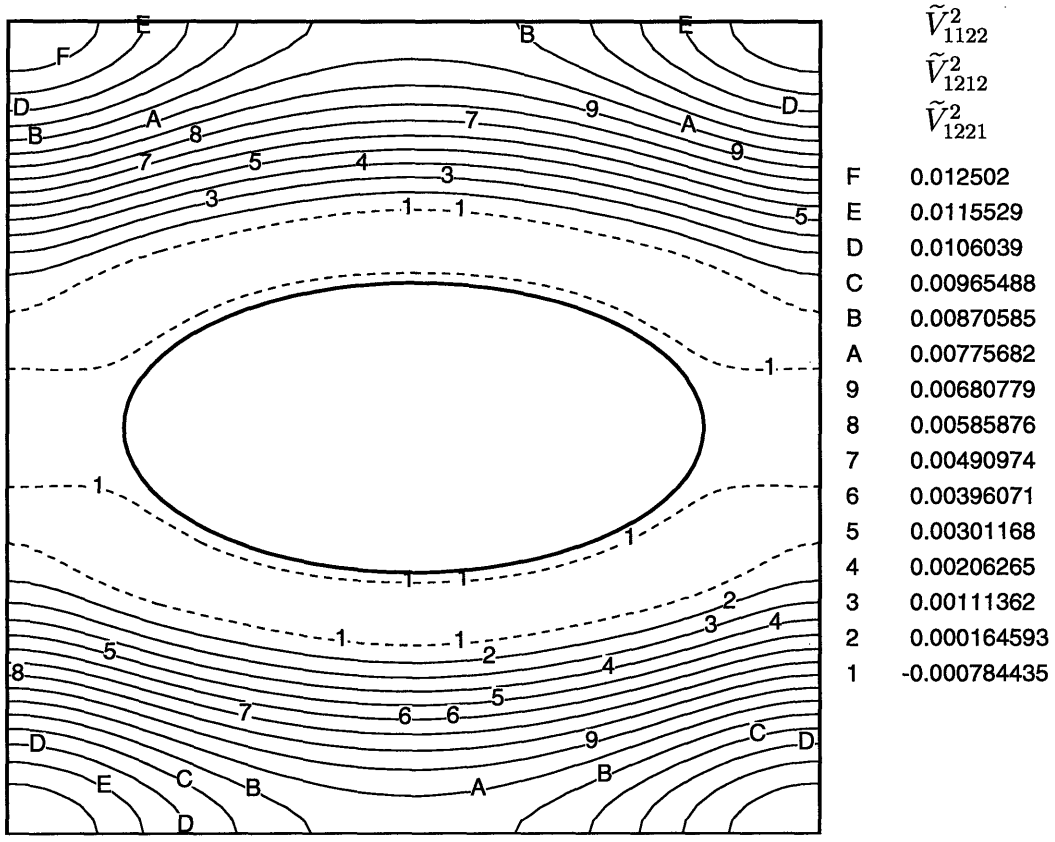

Figure D-19: Contours of $\tilde{V}^2_{1122}$ (or $\tilde{V}^2_{1212}$ or $\tilde{V}^2_{1221}$) from the $\mathcal{O}(2)$ cell problem for a square array of elliptical cylinders of volume fraction $\phi = 0.2$ and eccentricity $e = 2$.

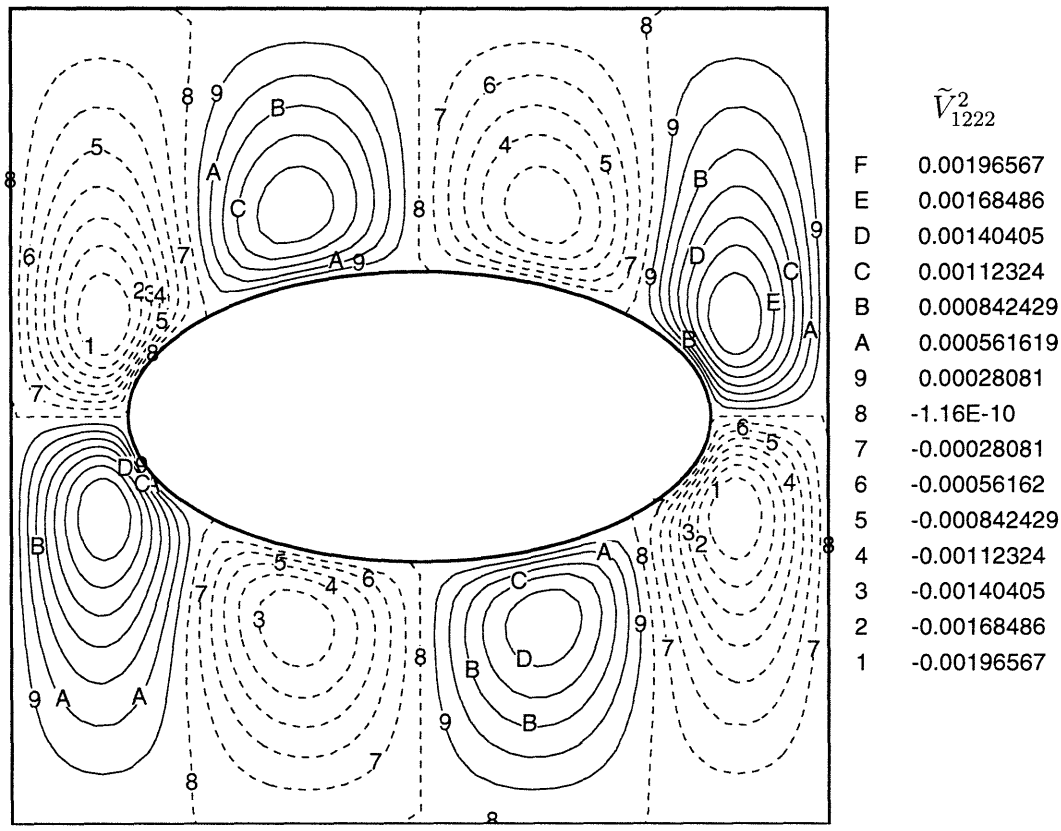

Figure D-20: Contours of $\widetilde{V}^2_{1222}$ from the $\mathcal{O}(2)$ cell problem for a square array of elliptical cylinders of volume fraction $\phi = 0.2$ and eccentricity $e = 2$.

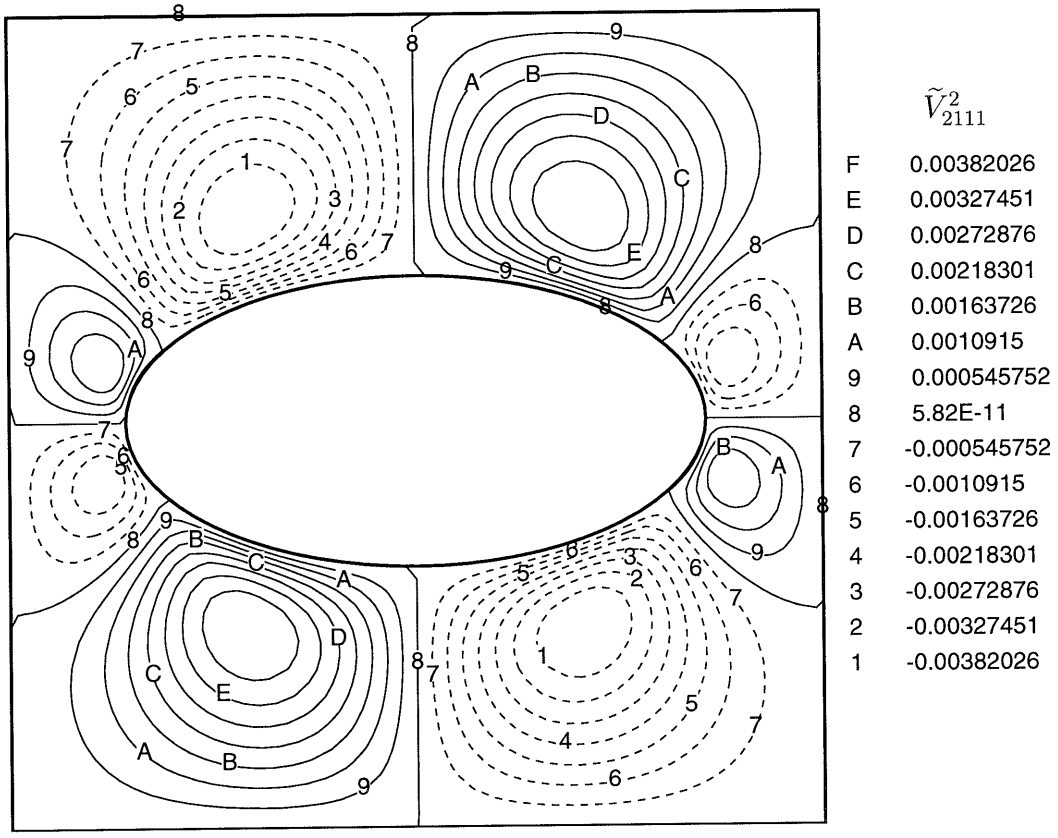

Figure D-21: Contours of $\widetilde{V}^2_{2111}$ from the $\mathcal{O}(2)$ cell problem for a square array of elliptical cylinders of volume fraction $\phi = 0.2$ and eccentricity $e = 2$.

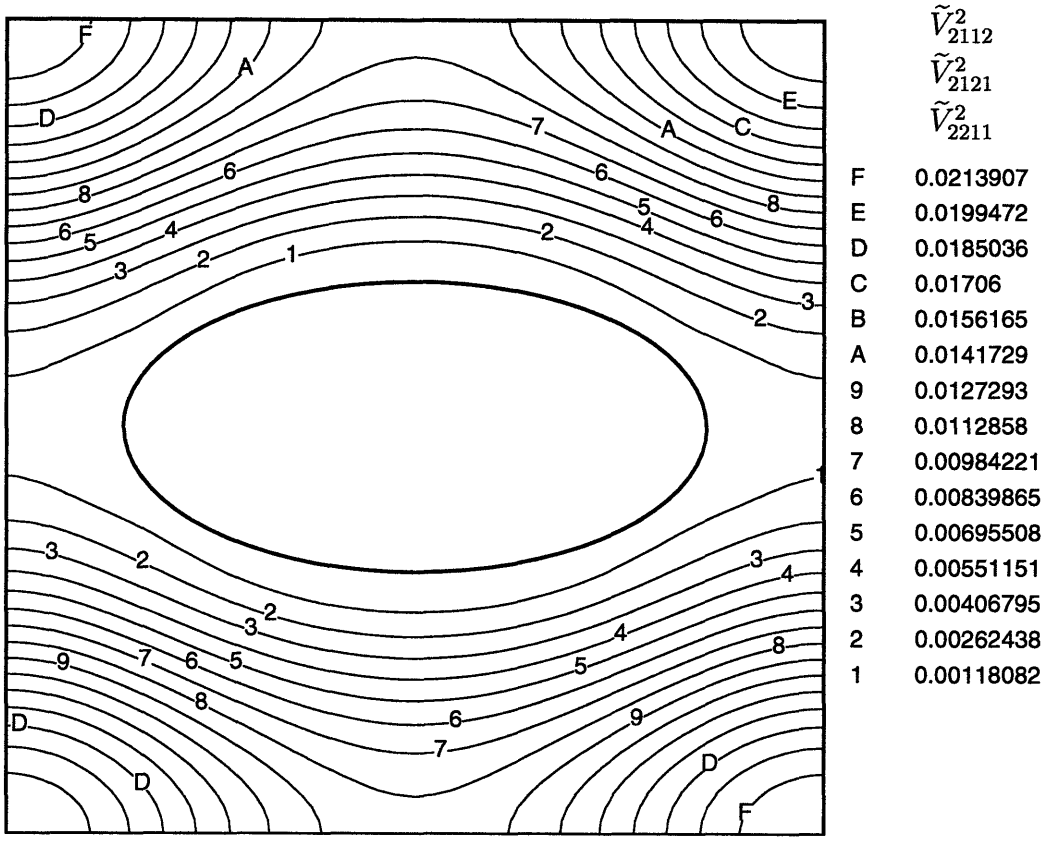

Figure D-22: Contours of $\tilde{V}^2_{2112}$ (or $\tilde{V}^2_{2121}$ or $\tilde{V}^2_{2211}$) from the $\mathcal{O}(2)$ cell problem for a square array of elliptical cylinders of volume fraction $\phi = 0.2$ and eccentricity $e = 2$.

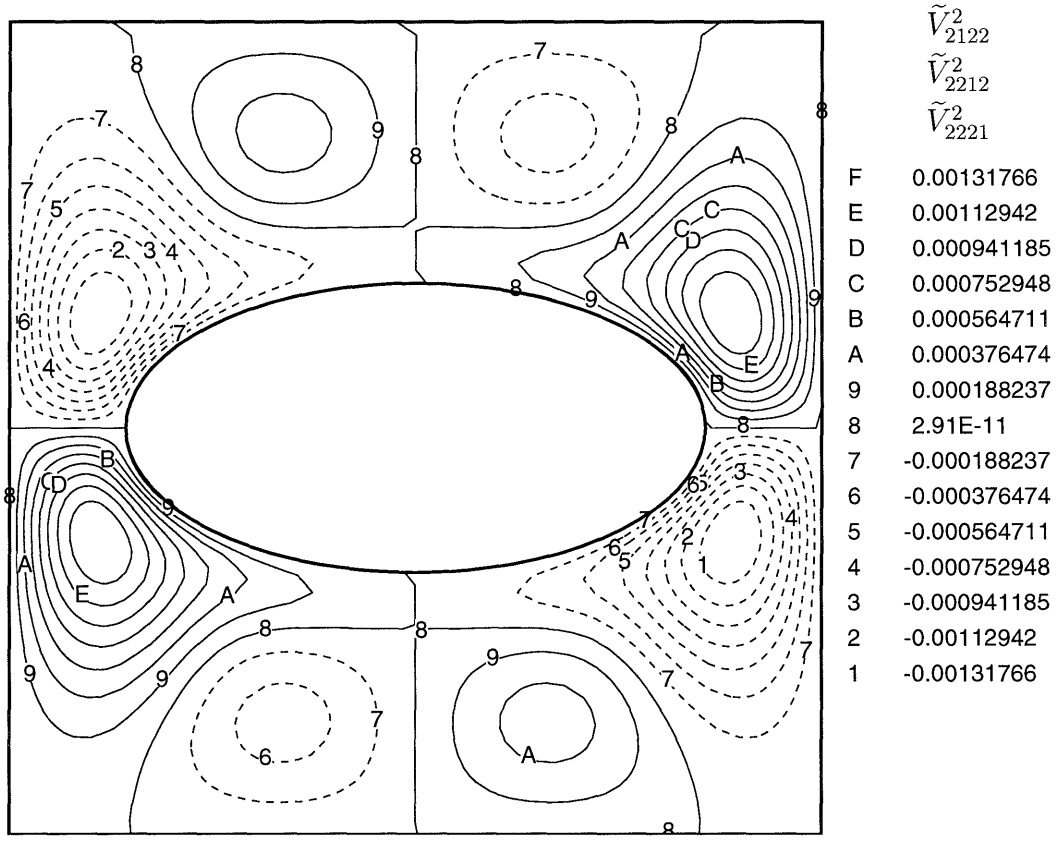

Figure D-23: Contours of $\widetilde{V}^2_{2122}$ (or $\widetilde{V}^2_{2212}$ or $\widetilde{V}^2_{2221}$) from the $\mathcal{O}(2)$ cell problem for a square array of elliptical cylinders of volume fraction $\phi = 0.2$ and eccentricity $e = 2$.

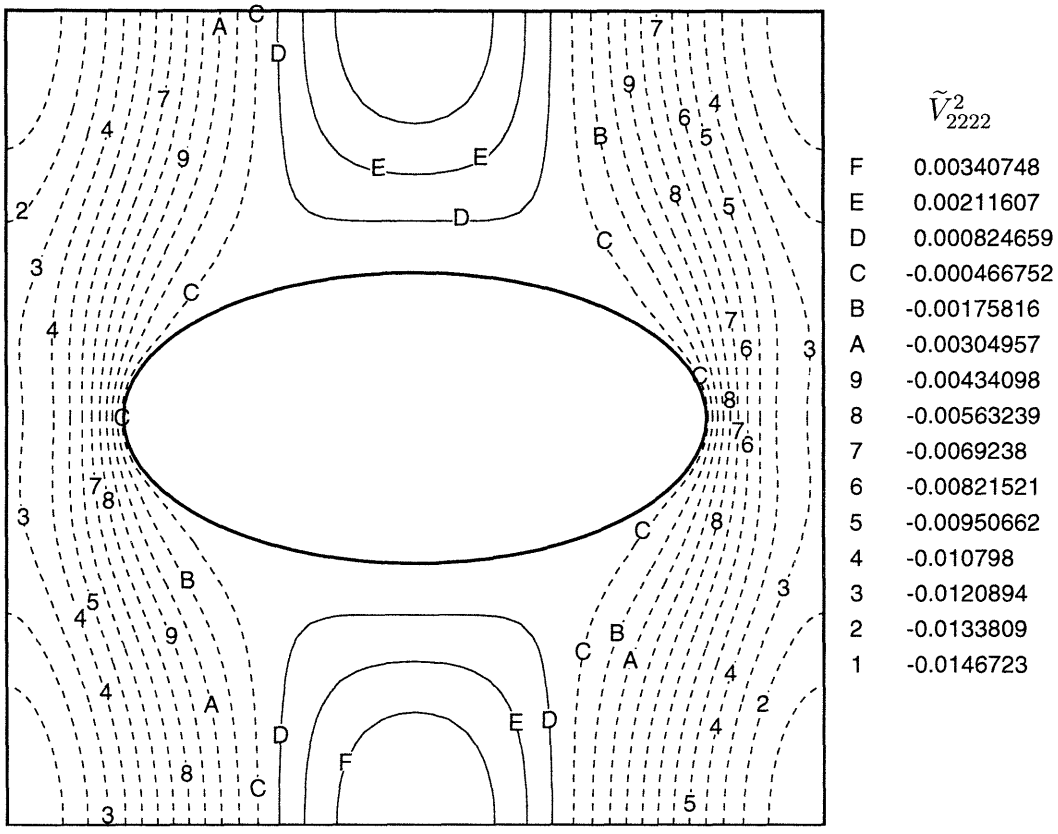

Figure D-24: Contours of $\tilde{V}^2_{2222}$ from the $\mathcal{O}(2)$ cell problem for a square array of elliptical cylinders of volume fraction $\phi = 0.2$ and eccentricity $e = 2$.

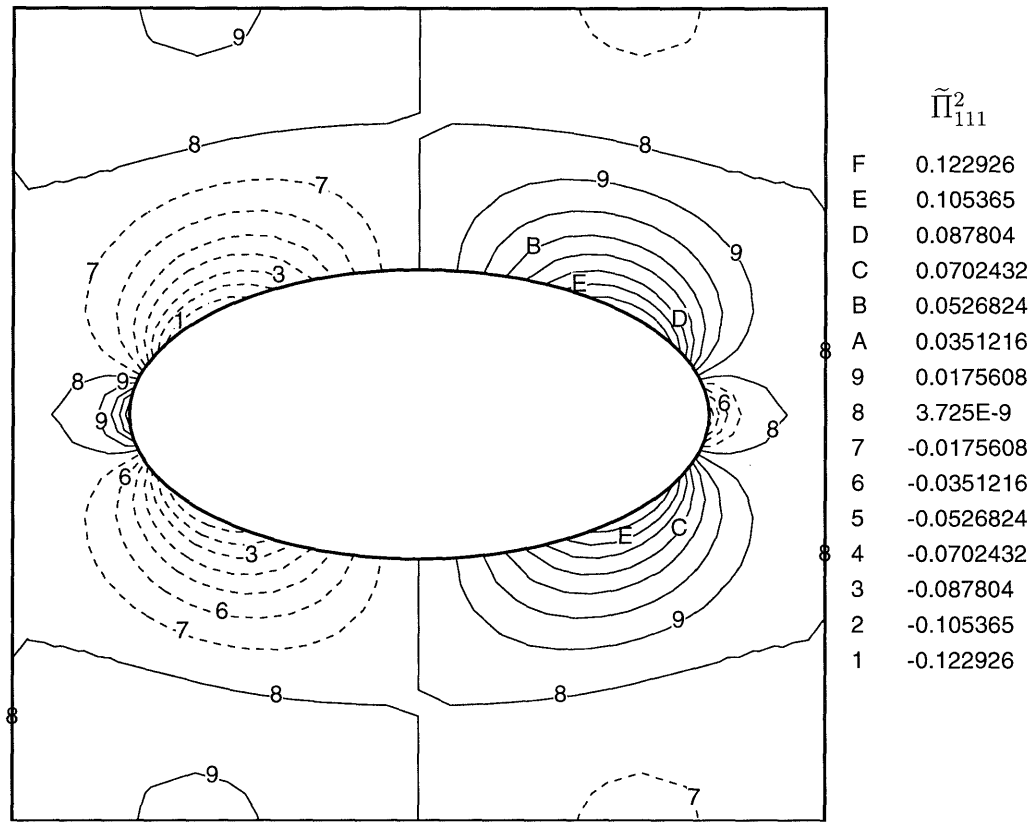

Figure D-25: Contours of $\widetilde{\Pi}^2_{111}$ from the $\mathcal{O}(2)$ cell problem for a square array of elliptical cylinders of volume fraction $\phi = 0.2$ and eccentricity $e = 2$.

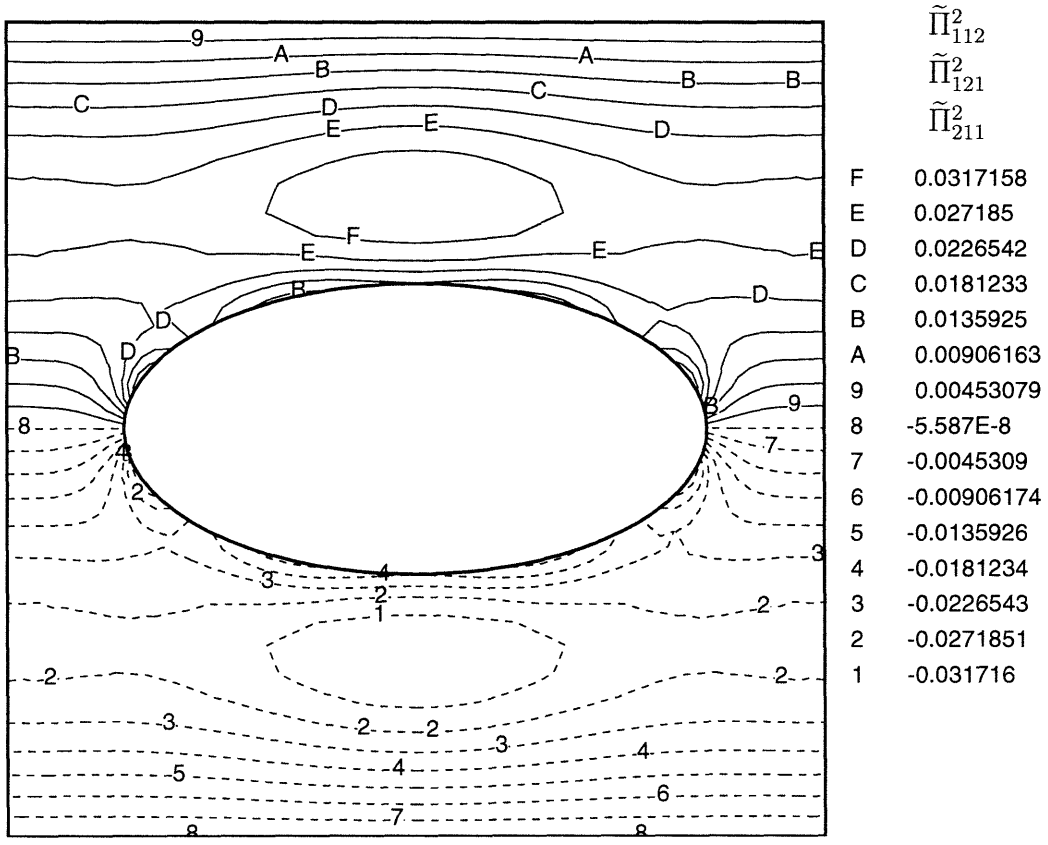

Figure D-26: Contours of $\tilde{\Pi}^2_{112}$ (or $\tilde{\Pi}^2_{121}$ or $\tilde{\Pi}^2_{211}$) from the $\mathcal{O}(2)$ cell problem for a square array of elliptical cylinders of volume fraction $\phi = 0.2$ and eccentricity $e = 2$.

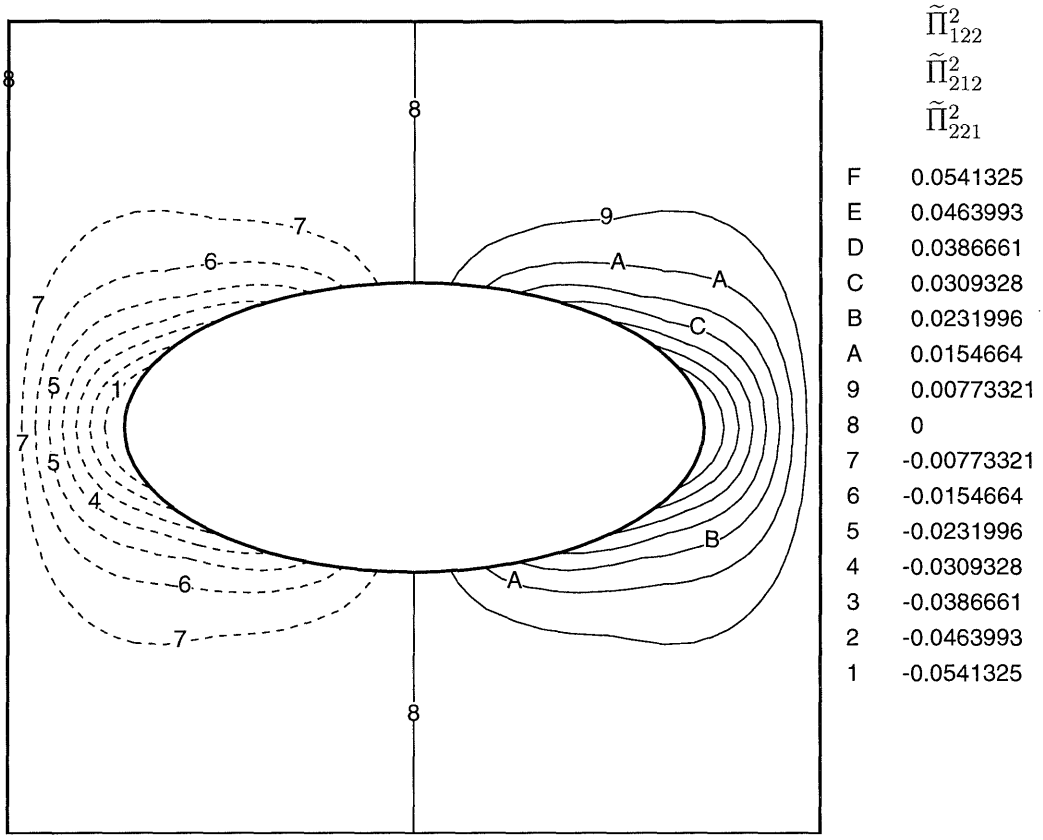

Figure D-27: Contours of $\tilde{\Pi}^2_{122}$ (or $\tilde{\Pi}^2_{212}$ or $\tilde{\Pi}^2_{221}$) from the $\mathcal{O}(2)$ cell problem for a square array of elliptical cylinders of volume fraction $\phi = 0.2$ and eccentricity $e = 2$.

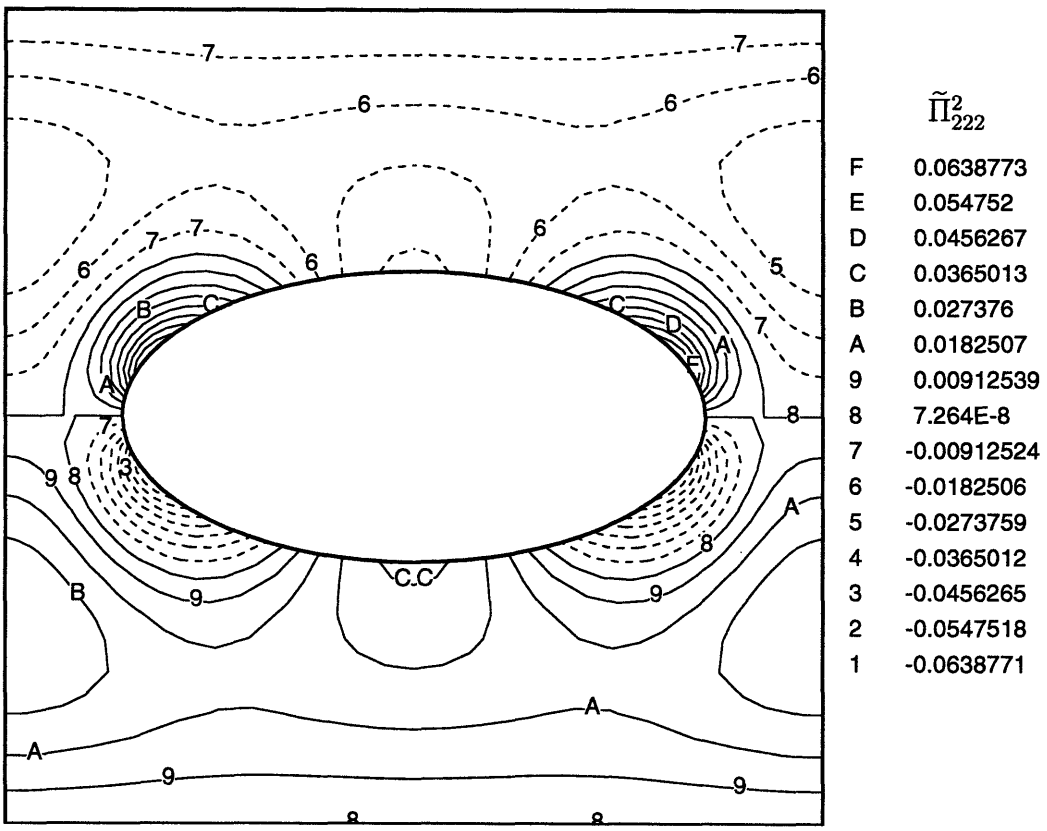

Figure D-28: Contours of $\tilde{\Pi}^2_{222}$ from the $\mathcal{O}(2)$ cell problem for a square array of elliptical cylinders of volume fraction $\phi = 0.2$ and eccentricity $e = 2$.

Bibliography

[1] ABRAMOWITZ, M. & STEGUN, I. A., 1972, *Handbook of Mathematical Functions*, Dover, NY., pp. -.

[2] ACRIVOS, A. & CHANG, E., 1986, "A Model for Estimating Transport Quantities in Two Phase Materials," *Phys. Fluids*, **29**, pp. 3-4.

[3] ADLER, P. M. & BRENNER, H., 1985, "Spatially Periodic Suspensions of Convex Particles in Linear Shear Flows.—I. Description and Kinematics," *Int. J. Multiphase Flow*, **11**, pp. 361-385.

[4] ADLER, P. M., ZUZOVSKY, M. & BRENNER, H., 1985, "Spatially Periodic Suspensions of Convex Particles in Linear Shear Flows.—II. Rheology," *Int. J. Multiphase Flow*, **11**, pp. 387-417.

[5] ADLER, P. M., NADIM, A. & BRENNER, H., 1990, "Rheological Models of Suspensions," *Adv. Chem. Eng.*, **15**, pp. 1-72.

[6] AFACAN, S. L. A. & MASLIYAH, J., 1994, "Steady Incompressible Laminar Flow in Porous Media," *Chem. Engng Sci.*, **49**, pp. xxxx-xxxx.

[7] ANDERSON, J. L. & KIM, J., 1987, "Fluid Dynamical Effects of Polymers Adsorbed to Spherical Particles," *J. Chem. Phys.*, **86**, pp. 5163-5173.

[8] ARIS, R., 1956, "," *Proc. Roy. Soc. Lond.*, **A235**, pp. 67-.

[9] AVELLANEDA, M. & TORQUATO, S., 1991, "Rigourous Link between Fluid Permeability, Electrical Conductivity, and Relaxation Times for Transport in Porous Media," *Phys. Fluids A*, **3**, pp. 2529-2540.

[10] BATYCKY, R. P., EDWARDS, D. A. & BRENNER, H., 1993, "Thermal Taylor Dispersion in an Insulated Circular Cylinder - I. Theory," *Int. J. Heat Mass Trans.*, **36**, pp. 4317-4325.

[11] BATYCKY, R. P., EDWARDS, D. A. & BRENNER, H., 1993, "Thermal Taylor Dispersion in an Insulated Circular Cylinder - II. Applications," *Int. J. Heat Mass Trans.*, **36**, pp. 4327-4333.

[12] BATYCKY, R. P., EDWARDS, D. A. & BRENNER, H., 1993, "Internal Energy Transport in Adiabatic Systems. Thermal Taylor Dispersion Phenomena," *Int. J. Non-linear Mech.*, **29**, pp. 639-664.

[13] BATYCKY, R. P., EDWARDS, D. A. & BRENNER, H., 1993, "Thermal Taylor Dispersion Phenomena in Nonadiabatic Systems," *Chem. Eng. Comm.*, **130**, pp. 53-104.

[14] BEAR, J., 1972, *Dynamics of Fluids in Porous Media*, American Elsevier, New York, pp. -.

[15] BEAVERS, G. S. & JOSEPH, D. D., 1967, "Boundary Conditions at a Naturally Permeable Wall," *J. Fluid Mech.*, **30**, pp. 197-207.

[16] BEAVERS, G. S., SPARROW, E. M. & MAGNUSON, R. A., 1970, "Experiments on Parallel Flows in a Channel and a Bounding Porous Medium," *J. Basic Eng.*, **92**, pp. 843-848.

[17] BERKOWITZ, B., 1989, "Boundary Conditions Along Permeable Fracture Walls: Influence on Flow and Conductivity," *Water Resources Res.*, **25**, pp. 1919-1922.

[18] BHARGAVA, S. K. & NIRMAL, C. S., 1989, "Heat Transfer in Generalized Couette Flow of Two Immiscible Newtonian Fluids through a Porous Channel: Use of Brinkman Model," *Indian J. Technol.*, **27**, pp. 211-214.

[19] BOSHENYATOV, B. V. & CHERNYSHEV, I. V., 1991, "The Effective Viscosity of a Microbubbly Medium," *Fluid Mech.: Soviet Res.*, **20**, pp. 124-129.

[20] BRENNER, H., 1970, "Rheology of Two-phase Systems," *Ann. Rev. Fluid Mech.*, **2**, pp. 137-.

[21] BRENNER, H., 1970, "Rheology of a Dilute Suspension of Dipolar Spherical Particles in an External Field," *J. Coll. Interface Sci.*, **32**, pp. 141-.

[22] BRENNER, H., 1972, "Suspension Rheology," *Prog. in Heat Mass Trans.*, **5**, pp. 89-129.

[23] BRENNER, H., 1974, "Rheology of a Dilute Suspension of Axisymmetric Brownian Particles," *Int. J. Multiphase Flow*, **1**, pp. 195-.

[24] BRENNER, H., 1980, "A General Theory of Taylor Dispersion Phenomena," *PhysicoChem. Hydrodyn.*, **1**, pp. 91-.

[25] BRENNER, H., 1980, "Dispersion resulting from Flow through Spatially Periodic Porous Media," *Phil. Trans. Roy. Soc. Lond.*, **A297**, pp. 81-.

[26] BRENNER, H., 1982, "A General Theory of Taylor Dispersion Phenomena," *PhysicoChem. Hydrodyn.*, **3**, pp. 139-.

[27] BRENNER, H., 1982, "Dispersion resulting from Flow through Spatially Periodic Porous Media," *Phil. Trans. Roy. Soc. Lond.*, **A307**, pp. 149-.

[28] BRENNER, H. & EDWARDS, D., 1993, *Macrotransport Processes*, Butterworth-Heinemann, pp. -.

[29] BRINKMAN, H. C., 1947, "A Calculation of the Viscosity and the Sedementation Constant for Solutions of Large Chain Molecules taking into account the Hampered Flow of the Solvent through these Molecules," *Physica*, **13**, pp. 447-448.

[30] BRINKMAN, H. C., 1947, "A Calculation of the Viscous Force Exerted by a Flowing Fluid on a Dense Swarm of Particles," *Appl. Sci. Res.*, **A1**, pp. 27-34.

[31] BRINKMAN, H. C., 1947, "On the Permeability of Media Consisting of Closely Packed Porous Particles," *Appl. Sci. Res.*, **A1**, pp. 81-86.

[32] BUYEVICH, Y. A. & SHCHELCHKOVA, I. N., 1978, "Flow of Dense Suspensions," *Prog. Aerospace Sci.*, **18**, pp. 121-150.

[33] CARMAN, W., 1937, "-," *Trans. Inst. Chem. Engrs.*, **15**, pp. 150-.

[34] CHANG, E. & ACRIVOS, A., 1986, "Rate of Heat Conduction from a Heated Sphere to a Matrix Containing Passive Spheres of a Different Conductivity," *J. Appl. Phys.*, **59**, pp. 3375-3382.

[35] CHANG, E. Y. & ACRIVOS, A., 1988, "The Effective Permeability of a Random Dispersion of Spheres," *PhysicoChem. Hydrodyn.*, **10**, pp. 579-584.

[36] CHANG, E. Y., YENDLER, B. S. & ACRIVOS, A., 1986, "A Model for Estimating the Effective Thermal Conductivity of a Random Suspension of Spheres," *Advances in Multiphase Flow*, -, pp. 35-54.

[37] CHANG, W. & JANG, J., 1989, "Non-Darcian Effects on Vortex Instability of a Horizontal Natural Convection Flow in a Porous Medium," *Int. J. Heat Mass Trans.*, **32**, pp. 529-539.

[38] CHAPMAN, S. & COWLING, T. G., 1961, *The Mathematical Theory of Non-Uniform Gasses, 2nd ed.*, Cambridge Univ. Press, Cambridge, pp. -.

[39] CHENG, P., 1978, "Heat Transfer in Geothermal Systems," *Advances in Heat Transfer*, **14**, pp. 1-105.

[40] CHENG, P., HSU, C. T. & CHOWDHURY, A., 1988, "Forced Convection in the Entrance Region of a Packed Channel With Axisymmetric Heating," *J. Heat Trans.*, **110**, pp. 946-954.

[41] CHENG, P. & MINKOWYCZ, W. J., 1977, "Free Convection about a Vertical Flat Plate Embedded in a Saturated Porous Medium with Application to Heat Transfer from a Dike," *J. Geophysics Res.*, **82**, pp. 2040-2044.

[42] CHILDRESS, S., 1972, "Viscous Flow Past a Random Array of Spheres," *J. Chem. Phys.*, **56**, pp. 2527-2539.

[43] CLERCX, H. J. H. & SCHRAM, P. P. J. M., 1992, "High-Frequency Effective Viscosity of Hard-Sphere Suspensions," *Phys. Rev. A*, **45**, pp. 860-872.

[44] DARCY, H. P. G., 1856, *Les Fontaines Publiques de la Ville de Dijon*, Victor Dalmont, Paris, pp. -.

[45] DU PLESSIS, J. P. & MASLIYAH, J. H., 1988, "Mathematical Modelling of Flow through Consolidated Isotropic Porous Media," *Transport Porous Media*, **3**, pp. 145-161.

[46] DURLOFSKY, L. & BRADY, J. F., 1987, "Analysis of the Brinkman Equation as a Model for Flow in Porous Media," *Phys. Fluids*, **30**, pp. 3329-3341.

[47] EDWARDS, D. A., SHAPIRO, M., BAR-YOSEPH, P. & SHAPIRA, M., 1990, "The Influence of Reynolds Number upon the Apparent Permeability of Spatially Periodic Arrays of Cylinders," *Phys. Fluids A*, **2**, pp. 45-55.

[48] EINSTEIN, A., 1906, "Eine neue Bestimmung der Moleküldimensionen," *Ann. Physik*, **19**, pp. 289-306.

[49] EINSTEIN, A., 1911, "Berichtigung zu meiner Arbeit: Eine neue Bestimmung der Moleküldimensionen," *Ann. Physik*, **34**, pp. 591-592.

[50] ERGUN, S., 1952, "Fluid Flow Through Packed Columns," *Chem. Eng. Progress*, **48**, pp. 89-94.

[51] ETHIER, C. R. & KAMM, R. D., 1989, "Flow Through Partially Gel-Filled Channels," *PhysicoChem. Hydrodyn.*, **11**, pp. 219-227.

[52] FELDERHOF, B. U., 1975, "Frictional Properties of Dilute Polymer Solutions. III. Translational-Frictional Coefficent," *Physica*, **80A**, pp. 63-75.

[53] FELDERHOF, B. U., 1975, "Frictional Properties of Dilute Polymer Solutions. IV. Intrinsic Viscosity," *Physica*, **80A**, pp. 172-188.

[54] FELDERHOF, B. U., 1976, "Rheology of Polymer Solutions. I. Local Flow Effects," *Physica*, **82A**, pp. 596-610.

[55] FELDERHOF, B. U., 1976, "Rheology of Polymer Solutions. II. Translation, Rotation and Viscosity," *Physica*, **82A**, pp. 611-622.

[56] FORCHHEIMER, P., 1901, "Wasserbewegung Durch Bodeu," *ForschHft. Ver. Dt. Ing.*, **45**, pp. 1782-1788.

[57] FREED, K. F. & MUTHUKUMAR, M., 1978, "On the Stokes Problem for a Suspension of Spheres at Finite Concentrations," *J. Chem. Phys.*, **68**, pp. 2088-2096.

[58] GIVLER, R. C. & ALTOBELLI, S. A., 1994, "A Determination of the Effective Viscosity for the Brinkman-Forchheimer flow model," *J. Fluid Mech.*, **258**, pp. 355-370.

[59] HABER, S. & MAURI, R., 1983, "Boundary Conditions for Darcy's Flow through Porous Media," *Int. J. Multiphase Flow*, **9**, pp. 561-574.

[60] HASIMOTO, H., 1959, "On the Periodic Fundamental Solution of the Stokes equations and their Applications to Viscous Flow past a Cubic Array of Spheres," *J. Fluid Mech.*, **5**, pp. 317-328.

[61] HAYES, R. E., 1990, "Simulation of Mixed Convection Heat Transfer at the Wall of a Packed Bed," *Num. Heat Trans. A*, **17**, pp. 217-230.

[62] HORN, F. J. M., 1971, "Calculation of Dispersion Coefficients by Means of Moments," *AIChE J.*, **17**, pp. 613-620.

[63] HOWELLS, I. D., 1974, "Drag Due to the Motion of a Newtonian Fluid through a Sparse Random Array of Small Fixed Rigid Objects," *J. Fluid Mech.*, **64**, pp. 449-475.

[64] HSU, C. T. & CHENG, P., 1985, "The Brinkman Model for Natural Convection about a Semi-infinite Vertical Flat Plate in a Porous Medium," *Int. J. Heat Mass Trans.*, **28**, pp. 683-696.

[65] IGUCHI, M. & MORITA, Z., 1992, "The Effective Viscosity and Effective Diffusivity of Bubbles in an Air-Water Vertical Bubbling Jet," *ISIJ Int.*, **32**, pp. 857-864.

[66] JEFFREY, D. J. & ACRIVOS, A., 1976, "The Rheological Properties of Suspensions of Rigid Particles," *AIChE J.*, **22**, pp. 417-432.

[67] JOSEPH, D. D., NIELD, D. A. & PAPANICOLAOU, G., 1982, "Nonlinear Equation Governing Flow in a Saturated Porous Medium," *Water Resources Res.*, **18**, pp. 1049-1052.

[68] KATTO, Y. & MASUAKA, T., 1967, "Criterion for the Onset of Convective Flow in a Fluid in a Porous Medium," *Int. J. Heat Mass Trans.*, **10**, pp. 297-309.

[69] KIM, S. & RUSSEL, W. B., 1985, "Modelling of Porous Media by Renormalization of the Stokes Equations," *J. Fluid Mech.*, **154**, pp. 269-286.

[70] KOPLIK, J. LEVIN, H. & ZEE, A., 1983, "Viscosity Renormalization in the Brinkman Equation," *Phys. Fluids*, **26**, pp. 2864-2870.

[71] LADD, A. J. C., 1990, "Hydrodynamic Trasport Coefficients of Random Dispersions of Hard Spheres," *J. Chem. Phys.*, **93**, pp. 3484-3494.

[72] LARSON, R. E. & HIGDON, J. J. L., 1986, "Microscopic Flow Near the Surface of Two-Dimensional Porous Media. Part 1. Axial Flow," *J. Fluid Mech.*, **166**, pp. 449-472.

[73] LUNDGREN, T. S., 1972, "Slow Flow Through Stationary Random Beds and Suspensions of Spheres," *J. Fluid Mech.*, **51**, pp. 273-299.

[74] MAJUMDAR, A. & TIEN, C. L., 1990, "Effects of Surface Tension on Film Condensation in a Porous Medium," *J. Heat Trans.*, **112**, pp. 751-757.

[75] MILNE, E. A., 1957, *Vector Mechanics*, Methuen, London, pp. -.

[76] MILNER, S. T., 1991, "Hydrodynamic Penetration into Parabolic Brushes," *Macromolecules*, **24**, pp. 3704-3705.

[77] MILOH, T. & BENVENISTE, Y., 1989, "On the Effective Viscosity of a Nondilute Emulsion of Two Stokes Fluids with Small Capillary Number," *Phys. Fluids A*, **1**, pp. 1915-1925.

[78] MISRAY, S. & VARANASI, S., 1991, "A Model for the Permeation Characteristics of Porous Membranes with Grafted Polyelectrolyte Brushes," *J. Colloid Interface Sci.*, **146**, pp. 251-275.

[79] NAKAYAMA, A., KOKUDAI, T. & KOYAMA, H., 1990, "Non-Darcian Boundary Layer Flow and Forced Convective Heat Transfer Over a Flat Plate in a Fluid-Saturated Porous Medium," *J. Heat Trans.*, **112**, pp. 157-162.

[80] NEALE, G., EPSTEIN, N. & NADER, W., 1973, "Creeping Flow Relative to Permeable Spheres," *Chem. Eng. Sci.*, **28**, pp. 1865-1874.

[81] NEALE, G. & NADER, W., 1974, "Practical Significance of Brinkman's Extension of Darcy's Law: Coupled Parallel Flows within a Channel and a Bounding Porous Medium," *Can. J. Chem. Eng.*, **52**, pp. 475-478.

[82] NITSCHE, L. C. & BRENNER, H., 1989, "Eulerian Kinematics of Flow through Spatially Periodic Models of Porous Media," *Arch. for Rat. Mech. and Analysis*, **107**, pp. 225-292.

[83] NUNAN, K. C. & KELLER, J. B., 1984, "Effective Viscosity of a Periodic Suspension," *J. Fluid Mech.*, **142**, pp. 269-287.

[84] OOMS, G., MIJNLIEFF, P. F. & BECKERS, H. L., 1970, "Frictional Force Exerted by a Flowing Fluid on a Permeable Particle, with Particular Reference to Polymer Coils," *J. Chem. Phys.*, **53**, pp. 4123-4130.

[85] PANGRLE, B. J., ALEXANDROU, A. N., DIXON, A. G. & DIBIASIO, D., 1991, "An Analysis of Laminar Fluid Flow in Porous Tube and Shell Systems," *Chem. Eng. Sci.*, **46**, pp. 2847-2855.

[86] PHILLIPS, R. J., DEEN, W. M. & BRADY, J. F., 1989, "Hindered Transport of Spherical Macromolecules in Fibrous Membranes and Gels," *AIChE J.*, **35**, pp. 1761-1769.

[87] PHILLIPS, R. J., DEEN, W. M. & BRADY, J. F., 1990, "Hindered Transport in Fibrous Membranes and Gels: Effect of Solute Size and Fiber Configuration," *J. Colloid Interface Sci.*, **139**, pp. 363-373.

[88] POP, I. & CHENG, P., 1992, "Flow Past a Circular Cylinder Embedded in a Porous Medium Based on the Brinkman Model," *Int. J. Engng Sci.*, **30**, pp. 257-262.

[89] POTANIN, A. A. & URIEV, N. B., 1991, "Microrheological Models of Aggregated Suspensions in Shear Flow," *J. Colloid Interface Sci.*, **142**, pp. 385-395.

[90] QIN, Y. & KALONI, P. N., 1992, "Steady Convection in a Porous Medium based upon the Brinkman Model," *IMA J. Appl. Math.*, **48**, pp. 85-95.

[91] REHBINDER, G., 1989, "Darcyan Flow with Relaxation Effect," *Appl. Sci. Res.*, **46**, pp. 45-72.

[92] RIPPS, D. L. & BRENNER, H., 1967, "The Stokes Resistance of a slightly Deformed Sphere—II. Intrinsic Resistance Operators for an Arbitrary Initial Flow," *Chem. Engng Sci.*, **10**, pp. 375-387.

[93] SAFFMAN, P. G., 1971, "On the Boundary Conditions at the Surface of a Porous Media," *Stud. Appl. Math*, **2**, pp. 93-101.

[94] SANGANI, A. S. & ACRIVOS, A., 1982, "Slow Flow Past Periodic Arrays of Cylinders with Application to Heat Transfer," *Int. J. Multiphase Flow*, **8**, pp. 193-206.

[95] SANGANI, A. S. & ACRIVOS, A., 1982, "Slow Flow through a Periodic Array of Spheres.," *Int. J. Multiphase Flow*, **8**, pp. 343-360.

[96] SANGANI, A. S. & BEHL, S., 1989, "The Planar Singular Solutions of Stokes and Laplace Equations and their Application to Transport Processes near Porous Surfaces," *Phys. Fluids A*, **1**, pp. 21-37.

[97] SANGANI, A. S. & YAO, C., 1988, "Transport Processes in Random Arrays of Cylinders.—II. Viscous Flow," *Phys. Fluids*, **31**, pp. 2435-2444.

[98] SASAKI, A., SHINYA, A. & SHOICHIRO, F., 1990, "Numerical Study on Freezing Heat Transfer in Water-Saturated Porous Media," *Num. Heat Trans. A*, **18**, pp. 17-32.

[99] SHAPIRO, M. & BRENNER, H., 1986, "Taylor Dispersion of Chemically Reactive Species: Irreversible First-order Reactions in Bulk and on Boundaries," *Chem. Engng Sci.*, **41**, pp. 1417-1433.

[100] SHAPIRO, M. & BRENNER, H., 1987, "Chemically Reactive Generalized Taylor Dispersion Phenomena," *AIChE J.*, **33**, pp. 1155-1167.

[101] SHEN, J. P. & DOI, M., 1990, "Effective Viscosity of Magnetic Fluids," *J. Phys. Soc. Japan*, **59**, pp. 111-117.

[102] SLATTERY, J. C., 1968, "Multiphase Viscoelastic Flow through Porous Media," *AIChE J.*, **14**, pp. 50-56.

[103] SLATTERY, J. C., 1969, "Single-phase Flow through Porous Media," *AIChE J.*, **15**, pp. 866-872.

[104] SLOBODOV, E. B., 1989, "Effective Viscosity of Liquid in Granular Bed at Moderate and Large Reynolds Numbers," *Theoretical Found. Chem. Eng.*, **23**, pp. 61-64.

[105] SPIELMAN, L. & GOREN, S. L., 1968, "Model for Predicting Pressure Drop and Filtration Efficiency in Fibrous Media," *Environ. Sci. and Tech.*, **2**, pp. 279-287.

[106] STRANG, W. G. & FIX, G. J., 1973, *An Analysis of the Finite Element Method*, Prentice-Hall, N.J., pp. -.

[107] TAM, C. K. W., 1969, "The Drag on a Cloud of Spherical Particles in Low Reynolds Number Flow," *J. Fluid Mech.*, **38**, pp. 537-546.

[108] TAYLOR, G. I., 1953, "," *Proc. Roy. Soc. Lond.*, **A219**, pp. 186-.

[109] TAYLOR, G. I., 1954, "The Dispersion of Matter in Turbulent Flow through a Pipe," *Proc. Roy. Soc. Lond.*, **A223**, pp. 446-468.

[110] TAYLOR, G. I., 1954, "," *Proc. Roy. Soc. Lond.*, **A225**, pp. 473-.

[111] TONG, T. W. & SUBRAMANIAN, E., 1985, "A Boundary-layer Analysis for Natural Convection in Vertical Porous Enclosures—Use of the Brinkman–extended Darcy Model," *Int. J. Heat Mass Trans.*, **28**, pp. 563-570.

[112] TSAY, R. & WEINBAUM, S., 1991, "Viscous Flow in a Channel with Periodic Cross-Bridging Fibres: Exact Solutions and Brinkman Approximation," *J. Fluid Mech.*, **226**, pp. 125-148.

[113] VAFAI, K. & TIEN, C. L., 1981, "Boundary and Inertia Effects on Flow and Heat Transfer in Porous Media," *Int. J. Heat Mass Trans.*, **24**, pp. 195-203.

[114] VAIDYANATHAN, G., SEKAR, R. & BALASUBRAMANIAN, R., 1991, "Ferro-convective Instability of Fluids Saturating a Porous Medium," *Int. J. Engng Sci.*, **29**, pp. 1259-1267.

[115] VAROQUI, R. & DEJARDIN, P., 1977, "Hydrodynamic Thickness of Adsorbed Polymers," *J. Chem. Phys.*, **66**, pp. 4395-4399.

[116] VASSEUR, P. & ROBILLARD, L., 1987, "The Brinkman Model for Boundary Layer Regime in a Rectangular Cavity with Uniform Heat Flux from the Side," *Int. J. Heat Mass Trans.*, **30**, pp. 717-726.

[117] VASSEUR, P., WANG, C. H. & SEN, M., 1989, "The Brinkman Model for Natural Convection in a Shallow Porous Cavity with Uniform Heat Flux," *Num. Heat Trans., A*, **15**, pp. 221-242.

[118] VASSEUR, P., WANG, C. H. & SEN, M., 1990, "Natural Convection in an Inclined Rectangular Porous Slot: the Brinkman-Extended Darcy Model," *J. Heat Trans.*, **112**, pp. 507-511.

[119] WALKER, K. & HOMSY, G. M., 1977, "A Note on Convective Instability in Boussinesq Fluids and Porous Media," *Trans. ASME J. Heat Trans.*, **99**, pp. 338-339.

[120] WHITAKER, S., 1966, "The Equations of Motion in Porous Media," *Chem. Engng Sci.*, **21**, pp. 291-300.

[121] WHITAKER, S., 1969, "Advances in Theory of Fluid Motion in Porous Media," *Ind. Eng. Chem. Fundamentals*, **61**, pp. 14-28.

[122] WIEGEL, F. W., 1980, *Fluid Flow Through Porous Macromolecular Systems*, Springer-Verlag, NY., pp. 12-14.

[123] WOODING, R. A., 1963, "Convection in a Saturated Porous Medium at Large Rayleigh Number or Peclet Number," *J. Fluid Mech.*, **15**, pp. 527-544.

[124] ZICK, A. A. & HOMSY, G. M., 1982, "Stokes Flow through Periodic Arrays of Spheres," *J. Fluid Mech.*, **115**, pp. 13-26.

[125] ZUZOVSKY, M., ADLER, P. M. & BRENNER, H., 1983, "Spatially Periodic Suspensions of Convex Particles in Linear Shear Flows.—III. Dilute Arrays of Spheres Suspended in Newtonian Fluids," *Phys. Fluids*, **26**, pp. 1714-1723.